

www.ceramics.org/ema2014

January 22-24, 2014 | DoubleTree by Hilton Orlando at Sea World® | Orlando, Fla., USA

ELECTRONIC MATERIALS AND APPLICATIONS 2014

Conference Program

Scan for meeting app.



Organized by
The American Ceramic Society and
The American Ceramic Society's Electronics Division and
Basic Science Division

Welcome Letter

Welcome to Electronic Materials and Applications 2014. Jointly programmed by the Electronics Division and Basic Science Division of The American Ceramic Society, EMA 2014 is the fifth in a series of annual international meetings focused on electroceramic materials and their applications in electronic, magnetic, dielectric and optical components, devices and systems.

The 2014 meeting features symposia focused on dielectrics, pyroelectrics and electrocalorics; ferroics and multiferroics; piezoelectrics, electrostrictors and magnetostrictors; thermoelectrics; superconductors; photovoltaics; LEDs; and materials for data storage. Other symposia emphasize broader themes covering structure, interfaces and novel characterization methods; doping, defects and nanoscale phenomena; multilayers, heterostructures and graded multi-functional materials; thin film integration and processing science; composites; and computational design of electronic materials.

The meeting also features plenary lectures by distinguished scientists, including James Bray, GE Global Research; Jürgen Rödel, Technische Universität Darmstadt, Germany; and Joseph V. Mantese, United Technologies Research Center. The technical program includes invited lectures, contributed papers, poster presentations, and provides ample opportunity for the exchange of information and ideas on the latest developments in the theory, experimental investigation and applications of electroceramic materials. The participants represent an international mix of industrial, university, and federal laboratory researchers, engineers, technologists and leaders. For students, there is a separate symposium that features best-paper awards and provides development and networking opportunities.

We are pleased to build on the previous successes of this conference series in providing a distinctive forum to address emerging needs, opportunities and key challenges in the field of electronic materials and applications. We anticipate that this year's meeting will continue to highlight the most recent scientific advances and technological innovations in the field, and to facilitate the interactions and collaborations that will help to shape its future.

The Electronics Division, Basic Science Division, symposium organizers, and staff from The American Ceramic Society thank you for joining us for EMA 2014. We hope you have a rewarding and beneficial meeting experience and very much look forward to your continued participation in future EMA meetings.

The 2014 Organizing Committee:

Steven C. Tidrow
Electronics Division



George A. Rossetti, Jr.
Basic Science Division



Haiyan Wang
Electronics Division



Table of Contents

Schedule At A Glance	2
Highlights of Student Research in Basic Science and Electronic Ceramics	
Student Symposium	3
Sponsors	3
Plenary Speakers.....	4-5
Symposia	6-7
Hotel Floorplan	7
Presenting Author List	8-10

Final Program

Wednesday Morning.....	11-13
Wednesday Afternoon	13-16
Thursday Morning	16-18
Thursday Afternoon	19-21
Friday Morning	22-23
Friday Afternoon	24-25
Abstracts	26
Author Index	83

Basic Science Division Officers

Chair: Wayne Kaplan
Chair-Elect: Eduardo Saiz
Vice Chair: Bryan Huey
Secretary: Shen Dillon

Electronics Division Officers

Trustee: Winnie Wong-Ng
Chair: Steven C. Tidrow
Chair-Elect: Timothy J. Haugan
Vice-chair: Haiyan Wang
Secretary: Geoff Brenneka
Secretary-Elect: Brady Gibbons

Schedule At A Glance

Tuesday – January 21, 2014

Registration	5:00 p.m. – 6:30 p.m.	Oceans Ballroom Foyer
--------------	-----------------------	-----------------------

Wednesday – January 22, 2014

Registration	7:30 a.m. – 6 p.m.	Oceans Ballroom Foyer
Opening Comments	8:30 a.m. – 8:45 a.m.	Indian
Plenary Session I	8:45 a.m. – 9:30 a.m.	Indian
Coffee Break	9:30 a.m. – 10 a.m.	Atlantic
Concurrent Technical Sessions	10 a.m. – 12:30 p.m.	Indian, Pacific, Coral A, Coral B, Mediterranean B/C
Lunch On Own	12:30 p.m. – 2 p.m.	
Poster Session Set-Up	12 p.m. – 5 p.m.	Atlantic/Arctic
Concurrent Technical Sessions	2 p.m. – 5:30 p.m.	Indian, Pacific, Coral A, Coral B, Mediterranean B/C
Coffee Break	3:30 p.m. – 4 p.m.	Atlantic
Poster Session & Reception	5:30 p.m. – 7:30 p.m.	Atlantic/Arctic
Basic Science Division Tutorial	7:45 p.m. – 9:45 p.m.	Coral A

Thursday – January 23, 2014

Registration	7:30 a.m. – 5:30 p.m.	Oceans Ballroom Foyer
Plenary Session II	8:30 a.m. – 9:30 a.m.	Indian
Coffee Break	9:30 a.m. – 10 a.m.	Atlantic
Concurrent Technical Sessions	10 a.m. – 12:30 p.m.	Indian, Pacific, Coral A, Coral B, Mediterranean B/C
Lunch On Own	12:30 p.m. – 2 p.m.	
Concurrent Technical Sessions	2 p.m. – 5:30 p.m.	Indian, Pacific, Coral A, Coral B, Mediterranean B/C
Coffee Break	3:30 p.m. – 4 p.m.	Atlantic
Conference Dinner	7 p.m. – 9 p.m.	Atlantic/Arctic

Friday – January 24, 2014

Registration	7:30 a.m. – 5:30 p.m.	Oceans Ballroom Foyer
Plenary Session III	8:30 a.m. – 9:30 a.m.	Indian
Coffee Break	9:30 a.m. – 10 a.m.	Atlantic
Concurrent Technical Sessions	10 a.m. – 12:30 p.m.	Indian, Pacific, Coral A, Coral B, Mediterranean B/C
Lunch On Own	12:30 p.m. – 2 p.m.	
Concurrent Technical Sessions	2 p.m. – 5:30 p.m.	Indian, Pacific, Coral A, Coral B, Mediterranean B/C
Coffee Break	3:30 p.m. – 4 p.m.	Atlantic

Highlights of Student Research in Basic Science and Electronic Ceramics – Student Symposium

Undergraduate student research is being conducted at universities all over the world, but rarely are these students allowed the opportunity to present their work at a meeting in front of their colleagues and esteemed professionals of the ceramics and materials community. This symposium will showcase undergraduate research to encourage innovation and involvement and to highlight the scientific contributions of undergraduate students to ceramics research.

Wednesday, January 22, 2014 – 12:40 p.m. – 1:50 p.m., Coral A

Thursday, January 23, 2014 – 12:40 p.m. – 1:55 p.m., Coral A

Special Thanks to Our Sponsors For Their Generosity



2014 EMA Plenary Speakers

Indian Room

Wednesday, January 22th

8:30 a.m. – 8:45 a.m. Opening Remarks



8:45 a.m. – 9:30 a.m.

James Bray, GE Global Research

Title: Electrical and Electronic Materials for Industrial Applications

Bray attended Georgia Institute of Technology and was graduated with a B.S. degree in physics in 1970. He received an M.S. in physics from the University of Illinois in 1971 and a Ph.D. in physics in 1974. While at Illinois, he worked under Professor John Bardeen on unusual mechanisms for superconductivity. He joined General Electric Global Research after graduation in September, 1974. Until June 1979, he worked as a theoretical condensed matter physicist in support of several programs. Since June 1979, he has held several technical management positions supervising R&D on various physical science topics, biotechnology, electronic materials processing (e.g., molecular beam epitaxy, chemical vapor deposition), electronic devices, electronic packaging, and high-temperature superconductivity. In 1996, he began work in the new GE Six-Sigma quality thrust and eventually acted as manager of the Measurements Systems Program, containing the bulk of the NDE projects. In 1998, he became manager of the new Optical Measurements and Processing Lab, focused on applied optics projects of many types. In 2001, he became Program Manager of the Superconducting Generator Program. He presently is a Chief Scientist within Electrical Technologies and Systems.

Thursday, January 23th



8:30 a.m. – 9:30 a.m.

Jürgen Rödel, Technische Universität Darmstadt, Germany

Title: Lead-free Piezoceramics: History, Achievements, Future

Rödel is a Professor in the Department for Materials and Geoscience at Technische Universität Darmstadt (Germany). He received a Diploma in Materials Science from Universität Erlangen-Nürnberg and a Ph.D. from the University of California at Berkeley. He completed postdoc periods at NIST, Gaithersburg, and TU Hamburg-Harburg. At TU Darmstadt part of his research is focused on processing of lead-free piezoceramics and high-temperature piezoelectrics as well as toughened piezoceramics. Next to the ceramics group, he initiated the center of electric fatigue at TU Darmstadt (SFB595). In Germany he served the Deutsche Forschungsgemeinschaft (DFG) a four-year term as speaker of the review board for Materials Science and a four-year term as regular member of same review board. Rödel is currently member of the grants committee on centers for collaborative studies of the DFG and was member of the selection committee for fellowships for the Alexander-von-Humboldt foundation. He received the DFG research award for young scientists (Heinz-Maier-Leibnitz-Price) in 1992 and the DFG research award for senior scientists (Gottfried Wilhelm Leibniz-Price) in 2009. He authored/coauthored more than 230 refereed publications and 4 patents.

2014 EMA Plenary Speakers

Indian Room

Friday, January 24th



8:30 a.m. – 9:30 a.m.

Joseph V. Mantese, United Technologies Research Center

Title: “Functional Electronic Materials in Integrated Commercial Building and Aerospace Systems

Mantese is a Research Fellow at United Technologies Corporation’s Research Center, specializing in electronic materials, components, sensors, and packaging. Prior to joining UTRC, Dr. Mantese was Department Head of Delphi Research Laboratories (Materials, Components, and Packaging). He was Section Leader at General Motors’ Research and Development Laboratories where he received an R&D 100 Award (1997) for the development of industrial scale plasma ion implantation. He was twice winner of General Motors’ Campbell Award (1990 and 1995) for scientific breakthroughs in materials science, and is an inductee in Delphi Corporation’s Hall of Fame (2000). In 2010 Dr. Mantese received UTRC’s Outstanding Achievement Award for his work related to multi-species chemical sensing. In 2013 he was inducted in the Connecticut Academy of Science and Engineering (CASE). Dr. Mantese is the holder of 33 patents pertaining to electronic materials, sensors, MEMS, and components. He is also the author of over 95 peer reviewed papers, a book on the fundamentals of graded ferroic materials, and three book chapters related to electronic materials and devices.

MEETING REGULATIONS

The American Ceramic Society is a nonprofit scientific organization that facilitates the exchange of knowledge meetings and publication of papers for future reference. The Society owns and retains full right to control its publications and its meetings. The Society has an obligation to protect its members and meetings from intrusion by others who may wish to use the meetings for their own private promotion purpose. Literature found not to be in agreement with the Society’s goals, in competition with Society services or of an offensive nature will not be displayed anywhere in the vicinity of the meeting. Promotional literature of any kind may not be displayed without the Society’s permission and unless the Society provides tables for this purpose. Literature not conforming to this policy or displayed in other than designated areas will be disposed. The Society will not permit unauthorized scheduling of activities during its meeting by any person or group when those activities are conducted at its meeting place in interference with its programs and scheduled activities. The Society does not object to appropriate activities by others during its meetings if it is consulted with regard to time, place, and suitability. Any person or group wishing to conduct any activity at the time and location of the Society meeting must obtain permission from the Executive Director or Director of Meetings, giving full details regarding desired time, place and nature of activity.

During oral sessions conducted during Society meetings, **unauthorized photography, videotaping and audio recording is prohibited.** Failure to comply may result in the removal of the offender from the session or from the remainder of the meeting.

The American Ceramic Society plans to take photographs and video at the conference and reproduce them in educational, news or promotional materials, whether in print, electronic or other media, including The American Ceramic Society’s website. By participating in the conference, you grant The American Ceramic Society the right to use your name and photograph for such purposes. All postings become the property of The American Ceramic Society.

Registration Requirements: Attendance at any meeting of the Society shall be limited to duly registered persons.

Disclaimer: Statements of fact and opinion are the responsibility of the authors alone and do not imply an opinion on the part of the officers, staff or members of The American Ceramic Society. The American Ceramic Society assumes no responsibility for the statements and opinions advanced by the contributors to its publications or by the speakers at its programs; nor does The American Ceramic Society assume any liability for losses or injuries suffered by attendees at its meetings. Registered names and trademarks, etc. used in its publications, even without specific indications thereof, are not to be considered unprotected by the law. Mention of trade names of commercial products does not constitute endorsement or recommendations for use by the publishers, editors or authors.

Final determination of the suitability of any information, procedure or products for use contemplated by any user, and the manner of that use, is the sole responsibility of the user. Expert advice should be obtained at all times when implementation is being considered, particularly where hazardous materials or processes are encountered.

Copyright © 2014. The American Ceramic Society (www.ceramics.org). All rights reserved.

Symposia

The 2014 Organizing Committee:

Steven C. Tidrow, Electronics Division

George A. Rosetti, Jr., Basic Science Division

Haiyan Wang, Electronics Division

S1: Functional and Multifunctional Electroceramics for Commercialization

Organizers: Steven C. Tidrow, The University of Texas – Pan American; Clive Randall, Pennsylvania State University; Shashank Priya, Virginia Polytechnic Institute and State University

S2: Multiferroic Materials and Multilayer Ferroic Heterostructures: Properties and Applications

Organizers: Melanie W. Cole, U.S. Army Research Laboratory; S. Pamir Alpay, University of Connecticut; Dietrich Hesse, Max-Planck-Institut für Mikrostrukturphysik, Germany; Ichiro Takeuchi, University of Maryland

S3: Structure of Emerging Perovskite Oxides: Bridging Length Scales and Unifying Experiment and Theory

Organizers: Igor Levin, NIST, David Cann, Oregon State University; John Daniels, University of South Wales, Australia; Jens Kreisl, LMGP, France; Pamela Thomas, University of Warwick, United Kingdom

S4: LEDs and Photovoltaics—Beyond the Light: Common Challenges and Opportunities

Organizers: Adam M. Scotch, OSRAM SYLVANIA; Erik D. Spörke, Sandia National Laboratories

S5: Structure and Properties of Interfaces in Electronic Materials

Organizers: John Blendell, Purdue University; R. Edwin García, Purdue University; Shen Dillon, University of Illinois; Wayne Kaplan, Technion, Israel; Nicholas Strandwitz, Lehigh University

S6: Thermoelectrics: Defect Chemistry, Doping and Nanoscale Effects

Organizers: Alp Sehirlioglu, Case Western Reserve University; Antoine Maignan, CRISMAT Laboratory, France; Jon Ihlefeld, Sandia National Laboratories; Anke Weidenkaff, EMPA, Switzerland

S7: Computational Design of Electronic Materials

Organizers: R. Prasad, University of Connecticut; Ghanshyam Pilania, Los Alamos National Laboratory; Mina Yoon, Oak Ridge National Laboratory; Blair Tuttle, Penn State University

S8: Advances in Memory Devices

Organizers: Bryan D. Huey, University of Connecticut; John Rodriguez, Texas Instruments

S9: Thin Film Integration and Processing Science

Organizers: Jon Ihlefeld, Sandia National Laboratories; Brady J. Gibbons, Oregon State University; Ronald G. Polcawich, Army Research Laboratory; Jon-Paul Maria, North Carolina State University

S10: Ceramic Composites for Defense Applications

Organizers: Edward P. Gorzkowski, Naval Research Laboratory; Ed Stutz, AFRL/RXPS, Wright-Patterson AFB; Ronald G. Polcawich, US Army Research Laboratory; Mason Wolak, Naval Research Laboratory

S11: Failure: The Greatest Teacher

Organizer: Geoff Brenneka, Sandia National Laboratories

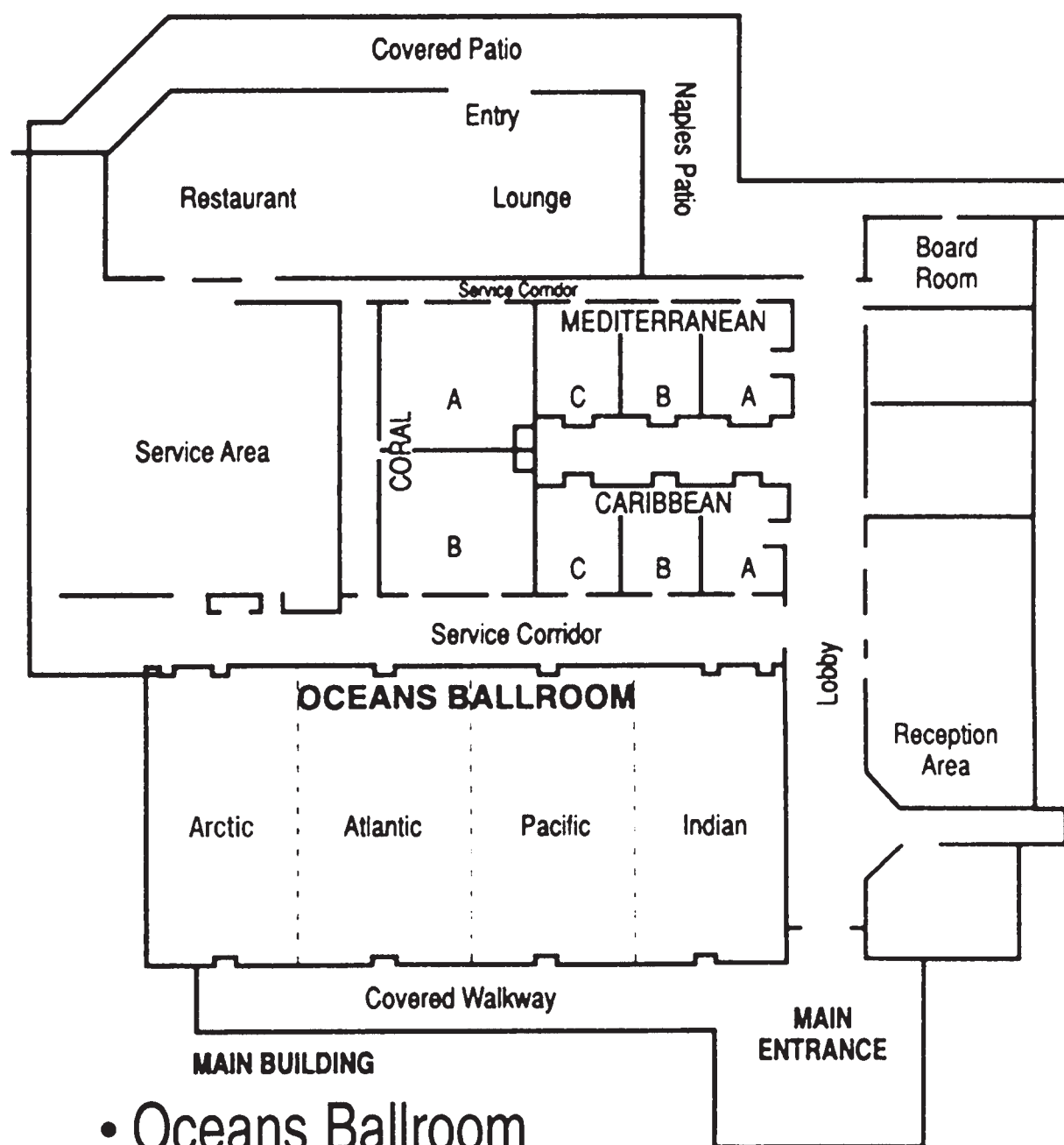
S12: Recent Developments in High-Temperature Superconductivity

Organizers: Haiyan Wang, Texas A&M University; Timothy J. Haugan, The Air Force Research Laboratory; Boris A. Maiorov, Los Alamos National Laboratory; QuanxiJia, Los Alamos National Laboratory

S13: Highlights of Undergraduate Student Research in Basic Science and Electronic Ceramics

Organizers: Aaron Lichtner, PCSA Programming Chair and University of Washington; Derek Miller, PCSA Council Chair and Ohio State University; Geoff Brennecke, Sandia National Laboratories

Doubletree by Hilton Floor Plan



Presenting Author List

Oral Presenters

Name	Date	Time	Room	Page Number	Name	Date	Time	Room	Page Number
A					F				
Akyildiz, H.I.	24-Jan	4:15PM	Coral B	25	Feng, L.	23-Jan	10:15AM	Caribbean B	18
Alberga, M.	24-Jan	11:00AM	Coral A	23	Field, T.	22-Jan	2:45PM	Mediterranean B/C	15
Alkoy, S.	22-Jan	12:00PM	Mediterranean B/C	13	Finkel, P.	22-Jan	4:30PM	Coral B	14
Alpay, S.	23-Jan	2:30PM	Coral A	20	Foley, B.M.	23-Jan	11:30AM	Pacific	17
Amemiya, N.	23-Jan	4:30PM	Mediterranean B/C	21	Foley, B.M.	23-Jan	12:40PM	Coral A	19
Ansell, T.	22-Jan	5:00PM	Coral B	14	Fontanella, J.J.	22-Jan	10:30AM	Mediterranean B/C	12
B					Fox, G.R.	24-Jan	2:00PM	Coral B	25
Bassiri-Gharb, N.	24-Jan	11:00AM	Coral B	23	Funakubo, H.	23-Jan	2:00PM	Indian	19
Batlogg, B.	23-Jan	2:30PM	Mediterranean B/C	21	Fusil, S.	22-Jan	12:00PM	Indian	11
Beanland, R.	22-Jan	11:00AM	Coral B	12	G				
Bellaiche, L.	22-Jan	2:30PM	Indian	14	Ganesh, P.	23-Jan	11:45AM	Coral A	18
Bellaiche, L.	23-Jan	10:00AM	Coral B	17	Garcia, V.	22-Jan	2:00PM	Mediterranean B/C	15
Berbano, S.S.	23-Jan	5:30PM	Pacific	19	Garofalini, S.H.	23-Jan	4:45PM	Caribbean B	20
Berry, H.D.	23-Jan	5:30PM	Caribbean B	20	Garrity, K.F.	22-Jan	12:15PM	Coral A	12
Bhaskaran, H.	22-Jan	4:15PM	Mediterranean B/C	15	Gelbstein, Y.	24-Jan	10:15AM	Coral A	23
Bhave, S.A.	23-Jan	4:30PM	Coral B	21	Govindaraju, N.	22-Jan	5:00PM	Pacific	13
Bishop, S.R.	23-Jan	4:45PM	Pacific	19	Gregg, M.	24-Jan	10:00AM	Indian	22
Bosak, A.	22-Jan	2:30PM	Coral B	14	Guo, H.	23-Jan	1:25PM	Coral A	19
Bosse, J.L.	22-Jan	1:05PM	Coral A	13	Guo, H.	24-Jan	2:30PM	Pacific	24
Bosse, J.L.	22-Jan	4:45PM	Mediterranean B/C	15	Guo, X.	24-Jan	4:00PM	Indian	24
Bray, J.W.	22-Jan	8:45AM	Indian	11	Guorong, L.	22-Jan	12:00PM	Pacific	11
Brennecke, G.L.	24-Jan	12:15PM	Coral B	23	H				
Bridger, K.	22-Jan	11:30AM	Mediterranean B/C	13	Hachmann, J.	23-Jan	10:30AM	Coral A	18
Brown-Shaklee, H.J.	24-Jan	2:30PM	Coral A	24	Haindl, S.	23-Jan	11:30AM	Mediterranean B/C	18
Bullard, T.	23-Jan	5:45PM	Mediterranean B/C	21	Han, J.	22-Jan	4:15PM	Pacific	13
Burch, M.J.	24-Jan	10:45AM	Coral B	23	Hang, T.	23-Jan	4:00PM	Pacific	19
Bux, S.	24-Jan	11:30AM	Coral A	23	Hao, R.	23-Jan	11:30AM	Caribbean B	18
C					Harris, D.T.	24-Jan	10:30AM	Coral B	23
Cantoni, C.	24-Jan	2:00PM	Mediterranean B/C	25	Haugan, T.	23-Jan	5:00PM	Mediterranean B/C	21
Carman, G.	23-Jan	11:15AM	Indian	17	Highland, M.	23-Jan	2:45PM	Coral B	21
Carter, J.J.	23-Jan	11:45AM	Coral B	18	Hill, M.D.	22-Jan	2:45PM	Pacific	13
Chan, C.K.	22-Jan	10:30AM	Caribbean B	12	Hopkins, P.	24-Jan	5:00PM	Coral A	25
Chan, H.M.	23-Jan	10:45AM	Caribbean B	18	Hordagoda, M.	22-Jan	2:30PM	Mediterranean B/C	15
Chang, J.P.	23-Jan	12:00PM	Indian	17	Hordagoda, M.	23-Jan	5:00PM	Indian	20
Chatain, D.	23-Jan	2:00PM	Caribbean B	20	Huang, J.	24-Jan	12:00PM	Mediterranean B/C	23
Chen, A.	24-Jan	12:15PM	Indian	22	Huey, B.	22-Jan	12:15PM	Indian	11
Chen, X.	22-Jan	4:45PM	Pacific	13	Huey, B.D.	22-Jan	11:30AM	Caribbean B	12
Chen, X.	23-Jan	12:00PM	Mediterranean B/C	19	Huey, B.D.	23-Jan	5:30PM	Coral B	21
Cho, S.	24-Jan	4:30PM	Coral A	25	I				
Chu, C.	23-Jan	10:00AM	Mediterranean B/C	18	Ihlefeld, J.	24-Jan	4:45PM	Coral B	25
Civale, L.	24-Jan	4:00PM	Mediterranean B/C	25	Ito, A.	24-Jan	11:00AM	Mediterranean B/C	23
Clem, P.	23-Jan	5:15PM	Coral B	21	J				
Corpuz, R.	24-Jan	4:30PM	Coral B	25	Jahangir, S.	23-Jan	12:55PM	Coral A	19
Cozzan, C.	23-Jan	1:10PM	Coral A	19	Jain, M.	23-Jan	4:00PM	Indian	20
Curtarolo, S.	22-Jan	10:30AM	Coral A	12	Jia, Q.X.	24-Jan	10:30AM	Indian	22
D					Jiao, J.	22-Jan	12:15PM	Pacific	11
Damjanovic, D.	22-Jan	10:30AM	Pacific	11	Jones, J.L.	22-Jan	4:00PM	Coral B	14
Davidson, B.A.	22-Jan	10:00AM	Indian	11	Jones, J.L.	24-Jan	11:30AM	Coral B	23
Dayal, K.	22-Jan	3:00PM	Indian	14	Joyce, D.	22-Jan	12:20PM	Mediterranean B/C	13
Dickey, E.C.	23-Jan	2:00PM	Pacific	19	Jung, J.	23-Jan	10:30AM	Caribbean B	18
Ding, J.	22-Jan	12:50PM	Coral A	13	K				
Ding, J.	23-Jan	5:45PM	Pacific	19	Kakimoto, K.	24-Jan	10:00AM	Pacific	22
Dkhil, B.	22-Jan	2:00PM	Coral B	14	Kalkur, T.	23-Jan	11:45AM	Indian	17
Dong, L.	22-Jan	4:45PM	Coral A	15	Kametani, F.	23-Jan	3:00PM	Mediterranean B/C	21
Donovan, B.F.	23-Jan	1:40PM	Coral A	19	Kaplan, W.D.	23-Jan	3:00PM	Caribbean B	20
Donovan, B.F.	24-Jan	3:00PM	Coral A	24	Kaplan, W.D.	24-Jan	2:30PM	Coral B	25
Dorr, K.	23-Jan	2:30PM	Indian	19	Kato, K.	24-Jan	11:30AM	Pacific	22
Dvorak, C.E.	24-Jan	4:45PM	Coral A	25	Kato, N.	23-Jan	11:15AM	Pacific	17
E					Kennedy, B.J.	23-Jan	10:30AM	Pacific	17
Ehmke, M.C.	22-Jan	4:45PM	Coral B	14	Kikuta, K.	24-Jan	11:15AM	Pacific	22
Eichel, R.A.	23-Jan	11:15AM	Coral B	17	Kim, E.	22-Jan	4:00PM	Pacific	13
Enriquez, E.	24-Jan	4:45PM	Indian	24	Kiss, T.	24-Jan	10:00AM	Mediterranean B/C	23
Evans, J.T.	22-Jan	3:00PM	Mediterranean B/C	15	Koenig, J.D.	24-Jan	9:45AM	Coral A	23
Evans, P.	22-Jan	11:45AM	Indian	11	Kowalski, B.	22-Jan	11:45AM	Pacific	11
					Kumakura, H.	23-Jan	2:00PM	Mediterranean B/C	21

Oral Presenters

Name	Date	Time	Room	Page Number	Name	Date	Time	Room	Page Number
Kumar, N.	23-Jan	4:30PM	Pacific	19	S				
Kutnjak, Z.	23-Jan	11:00AM	Pacific	17	Sachet, E.	23-Jan	4:00PM	Coral B	21
Kwon, Y.	22-Jan	12:00PM	Caribbean B	12	Sbrockey, N.M.	24-Jan	3:00PM	Indian	24
L					Sbrockey, N.M.	24-Jan	4:15PM	Indian	24
Lee, H.	24-Jan	2:30PM	Indian	24	Scheffler, M.	22-Jan	10:00AM	Coral A	12
Lenef, A.	22-Jan	10:00AM	Caribbean B	12	Scott, K.J.	24-Jan	2:45PM	Coral A	24
Levin, I.	23-Jan	2:30PM	Pacific	19	Sehirlioglu, A.	22-Jan	11:00AM	Pacific	11
Li, Q.	23-Jan	10:30AM	Mediterranean B/C	18	Seidel, J.	22-Jan	11:15AM	Indian	11
Lightfoot, P.	22-Jan	12:00PM	Coral B	12	Selvamanickam, V.	24-Jan	10:30AM	Mediterranean B/C	23
Liu, V.	23-Jan	11:15AM	Caribbean B	18	Sharma, A.	23-Jan	12:00PM	Pacific	17
Liu, X.	24-Jan	11:00AM	Pacific	22	Sharma, V.	23-Jan	11:00AM	Coral A	18
Lookman, T.	22-Jan	11:45AM	Coral A	12	Shelton, C.T.	23-Jan	2:30PM	Coral B	21
Loureiro, J.	24-Jan	4:15PM	Coral A	24	Siegel, D.	23-Jan	11:15AM	Coral A	18
Loureiro, J.	24-Jan	5:15PM	Coral A	25	Sinclair, D.	24-Jan	2:00PM	Coral A	24
Luo, J.	23-Jan	2:30PM	Caribbean B	20	Singh, D.J.	24-Jan	12:00PM	Coral A	23
Lynch, C.S.	23-Jan	11:00AM	Indian	17	Small, L.J.	24-Jan	3:15PM	Coral B	25
M					Song, S.	22-Jan	4:30PM	Pacific	13
Mackey, J.	24-Jan	4:00PM	Coral A	24	Spanier, J.	24-Jan	4:30PM	Indian	24
Maier, R.	22-Jan	1:20PM	Coral A	13	Spoerke, E.	22-Jan	12:15PM	Caribbean B	12
Maier, R.	23-Jan	10:30AM	Coral B	17	Spoerke, E.	23-Jan	5:15PM	Pacific	19
Maignan, A.	24-Jan	3:45PM	Coral A	24	Spoerke, E.	24-Jan	4:00PM	Coral B	25
Malic, B.	23-Jan	5:00PM	Coral B	21	Srinivasan, G.	23-Jan	11:30AM	Indian	17
Mantese, J.	24-Jan	8:30AM	Indian	22	Starr, J.D.	23-Jan	4:30PM	Indian	20
Maqbool, M.	23-Jan	12:00PM	Caribbean B	18	Stemmer, S.	24-Jan	11:00AM	Indian	22
May, S.	23-Jan	3:00PM	Indian	20	Strandwitz, N.C.	23-Jan	4:30PM	Caribbean B	20
Meier, D.	23-Jan	4:15PM	Indian	20	Sumpter, B.	23-Jan	10:00AM	Coral A	18
Mendez, J.E.	24-Jan	12:00PM	Coral B	23	Sun, N.	23-Jan	10:00AM	Indian	17
Mitic, V.	23-Jan	12:15PM	Pacific	17	T				
Moballeggh, A.	22-Jan	1:35PM	Coral A	13	Tagantsev, A.K.	22-Jan	2:00PM	Indian	14
Mueller, T.	22-Jan	11:00AM	Coral A	12	Takeuchi, I.	23-Jan	12:15PM	Indian	17
Mukherjee, D.	23-Jan	4:45PM	Indian	20	Tan, X.	22-Jan	11:30AM	Coral B	12
N					Tarantini, C.	24-Jan	1:30PM	Mediterranean B/C	25
Nahm, S.	24-Jan	1:30PM	Pacific	24	Terasaki, I.	24-Jan	3:15PM	Coral A	24
Nakhmanson, S.	23-Jan	4:00PM	Coral A	20	Thomas, P.A.	24-Jan	11:45AM	Pacific	22
Newman, N.	23-Jan	10:30AM	Indian	17	Tidrow, S.C.	22-Jan	5:15PM	Coral B	14
Nino, J.C.	24-Jan	12:00PM	Indian	22	Tomar, M.	23-Jan	11:45AM	Pacific	17
O					Tran, H.D.	22-Jan	4:30PM	Coral A	15
Okazaki, H.	23-Jan	11:00AM	Mediterranean B/C	18	Trolier-McKinstry, S.	24-Jan	2:00PM	Pacific	24
P					Tsurumi, T.	23-Jan	10:00AM	Pacific	17
Panasuk, G.Y.	23-Jan	5:30PM	Mediterranean B/C	21	U				
Pantelides, S.T.	22-Jan	4:00PM	Coral A	14	Uberuaga, B.P.	23-Jan	4:45PM	Coral A	21
Pardo, E.	23-Jan	4:00PM	Mediterranean B/C	21	V				
Pavunny, S.P.	22-Jan	3:15PM	Pacific	13	Vailionis, A.	23-Jan	2:00PM	Coral B	21
Perry, J.W.	22-Jan	10:00AM	Mediterranean B/C	12	Valanoor, N.	22-Jan	10:30AM	Indian	11
Pham, A.	23-Jan	4:30PM	Coral A	21	Valanoor, N.	24-Jan	10:00AM	Coral B	23
Ponomareva, I.	22-Jan	4:00PM	Indian	14	Valone, S.	23-Jan	3:00PM	Coral A	20
Post, E.	22-Jan	11:30AM	Pacific	11	Van de Walle, C.G.	22-Jan	2:30PM	Coral A	14
Prasertpalichat, S.	23-Jan	12:00PM	Coral B	18	Varghese, D.	22-Jan	3:15PM	Mediterranean B/C	15
R					W				
Ramanathan, S.	24-Jan	2:00PM	Indian	24	Wada, S.	23-Jan	11:45AM	Caribbean B	18
Randall, C.	23-Jan	11:00AM	Coral B	17	Wang, C.	22-Jan	11:30AM	Coral A	12
Ranjan, R.	22-Jan	10:30AM	Coral B	12	Wang, H.	24-Jan	5:00PM	Mediterranean B/C	25
Reaney, I.M.	22-Jan	10:00AM	Coral B	12	Watanabe, M.	23-Jan	4:15PM	Pacific	19
Reaney, I.M.	22-Jan	11:00AM	Indian	11	Wei, K.	24-Jan	10:45AM	Coral A	23
Reaney, I.M.	22-Jan	2:00PM	Pacific	13	Weidenkaff, A.	24-Jan	11:15AM	Coral A	23
Reimanis, I.	23-Jan	10:00AM	Caribbean B	18	Weiss, J.D.	24-Jan	4:30PM	Mediterranean B/C	25
Robles-Dutenhefner, P.	24-Jan	5:00PM	Indian	24	West, A.R.	23-Jan	3:00PM	Pacific	19
Rodriguez Pinilla, O.	23-Jan	5:15PM	Caribbean B	20	Whatmore, R.W.	24-Jan	11:45AM	Indian	22
Rodriguez, J.	22-Jan	5:15PM	Mediterranean B/C	15	Wilke, R.H.	24-Jan	2:45PM	Coral B	25
Roedel, J.	23-Jan	8:30AM	Indian	16	Windl, W.	22-Jan	3:00PM	Coral A	14
Rohrer, G.	23-Jan	4:00PM	Caribbean B	20	Wolak, M.A.	22-Jan	11:00AM	Mediterranean B/C	13
Rondinelli, J.	22-Jan	4:15PM	Indian	14	Wu, J.	24-Jan	11:30AM	Mediterranean B/C	23
Rossetti, G.A.	22-Jan	10:00AM	Pacific	11	Wu, M.	24-Jan	3:15PM	Indian	24
Rossetti, G.A.	23-Jan	2:00PM	Coral A	20					
Ruosi, A.	24-Jan	3:00PM	Mediterranean B/C	25					

Presenting Author List

Oral Presenters

Name	Date	Time	Room	Page Number	Name	Date	Time	Room	Page Number
Xi, X.	24-Jan	2:30PM	Mediterranean B/C	25	Zhang, S.	24-Jan	10:30AM	Pacific	22
					Zhang, Y.	24-Jan	12:15PM	Pacific	22
					Zollner, S.	24-Jan	11:30AM	Indian	22
Yang, H.	24-Jan	11:15AM	Indian	22	Zou, G.	23-Jan	3:15PM	Coral B	21
Yang, K.	22-Jan	4:30PM	Indian	14	Zubia, D.	22-Jan	11:00AM	Caribbean B	12
Yang, Y.	22-Jan	2:30PM	Pacific	13	Zunger, A.	22-Jan	2:00PM	Coral A	14
Yasui, S.	22-Jan	11:30AM	Indian	11					
Yokota, H.	22-Jan	3:00PM	Coral B	14					
Younis, A.	22-Jan	5:00PM	Mediterranean B/C	15					

Poster Presenters

Name	Date	Time	Room	Page Number	Name	Date	Time	Room	Page Number
Anders, J.	22-Jan	5:30PM	Atlantic/Arctic	16	Lin, F.	22-Jan	5:30PM	Atlantic/Arctic	16
Bin-Omran, S.H.	22-Jan	5:30PM	Atlantic/Arctic	15	Luo, H.	22-Jan	5:30PM	Atlantic/Arctic	15
Bishop, S.R.	22-Jan	5:30PM	Atlantic/Arctic	15	Mackey, J.	22-Jan	5:30PM	Atlantic/Arctic	16
Choi, H.	22-Jan	5:30PM	Atlantic/Arctic	16	Maqbool, M.	22-Jan	5:30PM	Atlantic/Arctic	16
Cortes-Pena, A.Y.	22-Jan	5:30PM	Atlantic/Arctic	16	Mensur-Alkoy, E.	22-Jan	5:30PM	Atlantic/Arctic	15
Gao, L.	22-Jan	5:30PM	Atlantic/Arctic	16	Mitic, V.	22-Jan	5:30PM	Atlantic/Arctic	15
Gelbstein, Y.	22-Jan	5:30PM	Atlantic/Arctic	16	Muñiz-Serrato, O.	22-Jan	5:30PM	Atlantic/Arctic	16
Gorzkowski, E.	22-Jan	5:30PM	Atlantic/Arctic	16	Ouyang, J.	22-Jan	5:30PM	Atlantic/Arctic	16
Han, Y.	22-Jan	5:30PM	Atlantic/Arctic	16	Panasyuk, G.Y.	22-Jan	5:30PM	Atlantic/Arctic	16
Haugan, T.	22-Jan	5:30PM	Atlantic/Arctic	16	Park, C.	22-Jan	5:30PM	Atlantic/Arctic	15
Haugan, T.J.	22-Jan	5:30PM	Atlantic/Arctic	16	Park, K.	22-Jan	5:30PM	Atlantic/Arctic	16
Kakemoto, H.	22-Jan	5:30PM	Atlantic/Arctic	16	Seshadri, D.	22-Jan	5:30PM	Atlantic/Arctic	16
Kalyani, A.K.	22-Jan	5:30PM	Atlantic/Arctic	15	Shinoda, R.	22-Jan	5:30PM	Atlantic/Arctic	15
Kato, K.	22-Jan	5:30PM	Atlantic/Arctic	16	Song, D.	22-Jan	5:30PM	Atlantic/Arctic	15
Khansur, N.H.	22-Jan	5:30PM	Atlantic/Arctic	16	Sumang, R.	22-Jan	5:30PM	Atlantic/Arctic	15
Kim, D.	22-Jan	5:30PM	Atlantic/Arctic	16	Wang, G.	22-Jan	5:30PM	Atlantic/Arctic	16
Kim, J.	22-Jan	5:30PM	Atlantic/Arctic	16	Whatmore, R.W.	22-Jan	5:30PM	Atlantic/Arctic	15
Kim, S.	22-Jan	5:30PM	Atlantic/Arctic	16	Woo, M.	22-Jan	5:30PM	Atlantic/Arctic	15
Kutnjak, Z.	22-Jan	5:30PM	Atlantic/Arctic	15	Xu, Y.	22-Jan	5:30PM	Atlantic/Arctic	15
Li, E.	22-Jan	5:30PM	Atlantic/Arctic	15	Yuan, Y.	22-Jan	5:30PM	Atlantic/Arctic	15
Li, Z.	22-Jan	5:30PM	Atlantic/Arctic	16	Zhu, T.	22-Jan	5:30PM	Atlantic/Arctic	16
Liau, L.C.	22-Jan	5:30PM	Atlantic/Arctic	16					

Wednesday, January 22, 2014

Plenary Session I

Room: Indian

Session Chair: Steven Tidrow, University of Texas - Pan American

8:30 AM

Opening Remarks

8:45 AM

(EMA-001-2014) Electrical and Electronic Materials for Industrial Applications (Invited)

J. W. Bray*, General Electric Global Research, USA

9:30 AM

Break

S1: Functional and Multifunctional Electroceramics for Commercialization

Ferroelectric Composition Design and Property Characterization

Room: Pacific

Session Chair: Sahn Nahm, Korea University

10:00 AM

(EMA-S1-001-2014) Influence of Thermal History on Structure-Property Relations in Lead Zirconate Titanate Ceramics (Invited)

C. Chung, G. A. Rossetti*, University of Connecticut, USA

10:30 AM

(EMA-S1-002-2014) Anelastic, dielectric and mixed electro-mechanical response in perovskite materials (Invited)

D. Damjanovic*, A. Biancoli, S. Hashemi Zadeh, Swiss Federal Institute of Technology - EPFL, Switzerland; T. Rojac, H. Ursic, Jozef Stefan Institute, Slovenia

11:00 AM

(EMA-S1-003-2014) High Temperature Ferroelectrics for Actuators: Recent Developments and Challenges (Invited)

A. Sehirlioglu*, Case Western Reserve University, USA

11:30 AM

(EMA-S1-004-2014) Characterization of Bariumtitanate by Thermal Analysis and Thermophysical Properties Techniques

E. Post*, E. Fueglein, NETZSCH Geraetebau GmbH, Germany; E. Lim, NETZSCH Instruments N.A., LLC, USA

11:45 AM

(EMA-S1-005-2014) Effects of dopants on depoling temperature in modified BiScO₃ - PbTiO₃

B. Kowalski*, A. Sehirlioglu, Case Western Reserve University, USA

12:00 PM

(EMA-S1-006-2014) Dielectric Relaxation of Pb(Mg_{1/3}Nb_{2/3})O₃-PbTiO₃ Relaxor Ferroelectric Ceramics in wide temperatures

L. Guorong*, L. Huang, W. Zhao, J. Zeng, L. Zheng, Shanghai Institute of Ceramics, Chinese Academy of Sciences, China; X. Xiong, Zhongshan University, China; A. Kassiba, Université du Maine, Avenue O. Messiaen, 72085 Le Mans, Cedex 09, France

12:15 PM

(EMA-S1-007-2014) The crystal growth and properties of PIMNT ternary single crystals

J. Jiao*, J. Chen, X. Li, X. Wang, S. Wang, X. Zhao, H. Luo, The Shanghai Institute of Ceramics, Chinese Academy of Sciences, China

S2: Multiferroic Materials and Multilayer Ferroic Heterostructures: Properties and Applications

Bismuth Ferrite

Room: Indian

Session Chair: Ichiro Takeuchi, University of Maryland

10:00 AM

(EMA-S2-001-2014) Magnetoelectric Control of Exchange Coupling in Monodomain BiFeO₃ Heterostructures (Invited)

B. A. Davidson*, W. Saenrang, S. Ryu, J. P. Podkaminer, D. Lee, J. Frederick, T. Kim, S. Baek, M. S. Rzchowski, University of Wisconsin, USA; J. W. Freeland, Argonne National Laboratory, USA; C. Eom, University of Wisconsin, USA

10:30 AM

(EMA-S2-002-2014) Phase evolution and structure-property correlations in rare-earth substituted bismuth ferrite thin films (Invited)

N. Valanoor*, University of New South Wales, Australia

11:00 AM

(EMA-S2-003-2014) RE-doped BiFeO₃: a critical appraisal of their potential applications (Invited)

I. M. Reaney*, University of Sheffield, United Kingdom

11:15 AM

(EMA-S2-004-2014) Domain walls and phase boundaries - new nanoscale functional elements in complex oxides (Invited)

J. Seidel*, The University of New South Wales, Australia

11:30 AM

(EMA-S2-005-2014) Piezoresponse behavior at a Morphotropic Phase Boundary in (Bi,Sm)FeO₃ Films (Invited)

S. Yasui*, Y. Ehara, T. Shiraishi, T. Shimizu, H. Funakubo, M. Itoh, Tokyo Institute of Technology, Japan; Y. Imai, H. Tajiri, Japan Synchrotron Radiation Research Institute/SPRING-8, Japan; O. Sakata, National Institute for Materials Science/SPRING-8, Japan; I. Takeuchi, University of Maryland, USA

11:45 AM

(EMA-S2-006-2014) Piezoelectric Nonlinearity and Dynamics of Electric-Field-Driven Structural Phase Transitions in Multiferroics (Invited)

M. Cosgriff, P. Chen, University of Wisconsin-Madison, USA; J. Jo, Gwangju Institute of Science and Technology, Republic of Korea; Z. Chen, L. Chen, Nanyang Technological University, Singapore; P. Evans*, University of Wisconsin-Madison, USA

12:00 PM

(EMA-S2-007-2014) Ferroelectric field effect with supertetragonal BiFeO₃

S. Fusil*, V. Garcia, Unité Mixte CNRS/Thales, France; H. Yamada, National Institute of Advanced Industrial Science and Technology (AIST), Japan; M. Marinova, Laboratoire de Physique des Solides, France; S. Boyn, Unité Mixte CNRS/Thales, France; A. Gloter, Laboratoire de Physique des Solides, France; J. Villegas, M. Bibes, A. Barthelemy, Unité Mixte CNRS/Thales, France

12:15 PM

(EMA-S2-008-2014) Domain and Domain Boundary Influences on switching for Multiferroics (Invited)

L. Ye, J. Leveille, A. McDannald, B. Moffitt, N. Polomoff, M. Jain, University of Connecticut, USA; J. Ihlefeld, Sandia National Laboratories, USA; B. Huey*, University of Connecticut, USA

S3: Structure of Emerging Perovskite Oxides: Bridging Length Scales and Unifying Experiment and Theory

Local Structure and Phase Transitions

Room: Coral B

Session Chair: Igor Levin, National Institute of Standards and Technology

10:00 AM

(EMA-S3-001-2014) Critical Issues in Ferroelectrics: a TEM perspective (Invited)

I. M. Reaney*, University of Sheffield, United Kingdom

10:30 AM

(EMA-S3-002-2014) Local structural disorder and its influence on the average global structure and ferroelectric properties of lead-free $\text{Na}_1/2\text{Bi}_{1/2}\text{TiO}_3$ (Invited)

R. Ranjan*, B. Rao, Indian Institute of Science Bangalore, India

11:00 AM

(EMA-S3-003-2014) Scale-dependent symmetries in $\text{Na}_0.5\text{Ba}_{0.5}\text{TiO}_3$ (Invited)

R. Beanland*, D. Keeble, University of Warwick, United Kingdom; S. Gorfman, Universitat Siegen, Germany; P. Thomas, University of Warwick, United Kingdom

11:30 AM

(EMA-S3-004-2014) Perovskite Phases and Their Transformations in Lead-Free Piezoelectric Ceramics (Invited)

H. Guo, C. Ma, X. Tan*, Iowa State Univ, USA

12:00 PM

(EMA-S3-005-2014) Unusual Phase Behaviour in NaNbO_3 and its Derivatives (Invited)

P. Lightfoot*, University of St Andrews, United Kingdom

S4: LEDs and Photovoltaics - Beyond the Light: Common Challenges and Opportunities

LED and PV Materials

Room: Caribbean B

Session Chairs: Adam Scotch, OSRAM SYLVANIA, Inc.; Erik Spoerke, Sandia National Laboratories

10:00 AM

(EMA-S4-001-2014) Scattering and Light Extraction from Bulk Polycrystalline Ceramic Phosphors (Invited)

A. Lenef*, J. Kelso, A. Piquette, OSRAM SYLVANIA Inc, USA

10:30 AM

(EMA-S4-002-2014) Spatially Resolved Chemical and Electronic Structure of Thin-Film Photovoltaics (Invited)

C. K. Chan*, G. L. Kellogg, Sandia National Laboratories, USA; L. Mansfield, R. Noufi, National Renewable Energy Laboratory, USA

11:00 AM

(EMA-S4-003-2014) Experimental and Simulated Selective-Area Growth of CdTe (Invited)

D. Zubia*, B. A. Aguirre, R. Ordonez, F. Anwar, University of Texas, El Paso, USA; H. Prieto, C. Sanchez, M. T. Salazar, A. A. Pimentel, J. R. Michael, Sandia National Laboratories, USA; X. Zhou, University of Texas, El Paso, USA; J. C. McClure, G. N. Nielson, J. L. Cruz-Campa, Sandia National Laboratories, USA

11:30 AM

(EMA-S4-004-2014) Nanoscale Mapping of Performance in Photovoltaics (Invited)

Y. Kutes, J. Bosse, A. Lluberes, University of Connecticut, USA; J. Cruz-Campa, E. D. Spoerke, Sandia National Labs, USA; B. D. Huey*, University of Connecticut, USA

12:00 PM

(EMA-S4-005-2014) Initial Stage of Electrodeposited Copper on Molybdenum substrate for Solar Application

Y. Kwon*, S. Chun, S. Cho, H. Cho, Sungkyunkwan University, Republic of Korea

12:15 PM

(EMA-S4-006-2014) Supramolecular Building Blocks for Hybrid Photovoltaics

E. Spoerke*, D. Gough, J. Wheeler, K. Leong, V. Stavila, M. Foster, T. Lambert, M. Allendorf, Sandia National Laboratories, USA

S7: Computational Design of Electronic Materials

Materials Informatics

Room: Coral A

Session Chair: R. Ramprasad, University of Connecticut

10:00 AM

(EMA-S7-001-2014) Big Data of Materials Science from First Principles — Critical Next Steps (Invited)

M. Scheffler*, Fritz Haber Institute of Max Planck Society, Germany

10:30 AM

(EMA-S7-002-2014) The high-throughput highway to computational materials design (Invited)

S. Curtarolo*, M. Buongiorno Nardelli, Duke University, USA; N. Mingo, J. Carrete, CEA, France; K. Yang, Duke University, USA

11:00 AM

(EMA-S7-003-2014) The origins of hole traps in hydrogenated nanocrystalline and amorphous silicon revealed through machine learning (Invited)

T. Mueller*, Johns Hopkins University, USA; E. Johlin, J. C. Grossman, Massachusetts Institute of Technology, USA

11:30 AM

(EMA-S7-004-2014) Accelerating Materials Property Predictions Using Machine Learning

C. Wang*, University of Connecticut, USA; G. Pilania, Los Alamos National Laboratory, USA; R. Ramprasad, University of Connecticut, USA

11:45 AM

(EMA-S7-005-2014) Information-driven approaches to materials discovery (Invited)

T. Lookman*, Los Alamos National Laboratory, USA

12:15 PM

(EMA-S7-006-2014) First Principles Search for Functional ABC Materials

K. F. Garrity*, K. M. Rabe, D. Vanderbilt, Rutgers University, USA

S10: Ceramic Composites for Defense Applications

Nano, Piezo and Bio-derived Composites

Room: Mediterranean B/C

Session Chair: Edward Gorzkowski, Naval Research Laboratory

10:00 AM

(EMA-S10-001-2014) Nanocomposite and Hybrid Materials for Efficient High Energy Density Capacitors (Invited)

J. W. Perry*, Georgia Tech, USA

10:30 AM

(EMA-S10-002-2014) Electrical Properties of Nanodielectrics Consisting of Polymers Containing Oxide Nanoparticles (Invited)

J. J. Fontanella*, J. F. Lomax, C. A. Edmondson, M. C. Wintersgill, U. S. Naval Academy, USA; M. A. Wolak, J. P. Calame, U. S. Naval Research Laboratory, USA; M. A. Westgate, U. S. Naval Academy, USA

11:00 AM

(EMA-S10-003-2014) Interface-modified Multilayer Polymer Films for High Energy Density Capacitors (Invited)

M. A. Wolak*, J. S. Shirk, US Naval Research Laboratory, USA; M. Mackey, Z. Zhou, E. Baer, Case Western Reserve University, USA

11:30 AM

(EMA-S10-004-2014) Performance of Wide-Temperature, High-Power Ceramic Filter Capacitors (Invited)

K. Bridger*, A. V. Cooke, D. Kohlhafer, E. Passaro, Activesignaltech.com, USA; W. Schulze, R. Dempsey, S. Arrasmith, Alfred University, USA; J. Weigner, Lockheed Martin, USA; F. Duva, Novacap, USA

12:00 PM

(EMA-S10-005-2014) Continuous Fabrication of Piezoceramic Fibers and Ribbons by a Novel Alginate Gelation Method and Electrical Properties of 1-3 Piezocomposites

S. Alkoy*, Gebze Institute of Technology, Turkey; E. Mensur-Alkoy, Maltepe University, Turkey; R. Olukent, S. Dursun, Gebze Institute of Technology, Turkey; A. Berksoy-Yavuz, ENS Piezodevices Ltd., Turkey; M. Kaya, Gebze Institute of Technology, Turkey

12:20 PM

(EMA-S10-006-2014) DNA based Bio-Polymer Hybrid Thin Films for Capacitor Applications

D. Joyce*, AFRL, USA

S13: Highlights of Undergraduate Student Research in Basic Science and Electronic Ceramics

Student Finalist Presentations, Wednesday

Room: Coral A

Session Chair: Geoff Brennecka, Sandia National Laboratories

12:40 PM

Introduction

Geoff Brennecka, Sandia National Laboratories

12:50 PM

(EMA-S13-001-2014) Conductivity in nanostructured ceria: space- and time- resolved mapping of ionic dynamics

J. Ding*, Georgia Institute of Technology, USA; E. Strelcov, S. Kalinin, Oak Ridge National Laboratory, USA; N. Bassiri-Gharb, Georgia Institute of Technology, USA

1:05 PM

(EMA-S13-002-2014) Crystallization Kinetics of Phase Change Memory Films by Atomic Force Microscopy

J. L. Bosse*, B. D. Huey, University of Connecticut, USA; I. Grishin, O. V. Kolosov, Institute of Materials Science, United Kingdom

1:20 PM

(EMA-S13-003-2014) Investigation of Defect Dipole Kinetics in the Ferroelectric and Paraelectric Phases of Acceptor Doped BaTiO₃ Single Crystals

R. Maier*, T. Pomorski, P. Lenahan, C. Randall, The Pennsylvania State University, USA

1:35 PM

(EMA-S13-004-2014) Investigation of the nature and mechanism of resistive switching in TiO_{2-x}

A. Moballeggh*, E. C. Dickey, NC State University, USA

S1: Functional and Multifunctional Electroceramics for Commercialization

Dielectrics: Design and Synthesis

Room: Pacific

Session Chairs: Igor Levin, National Institute of Standards and Technology; Anthony West, University of Sheffield

2:00 PM

(EMA-S1-008-2014) Commercialising Research: Materials Discovery to Prototype Devices (Invited)

I. M. Reaney*, University of Sheffield, United Kingdom

2:30 PM

(EMA-S1-009-2014) Phase transition and strain glass in (1-x)(Bi^{1/2}Na^{1/2})TiO₃-xBaTiO₃ (x < 7%)

Y. Yao, Y. Yang*, Xi'an Jiaotong University, China; X. Tan, Iowa State University, USA; X. Ren, Xi'an Jiaotong University, China

2:45 PM

(EMA-S1-010-2014) Crystal Chemical Strategies for Reducing the Dielectric Loss for Commercially Significant Polycrystalline Temperature-Compensated Microwave Dielectric Oxides using "Non-Critical" Materials (Invited)

M. D. Hill*, Trans-Tech Inc., USA

3:15 PM

(EMA-S1-011-2014) Thin Films of High-k Dielectric Material LaGdO₃ for Logic and Memory Devices

S. P. Pavunny*, University of Puerto Rico, USA; J. F. Scott, University of Cambridge, United Kingdom; R. S. Katiyar, University of Puerto Rico, USA

3:30 PM

Break

4:00 PM

(EMA-S1-012-2014) Affecting Factors on the Microwave Dielectric Properties of CaMgSi₂O₆ Glass-Ceramics

Y. Eoh, B. Choi, E. Kim*, Kyonggi University, Republic of Korea

4:15 PM

(EMA-S1-013-2014) Synthesis of BaTiO₃ Nanopowders using TiO₂ Nanoparticles by Hydrothermal Method

J. Han*, M. Joung, J. Kim, Y. Lee, S. Nahm, Korea University, Republic of Korea; Y. Choi, Samsung Chemicals Nanotechnology, Material R&D Team, Republic of Korea

4:30 PM

(EMA-S1-014-2014) Effects of Bi(Mg^{1/2}Ti^{1/2})O₃ addition on the nanostructure and dielectric properties of modified SrTiO₃ by LPP(Liquid Phase Precursor) method

S. Song*, SungKyunKwan Univ., Republic of Korea

4:45 PM

(EMA-S1-015-2014) Enhanced Dielectric and Ferroelectric Characteristics in Ba_{1-x}CaxTiO₃ Ceramics

X. Chen*, X. Zhu, W. Zhang, Zhejiang University, China

5:00 PM

(EMA-S1-016-2014) Nanocrystalline Diamond as a Dielectric Material

R. Singh, N. Govindaraju*, Oklahoma State University, USA

S2: Multiferroic Materials and Multilayer Ferroic Heterostructures: Properties and Applications

Theory and Modeling

Room: Indian

Session Chair: Pamir Alpay, IMS, University of Connecticut

2:00 PM

(EMA-S2-009-2014) Antiferroelectricity and Antiferroelectric Domain Walls (Invited)

A. K. Tagantsev*, Swiss Federal Institute of Technology, EPFL, Switzerland; A. K. Tagantsev, Ioffe Physical Technical Institute, Russian Federation

2:30 PM

(EMA-S2-010-2014) Switching Magnetic Ordering by an Electric field in Multiferroics (Invited)

L. Bellaiche*, University of Arkansas, USA

3:00 PM

(EMA-S2-011-2014) Multiscale Atomistics for Defects in Electronic Materials (Invited)

K. Dayal*, J. Marshall, Carnegie Mellon University, USA

3:30 PM

Break

4:00 PM

(EMA-S2-012-2014) Dynamics of the soft mode in ferroelectric PbTiO₃ from atomistic simulations (Invited)

I. Ponomareva*, University of South Florida, USA

4:15 PM

(EMA-S2-013-2014) Theoretical Design Strategies for New Multiferroics (Invited)

J. Rondinelli*, Drexel University, USA

4:30 PM

(EMA-S2-014-2014) Electromagnetic Modeling of Microwave-Assisted Low-Temperature Growth of Thin Films in Solution (Invited)

K. Yang*, B. Rejee-Jayan, K. Harrison, C. Wang, University of Texas at Austin, USA; M. Cole, U.S. Army Research Laboratory, USA; A. Manthiram, A. E. Yilmaz, University of Texas at Austin, USA

S3: Structure of Emerging Perovskite Oxides: Bridging Length Scales and Unifying Experiment and Theory

Local Structure and Ferroelectric Domains

Room: Coral B

Session Chairs: Pamela Thomas, University of Warwick; David Cann, University of Oregon

2:00 PM

(EMA-S3-006-2014) The physics of relaxors in relation with other complex systems (Invited)

S. Prosandeev, Laboratoire SPMS, Ecole Centrale Paris - CNRS, France; S. Prosandeev, Physics Department and Institute for Nanoscience and Engineering, University of Arkansas, USA; B. Dkhil*, Laboratoire SPMS, Ecole Centrale Paris - CNRS, France

2:30 PM

(EMA-S3-007-2014) Diffuse scattering in lead-containing perovskites (Invited)

A. Bosak*, European Synchrotron Radiation Facility, France; D. Chernyshov, Swiss-Norwegian Beam Lines at the ESRF, France; R. Burkovsky, M. Kirsch, European Synchrotron Radiation Facility, France; S. Vakhrushev, Ioffe Physico-Technical Institute, Russian Federation

3:00 PM

(EMA-S3-008-2014) Local structure analysis on complex PbZr_{1-x}Ti_xO₃ (Invited)

H. Yokota*, Chiba University, Japan; N. Zhang, Simon Fraser University, Canada; P. Thomas, University of Warwick, United Kingdom; M. Glazer, University of Oxford, United Kingdom

3:30 PM

Break

4:00 PM

(EMA-S3-009-2014) The role of domain wall displacement in achieving superior properties of lead-free ceramics: insights from in situ diffraction (Invited)

J. L. Jones*, North Carolina State University, USA

4:30 PM

(EMA-S3-010-2014) Ferroelectric phase transitions and large energy conversion in domain engineered ferroic crystals (Invited)

P. Finkel*, A. Amin, Naval Undersea Warfare Center, USA; S. Lofland, Rowan University, USA

4:45 PM

(EMA-S3-011-2014) Correlation of Domain Processes and Properties in Future Piezoceramics

M. C. Ehmke*, J. Blendell, Purdue University, USA; K. J. Bowman, Illinois Institute of Technology, USA

5:00 PM

(EMA-S3-012-2014) Depolarization Mechanisms in High Temperature Piezoceramics

T. Ansell*, D. Cann, Oregon State University, USA

5:15 PM

(EMA-S3-013-2014) Bridging Length Scales in the Design of Advanced Perovskite Materials

S. C. Tidrow*, University of Texas - Pan American, USA

S7: Computational Design of Electronic Materials

Design of Materials with Novel Architectures

Room: Coral A

Session Chairs: Tim Mueller, Johns Hopkins University; Blas Ueberuaga, Los Alamos National Laboratory

2:00 PM

(EMA-S7-007-2014) The Inverse Problem in Nano science and in materials theory: (Invited)

A. Zunger*, University of Colorado, Boulder, USA

2:30 PM

(EMA-S7-008-2014) Controlling the Conductivity of Two-Dimensional Conductors (Invited)

C. G. Van de Walle*, H. Peelaers, University of California, USA

3:00 PM

(EMA-S7-009-2014) First-Principles Assisted Design of Molecular Scale Graphane Analogues (Invited)

W. Windl*, O. D. Restrepo, J. Goldberger, The Ohio State University, USA

3:30 PM

Break

4:00 PM

(EMA-S7-010-2014) Density functional theory and microscopy: A combination tool for the design of new materials (Invited)

S. T. Pantelides*, Vanderbilt University, USA; S. J. Pennycook, Oak Ridge National Laboratory, USA

4:30 PM

(EMA-S7-011-2014) First-principles design of organo-Sn polymeric dielectrics

H. D. Tran*, A. Kumar M.K., C. Wang, A. Baldwin, R. Ma, G. Sotzing, R. Ramprasad, Institute of Materials Science, University of Connecticut, USA

4:45 PM

(EMA-S7-012-2014) Theoretical Study on Strain Induced Variations in Electronic Properties of Ultrathin MoS₂ Sheets

L. Dong*, A. Dongare, University of Connecticut, USA; R. Namburu, T. O'Regan, M. Dubey, U.S. Army Research Laboratory, USA

S8: Advances in Memory Devices

Ferroelectric and Resistive Data Storage

Room: Mediterranean B/C

Session Chair: Bryan Huey, University of Connecticut

2:00 PM

(EMA-S8-001-2014) Ferroelectric tunnel junctions (Invited)

V. Garcia*, Unité Mixte CNRS/Thales, France

2:30 PM

(EMA-S8-002-2014) Enhanced ferroelectric properties in epitaxial La-doped PZT films at low concentrations of La-doping

M. Hordagoda*, D. Mukherjee, University of South Florida, USA; D. Ghosh, J. Jones, University of Florida, USA; P. Mukherjee, S. Witanachchi, University of South Florida, USA

2:45 PM

(EMA-S8-003-2014) Composition-Dependence of Piezoresponse in Ferroelectric Nanotubes

T. Field*, N. Bassiri-Gharb, Georgia Institute of Technology, USA

3:00 PM

(EMA-S8-004-2014) Ferroelectric Circuit Equations

J. T. Evans*, Radiant Technologies, Inc., USA

3:15 PM

(EMA-S8-005-2014) Grain boundary initiated DC breakdown of Ferroelectric films and push-pull failures of series connected capacitors (Invited)

D. Varghese*, Texas Instruments, USA; M. Masuduzzaman, Purdue University, USA; J. Rodriguez, S. Krishnan, Texas Instruments, USA; M. Alam, Purdue University, USA

3:45 PM

Break

4:15 PM

(EMA-S8-006-2014) On the electro-optical properties and applications of phase change materials (Invited)

P. Hosseini, C. Rios, G. Rodriguez-Hernandez, University of Oxford, United Kingdom; Y. Au, C. Wright, University of Exeter, United Kingdom; W. H. Pernice, Karlsruhe Institute of Technology, Germany; H. Bhaskaran*, University of Oxford, United Kingdom

4:45 PM

(EMA-S8-007-2014) Crystallization Kinetics of Phase Change Memory Films by Atomic Force Microscopy

J. L. Bosse*, B. D. Huey, University of Connecticut, USA; I. Grishin, O. V. Kolosov, Institute of Materials Science, United Kingdom

5:00 PM

(EMA-S8-008-2014) Ceria Nanocrystals Based Memristors

A. Younis*, University of New South Wales, Australia

5:15 PM

(EMA-S8-009-2014) An 8MHz 165uA/MHz Zero Leakage Non-Volatile Logic based Microcontroller Exhibiting 100% Digital State Retention at VDD=0V with <400ns Wakeup and Sleep Transitions

J. Rodriguez*, S. Bartling, S. Khanna, M. Clinton, H. McAdams, S. Summerfelt, Texas Instruments, USA

Poster Session

Room: Atlantic/Arctic

5:30 PM

(EMA-S1-P001-2014) Effect of viscosity and thickness in PZT-PZNN tape casting process for energy harvesting system

D. Song*, M. Woo, D. Cho, T. Sung, Hanyang University, Republic of Korea; S. Nahm, Korea University, Republic of Korea

(EMA-S1-P002-2014) Mechanism behind enhanced piezoresponse in high performance piezoceramics

A. K. Kalyani*, Indian Institute of Science, India; A. James, DMRL, India; R. Ranjan, Indian Institute of Science, India

(EMA-S1-P004-2014) Thickness Optimization of 0.69PZT-0.31PZNN thick film for energy harvesting module

M. Woo*, D. Song, D. Cho, T. Sung, Hanyang University, Republic of Korea; S. Nahm, Korea University, Republic of Korea

(EMA-S1-P005-2014) Studies on magnetic and structural properties of Ba(Co_{1-x}Mn_x)O_{3-δ} using synchrotron X-ray spectroscopy

R. Shinoda*, Osaka Prefecture University, Japan; Y. Okamoto, Japan Atomic Energy Agency(JAEA-Tokai), Japan; A. Iwase, T. Matsui, Osaka Prefecture University, Japan

(EMA-S1-P006-2014) Fabrication of Textured Lead-free (K,Na)NbO₃ Ceramics by Alginate Gelation and Templated Grain Growth

E. Mensur-Alkoy*, Maltepe University, Turkey; A. Berksoy-Yavuz, ENS Piezodevices Ltd., Turkey; S. Alkoy, Gebze Institute of Technology, Turkey

(EMA-S1-P007-2014) Effect of buffer layer and microstructure on the thermochromic properties of VO₂ thin film

H. Koo, J. Cho, S. Bae, C. Park*, S. Ahn, Seoul National University, Republic of Korea

(EMA-S1-P008-2014) Dielectric properties of rare earth doped BaTiO₃ ceramics and Curie Weiss law

V. Mitic*, V. Paunovic, M. Miljkovic, B. Jordovic, University of Nis and Institute of Technical Sciences of SASA, Serbia

(EMA-S1-P009-2014) Influence of Li-B-Si and Ba-Zn-B additions on the sintering and microwave dielectric properties of Ba-Nd-Ti ceramics

E. Li*, S. Zhang, University of Electronic Science and Technology of China, China

(EMA-S1-P010-2014) The thermal and dielectric properties of Mn-doped (1-x) ZrTi₂O₆-xZnNb₂O₆ filled PTFE composites

Y. Yuan*, C. Zhong, Univ. of Electron. Sci. and Tech. of China, China

(EMA-S1-P011-2014) Kinetics and equilibria of Schottky defect formation in the radiation detector TlBr

S. R. Bishop*, M. Kuhn, H. Tuller, Massachusetts Institute of Technology, USA

(EMA-S1-P012-2014) Effect of K-doping on the antiferroelectric to ferroelectric phase transition in (Ag_{0.05}Na_{0.95})NbO₃ ceramics

Y. Xu*, X. Tan, Iowa state university, USA; Y. Feng, Xi'an Jiaotong University, China

(EMA-S1-P013-2014) Effects of Annealing in Pb(Yb_{1/2}Nb_{1/2})O₃-PbTiO₃ Ceramics Near the Morphotopic Phase Boundary

R. Sumang*, Naresuan University, Thailand; S. Prasertpalichat, Oregon State University, USA; T. Bongkarn, Naresuan University, Thailand; D. Cann, Oregon State University, USA

(EMA-S2-P039-2014) Electrocaloric Materials and Dielectric Refrigeration: Novel Developments and Future Perspectives

Z. Kutnjak*, B. Rozic, B. Malic, H. Ursic, Jozef Stefan Institute, Slovenia; Q. M. Zhang, The Pennsylvania State University, USA

(EMA-S2-P040-2014) Improved pyroelectric performances of PMNT single crystals used for infrared detectors

H. Luo*, The Shanghai Institute of Ceramics, Chinese Academy of Sciences, China

(EMA-S2-P041-2014) Structure and ferroelectric/magnetic properties of Mn-doped bismuth iron titanate Aurivillius thin films

L. Keeney, T. Maity, M. Schmidt, N. Deepak, S. Roy, A. Amann, M. E. Pemble, R. W. Whatmore*, Tyndall National Institute, Ireland

(EMA-S2-P047-2014) Strain Dependence of Polarization and Dielectric response in Epitaxial (BaxSr1-x)TiO₃ Thin Films

S. H. Bin-Omran*, King Saud University, Saudi Arabia

(EMA-S3-P034-2014) Thin Film Growth by Pulsed Laser Deposition of Dielectric Materials

G. Kozlowski, J. Anders*, Wright State University, USA; C. Stutz, J. Jones, S. Smith, G. Landis, AFRL (Air Force Research Laboratory), USA

(EMA-S3-P035-2014) Electric-field induced microscopic strain response in functional ceramic/ceramic composite materials

N. H. Khansur*, J. Daniels, University of New South Wales, Australia

(EMA-S3-P038-2014) Enhanced Light emission from Erbium Oxide nanoparticles for Electronic and Optical Devices Applications

M. Maqbool*, Qatar University, Qatar

(EMA-S3-P042-2014) The non-volatile control of 2DEG conductance at oxide interfaces

S. Kim*, Korea Institute of Science and Technology, Republic of Korea; D. Kim, Seoul National University, Republic of Korea; Y. Kim, S. Moon, M. Kang, J. Choi, Korea Institute of Science and Technology, Republic of Korea; H. Jang, Seoul National University, Republic of Korea; S. Kim, J. Choi, S. Yoon, H. Chang, C. Kang, S. Lee, Korea Institute of Science and Technology, Republic of Korea; S. Hong, Seoul National University, Republic of Korea; J. Kim, S. Baek, Korea Institute of Science and Technology, Republic of Korea

(EMA-S3-P043-2014) Non-volatile electroresistive diode of PZT/LAO/STO heterostructure

S. Kim, Korea Institute of Science and Technology, Republic of Korea; C. Park, Seoul National University, Republic of Korea; J. Kim*, S. Baek, Korea Institute of Science and Technology, Republic of Korea

(EMA-S3-P045-2014) Preparation and Characterization of Self-Assembled, Percolative BaTiO₃-CoFe₂O₄ Nanocomposites via Magnetron Co-sputtering

Q. Yang, W. Zhang, M. Yuan, L. Kang, J. Feng, J. Ouyang*, Shandong University, China

(EMA-S4-P014-2014) Encapsulation Process of OLED Using a LMPA-Epoxy Double Layered Structure

H. Choi*, E. Im, C. Moon, Hoseo University, Republic of Korea

(EMA-S4-P015-2014) Change of the Heat Dissipation Characteristics According to the Emissivity at the Surface of LED Module

K. Park*, C. Moon, Hoseo Univ, Republic of Korea

(EMA-S4-P017-2014) Effective activated carbon based counter electrode for dye sensitized solar cells: electrochemical study

Z. Li*, M. Akhtar, W. Lee, O. Yang, Chonbuk National University, Republic of Korea

(EMA-S5-P018-2014) Effect of MMT Addition on Tensile Properties of Graphene Oxide/Chitosan Nanocomposites

D. Kim*, Y. Mithlesh, K. Rhee, Kyunghee University, Republic of Korea

(EMA-S5-P037-2014) Redox behavior of (Ba,Sr)(Ti,Zr)O₃ systems

Y. Han*, G. Song, Sungkyunkwan University, Republic of Korea

(EMA-S6-P019-2014) Marine and Automotive Thermoelectric Generators Development in the Frame of the EC - PowerDriver Project

Y. Gelbstein*, Ben Gurion University, Israel; J. Tunbridge, R. Dixon, Intrinsiq Materials Ltd, United Kingdom; M. Reece, H. Ning, Queen Mary University of London, United Kingdom; R. Gilchrist, Jaguar Land Rover, United Kingdom; R. Summers, Halyard Ltd, United Kingdom; I. Agote, TECNALIA Research and Innovation, Spain; I. Dimitriadou, K. Simpson, European Thermodynamics Ltd, United Kingdom; C. Rouaud, P. Feulner, Ricardo, United Kingdom; S. Rivera, Nanoker Research SL, Spain; M. Husband, Rolls Royce PLC, United Kingdom; J. Crossley, I. Robinson, Thermex Ltd, United Kingdom

(EMA-S6-P020-2014) Enhanced thermoelectric performance in bismuth telluride based alloys by multi-scale microstructural effects

T. Zhu*, L. Hu, Zhejiang University, China

(EMA-S6-P021-2014) Surface Flatness of Fe₂VAI-based Epitaxial Thin-films Prepared by Ion Beam Sputtering Technique

K. Kato*, K. Iwasaki, TOYOTA BOSHOKU CORPORATION, Japan; Y. Furuta, T. Miyawaki, H. Asano, T. Takeuchi, Nagoya University, Japan

(EMA-S6-P022-2014) Uncertainty analysis of Seebeck coefficient and electrical resistivity characterization

J. Mackey*, University of Akron, USA; A. Sehirlioglu, Case Western Reserve University, USA; F. Dynys, NASA Glenn Research Center, USA

(EMA-S6-P023-2014) Transient thermoelectric solution employing Green's functions

J. Mackey*, University of Akron, USA; A. Sehirlioglu, Case Western Reserve University, USA; F. Dynys, NASA Glenn Research Center, USA

(EMA-S6-P024-2014) Thermoelectric properties of Ba₂NaNb₅O₁₅ orient ceramics, and its hopping enhancement

H. Kakemoto*, T. Kawano, H. Irie, University of Yamanashi, Japan

(EMA-S6-P025-2014) High Pressure Processing of Bulk Nanoscale Thermoelectrics

E. Gorzkowski*, J. Wollmershauser, B. Feigelson, Naval Research Laboratory, USA

(EMA-S7-P026-2014) Energetics for lead migration across Pt/PbTiO₃ and Pt₃Pb/PbTiO₃ interfaces: A computation study

F. Lin*, A. Chernatynskiy, S. R. Phillpot, J. C. Nino, University of Florida, USA; J. L. Jones, North Carolina State University, USA; S. B. Sinnott, University of Florida, USA

(EMA-S9-P027-2014) Design and fabrication of ceramic-based inverters using ZnO and TiO₂ films assembled by wet processing technique

L. C. Liao*, Y. Lin, Yuan Ze University, Taiwan

(EMA-S9-P028-2014) Optical properties of nanostructured anatase thin films formed by the low temperature aqueous sol gel – flow coating approach

O. Muñoz-Serrato*, J. Serrato-Rodríguez, Universidad Michoacana de San Nicolás de Hidalgo, Mexico; T. Ishibashi, Nagaoka University of Technology, Japan

(EMA-S12-P029-2014) Cryogenic Propulsion Technologies for 45 Megawatt Electric Aircraft

G. Y. Panasyuk*, UES Inc., USA; T. J. Haugan, Air Force Research Laboratory, USA

(EMA-S12-P030-2014) Development of high energy density SMES devices with YBCO wire

D. Latypov, BerrieHill Research Corp., USA; T. Bullard, UES Inc., USA; T. Haugan*, The Air Force Research Laboratory, USA

(EMA-S12-P044-2014) Stability of structures in K-intercalated iron selenide superconductors

G. Wang*, Y. Liu, T. Ying, X. Lai, S. Jin, X. Chen, Chinese Academy of Sciences, China

(EMA-S12-018-2014) Optimizing Flux Pinning of YBCO Superconductor with BaSnO₃+Y₂BaCuO₅ Mixed Phase Additions

M. P. Sebastian, AFRL, USA; G. Y. Panasyuk, UES, USA; H. Wang, Texas A & M University, USA; T. J. Haugan*, J. N. Reichart, AFRL, USA

(EMA-S13-P031-2014) Lithium Titanate as Anode Material in Lithium-Ion Batteries

D. Seshadri*, Case Western Reserve University, USA; M. Shirkpour, M. Doeff, Lawrence Berkeley National Laboratory, USA

(EMA-S13-P032-2014) Effects of High Energy X Ray and Proton Irradiation on Lead Zirconate Titanate Thin Films' Dielectric and Piezoelectric Response

Y. Bastani, A. Y. Cortes-Pena*, A. D. Wilson, Georgia Institute of Technology, USA; S. Gerardin, M. Bagatin, A. Paccagnella, University of Padova, Italy; N. Bassiri-Gharb, Georgia Institute of Technology, USA

(EMA-S13-P033-2014) Co-fired Multilayer Ceramic Batteries for Safe Electrochemical Energy Storage

L. Gao*, A. Baker, S. S. Berbano, C. Randall, The Pennsylvania State University, USA

Thursday, January 23, 2014

Plenary Session II

Room: Indian

Session Chair: George Rossetti, University of Connecticut

8:30 AM

(EMA—002-2014) Lead-free piezoceramics: History, achievements, future (Invited)

J. Roedel*, Technische Universität Darmstadt, Germany

9:30 AM

Break

S1: Functional and Multifunctional Electroceramics for Commercialization

Multifunctional Properties in Oxides

Room: Pacific

Session Chairs: Dragan Damjanovic, Swiss Federal Institute of Technology - EPFL; Pamela Thomas, University of Warwick

10:00 AM

(EMA-S1-017-2014) Polarization Mechanism and New Trend of Dielectric Study (Invited)

T. Tsurumi*, K. Takeda, T. Hoshina, Tokyo Institute of Technology, Japan

10:30 AM

(EMA-S1-018-2014) Using high resolution neutron diffraction to study the impact of Jahn-Teller active Mn³⁺ on strain effects and phase transitions in Manganites Perovskites (Invited)

B. J. Kennedy*, The University of Sydney, Australia

11:00 AM

(EMA-S1-019-2014) New Soft Composite Multiferroics and Solid Spin Modulated Multiferroics Structures

Z. Kutnjak*, B. Rozic, Jozef Stefan Institute, Slovenia; M. Jagodic, Institute of Mathematics, Physics and Mechanics, Slovenia; S. Gyergyek, M. Drofenik, D. Arcon, Jozef Stefan Institute, Slovenia

11:15 AM

(EMA-S1-020-2014) Photocatalytic property of ferroelectric (Na,K) NbO₃

N. Kato*, K. Kakimoto, Nagoya Institute of Technology, Japan; M. Wegner, A. Roosen, University of Erlangen-Nuremberg, Germany

11:30 AM

(EMA-S1-021-2014) Glass-like Thermal Conductivity of (010)-Textured Lanthanum-doped Strontium Niobate Synthesized with Wet Chemical Deposition

B. M. Foley*, University of Virginia, USA; H. J. Brown-Shaklee, M. J. Campion, D. L. Medlin, P. G. Clem, J. Ihlefeld, Sandia National Laboratories, USA; P. E. Hopkins, University of Virginia, USA

11:45 AM

(EMA-S1-022-2014) Surface plasmon resonance based magnetic field sensor using N:ZnO thin film

K. Jindal, University of Delhi, India; M. Tomar*, Miranda House, University of Delhi, India; V. Gupta, University of Delhi, India

12:00 PM

(EMA-S1-023-2014) Development of MEMS based E-nose for the detection of harmful gases

A. Sharma*, R. Gupta, P. Tyagi, A. Singh, L. Rana, M. Tomar, V. Gupta, University of Delhi, India

12:15 PM

(EMA-S1-024-2014) From the Heywang model to the fractal electronics properties intergranular capacity relations

V. Mitic*, V. Paunovic, L. Kocic, University of Nis and Institute of Technical Sciences of SASA, Serbia

S2: Multiferroic Materials and Multilayer Ferroic Heterostructures: Properties and Applications

Multiferroic Devices

Room: Indian

Session Chair: Greg Carman, UCLA

10:00 AM

(EMA-S2-015-2014) Magnetoelectric Multiferroic Heterostructures and Low-Power Devices (Invited)

N. Sun*, Northeastern University, USA

10:30 AM

(EMA-S2-016-2014) Loss Mechanism in Modern Microwave Dielectrics (Invited)

N. Newman*, S. Zhang, L. Liu, Arizona State University, USA

11:00 AM

(EMA-S2-017-2014) Strain mediated magnetoelectric coupling using substrate constrained thin film ferroelectrics (Invited)

C. S. Lynch*, J. Cui, J. Hockel, UCLA, USA

11:15 AM

(EMA-S2-018-2014) Strain Mediated Multiferroics: Reorientation of Single Domain Magnetic Moments (Invited)

G. Carman*, UCLA, USA

11:30 AM

(EMA-S2-019-2014) Field-directed Assembly of Ferrite-Ferroelectric Core-Shell Nanofibers and Studies on Magneto-electric Interactions (Invited)

G. Sreenivasulu, M. Popov, K. Sharma, G. Srinivasan*, Oakland University, USA

11:45 AM

(EMA-S2-020-2014) Ferroelectric and Multiferroic Hetero-structure Devices for Adaptive RF Circuit Applications (Invited)

T. Kalkur*, University of Colorado, USA

12:00 PM

(EMA-S2-021-2014) Synthesis and Integration of Multifunctional Materials based on Complex Oxides and their Heterostructures (Invited)

J. P. Chang*, UCLA, USA

12:15 PM

(EMA-S2-022-2014) PZT/FeGa non-linear microcantilevers as robust multiferroic memory devices

I. Takeuchi*, University of Maryland, USA

S3: Structure of Emerging Perovskite Oxides: Bridging Length Scales and Unifying Experiment and Theory

Inhomogeneities, Nonstoichiometry, and Point Defects

Room: Coral B

Session Chairs: Philip Lightfoot, University of St Andrews; Alexei Bosak, European Synchrotron Radiation Facility

10:00 AM

(EMA-S3-014-2014) Peculiar Inhomogeneous States in Ferroelectrics and Multiferroics (Invited)

L. Bellaiche*, University of Arkansas, USA

10:30 AM

(EMA-S3-015-2014) Investigation of Defect Dipole Kinetics in the Ferroelectric and Paraelectric Phases of Acceptor Doped BaTiO₃ Single Crystals (Invited)

R. Maier*, T. Pomorski, P. Lenahan, C. Randall, The Pennsylvania State University, USA

11:00 AM

(EMA-S3-016-2014) Dynamics of Point Defects in Perovskite Dielectric Materials

C. Randall*, D. P. Shay, R. A. Maier, J. A. Bock, The Pennsylvania State University, USA; S. Lee, KICET, Republic of Korea

11:15 AM

(EMA-S3-017-2014) Impact of Non-Stoichiometry and Aliovalent Doping on Materials Properties of Functional Oxides – from Ferroelectrics to Lithium-Ion Battery Cathode Materials (Invited)

R. A. Eichel*, RWTH Aachen University, Germany

11:45 AM

(EMA-S3-018-2014) Synthesis and Crystal Structure of Perovskite Dielectric (Na,Li)(Nb,Ta)O₃

J. J. Carter*, University of Florida, USA; I. Levin, NIST, USA

12:00 PM

(EMA-S3-019-2014) Effects of A-site Stoichiometry in 1-x(Bi_{0.5}Na_{0.5}TiO₃)-xBaTiO₃ Ceramics Near the Morphotropic Phase Boundary (MPB)

S. Prasertpalichat*, D. Cann, Oregon State University, USA

S5: Structure and Properties of Interfaces in Electronic Materials

Transport at Interfaces

Room: Caribbean B

Session Chair: Nick Strandwitz, Lehigh University

10:00 AM

(EMA-S5-001-2014) The Role of Grain Boundaries in the Internal Reduction of Ni²⁺ in YSZ (Invited)

I. Reimanis*, Colorado School of Mines, USA; J. T. White, Los Alamos National Laboratory, USA; J. Tong, Colorado School of Mines, USA; J. R. O'Brien, Quantum Design, Incorporated, USA; A. Morrissey, Colorado School of Mines, USA

10:15 AM

(EMA-S5-002-2014) Dopant Effects on Cation Diffusion in α -Al₂O₃

L. Feng*, S. Dillon, University of Illinois at Urbana Champaign, USA

10:30 AM

(EMA-S5-003-2014) Transport mechanism by gas/solid interactions in metal-oxide semiconductor interfaces

J. Jung*, S. Lee, Kyungnam University, Republic of Korea

Consequences of Interfaces

Room: Caribbean B

Session Chair: Shen Dillon, University of Illinois at Urbana-Champaign

10:45 AM

(EMA-S5-004-2014) Novel Ceramic Metal Nanostructures by Reduction of Mixed Oxides (Invited)

H. M. Chan*, M. Kracum, K. Anderson, A. Kundu, Lehigh University, USA

11:15 AM

(EMA-S5-005-2014) Interface-dependent electrochemical behaviour of nanostructured manganese (IV) oxide (Mn₃O₄)

V. Liu*, Y. Ng, B. Okatan, K. Bogle, R. Amal, V. Nagarajan, University of New South Wales, Australia

11:30 AM

(EMA-S5-006-2014) In Situ Testing of High Strength Niobium-Sapphire Interfaces at the Nanoscale

R. Hao*, E. Saiz, F. Giuliani, Imperial College London, United Kingdom

11:45 AM

(EMA-S5-007-2014) Dielectric & Piezoelectric Enhancement of Potassium Niobate/Barium Titanate Nano-complex Ceramics with Parallel Configuration of Structure-gradient Regions

S. Wada*, University of Yamanashi, Japan

12:00 PM

(EMA-S5-008-2014) Cylindrical and Ring Micro and Nano laser on optical fibers and titanium oxide nanotubes/nanowires

M. Maqbool*, Qatar University, Qatar; G. Ali, Pakistan Institute of Engineering & Applied Sciences, Pakistan

S7: Computational Design of Electronic Materials

Design of Energy Materials

Room: Coral A

Session Chair: Mina Yoon, Oak Ridge National Laboratory

10:00 AM

(EMA-S7-014-2014) Computationally Guided Design of Nanostructured Soft Matter and Multicomponent Materials for Energy Science (Invited)

B. Sumpter*, Oak Ridge National Laboratory, USA

10:30 AM

(EMA-S7-015-2014) Virtual high-throughput and Big Data techniques for the discovery and design of new organic semiconductors (Invited)

J. Hachmann*, University at Buffalo, SUNY, USA

11:00 AM

(EMA-S7-016-2014) Evolutionary search for the Crystal Structures of Novel Polymer Dielectrics

V. Sharma*, C. Wang, University of Connecticut, USA; Q. Zhu, Los Alamos National Laboratory, USA; G. Pilania, Stony Brook University, USA; A. R. Oganov, Los Alamos National Laboratory, USA; G. Sotzing, University of Connecticut, USA; S. Kumar, Columbia University, USA; R. Ramprasad, University of Connecticut, USA

11:15 AM

(EMA-S7-017-2014) Charge transport in lithium peroxide: relevance for rechargeable metal-air batteries (Invited)

M. Radin, D. Siegel*, University of Michigan, USA

11:45 AM

(EMA-S7-018-2014) Understanding the origin of high-rate intercalation pseudocapacitance in Nb₂O₅ crystals

P. Ganesh*, Oak Ridge National Laboratory, USA; A. Lubimtsev, Pennsylvania State University, USA; P. Kent, B. Sumpter, Oak Ridge National Laboratory, USA

S12: Recent Developments in High-Temperature Superconductivity

New Superconductors and Their Progress

Room: Mediterranean B/C

Session Chair: Haiyan Wang, Texas A&M University

10:00 AM

(EMA-S12-001-2014) High T_c via the Mesoscopic Structure Route (Invited)

C. Chu*, L. Deng, Texas Center for Superconductivity at the University of Houston, USA

10:30 AM

(EMA-S12-002-2014) Pushing the T_c-J_c-H_{c2} Boundaries of Iron-Chalcogenide Superconductors (Invited)

Q. Li*, Brookhaven National Lab, USA

11:00 AM

(EMA-S12-003-2014) Role of Excess Fe in Iron Chalcogenide Superconductor (Invited)

H. Okazaki*, T. Yakaguchi, T. Watanabe, K. Deguchi, S. Demura, S. Denholme, T. Ozaki, National Institute for Materials Science, Japan; Y. Mizuguchi, Tokyo Metropolitan University, Japan; H. Takeya, National Institute for Materials Science, Japan; T. Oguchi, Osaka University, Japan; Y. Takano, National Institute for Materials Science, Japan

11:30 AM

(EMA-S12-004-2014) Fe-based Superconducting Thin Film Case Studies: From Fundamental Properties to Functional Devices (Invited)

S. Haindl*, University of Tuebingen, Germany

12:00 PM

(EMA-S12-005-2014) Progresses on the study of iron selenide based superconductors (Invited)

X. Chen*, Institute of Physics, Chinese Academy of Sciences, China

S13: Highlights of Undergraduate Student Research in Basic Science and Electronic Ceramics

Student Finalist Presentations, Thursday

Room: Coral A

Session Chair: Geoff Brennecke, Sandia National Laboratories

12:40 PM

(EMA-S13-005-2014) Glass-like Thermal Conductivity of (010)-Textured Lanthanum-doped Strontium Niobate Synthesized with Wet Chemical Deposition

B. M. Foley*, University of Virginia, USA; H. J. Brown-Shaklee, M. J. Campion, D. L. Medlin, P. Clem, J. Ihlefeld, Sandia National Laboratories, USA; P. Hopkins, University of Virginia, USA

12:55 PM

(EMA-S13-006-2014) In-situ investigation of dewetting kinetics in polycrystalline platinum thin films via confocal laser microscopy

S. Jahangir*, N. Valanoor, University of New South Wales, Australia; J. Ihlefeld, Sandia National Labs, USA

1:10 PM

(EMA-S13-007-2014) New models for polarization reversal in poled ferroelectric ceramics

C. Cozzan*, University of Florida, USA; J. E. Daniels, University of New South Wales, Australia; J. L. Jones, North Carolina State University, USA

1:25 PM

(EMA-S13-008-2014) Microstructural origin for the piezoelectricity evolution in $(K_{0.5}Na_{0.5})NbO_3$ -based lead-free ceramics

H. Guo*, Iowa State University, USA; S. Zhang, Pennsylvania State University, USA; S. P. Beckman, X. Tan, Iowa State University, USA

1:40 PM

(EMA-S13-009-2014) Temperature dependent thermal conductivity of nano-grained Barium Titanate ($BaTiO_3$)

B. F. Donovan*, B. M. Foley, University of Virginia, USA; J. Ihlefeld, B. McKenzie, Sandia National Laboratories, USA; P. Hopkins, University of Virginia, USA

S1: Functional and Multifunctional Electroceramics for Commercialization

Defect Dynamics, Disorder, and Reliability

Room: Pacific

Session Chairs: Susan Trolier-McKinstry, Penn State; Clive Randall, Penn State University

2:00 PM

(EMA-S1-025-2014) Electrochemical Point Defect Dynamics in Ionic Ceramics (Invited)

E. C. Dickey*, A. Mobbalegh, North Carolina State University, USA

2:30 PM

(EMA-S1-026-2014) Local-Structure Origins of Properties in Perovskite Ferroelectrics: A Combined-Technique Approach (Invited)

I. Levin*, NIST, USA

3:00 PM

(EMA-S1-027-2014) Voltage-dependent resistance phenomena in electroceramics (Invited)

A. R. West*, University of Sheffield, United Kingdom

3:30 PM

Break

4:00 PM

(EMA-S1-028-2014) Electrical Partial Discharge as a Non-destructive Method for Reliability Evaluation of Piezoelectric Ceramics

T. Hang*, J. Glaum, B. Phung, M. Hoffman, The University of New South Wales, Australia

4:15 PM

(EMA-S1-029-2014) Impedance spectroscopy and material design of lead-free alkali niobate piezoelectric ceramics

M. Watanabe*, K. Kakimoto, I. Kagomiya, Nagoya Institute of Technology, Japan

4:30 PM

(EMA-S1-030-2014) Fatigue mechanisms in Pb-free Piezoelectric Ceramics

N. Kumar*, T. Ansell, D. Cann, Oregon State University, USA

4:45 PM

(EMA-S1-031-2014) Electrochemically and optically derived oxygen stoichiometry and redox kinetics of $(Pr,Ce)O_{2-\delta}$ thin films (Invited)

S. R. Bishop*, Kyushu University, Japan; J. Kim, D. Chen, Massachusetts Institute of Technology, USA; L. Zhao, Kyushu University, Japan; H. Tuller, Massachusetts Institute of Technology, USA

5:15 PM

(EMA-S1-032-2014) "Phased and Confused": Exploring the Evolution of Phase Chemistry in NaSICON Ion Conducting Ceramics

E. Spoeke*, N. Bell, J. S. Wheeler, C. Edney, D. Ingersoll, Sandia National Laboratories, USA

5:30 PM

(EMA-S1-033-2014) Bulk Ionic Conductivity of Glass and Glass-Ceramic Lithium Thiophosphate Solid Electrolytes for Solid-state Batteries & Electrochemical Capacitors

S. S. Berbano*, M. Mirsaneh, M. T. Lanagan, C. A. Randall, The Pennsylvania State University, USA

5:45 PM

(EMA-S1-034-2014) Conductivity in nanostructured ceria: space- and time- resolved mapping of ionic dynamics

J. Ding*, Georgia Institute of Technology, USA; E. Strelcov, S. Kalinin, Oak Ridge National Laboratory, USA; N. Bassiri-Gharb, Georgia Institute of Technology, USA

S2: Multiferroic Materials and Multilayer Ferroic Heterostructures: Properties and Applications

Materials Synthesis and Epitaxial Systems

Room: Indian

Session Chair: Valanoor Nagarajan, University of New South Wales

2:00 PM

(EMA-S2-023-2014) Domain structure of (100)/(010)-oriented epitaxial $PbTiO_3$ -based thin films with in-plane polarization (Invited)

H. Funakubo*, Y. Ehara, T. Nakashima, Tokyo Institute of Technology, Japan; T. Yamada, Nagoya University, Japan

2:30 PM

(EMA-S2-024-2014) Ferroic order and switching controlled by reversible elastic strain (Invited)

K. Dorr*, E. Guo, MLU Halle-Wittenberg, Germany; M. D. Biegalski, H. M. Christen, ORNL, USA; S. Das, IFW Dresden, Germany; R. Roth, MLU Halle-Wittenberg, Germany; L. Schultz, A. Herklotz, IFW Dresden, Germany

3:00 PM

(EMA-S2-025-2014) The effect of interfacial octahedral behavior in ferromagnetic manganite heterostructures (Invited)

E. Moon, S. May*, Drexel University, USA

3:30 PM

Break

4:00 PM

(EMA-S2-026-2014) Biphasic Magnetoelectric Multiferroic Nanocomposite Films (Invited)

M. Jain*, University of Connecticut, USA

4:15 PM

(EMA-S2-027-2014) Exotic functional domain walls in multiferroics (Invited)

D. Meier*, ETH Zürich, Switzerland

4:30 PM

(EMA-S2-028-2014) Multiferroics Within a Fiber: Janus-type Nanomaterials Synthesized via Electrospinning and Electrospray Techniques

J. D. Starr*, J. S. Andrew, University of Florida, USA

4:45 PM

(EMA-S2-029-2014) Magnetic and ferroelectric property enhancement of PZT/LSMO multiferroic thin films using dual laser ablation

M. Hordagoda, D. Mukherjee*, H. Robert, P. Mukherjee, S. Witanachchi, University of South Florida, USA

5:00 PM

(EMA-S2-030-2014) The effect of La doping on the ferroelectric and magnetic properties of PZT/LSMO multiferroic heterostructures

M. Hordagoda*, D. Mukherjee, University of South Florida, USA; D. Ghosh, J. Jones, University of Florida, USA; P. Mukherjee, S. Witanachchi, University of South Florida, USA

S5: Structure and Properties of Interfaces in Electronic Materials

Thermodynamics of Interfaces

Room: Caribbean B

Session Chair: Edwin Garcia, Purdue University

2:00 PM

(EMA-S5-009-2014) Orientation relationships of copper crystals on sapphire surfaces: how much does the interface matter? (Invited)

D. Chatain*, Aix-Marseille University, CNRS, France

2:30 PM

(EMA-S5-010-2014) Extending CALPHAD Methods to Model Grain Boundaries and Nanocrystalline Materials (Invited)

N. Zhou, J. Luo*, UCSD, USA

3:00 PM

(EMA-S5-011-2014) Equilibrium State of the Solid-Solid Ni-YSZ(111) Interface (Invited)

H. (Bratt) Nahor, H. Meltzman, W. D. Kaplan*, Technion - Israel Institute of Technology, Israel

3:30 PM

Break

Structure and Composition of Interfaces

Room: Caribbean B

Session Chair: John Blendell, Purdue University

4:00 PM

(EMA-S5-012-2014) Phase and Orientation Relationships for Interfaces in Electronic Ceramic Heterostructures Determined by Combinatorial Substrate Epitaxy (Invited)

G. Rohrer*, P. Salvador, Carnegie Mellon University, USA

4:30 PM

(EMA-S5-013-2014) Crystallization of Atomic Layer Deposited Aluminum Oxide Films (Invited)

N. C. Strandwitz*, D. Weisberg, Lehigh University, USA

4:45 PM

(EMA-S5-014-2014) Molecular Dynamics Simulations of the Lu in Silicate Intergranular Films in Silicon Nitride: Growth and the Role of Oxygen on Adsorption (Invited)

S. H. Garofalini*, Y. Jiang, Rutgers University, USA

5:15 PM

(EMA-S5-015-2014) Comparative method behavior interaction potential surface to a structure (Al₂O₃(ZnO/SnO₂)+TiO₂) in low isotropic model with multiple harmonic oscillators single bond

O. Rodriguez Pinilla*, Universidad Autónoma de Colombia, Colombia

5:30 PM

(EMA-S5-016-2014) The Study of Magnetic Properties of A_(1-x)Mn_xA' (A=Zn,Cd and A'=S,Te,Se) at Critical Region Using High Temperature Series Expansion Extrapolated with Pade Approximants

H. D. Berry*, Dilla University, Ethiopia

S7: Computational Design of Electronic Materials

Computational Methods for Novel Oxides

Room: Coral A

Session Chair: Ghanshyam Pilania

2:00 PM

(EMA-S7-019-2014) A Phenomenological Theory for Ferroelectric Solid Solutions (Invited)

G. A. Rossetti*, University of Connecticut, USA; A. A. Heitmann, Naval Undersea Warfare Center, USA

2:30 PM

(EMA-S7-020-2014) Modeling Electrothermal Properties of Polarizable Dielectric Materials (Invited)

S. Alpay*, G. A. Rossetti, University of Connecticut, USA

3:00 PM

(EMA-S7-021-2014) Generalized Atomistic Models for Metal-Metal Oxide Composites (Invited)

S. Valone*, Los Alamos National Laboratory, USA; M. I. Baskes, University of California San Diego, USA; X. Liu, R. L. Martin, Los Alamos National Laboratory, USA; K. Kolluri, University of Pennsylvania, USA; S. R. Atlas, University of New Mexico, USA; G. Pilania, Los Alamos National Laboratory, USA

3:30 PM

Break

4:00 PM

(EMA-S7-022-2014) Computational design of multifunctional layered oxides across length scales (Invited)

S. Nakhmanson*, University of Connecticut, USA

4:30 PM

(EMA-S7-023-2014) Accurate descriptions of Hellmann-Feynman forces in understanding ferromagnetic ZnOCoH

A. Pham*, M. H. Al Assadi, University of New South Wales, Australia; C. J. Gil, University of Florida, USA; A. Yu, S. Li, University of New South Wales, Australia

4:45 PM

(EMA-S7-013-2014) Defect kinetics in oxides from long time simulations (Invited)

B. P. Uberuaga*, Los Alamos National Laboratory, USA

S9: Thin Film Integration and Processing Science

Epitaxial and Functional Oxide Thin Films

Room: Coral B

Session Chairs: Brady Gibbons, Oregon State University; Rudeger Wilke, The Pennsylvania State University

2:00 PM

(EMA-S9-001-2014) Strain engineering via octahedral distortions in epitaxial perovskite oxide films (Invited)

A. Vaillonis*, Stanford University, USA; H. Boschker, M. Huijben, G. Koster, G. Rijnders, University of Twente, Netherlands

2:30 PM

(EMA-S9-002-2014) Epitaxial integration of commensurate cubic oxides on GaN

C. T. Shelton*, E. Paisley, E. Sachet, I. Bryan, NCSU, USA; M. Bügler, TU Berlin, Germany; M. Biegalski, Oak Ridge National Laboratory, USA; J. LeBeau, B. Gaddy, S. Mita, R. Collazo, Z. Sitar, D. Irving, NCSU, USA; A. Hoffmann, TU Berlin, Germany; J. Maria, NCSU, USA

2:45 PM

(EMA-S9-003-2014) In-situ X-ray Studies of the Synthesis and Properties of Polar and Ferroelectric Thin Film Heterostructures (Invited)

M. Highland*, E. Perret, C. Folkman, Argonne National Laboratory, USA; C. Thompson, Northern Illinois University, USA; D. Fong, S. Streiffer, G. Stephenson, J. Eastman, P. Fuoss, Argonne National Laboratory, USA

3:15 PM

(EMA-S9-004-2014) Carbon Nanotubes Integrated with Superconducting NbC

G. Zou*, Soochow University, China; H. Luo, NMSU, USA; T. McCleskey, Q. Jia, LANL, USA

3:30 PM

Break

4:00 PM

(EMA-S9-005-2014) High mobility CdO: Towards monolithically integrated plasmonic devices (Invited)

E. Sachet*, C. T. Shelton, M. Kang, S. Franzen, J. Maria, North Carolina State University, USA

4:30 PM

(EMA-S9-006-2014) High kt₂×Q, Multi-frequency Lithium Niobate Resonators (Invited)

S. A. Bhavne*, Cornell University, USA

5:00 PM

(EMA-S9-007-2014) Ba_{0.5}Sr_{0.5}TiO₃ Thin Film Capacitors for Microwave Antenna

B. Malic*, Jozef Stefan Institute, Slovenia; S. Glinsek, Brown University, USA; B. Kmet, T. Pecnik, Jozef Stefan Institute, Slovenia; V. Furlan, Centre of Excellence SPACE.SI, Slovenia; M. Vidmar, University of Ljubljana, Slovenia

5:15 PM

(EMA-S9-008-2014) VO₂ Thin Film Electrochromic Window Behavior Dependence on Doping and Strain State

P. Clem*, C. Edney, J. Custer, C. Nordquist, T. Jordan, J. Hunker, Sandia National Laboratories, USA

5:30 PM

(EMA-S9-009-2014) Nanoscale Mapping of Microscale Piezoactuators (Invited)

M. Rivas, J. L. Bosse, L. Ye, University of Connecticut, USA; R. Keech, S. Trolier McKinstry, Penn State University, USA; R. Polcawich, U.S. Army Research Laboratory, USA; B. D. Huey*, University of Connecticut, USA

S12: Recent Developments in High-Temperature Superconductivity

Superconductors and Their Applications

Room: Mediterranean B/C

Session Chair: Timothy Haugan, Air Force Research Laboratory

2:00 PM

(EMA-S12-006-2014) Development of MgB₂ and (Ba(Sr),K)Fe₂As₂ wires (Invited)

H. Kumakura*, S. Ye, Z. Gao, A. Matsumoto, K. Togano, National Institute for Materials Science, Japan

2:30 PM

(EMA-S12-022-2014) Slow Abrikosov to fast moving Josephson vortex transition in REFeAs(O,F) (Invited)

P. J. Moll, ETH Zurich, Switzerland; L. Balicas, National High Magnetic Field Laboratory, USA; D. Geshkenbein, G. Blatter, J. Karpinski, N. D. Zhigadlo, B. Batlogg*, ETH Zurich, Switzerland

3:00 PM

(EMA-S12-008-2014) Grain structure in macroscopically untextured Bi₂212 round wires – Where does the current flow? (Invited)

F. Kametani*, J. D. Jiang, N. Craig, M. Matras, E. E. Hellstrom, D. C. Larbalestier, National High Magnetic Field Laboratory, USA

3:30 PM

Break

4:00 PM

(EMA-S12-009-2014) AC loss in coated conductor coils in DC bias current (Invited)

E. Pardo*, J. Souc, J. Kovac, Institute of Electrical Engineering, Slovak Academy of Sciences, Slovakia

4:30 PM

(EMA-S12-010-2014) Recent Progress of R&D Project of Fundamental Technologies for Accelerator Magnets Using Coated Conductors (Invited)

N. Amemiya*, Kyoto University, Japan; T. Kurusu, Toshiba Corporation, Japan; T. Ogitsu, High Energy Accelerator Research Organization, Japan; Y. Mori, Kyoto University, Japan; K. Noda, National Institute of Radiological Sciences, Japan; M. Yoshimoto, Japan Atomic Energy Agency, Japan

5:00 PM

(EMA-S12-011-2014) Cryogenic and superconducting drivetrains and components for all-electric or hybrid-electric aircraft propulsion (Invited)

T. Haugan*, The Air Force Research Laboratory, USA; G. Y. Panasyuk, T. Bullard, UES Inc., USA; D. Latypov, BerrieHill Research Corp., USA

5:30 PM

(EMA-S12-012-2014) Electric Aircraft Concept: Impact of Superconductor/Cryogenic Power Systems for Aircraft Propulsion

G. Y. Panasyuk*, UES Inc., USA; T. J. Haugan, Air Force Research Laboratory, USA

5:45 PM

(EMA-S12-013-2014) An Investigation into the Nickel Doped Paratacamite Group of Minerals as Potential Superconducting Materials

T. Bullard*, UES Inc., USA; T. Haugan, The Air Force Research Laboratory, AFRL/RQOM, USA; L. Brunke, University of Dayton Research Institute, USA

Friday, January 24, 2014

Plenary Session III

Room: Indian

Session Chair: Haiyan Wang, Texas A&M University

8:30 AM

(EMA—003-2014) Functional Electronic Materials in Integrated Commercial Building and Aerospace Systems (Invited)

J. Mantese*, United Technologies Research Center, USA

9:30 AM

Break

S1: Functional and Multifunctional Electroceramics for Commercialization

Lead-Free Piezoelectrics

Room: Pacific

Session Chairs: Takaaki Tsurumi, Tokyo Institute of Technology; Sean Bishop, Kyushu University

10:00 AM

(EMA-S1-035-2014) Processing and Microstructure Control of (Na,K)NbO₃-based Lead-free Piezoceramics (Invited)

K. Kakimoto*, Nagoya Institute of Technology, Japan

10:30 AM

(EMA-S1-036-2014) Recent Developments on Lead Free Ferroelectric Materials (Invited)

S. Zhang*, T. Shrout, Pennsylvania State University, USA

11:00 AM

(EMA-S1-037-2014) Large electric field-induced strain in La-modified [(Bi_{1/2}Na_{1/2})_{0.95}Ba_{0.05}]TiO₃ lead-free ceramics

X. Liu*, X. Tan, Iowa State University, USA

11:15 AM

(EMA-S1-038-2014) Preparation of (K,Na)(Nb,Ta)O₃ based Lead Free Piezoelectrics Using Novel Sintering Aid

K. Kikuta*, EcoTopia Scienc Institute, Nagoya University, Japan

11:30 AM

(EMA-S1-039-2014) Piezoelectric properties of lead-free niobate ceramics with controlled grain size

K. Kato*, K. Kakimoto, Nagoya Institute of Technology, Japan; K. Hatano, K. Kobayashi, Y. Doshida, Taiyo Yuden Co., Ltd., Japan

11:45 AM

(EMA-S1-040-2014) Electric field-induced structure in NBT-based relaxors (Invited)

P. A. Thomas*, D. I. Woodward, D. S. Keeble, D. Walker, S. Anand, University of Warwick, United Kingdom

12:15 PM

(EMA-S1-041-2014) Correlation between Piezoelectric Properties and Phase Co-existence in (Ba,Ca)(Ti,Zr)O₃ Ceramics

Y. ZHANG*, J. Glaum, University of New South Wales, Australia; C. Groh, Technische Universität Darmstadt, Germany; M. C. Ehmke, J. Blendell, Purdue University, USA; M. Hoffman, University of New South Wales, Australia

S2: Multiferroic Materials and Multilayer Ferroic Heterostructures: Properties and Applications

Novel Multiferroic Materials and Other Functional Oxides I

Room: Indian

Session Chair: Jonathan Spanier, Drexel University

10:00 AM

(EMA-S2-031-2014) Characteristics of PZTFT: A New Room-Temperature Multiferroic (Invited)

D. M. Evans, Queens University Belfast, United Kingdom; M. Alexe, University of Warwick, United Kingdom; J. F. Scott, University of Cambridge, United Kingdom; M. Gregg*, Queens University Belfast, United Kingdom

10:30 AM

(EMA-S2-032-2014) Polymer-assisted deposition for a wide range of epitaxial ferroic metal-oxide films (Invited)

Q. X. Jia*, Los Alamos National Laboratory, USA; M. Jain, University of Connecticut, USA; H. Luo, Texas A&M University, USA; E. Bauer, Los Alamos National Laboratory, USA; H. Wang, Texas A&M University, USA; T. M. McCleskey, A. K. Burrell, Los Alamos National Laboratory, USA

11:00 AM

(EMA-S2-033-2014) Controlling Metal-to-Insulator Transitions in Complex Oxide Heterostructures (Invited)

S. Stemmer*, University of California, Santa Barbara, USA

11:15 AM

(EMA-S2-034-2014) Vertical interface effects in multiferroic nanocomposite thin films (Invited)

H. Yang*, Soochow University, China; H. Wang, Texas A&M University, USA; J. L. MacManus-Driscoll, University of Cambridge, United Kingdom; Q. Jia, Los Alamos National Laboratory, USA

11:30 AM

(EMA-S2-035-2014) Electronic and Vibrational Properties of Complex Metal Oxides (Invited)

S. Zollner*, New Mexico State University, USA

11:45 AM

(EMA-S2-036-2014) Ferroelectric behaviour in strained thin films of anatase TiO₂ (Invited)

N. Deepak, M. E. Pemble, L. Keeney, R. W. Whatmore*, Tyndall National Institute, Ireland

12:00 PM

(EMA-S2-037-2014) Energy Landscape in Frustrated Systems: Cation Hopping in Pyrochlores (Invited)

J. C. Nino*, U of Florida, USA

12:15 PM

(EMA-S2-038-2014) Formation mechanisms and functionalities in a new supercell structure by the co-growth of BiFeO₃ and BiMnO₃

A. Chen*, Los Alamos National Laboratory, USA; Y. Zhu, Texas A&M University, USA; Z. Bi, Los Alamos National Laboratory, USA; H. Zhou, North Carolina State University, USA; J. L. MacManus-Driscoll, University of Cambridge, United Kingdom; J. Narayan, North Carolina State University, USA; Q. Jia, Los Alamos National Laboratory, USA; H. Wang, Texas A&M University, USA

S6: Thermoelectrics: Defect Chemistry, Doping and Nanoscale Effects

Theory and Novel Materials

Room: Coral A

Session Chair: Doreen Edwards, Alfred University

9:45 AM

(EMA-S6-001-2014) Recent Progress in the Development of Thermoelectric Generators (Invited)

J. D. Koenig*, Fraunhofer IPM, Germany

10:15 AM

(EMA-S6-002-2014) Methods of Thermoelectric Efficiency Enhancement for Power Generation Applications (Invited)

Y. Gelbstein*, Ben-Gurion University, Israel

10:45 AM

(EMA-S6-003-2014) Nano-scale Enhancement via Bottom-up Processing of Thermoelectric Materials

K. Wei*, G. S. Nolas, University of South Florida, USA

11:00 AM

(EMA-S6-004-2014) Alkaline earth hexaborides: the effect of dopant additions on thermoelectric properties

M. Alberg*, D. D. Edwards, Alfred University, USA

11:15 AM

(EMA-S6-014-2014) Synthesis of nanostructured Oxides and Oxynitrides for thermoelectric converters

A. Weidenkaff*, W. Xie, X. Xiao, L. Sagarna, G. Saucke, P. Thiel, L. Karvonen, A. Shkabko, EMPA, Switzerland

11:30 AM

(EMA-S6-006-2014) High Performance, High Efficiency Rare-Earth-Based Thermoelectric Materials for Space Power Generation Applications (Invited)

S. Bux*, T. Vo, Jet Propulsion Laboratory/California Institute of Technology, USA; J. Grenkemper, Y. Hu, University of California Davis, USA; J. Ma, S. Clarke, University of California Los Angeles, USA; J. Pfluger, California Institute of Technology, USA; C. Huang, D. Uhl, T. Caillat, P. Von Allmen, Jet Propulsion Laboratory/California Institute of Technology, USA; S. Kauzlarich, University of California Davis, USA; J. Fleuriel, Jet Propulsion Laboratory/California Institute of Technology, USA

12:00 PM

(EMA-S6-007-2014) Discovering New and Old Thermoelectrics Using Transport Theory (Invited)

D. J. Singh*, Oak Ridge National Laboratory, USA

S9: Thin Film Integration and Processing Science

Processing and Integration of Ferroelectric Thin Films

Room: Coral B

Session Chair: Jon Ihlefeld, Sandia National Laboratories

10:00 AM

(EMA-S9-019-2014) Understanding dewetting in metallic thin films through in-situ scanning confocal laser microscopy (Invited)

N. Valanoor*, University of New South Wales, Australia

10:30 AM

(EMA-S9-011-2014) Flux-assisted growth of BaTiO₃ thin films

D. T. Harris*, M. J. Burch, J. Ihlefeld, P. G. Lam, J. Li, E. C. Dickey, J. Maria, North Carolina State University, USA

10:45 AM

(EMA-S9-012-2014) Microstructural Characterization of Flux-Grown BaTiO₃ Thin Films

M. J. Burch*, D. T. Harris, J. Li, J. Maria, E. C. Dickey, North Carolina State University, USA

11:00 AM

(EMA-S9-013-2014) Chemical Solution Processing of High Performance Piezoelectric Thin and Ultra-Thin Films (Invited)

N. Bassiri-Gharb*, Y. Bastani, S. Brewer, Georgia Institute of Technology, USA

11:30 AM

(EMA-S9-014-2014) In situ x-ray diffraction during crystallization of solution-derived ferroelectric films (Invited)

J. L. Jones*, North Carolina State University, USA; S. Mhin, University of Florida, USA; G. L. Brennecke, J. Ihlefeld, Sandia National Laboratories, USA; R. G. Polcawich, L. M. Sanchez, US Army Research Laboratory, USA

12:00 PM

(EMA-S9-015-2014) Compositional Study of Solution Deposited (Bi_{0.5}Na_{0.5})TiO₃ - (Bi_{0.5}K_{0.5})TiO₃ - Bi(Mg_{0.5}Ti_{0.5})O₃ Thin Films

J. E. Mendez*, J. Walenza-Slabe, N. Kumar, D. P. Cann, B. J. Gibbons, Oregon State University, USA

12:15 PM

(EMA-S9-016-2014) Solution-Derived Bi(Zn,Ti)O₃ - BaTiO₃ Thin Films with Bulk-like Permittivity

R. P. Wilkerson, University of California - Berkeley, USA; K. E. Meyer, New Mexico Institute of Mining and Technology, USA; P. G. Kotula, G. L. Brennecke*, Sandia National Laboratories, USA

S12: Recent Developments in High-Temperature Superconductivity

YBCO based Coated Conductors, Pinning Properties and Applications

Room: Mediterranean B/C

Session Chair: Judy Wu, University of Kansas

10:00 AM

(EMA-S12-014-2014) Improvement of Spatial Homogeneity and In-field Critical Current in RE-123 Coated Conductors (Invited)

T. Kiss*, K. Higashikawa, S. Gangl, K. Imamura, M. Inoue, Kyushu University, Japan; T. Taneda, A. Ibi, T. Yoshida, M. Yoshizumi, T. Izumi, Y. Shiohara, International Superconductivity Technology Center, Japan; K. Kimura, T. Koizumi, N. Aoki, T. Hasegawa, SWCC Showa cable systems Co., Ltd, Japan

10:30 AM

(EMA-S12-015-2014) Status of coated conductor development for coil applications in high magnetic fields at low temperatures (Invited)

V. Selvamanickam*, A. Xu, Y. Liu, N. Khatir, L. Delgado, E. Galtsyan, X. Li, G. Majkic, University of Houston, USA

11:00 AM

(EMA-S12-016-2014) Laser Chemical Vapor Deposition for High-J_c YBa₂Cu₃O_{7-δ} films (Invited)

A. Ito*, P. Zhao, T. Goto, Institute for Materials Research, Tohoku University, Japan

11:30 AM

(EMA-S12-017-2014) Kinetics and dynamics of double doping nanostructure self-assembly in YBCO films (Invited)

J. Wu*, J. Baca, J. Shi, University of Kansas, USA; T. Haugan, M. Sabastian, U.S. Air Force Research Laboratory, USA; B. Maiorov, T. Holesinger, Los Alamos National Laboratory, USA

12:00 PM

(EMA-S12-019-2014) Designed Flux Pinning Landscapes in YBa₂Cu₃O_{7-δ} Thin Films by incorporating CoFe₂O₄:CeO₂ Vertically Aligned Nanocomposites

J. Huang*, C. Tsai, L. Chen, H. Wang, Texas A&M University, USA

S1: Functional and Multifunctional Electroceramics for Commercialization

Piezoelectric Energy Harvesting

Room: Pacific

Session Chair: Shujun Zhang, Penn State University

1:30 PM

(EMA-S1-042-2014) Synthesis of K_{0.5}NbO₃ Nanowires and Their Application to Flexible Piezoelectric Energy Harvesters (Invited)

S. Nahm*, M. Joung, H. Xu, J. Kim, I. Seo, Korea University, Republic of Korea; S. Yoon, C. Kang, Korea Institute of Science and Technology, Republic of Korea

2:00 PM

(EMA-S1-043-2014) Confinement Printing of Thin Film Lead Zirconate Titanate (Invited)

S. Trolier-McKinstry*, A. Welsh, Penn State, USA; D. Dezest, L. Nicu, CNRS, France

2:30 PM

(EMA-S1-044-2014) Microstructural origin for the piezoelectricity evolution in (K_{0.5}Na_{0.5})NbO₃-based lead-free ceramics

H. Guo*, Iowa State University, USA; S. Zhang, Pennsylvania State University, USA; S. P. Beckman, X. Tan, Iowa State University, USA

S2: Multiferroic Materials and Multilayer Ferroic Heterostructures: Properties and Applications

Novel Multiferroic Materials and Other Functional Oxides II

Room: Indian

Session Chair: Nick Sbrockey, Structured Materials Industries, Inc.

2:00 PM

(EMA-S2-039-2014) Metal-insulator transition-based oxide electronics (Invited)

S. Ramanathan*, Harvard Univ, USA

2:30 PM

(EMA-S2-040-2014) Reversible redox reactions in epitaxial SrCoO_x oxygen sponges (Invited)

H. Lee*, Oak Ridge National Laboratory, USA

3:00 PM

(EMA-S2-041-2014) Voltage Tunable Microwave Resonators Fabricated with MOCVD deposited Ba_{1-x}Sr_xTiO₃ Films (Invited)

N. M. Sbrockey*, Structured Materials Industries, Inc., USA; T. Kalkur, E. Nowe, University of Colorado at Colorado Springs, USA; S. Alpay, H. Khassaf, University of Connecticut, USA; G. S. Tompa, Structured Materials Industries, Inc., USA

3:15 PM

(EMA-S2-042-2014) Deposition of YIG and BST Films on Metals and Growth of Low-Damping Nanometer-Thick YIG Films (Invited)

M. Wu*, Y. Sun, T. Liu, H. Chang, M. Kabatek, Y. Song, W. Schneider, Colorado State University, USA; V. Vlaminck, H. Schultheiss, A. Hoffmann, Argonne National Laboratory, USA

3:30 PM

Break

4:00 PM

(EMA-S2-043-2014) Monolithic Multiferroic Thin Film Heterostructure Fabrication via an Automated Chemical Solution Deposition Process (Invited)

X. Guo*, H. Song, Y. Wang, K. K. Li, Y. K. Zou, H. Jiang, Boston Applied Technologies, Inc., USA; S. S. Puranam, A. Gopinath, University of Minnesota, USA; M. Wu, Colorado State University, USA

4:15 PM

(EMA-S2-044-2014) MOCVD of Complex Oxides for Multiferroic and Multiferroic Composite Thin Film Production (Invited)

G. S. Tompa, N. M. Sbrockey*, Structured Materials Industries, Inc., USA

4:30 PM

(EMA-S2-045-2014) A facile route for single-crystal heteroepitaxial ferroic perovskite oxide thin films (Invited)

J. Spanier*, Drexel University, USA

4:45 PM

(EMA-S2-046-2014) Hardware Modifications of ARL's MOCVD System and Fabrication of SrTiO₃ Thin Films

E. Enriquez*, UTSA, USA; D. Shreiber, M. Will-Cole, Army Research Lab, USA

5:00 PM

(EMA-S2-047-2014) CoWO₄ nanoparticles synthesized by microwave-hydrothermal technology: catalytic oxidation of terpenes

A. Dias, P. Robles-Dutenehner*, UFOP, Brazil

S6: Thermoelectrics: Defect Chemistry, Doping and Nanoscale Effects

Oxides, Films and Defects

Room: Coral A

Session Chair: Sabah Bux, Jet Propulsion Laboratory/California Institute of Technology

2:00 PM

(EMA-S6-008-2014) Understanding the defect chemistry to control electrical conduction in polar titanates (Invited)

D. Sinclair*, University of Sheffield, United Kingdom

2:30 PM

(EMA-S6-009-2014) High temperature thermoelectric properties of SrTiO₃ under controlled pO₂

H. J. Brown-Shaklee*, P. A. Sharma, J. Ihlefeld, Sandia National Laboratories, USA

2:45 PM

(EMA-S6-010-2014) The effects of niobium doping and oxygen partial pressure on the thermoelectric properties of beta-gallia rutile intergrowths

K. J. Scott*, M. Alberga, D. D. Edwards, Alfred University, USA

3:00 PM

(EMA-S6-011-2014) Temperature dependent thermal conductivity of nano-grained Barium Titanate (BaTiO₃)

B. F. Donovan*, B. M. Foley, University of Virginia, USA; J. Ihlefeld, B. B. McKenzie, Sandia National Laboratories, USA; P. E. Hopkins, University of Virginia, USA

3:15 PM

(EMA-S6-012-2014) Spin-state control in cobalt oxides (Invited)

I. Terasaki*, Nagoya University, Japan

3:45 PM

(EMA-S6-013-2014) Thermoelectric transition metal oxides and sulfides: a comparison between itinerant ferromagnets

A. Maignan*, LABORATOIRE CRISMAT CNRS ENSICAEN UCBN, France

4:00 PM

(EMA-S6-005-2014) Si/Ge Nano-structured with Tungsten Silicide Inclusions

J. Mackey*, University of Akron, USA; A. Sehirlioglu, Case Western Reserve University, USA; F. Dynys, Nasa Glenn Research Center, USA

4:15 PM

(EMA-S6-015-2014) Cutting-Edge Room Temperature Thermoelectric Properties of AZO Thin Films

J. Loureiro*, R. Santos, J. Figueira, M. Ferreira, I3N-CENIMAT/UNINOVA, Portugal; S. Reparaz, C. Sotomayor, Catalan Institute of Nanoscience and Nanotechnology ICN2, Spain; R. Martins, I. Ferreira, I3N-CENIMAT/UNINOVA, Portugal

4:30 PM

(EMA-S6-016-2014) All-solution processed InGaO₃(ZnO)_m superlattice films with coarsened grains of c-axis preferred orientation

S. Cho*, Y. Kwon, H. Cho, Sungkyunkwan University, Republic of Korea

4:45 PM

(EMA-S6-017-2014) Thermoelectric Oxide Ga_{3-x}In_{5+x}Sn₂O₁₆ Properties Using Spark Plasma Sintering

C. E. Dvorak*, D. Edwards, Alfred University, USA

5:00 PM

(EMA-S6-018-2014) Experimental determination of phonon mean free paths in complex crystals

P. Hopkins*, B. M. Foley, B. F. Donovan, R. Cheaito, J. T. Gaskins, University of Virginia, USA; H. J. Brown-Shaklee, J. Ihlefeld, Sandia National Laboratories, USA

5:15 PM

(EMA-S6-019-2014) Thermoelectric modules using p-type CuZnO and n-type NiZnO thin film oxides

J. Loureiro*, R. Santos, J. Figueira, M. Ferreira, A. Rodrigues, R. Martins, I. Ferreira, I3N-CENIMAT/UNINOVA, Portugal

S9: Thin Film Integration and Processing Science

Substrates, Metallization, and Integration

Room: Coral B

Session Chair: Edward Sachet, North Carolina State University

2:00 PM

(EMA-S9-017-2014) Seed Layer TiO₂ Structure Impact on {111}-Textured Pt Electrodes for PZT Devices (Invited)

G. R. Fox*, Fox Materials Consulting, LLC, USA; D. M. Potrepka, R. G. Polcawich, US Army Research Laboratory, USA; D. A. Cullen, Oak Ridge National Laboratory, USA

2:30 PM

(EMA-S9-018-2014) The Influence of Microscopic Degrees of Freedom on Equilibrated Orientation Relationships between Pt and SrTiO₃

G. Atiya, A. Altberg, V. Mikhelashvili, G. Eisenstein, W. D. Kaplan*, Technion - Israel Institute of Technology, Israel

2:45 PM

(EMA-S9-010-2014) Adaptive Optics Systems Based on PZT Thin Films with Integrated ZnO Electronics (Invited)

R. H. Wilke*, R. L. Johnson-Wilke, M. L. Wallace, The Pennsylvania State University, USA; J. I. Ramirez, T. L. Jackson, The Pennsylvania State University, USA; V. Cotroneo, S. McMuldroch, P. B. Reid, D. A. Schwartz, Harvard-Smithsonian Center for Astrophysics, USA; S. Trolier-McKinstry, The Pennsylvania State University, USA

3:15 PM

(EMA-S9-020-2014) Electrochromism vs. the Bugs: Developing WO₃ Thin Film Windows to Control Photoactive Biological Systems

L. J. Small*, S. Wolf, E. Courchaine, V. S. Vandelinder, D. R. Wheeler, G. Bachand, E. D. Spörke, Sandia National Laboratories, USA

3:30 PM

Break

4:00 PM

(EMA-S9-021-2014) Molecular "Popoids": Assembling Functional Supramolecular Nanocrystal Films on Chemically-Modified Surfaces

E. Spörke*, D. V. Gough, J. S. Wheeler, T. N. Lambert, V. Stavila, K. Leong, M. D. Allendorf, Sandia National Laboratories, USA

4:15 PM

(EMA-S9-022-2014) Nucleation and Passivation of Al₂O₃ and TiO₂ Thin Films Formed by Atomic Layer Deposition on Polymeric Substrates

H. I. Akyildiz*, Y. Sun, J. S. Jur, North Carolina State University, USA

4:30 PM

(EMA-S9-023-2014) Fabrication of superhydrophobic silica-stainless steel composite through electrophoretic deposition

R. Corpuz*, MSU-IIT, Philippines; L. De Juan, University of the Philippines Diliman, Philippines

4:45 PM

(EMA-S9-024-2014) Sodium ion conductivity and scaling effects in NASICON thin films prepared via chemical solution deposition

J. Ihlefeld*, W. Meier, M. Rodriguez, B. B. McKenzie, A. Allen, M. Blea, A. McDaniel, Sandia National Laboratories, USA

S12: Recent Developments in High-Temperature Superconductivity

New Superconductors, New Structures and Pinning Properties

Room: Mediterranean B/C

Session Chair: Claudia Antoni, Oak Ridge National Laboratory

1:30 PM

(EMA-S12-020-2014) High critical current densities in Ba-122 thin films by self-assembled and artificial pin arrays (Invited)

C. Tarantini*, F. Kametani, J. D. Weiss, J. Jiang, E. E. Hellstrom, J. Jaroszynski, National High Magnetic Field Laboratory, USA; S. Lee, C. Eom, University of Wisconsin, USA; D. C. Larbalestier, National High Magnetic Field Laboratory, USA

2:00 PM

(EMA-S12-021-2014) Exploring the variables controlling superconductivity in 122 arsenides by local-probe microscopy and spectroscopy techniques (Invited)

C. Antoni*, M. Pan, K. Gofryk, A. Sefat, B. I. Saparov, A. F. May, W. Lin, M. A. McGuire, B. C. Sales, Oak Ridge National Laboratory, USA

2:30 PM

(EMA-S12-007-2014) MgB₂ thin films for electronics and RF applications (Invited)

X. Xi*, Temple University, USA

3:00 PM

(EMA-S12-023-2014) Artificially engineered superlattices of pnictide superconductor (Invited)

C. Eom, A. Ruosi*, University of Wisconsin-Madison, USA

3:30 PM

Break

4:00 PM

(EMA-S12-024-2014) Vortex pinning and dynamics in Fe-based superconductors with naturally-grown and engineered pinning landscapes (Invited)

L. Civale*, Los Alamos National Laboratory, USA

4:30 PM

(EMA-S12-025-2014) Improvement and limitations of critical current densities in K-doped ferropnictide BaFe₂As₂ bulks and wires (Invited)

J. D. Weiss*, J. Jiang, C. Tarantini, F. Kametani, A. Polyanski, B. Hainsey, D. Larbalestier, E. Hellstrom, Florida State University, USA

5:00 PM

(EMA-S12-026-2014) Enhanced Superconducting Properties of FeSe_{0.1}Te_{0.9} Thin Films on STO and Glass Substrates

L. Chen, J. Huang, C. Tsai, Y. Zhu, J. Jian, A. Chen, Z. Bi, F. Khatkhatay, Texas A&M University, USA; N. Cornell, A. Zakhidov, University of Texas at Dallas, USA; H. Wang*, Texas A&M University, USA

Wednesday, January 22, 2014

Plenary Session I

Room: Indian

Session Chair: Steven Tidrow, University of Texas - Pan American

8:45 AM

(EMA-001-2014) Electrical and Electronic Materials for Industrial Applications (Invited)

J. W. Bray*, General Electric Global Research, USA

This talk will focus on emerging needs, opportunities and challenges for electrical and electronic materials in energy, power conversion, aviation, lighting, and transportation, as seen from an industry perspective. There will be some emphasis on experiences at GE and on ceramics.

S1: Functional and Multifunctional Electroceramics for Commercialization

Ferroelectric Composition Design and Property Characterization

Room: Pacific

Session Chair: Sahn Nahm, Korea University

10:00 AM

(EMA-S1-001-2014) Influence of Thermal History on Structure-Property Relations in Lead Zirconate Titanate Ceramics (Invited)

C. Chung, G. A. Rossetti*, University of Connecticut, USA

This talk will describe the influence of thermal history on the crystal structure, microstructure and properties of un-doped lead zirconate titanate (PZT) ceramics prepared by the sold-gel method. Long annealing above the Curie temperature after sintering resulted in a sharpening of the paraelectric to ferroelectric phase transition, larger extrinsic contributions to the dielectric response, and a higher degree of irreversible domain wall motion without a change in grain size. The changes in properties observed on annealing all showed extrema near the morphotropic phase boundary (MPB). The evolution of structural and dielectric properties with annealing time showed that dense ceramics cooled from high-temperature by natural convection were not in their equilibrium state near the MPB. However, no evidence of phase decomposition to form an equilibrium mixture of tetragonal and rhombohedral phases was found after annealing. Instead, a slow relaxation process was revealed that involved redistribution in the fractions of the two phases, a decrease in cell volume, an increase in spontaneous strain, and a coarsening of the domain structure that correlated with increased domain wall contributions to the permittivity. The results show that the domain structure and properties of PZT compositions near the MPB can be adjusted without dopants by processing under different thermal histories.

10:30 AM

(EMA-S1-002-2014) Anelastic, dielectric and mixed electro-mechanical response in perovskite materials (Invited)

D. Damjanovic*, A. Biancoli, S. Hashemi Zadeh, Swiss Federal Institute of Technology - EPFL, Switzerland; T. Rojac, H. Ursic, Jozef Stefan Institute, Slovenia

We report on a study of anelastic, dielectric and mixed, direct and converse piezoelectric / electro-mechanical responses of several materials with perovskite structure. The investigated materials include ferroelectric, paraelectric and relaxor materials such as $\text{Pb}(\text{Zr,Ti})\text{O}_3$, $(\text{Ba,Ca})(\text{Zr,Ti})\text{O}_3$, $(\text{Ba,Sr})\text{TiO}_3$, BiFeO_3 and $\text{Pb}(\text{Mg}_{1/3}\text{Nb}_{2/3})\text{O}_3$. The elastic, dielectric and piezoelectric / electro-mechanical properties are examined as a function of temperature

and frequency. Our study reveals that in some cases where usually only electrical processes are discussed (e.g., increase of dielectric loss at low frequencies, relaxor behavior), there appears to be a strong coupling with mechanical properties. This leads to non-negligible dependence of piezoelectric and anelastic coefficients on temperature and frequency. Implication of these results on understanding of properties of perovskite materials are discussed

11:00 AM

(EMA-S1-003-2014) High Temperature Ferroelectrics for Actuators: Recent Developments and Challenges (Invited)

A. Schirlioglu*, Case Western Reserve University, USA

A variety of piezoelectric applications have been driving the research in development of new high temperature ferroelectrics; ranging from broader markets such as fuel and gas modulation and deep well oil drilling to very specific applications such as thermoacoustic engines and ultrasonic drilling on the surface of Venus. The focus has been mostly on increasing the Curie temperature. However, greater challenges for high temperature ferroelectrics limit the operating temperature to levels much below the Curie temperature. These include enhanced loss tangent and dc conductivity at high fields as well as depoling due to thermally activated domain rotation. The initial work by Eitel et al. [Jpn. J. Appl. Phys., 40 [10, Part 1] 5999-6002 (2001)] increased interest in investigation of Bismuth containing perovskites in solid solution with lead titanate. Issues that arise vary from solubility limits to increased tetragonality; the former one prohibits processing of morphotropic phase boundary, while the latter one impedes thorough poling of the polycrystalline ceramics. This talk will summarize recent advances in development of high temperature piezoelectrics and provide information about challenges encountered as well as the approaches taken to improve the high temperature behavior of ferroelectrics with a focus on applications that employ the converse piezoelectric effect.

11:30 AM

(EMA-S1-004-2014) Characterization of Bariumtitanate by Thermal Analysis and Thermophysical Properties Techniques

E. Post*, E. Fueglein, NETZSCH Geraetebau GmbH, Germany; E. Lim, NETZSCH Instruments N.A., LLC, USA

BaTiO_3 is one of the classical ferroelectric materials with orthorhombic crystal lattice at room temperature and a Curie temperature at around 120°C. It undergoes several solid state phase transitions between -120°C and the melting at about 1625 °C. Thermal Analysis methods can help with the characterization of these structural changes, typically investigated by Differential Scanning Calorimetry (DSC). For studying of the sintering behavior the dilatometry is often employed. Impurities in the raw material like carbonates can easily be detected by Thermogravimetry (TG) coupled to evolved gas analysis, e.g. mass spectrometry (MS). Last but not least the thermal diffusivity/conductivity can be determined by LFA technique. BaTiO_3 samples were characterized by DSC, TG-DSC-MS, dilatometry and LFA. The methods and the results will be explained and discussed.

11:45 AM

(EMA-S1-005-2014) Effects of dopants on depoling temperature in modified BiScO_3 - PbTiO_3

B. Kowalski*, A. Schirlioglu, Case Western Reserve University, USA

In recent years there has been a renewed interest for high temperature piezoelectrics for both terrestrial and aerospace applications. These applications are limited in part by the operating temperature, which is usually taken as one half of the Curie temperature (T_c), and is ~200°C for one of the most widely used commercial piezoelectrics, $\text{Pb}(\text{Zr,Ti})\text{O}_3$ (PZT). In an effort to increase T_c , subsequent research into high temperature $\text{Bi}(\text{B}'\text{B}'')\text{O}_3$ - PbTiO_3 piezoelectrics led to the discovery of the morphotropic phase boundary (MPB) in the high- T_c BiScO_3 - PbTiO_3 (BS-PT) system with a T_c of 460°C

and a d_{33} of 460 pm/V. The T_c marks the ferroelectric to paraelectric phase transformation and while, in general, a phase transformation leads to thermal depoling in piezoelectrics with low or moderate T_c s, for high T_c piezoelectrics thermally assisted dipole rotation can lead to randomization of domains at temperatures below T_c . It becomes necessary to determine the depoling temperature (T_d) which dictates the actual working temperature range. By doping for Sc and Ti the T_d can be shifted while maintaining similar electromechanical properties as a function of temperature. The effect of this B-site doping on depoling temperature has been explored through the characterization of microstructure and weak/high field measurements.

12:00 PM

(EMA-S1-006-2014) Dielectric Relaxation of Pb(Mg_{1/3}Nb_{2/3})O₃-PbTiO₃ Relaxor Ferroelectric Ceramics in wide temperatures

L. Guorong*, L. Huang, W. Zhao, J. Zeng, L. Zheng, Shanghai Institute of Ceramics, Chinese Academy of Sciences, China; X. Xiong, Zhongshan University, China; A. Kassiba, Université du Maine, Avenue O. Messiaen, 72085 Le Mans, Cedex 09, France

PMN-PT based relaxor ferroelectric materials perform a high dielectric, piezoelectric and electro-optical properties. Many reports shown that these excellent properties are owing to the complex perovskite ABO₃ structures. The electric field can easily change the structural to increase the macro polarization, thus the high properties are obtained because all electric properties are proportional the polarization or its change. Dielectric coefficient is sensitive to the polarization change, the dielectric relaxation can be used to understand the structure change, e.g., the cations or the oxygen vacancy movements, phase transition, micro and nano domains transition. But few study report the dielectric relaxation coming from A, B, and O together. This study presents the A, B and O relaxation of PMN-PT based ferroelectric ceramics. The compositions are 0.65PMN O₃-(0.35-y) PT + yBaTiO₃, which are near the MPB where Ba partly replace Pb. Dielectric coefficient versus frequencies were measured in the temperature of -120 ~ 300°C. Dielectric relaxation occurring in the different temperatures are considered to result from A, B cation, and O vacancy. Raman spectroscopy, XRD, hysteresis loops, and the mechanical and loss versus frequencies in wide temperature range support the consideration. High piezoelectric properties at low temperatures can be explained by the A cation relaxation.

12:15 PM

(EMA-S1-007-2014) The crystal growth and properties of PIMNT ternary single crystals

J. Jiao*, J. Chen, X. Li, X. Wang, S. Wang, X. Zhao, H. Luo, The Shanghai Institute of Ceramics, Chinese Academy of Sciences, China

Ternary single crystals xPb(In_{1/2}Nb_{1/2})O₃-yPb(Mg_{1/3}Nb_{2/3})O₃-zPbTiO₃ (PIN-PMN-PT100x/100y/100z) have drawn attentions in recent years both owing to their high Curie temperature T_c and excellent piezoelectric properties near MPB. The PIMNT crystals were grown directly from melt by the Bridgman method for mass production, and the size reached $\Phi 75 \times 80$ mm³. The dielectric, ferroelectric and piezoelectric properties of PIMNT crystals with the composition near MPB were investigated. For PIMNT29/44/27, the depolarization temperature reaches up to $T_{rt} \sim 116^\circ\text{C}$, and $T_c \sim 172^\circ\text{C}$. For <001>-oriented PIMNT the coercive field E_c is 6.8 kV/cm, which is two times larger than that of PMNT crystal. The high piezoelectric constant $d_{33} \sim 2300$ pC/N was obtained. Compared with PMNT, the higher T_c and larger coercive field E_c make PIMNT crystals more broad range of practical device applications.

S2: Multiferroic Materials and Multilayer Ferroic Heterostructures: Properties and Applications

Bismuth Ferrite

Room: Indian

Session Chair: Ichiro Takeuchi, University of Maryland

10:00 AM

(EMA-S2-001-2014) Magnetoelectric Control of Exchange Coupling in Monodomain BiFeO₃ Heterostructures (Invited)

B. A. Davidson*, W. Saenrang, S. Ryu, J. P. Podkaminer, D. Lee, J. Frederick, T. Kim, S. Baek, M. S. Rzechowski, University of Wisconsin, USA; J. W. Freeland, Argonne National Laboratory, USA; C. Eom, University of Wisconsin, USA

Multiferroic materials that exhibit coupling of ferroelectric and antiferromagnetic ordering can form the basis of exchange-coupled heterostructures providing electric-field control of magnetization. Such structures provide new directions for novel spintronic devices, such as magnetic tunnel junctions whose resistance state is controlled by ferroelectric polarization. Here we investigate exchange coupling between monodomain multiferroic BiFeO₃ (BFO) and a ferromagnetic Co overlayer, using x-ray magnetic circular dichroism (XMCD), linear dichroism (XMLD) and anisotropic magnetoresistance (AMR). We demonstrate that the exchange coupling between BFO and Co occurs without the contribution of domain walls. The Co magnetization rotates by $\sim 20^\circ$ upon electric polarization reversal in the BFO at temperatures below ~ 150 K. Our AMR results, in which the Co longitudinal resistance (ρ_{xx}) changes upon inverting the BFO polarization, confirm the XMCD observation of Co magnetization rotation at low temperature. Its absence above 150 K may be explained by a magnetic surface dead layer in BFO, as revealed by XMLD measurements in surface-sensitive and bulk-sensitive configurations. In addition, the linear dichroism (LD) of BFO at low temperature is very large ($\sim 35\%$). These results are an important step toward intrinsic (i.e., not domain-wall mediated) room-temperature magnetoelectric device applications.

10:30 AM

(EMA-S2-002-2014) Phase evolution and structure-property correlations in rare-earth substituted bismuth ferrite thin films (Invited)

N. Valanoor*, University of New South Wales, Australia

The discovery of a morphotropic phase boundary (MPB) in Sm³⁺-substituted BFO thin films by combinatorial thin-film synthesis strategy (Fujino et al, Appl. Phys. Lett. 2008) motivates the talk. This particular boundary represents a structural phase transition from the ferroelectric rhombohedral phase to an orthorhombic phase exhibiting a double hysteresis in polarization vs. electric field (P-E) loops. Subsequent investigations using smaller trivalent A-site rare-earth (RE³⁺) dopants (RE = Dy, Gd and Sm) revealed the universal occurrence of the structural transition and concomitant change in the ferroelectric properties independent of the RE dopant species. The enhancement is correlated to the presence of a competing intermediate antipolar phase with the rhombohedral ferroelectric and non-polar orthorhombic phase. As a final step we show that the presence of the phase boundary can be systematically tuned in multilayered heterostructures. This work is a collaborative effort with the University of Maryland (Takeuchi group), Connecticut (Alpay/Wells group), Rutgers (Rabe group), ORNL (Borisevich and Kalinin), NAS Ukraine (Morozovska) and the National Chiao Tung University (Y.-H. Chu).

11:00 AM

(EMA-S2-003-2014) RE-doped BiFeO₃: a critical appraisal of their potential applications (Invited)

I. M. Reaney*, University of Sheffield, United Kingdom

It has been over 10 years since the first papers on BiFeO₃ were published suggesting the possibility of new devices based on magneto-electric coupling. However, no BiFeO₃-based devices have emerged despite extensive investigation by leading materials chemists and physicists. The question therefore is do these materials have genuine potential for applications. From a materials perspective, BiFeO₃ is conducting, its phase transition is too high and it is anti- rather than ferromagnetic. Three strong reasons why it is not suitable for magnetoelectric devices. This presentation will review how far have we come in solving these problems and suggests some novel ways in which BiFeO₃ could yield useful functional behaviour.

11:15 AM

(EMA-S2-004-2014) Domain walls and phase boundaries - new nanoscale functional elements in complex oxides (Invited)

J. Seidel*, The University of New South Wales, Australia

Interfaces and topological boundaries in complex oxide materials, such as domain walls and morphotropic phase boundaries, have recently received increasing attention due to the fact that their properties, which are linked to the inherent order parameters of the material, its structure and symmetry, can be completely different from that of the bulk material [1]. I will present an overview of recent results on electronic and optical properties of ferroelectric phase boundaries, domain walls, and topological defects in multiferroic materials [2, 3, 4]. The origin and nature of the observed confined nanoscale properties is probed using a combination of nanoscale transport measurements based on scanning probe methods, high resolution transmission electron microscopy and first-principles density functional computations. I will also give an outlook on how these special properties can be found in other material systems and discuss possible future applications [5]. 1. J. Seidel, et al., Nature Materials 8, 229 (2009) 2. J. Seidel, et al., J. Phys. Chem. Lett. 3, 2905 (2012) 3. J. Seidel, et al., Phase Trans. 86, 53 (2013) 4. A. Lubk et al., Nano Lett. 13, 1410 (2013) 5. G. Catalan, J. Seidel, R. Ramesh, and J. Scott, Rev. Mod. Phys. 84, 119 (2012)

11:30 AM

(EMA-S2-005-2014) Piezoresponse behavior at a Morphotropic Phase Boundary in (Bi,Sm)FeO₃ Films (Invited)

S. Yasui*, Y. Ehara, T. Shiraishi, T. Shimizu, H. Funakubo, M. Itoh, Tokyo Institute of Technology, Japan; Y. Imai, H. Tajiri, Japan Synchrotron Radiation Research Institute/SPRING-8, Japan; O. Sakata, National Institute for Materials Science/SPRING-8, Japan; I. Takeuchi, University of Maryland, USA

Piezoelectric microelectromechanical-systems (MEMS) are widely used for actuators, sensors and other devices. Pb-contained piezoelectric materials such as Pb(Zr,Ti)O₃ [PZT] and Pb(Mg,Nb)O₃-PbTiO₃ [PMN-PT] with superior piezoresponse and electromechanical properties are commonly used in piezo-MEMS. However, Pb-based materials are toxic, and there is an urgent need to replace those materials. In this work, we propose Pb-free (Bi,Sm)FeO₃ [BSFO] as a new piezoelectric material which has a perovskite structure. Epitaxial BSFO films prepared on (100)SrRuO₃/(100)SrTiO₃ substrates by pulsed laser deposition display robust piezoresponse at the morphotropic phase boundary composition. The origin of piezoelectricity is investigated by in-situ synchrotron-HR-XRD under pulsed applied electric field. We find that the large piezoresponse in BSFO at this composition originates from an extrinsic effect of field-induced phase transition from an antiferroelectric phase to a ferroelectric phase. Maximum longitudinal piezoresponse (d_{33}) of approximately 240 pm/V was detected based on displacement of diffraction peaks measured under electric field.

11:45 AM

(EMA-S2-006-2014) Piezoelectric Nonlinearity and Dynamics of Electric-Field-Driven Structural Phase Transitions in Multiferroics (Invited)

M. Cosgriff, P. Chen, University of Wisconsin-Madison, USA; J. Jo, Gwangju Institute of Science and Technology, Republic of Korea; Z. Chen, L. Chen, Nanyang Technological University, Singapore; P. Evans*, University of Wisconsin-Madison, USA

Bismuth ferrite thin films and heterostructures have a series of properties that result from the existence of several competing structural phases. We have shown using time-resolved synchrotron x-ray microdiffraction techniques that the functional consequences of this competition of phases include nonlinearity of the piezoelectric response of thin films and rapid reversible field-induced structural phase transitions. In thin films of BiFeO₃ grown on substrates with relatively large lattice constants, the system is effectively far from the phase transition and only the piezoelectric nonlinearity is observed. Multiple structural phases, however, can be simultaneously stabilized by compressive stress on substrates with smaller lattice constants. Applied electric fields redistribute intensity among the reflections arising from these competing phases on a characteristic timescale of approximately 100 ns. The transition between phases can be driven in the opposite direction by reversing the sign of the applied electric field, leading to the possibility that phase transitions can be rapidly and reversibly applied in device structures.

12:00 PM

(EMA-S2-007-2014) Ferroelectric field effect with supertetragonal BiFeO₃

S. Fusil*, V. Garcia, Unité Mixte CNRS/Thales, France; H. Yamada, National Institute of Advanced Industrial Science and Technology (AIST), Japan; M. Marinova, Laboratoire de Physique des Solides, France; S. Boyn, Unité Mixte CNRS/Thales, France; A. Gloter, Laboratoire de Physique des Solides, France; J. Villegas, M. Bibes, A. Barthélemy, Unité Mixte CNRS/Thales, France

Ferroelectric field-effect allows non-volatile electrical control of electronic devices. We exploit a recently discovered high polarization polymorph of BiFeO₃ with giant axial ratio (T-BFO) to achieve field-induced changes at room temperature. This active material is used as a gate in three-terminal lateral devices as well as a barrier in tunnel junctions. We report a large ferroelectric field-effect in perovskite heterostructures composed of the Mott insulator CaMnO₃ (CMO) and the ferroelectric T-BFO. Upon polarization reversal of the T-BFO ferroelectric gate, the CMO channel exhibits a non-volatile resistance switching by a factor of 4 around room temperature, and up to a factor of 10 at 200 K [1]. In ferroelectric tunnel junctions, switching the polarisation and consequently their asymmetric electrostatic potential distribution yields tunnel electroresistance (TER). Tunnel junctions based on T-BFO tunnel barriers exhibit very large TER (>10000 at 300K). Using piezoresponse force microscopy, we illustrate that the changes in resistance are related to the nucleation and domain growth in BiFeO₃ [2]. [1] H. Yamada et al., Scientific Reports (accepted). [2] H. Yamada et al., ACS Nano 7, 5385-5390 (2013)

12:15 PM

(EMA-S2-008-2014) Domain and Domain Boundary Influences on switching for Multiferroics (Invited)

L. Ye, J. Leveille, A. McDannald, B. Moffitt, N. Polomoff, M. Jain, University of Connecticut, USA; J. Ihlefeld, Sandia National Laboratories, USA; B. Huey*, University of Connecticut, USA

Switching in ferroelectrics and multiferroics is directly observed High Speed SPM. Building on previous work visualizing domains and domain walls, domain wall densities are presented as a function of polarization variants for BFO, as well as with respect to composition for PZT. The influence of such domain boundaries on switching processes, switching speeds, and even electronic and

thermal transport are reported. This includes electron transport in the vicinity of switched domains, in some cases profoundly affecting new domain nucleation and growth. Direct indications of magnetic and ferroelectric coupling are mapped as well.

S3: Structure of Emerging Perovskite Oxides: Bridging Length Scales and Unifying Experiment and Theory

Local Structure and Phase Transitions

Room: Coral B

Session Chair: Igor Levin, National Institute of Standards and Technology

10:00 AM

(EMA-S3-001-2014) Critical Issues in Ferroelectrics: a TEM perspective (Invited)

I. M. Reaney*, University of Sheffield, United Kingdom

The advancement of TEM techniques in the last 10 years has been little short of astonishing. Moreover, focused ion beam thinning has improved dramatically, revolutionising sample preparation and allowing bespoke regions of a device/material to be studied. Up until ~2000, lab based advanced TEM techniques utilised a combination of diffraction contrast imaging, PEELS/EDS, high resolution imaging and electron diffraction. These conventional techniques are very powerful and are the basis of all initial studies but a plethora of further techniques are now available such as fast fourier filtering to directly image local structure, aberration corrected STEM/TEM using HAADF for atomic resolution density contrast imaging, digital LACBED for the determination of local symmetry and ultra high spatial resolution PEELS for compositional analysis at the atomic level. This presentation illustrates how these new techniques supplemented by conventional TEM give new insight into domain structure, defect chemistry and atomic structure of ferroelectrics.

10:30 AM

(EMA-S3-002-2014) Local structural disorder and its influence on the average global structure and ferroelectric properties of lead-free $\text{Na}_1/2\text{Bi}_{1/2}\text{TiO}_3$ (Invited)

R. Ranjan*, B. Rao, Indian Institute of Science Bangalore, India

A comparative study of the local and global structures of electrically poled and unpoled specimens of $\text{Na}_1/2\text{Bi}_{1/2}\text{TiO}_3$ by electron, synchrotron and neutron diffraction, in conjunction with first principles study, proved that the recently reported monoclinic (Cc) structure does not correspond to the ground state. The monoclinic like distortion observed in high resolution bulk diffraction techniques is rather a manifestation of lattice strain induced by localized in-phase tilted octahedral regions which are incompatible with the global rhombohedral (R3c) structure. The ground state rhombohedral (R3c) structure is clearly revealed in bulk diffraction techniques once the system is freed from the structural heterogeneity due to the local in-phase tilted octahedral regions. The study also demonstrates the predominant role of rhombohedral incompatible in-phase octahedral tilts in determining the polar properties of this ferroelectric compound.

11:00 AM

(EMA-S3-003-2014) Scale-dependent symmetries in $\text{Na}_0.5\text{Ba}_{0.5}\text{TiO}_3$ (Invited)

R. Beanland*, D. Keeble, University of Warwick, United Kingdom; S. Gorfman, Universität Siegen, Germany; P. Thomas, University of Warwick, United Kingdom

Sodium Bismuth Titanate (NBT) is a leading contender to replace the environmentally toxic lead-containing piezoelectrics. Studies of NBT have revealed a complex interplay between structure and

symmetry, often leading to contradictory interpretations of experimental data. Here, we summarize investigations from several methods including birefringence, X-ray, neutron and electron diffraction and transmission electron microscopy. Neutron diffraction data, in agreement with observations from several groups, show Bi-O bond lengths are $\sim 2.2\text{\AA}$. This is inconsistent with a conventional R3c a-a-a- perovskite structure. Nevertheless, on the scale of a few nm in a clean high-quality crystal, we present evidence for the average structure of NBT being rhombohedral at room temperature using new 'digital' electron diffraction measurements, while X-ray diffraction data and birefringence microscopy results often point to a monoclinic symmetry. We reconcile these observations by considering the differences between local and average structure as sampled by the different techniques. We also show that defects have a crucial role to play, especially those which form due to the breaking of symmetry, since their local structure is – by definition – different from that of the bulk. We show how their interaction can lead to a complex microstructure and consider their role in phase transformations and functional properties.

11:30 AM

(EMA-S3-004-2014) Perovskite Phases and Their Transformations in Lead-Free Piezoelectric Ceramics (Invited)

H. Guo, C. Ma, X. Tan*, Iowa State Univ, USA

TEM study was carried out on the $(\text{Bi}_{1/2}\text{Na}_{1/2})\text{TiO}_3$ -, $(\text{K}_{0.5}\text{Na}_{0.5})\text{NbO}_3$ - and BaTiO_3 -based piezoceramics. Using a novel method for analysis of the multi-domain state, we discovered a new phase boundary in $(1-x)(\text{Bi}_{1/2}\text{Na}_{1/2})\text{TiO}_3$ - $x\text{BaTiO}_3$; the observations support the recently proposed Cc symmetry for pure $(\text{Bi}_{1/2}\text{Na}_{1/2})\text{TiO}_3$, and, more importantly, indicate the crystal structure evolves into the R3c symmetry with the addition of BaTiO_3 , forming a Cc/R3c phase boundary at $x = 3\sim 4\%$. In the poling field Epol vs. composition x phase diagram for polycrystalline ceramics, this phase boundary exists with Epol below 5.5 kV/mm; the Cc phase is transformed to the R3c phase during poling at higher fields. The results reported here provide the microstructural origin for the previously unexplained strain behavior and clarify the low- BaTiO_3 -content phase relationship in this popular lead-free piezoelectric system. In the $0.948(\text{K}_{0.5}\text{Na}_{0.5})\text{NbO}_3$ - 0.052LiSbO_3 ceramic, it was found that the origin of the excellent piezoelectric performance was due to a tilted monoclinic phase that emerges when poling fields greater than 14 kV/cm were applied. During poling of the $0.5\text{Ba}(\text{Ti}_{0.8}\text{Zr}_{0.2})\text{O}_3$ - $0.5(\text{Ba}_{0.7}\text{Ca}_{0.3})\text{TiO}_3$ ceramic, it was observed that the initial multidomain state transformed to a single domain state at very low fields ($2\sim 4\text{ kV/cm}$), then reappeared at higher poling fields.

12:00 PM

(EMA-S3-005-2014) Unusual Phase Behaviour in NaNbO_3 and its Derivatives (Invited)

P. Lightfoot*, University of St Andrews, United Kingdom

Sodium niobate, NaNbO_3 , is one of the most structurally complex ferroelectric perovskites known, and has enjoyed renewed interest as a potential replacement for PZT, owing to its high piezoelectric responses. In this talk I will present two unusual aspects of the structural chemistry of NaNbO_3 and its derivatives. First, the high temperature phase diagram of NaNbO_3 itself, within which we have suggested new crystallographic models for two of the more complex and elusive phases (R and S), both of which adopt complex long-range modulations of the basic perovskite structure, due to unusual octahedral tilt patterns. Second, the compositional phase diagram, at ambient temperature, of the Li-doped system $\text{Li}_x\text{Na}_{1-x}\text{NbO}_3$. Here we find an unusual phase co-existence/competition whereby the phases present depend on a variety of factors including simply the time that the as-made samples are left standing under ambient conditions. Both these observations suggest there is an unusually high level of inherent structural frustration in NaNbO_3 -based perovskites, which merits further study by a wider range of experimental and theoretical techniques. For each of our studies we use primarily powder

diffraction (especially neutron diffraction) to probe the long range structure of our materials. We also use solid state NMR to complement this, which reveals details of the local structure.

S4: LEDs and Photovoltaics - Beyond the Light: Common Challenges and Opportunities

LED and PV Materials

Room: Caribbean B

Session Chairs: Adam Scotch, OSRAM SYLVANIA, Inc.; Erik Spörke, Sandia National Laboratories

10:00 AM

(EMA-S4-001-2014) Scattering and Light Extraction from Bulk Polycrystalline Ceramic Phosphors (Invited)

A. Lenef*, J. Kelso, A. Piquette, OSRAM SYLVANIA Inc, USA

Ceramic phosphors are advantageous for LED conversion because of their excellent thermal and optical properties. High luminance applications, such as automotive or projection in particular, have large benefits with ceramic phosphors because of the increased thermal conduction through the ceramic and consequent reduction in thermal quenching. A second benefit of polycrystalline ceramic phosphors is their high light extraction efficiency because of the combination of very low optical losses in the bulk material and process controllable volume scattering. Light extraction can be understood as a light recycling effect in which rays initially emitted outside the critical angle cone of the phosphor-external medium interface will have some probability of escape after volume scattering by pores or grain boundary interfaces in the ceramic. We first discuss the light extraction problem through spontaneous emission into scattering-coupled trapped and free radiation modes. This is an alternative picture to the geometric optics picture of light-recycling by scatterers. Then we describe modeling and experimental data, showing the relation between the scattering length and extraction in typical LED configurations with Ce:GdYAG ceramic phosphors. Finally, we show some examples of surface enhanced extraction from high transparency ceramic phosphors with the potential for high overall conversion efficiency.

10:30 AM

(EMA-S4-002-2014) Spatially Resolved Chemical and Electronic Structure of Thin-Film Photovoltaics (Invited)

C. K. Chan*, G. L. Kellogg, Sandia National Laboratories, USA; L. Mansfield, R. Noufi, National Renewable Energy Laboratory, USA

Thin-film chalcogenide semiconductors make promising photovoltaic materials because of their high optical absorption and potentially low-cost manufacturing. $\text{Cu}(\text{In}_{1-x}\text{Ga}_x)\text{Se}_2$ (CIGS) has been a particularly interesting material because, despite its disordered microcrystalline structure, it holds the record for thin-film solar power conversion efficiency (> 20%). Even with this achievement, large-scale commercialization of this technology has been limited by manufacturing problems. It is believed that variations in chemical composition are affecting local electronic structure properties that then impact charge separation, charge transport, and carrier recombination in a device. Spectroscopic microscopies with chemical and electronic structure information have become important tools for understanding the complex structure-property-performance relationships of CIGS materials and devices. This presentation will provide an overview of various microscopy efforts to characterize the spatially varying chemical and electronic structure of CIGS. Recent results from our novel application of low-energy electron microscopy (LEEM) and photoemission electron microscopy (PEEM) to CIGS will be highlighted. By combining insights gained from these spectroscopic microscopy tools, a model explaining CIGS device performance and manufacturing challenges is proposed.

11:00 AM

(EMA-S4-003-2014) Experimental and Simulated Selective-Area Growth of CdTe (Invited)

D. Zubia*, B. A. Aguirre, R. Ordóñez, F. Anwar, University of Texas, El Paso, USA; H. Prieto, C. Sanchez, M. T. Salazar, A. A. Pimentel, J. R. Michael, Sandia National Laboratories, USA; X. Zhou, University of Texas, El Paso, USA; J. C. McClure, G. N. Nielson, J. L. Cruz-Campa, Sandia National Laboratories, USA

Cadmium telluride (CdTe) thin-film photovoltaics has surpassed crystalline silicon in cost-efficiency in the multi-kilowatt market as a result of its favorable material properties and relatively low manufacturing cost. CdTe has a high absorption coefficient (>104 cm⁻¹) and ideal bandgap (~1.5 eV) with a theoretical maximum efficiency of ~30%. However, the highest reported efficiency is 18.7% for laboratory scale devices and 14.4% for modules. The difference between the actual and theoretical maximum efficiencies is due to a low open-circuit voltage ($V_{oc} < 1$ V) which has been partially attributed to charge recombination at the interface. The large lattice mismatch (~10%) between CdTe on CdS results in a high defect density near the junction. Moreover, morphological inhomogeneity of the CdTe polycrystalline grains is another source of loss. In this paper, experimental and simulated growth of CdTe on nanopatterned CdS substrates is presented. The selective-area deposition of CdTe on CdS via close-space sublimation is used to study the effect of window size (2 μm and 300 nm) on grain growth. The basic fabrication procedures for each of the layers (CdS, SiO₂ and CdTe) and achieving selective-area growth are presented. Selective-area growth of both micro- and nano-scale CdTe islands on CdS substrates using close-spaced sublimation is demonstrated.

11:30 AM

(EMA-S4-004-2014) Nanoscale Mapping of Performance in Photovoltaics (Invited)

Y. Kutes, J. Bosse, A. Llubes, University of Connecticut, USA; J. Cruz-Campa, E. D. Spörke, Sandia National Labs, USA; B. D. Huey*, University of Connecticut, USA

Progress is reported in the development of a new measurement scheme for nanoscale mapping of PV performance. Solar cell specimens are illuminated during simultaneous scanning with conductive atomic force microscopy (cAFM). Uniquely, a series of images is acquired for a single area, incrementing the applied bias and/or illumination conditions from one image to the next. The local I/V or I/intensity relationship for any given location is then easily measured based on the cAFM contrast (current) from each distinct image (voltage or intensity). This provides drift-free, high spatial resolution photoconduction maps based on the resulting array of I/V or I/intensity spectra (up to 65,536 are presented from a single experiment on a 5 nm pitch). Beyond maps of the photoconductivity, typically ranging from 0 to 500 pSiemens (pS) depending on the location, the short circuit current, open circuit potential, power, and fill factor are also mapped with equivalent resolution. The PV performance of microstructured as well as essentially identical but continuous CdTe-CdS films will specifically be compared, and related to orientations within the polycrystalline cell based on EBSD results. For the CdTe-CdS films, enhanced photoconductivity is clearly observed for certain grains, and grain boundaries are clearly resolved, confirming the importance of microstructural control and grain boundary conductivity on polycrystalline PV performance.

12:00 PM

(EMA-S4-005-2014) Initial Stage of Electrodeposited Copper on Molybdenum substrate for Solar Application

Y. Kwon*, S. Chun, S. Cho, H. Cho, Sungkyunkwan University, Republic of Korea

Thin films including CdTe and $\text{Cu}(\text{In,Ga})\text{Se}_2$ (CIGS) have been considered as a promising solar cell due to their low cost and flexibility. In particular, CIGS solar cell has attracted since its large

optical absorption coefficient is suitable for high conversion efficiency. Recently, the CIGS solar cell with 20.3 % efficiency was achieved by co-evaporation method. However, vacuum process exhibited a limitation in cost reduction coming from wasted materials and high capital investment. Thus, electrodeposition method which can provide high quality film, high rate process and very low cost starting materials has been suggested as breakthrough. However, electrodeposition method shows the lower conversion efficiency than vacuum process, since optimization is not sufficient yet. Even though nucleation and growth mechanism is effective in uniformity and performance of solar cell, the fundamental research was not proceeded. In this study, to clear the effect of initial stage of electrodeposition, electrolyte consists of CuSO₄, H₂SO₄, and Na₂SO₄ was used. The applied potential and ion concentration was varied to analyze the growth mechanism of copper. After the deposition, SEM was employed to confirm the surface morphology. The crystallinity was characterized by XRD.

12:15 PM

(EMA-S4-006-2014) Supramolecular Building Blocks for Hybrid Photovoltaics

E. Spoecker*, D. Gough, J. Wheeler, K. Leong, V. Stavila, M. Foster, T. Lambert, M. Allendorf, Sandia National Laboratories, USA

The continued development of efficient new materials systems for next generation photovoltaics (PV) will require the creative integration of multifunctional materials, interacting cooperatively at a molecular scale. We explore here metal organic frameworks (MOFs) as highly porous, supramolecular crystalline materials, whose chemistry and structure can be tailored to influence their intermolecular interactions, optical absorption, and electronic properties. Moreover, the porosity and rich chemical functionality of these materials makes them attractive templates for the organized integration of donor and acceptor materials within the MOF architecture. Guided by periodic Density Functional Theory calculations, we have synthesized and characterized a family of MOFs in an effort to explore the nanoscale ordering and energy-transfer processes of both organic and inorganic donors and acceptors, organized by the molecular MOF architectures. Exploiting these chemically and structurally versatile supramolecular structures represents a promising new approach for next generation photovoltaic development.

S7: Computational Design of Electronic Materials

Materials Informatics

Room: Coral A

Session Chair: R. Ramprasad, University of Connecticut

10:00 AM

(EMA-S7-001-2014) Big Data of Materials Science from First Principles — Critical Next Steps (Invited)

M. Scheffler*, Fritz Haber Institute of Max Planck Society, Germany

Using first-principles electronic-structure codes, a huge number of materials has been studied in recent years. The amount of already created data is immense. Thus, the field is facing the challenges of “Big Data”, which are often characterized in terms of “the four V”: Volume (amount of information), Variety (heterogeneity), Veracity (uncertainty of the quality), and Velocity at which data may change or arrive. A further critical issue for achieving novel scientific insight with these data concerns an additional “A”, i.e. the Big Data Analysis. For first-principles computational materials science, the two key issues from the above five concern veracity and analysis, and this is what I will focus on in this talk: 1) Veracity of the calculated results refers to the reliability and range of validity of the employed methodology (e.g. pseudopotentials, basis sets) and, in particular, of the exchange-correlation functional. 2) Development

of data-analysis tools largely concerns the identification of descriptors, *d*, of a certain property, *P*, for example the transport band gap of semiconductors, across all studied materials. Knowledge of *P*(*d*) enables us to identify “white spots” (missing data points), to interpolate between calculated data, to (mildly) extrapolate, and to identify outliers with possibly novel types of physics. (*) In collaboration with X. Ren, L. Ghiringhelli, C. Draxl

10:30 AM

(EMA-S7-002-2014) The high-throughput highway to computational materials design (Invited)

S. Curtarolo*, M. Buongiorno Nardelli, Duke University, USA; N. Mingo, J. Carrete, CEA, France; K. Yang, Duke University, USA

High-throughput computational materials design is an emerging area of materials science [1]. By combining advanced thermodynamic and electronic-structure methods with intelligent data mining and database construction, and exploiting the power of current supercomputer architectures, scientists generate, manage and analyze enormous data repositories for the discovery of novel materials. The key for discovering new materials is the availability of descriptors. These are physically sound empirical quantities, not necessarily observables, connecting the calculated microscopic parameters to macroscopic properties of the materials. In this talk (i) we provide a current snapshot of this rapidly evolving field, (ii) we highlight the challenges and opportunities that lie ahead, and (iii) we illustrate the needs and goals of the communities involved: open and free repositories with widely accepted standards. [1] Nature Mater 12, 191 (2013).

11:00 AM

(EMA-S7-003-2014) The origins of hole traps in hydrogenated nanocrystalline and amorphous silicon revealed through machine learning (Invited)

T. Mueller*, Johns Hopkins University, USA; E. Johlin, J. C. Grossman, Massachusetts Institute of Technology, USA

The discovery and design of new materials can be accelerated by the identification of simple descriptors of material properties. However the identification of the most relevant descriptors and how they relate to the properties of interest is not always obvious. I will demonstrate how machine learning, in the form of genetic programming, can be used to identify relevant descriptors for predicting hole trap depths in hydrogenated nanocrystalline and amorphous silicon. Amorphous silicon is an inexpensive and flexible photovoltaic material, but its efficiency is limited by low hole mobility. We have evaluated 243 structural descriptors of amorphous silicon to identify those that are most indicative of the hole trap depth. Our calculations reveal three general classes of structural features that influence hole trap depth and predict that multiple interacting defects may result in deeper traps than isolated defects. I will discuss how these results suggest a possible mechanism for the Staebler-Wronski effect, in which exposure to light degrades the performance of amorphous silicon over time.

11:30 AM

(EMA-S7-004-2014) Accelerating Materials Property Predictions Using Machine Learning

C. Wang*, University of Connecticut, USA; G. Pilania, Los Alamos National Laboratory, USA; R. Ramprasad, University of Connecticut, USA

The materials discovery process is an expensive and time-consuming endeavor. It can be significantly expedited and simplified if we can learn effectively from past knowledge. In this work a similarity-based machine learning method supplemented with a feature selection algorithm is developed for materials property predictions. We show that such a learning method can effectively determine the most relevant attributes of the building blocks of a system that controls specific material properties, and can thus allow us perform targeted and efficient chemical space searches. In the present study,

a family of C, Si, Ge and Sn-based hybrid polymers is considered as an example, with the initial property dataset generated using high throughput density functional theory (DFT) computations. For the polymeric chains studied in this work, a chemo-structural fingerprint vector is defined. We first use our machine learning approach to determine the proper components of the fingerprint vector that most control a certain property. Trained machine learning models then predict a plethora of properties of an enormous number of new polymers within the same family, and reveal hidden correlations between properties, at negligible cost with high fidelity. The strategy developed in this work allows us to systematically explore the chemical spaces, and can significantly accelerate the discovery of new application specific materials.

11:45 AM

(EMA-S7-005-2014) Information-driven approaches to materials discovery (Invited)

T. Lookman*, Los Alamos National Laboratory, USA

With a focus on a particular example from the literature (i.e. piezoelectrics), I will try to provide a perspective on approaches used towards the problem of finding materials with targeted properties. I will then suggest how one might devise a "learning" approach to such a problem.

12:15 PM

(EMA-S7-006-2014) First Principles Search for Functional ABC Materials

K. F. Garrity*, K. M. Rabe, D. Vanderbilt, Rutgers University, USA

There has been great interest and success in using first principles calculations to understand and predict the properties of functional materials, but these studies have frequently focused on a relatively small range of compounds. In this work, we use targeted high-throughput calculations to search for functional ABC materials, an under-explored group of highly tunable semiconductors and metals. In particular, we focus on the competing structural distortions of the hexagonal $P6_3mmc$ structure. We have previously pointed out that insulating ABC materials with polar distortions can be ferroelectric, while competing polar and anti-polar distortions produce antiferroelectrics. In this work, we consider the magnetic properties of hexagonal ABC metals and how they couple to an anti-polar structural distortion. We find several candidate materials which have a Martensitic phase transition which will alter their magnetic properties, and this coupling of structural and magnetic degrees of freedom may allow these materials to display the giant magnetocaloric effect or function as ferromagnetic shape-memory materials. We also briefly introduce the recently developed GBRV high-throughput pseudopotential library used in this work.

S10: Ceramic Composites for Defense Applications

Nano, Piezo and Bio-derived Composites

Room: Mediterranean B/C

Session Chair: Edward Gorzkowski, Naval Research Laboratory

10:00 AM

(EMA-S10-001-2014) Nanocomposite and Hybrid Materials for Efficient High Energy Density Capacitors (Invited)

J. W. Perry*, Georgia Tech, USA

Metal oxide/polymer nanocomposites and organic/inorganic hybrid materials are promising candidates for high energy density capacitor applications. We are investigating two major areas of contemporary dielectrics that include nanocomposites of surface modified BaTiO₃ nanoparticles in polymer hosts and organically modified silica hybrid sol-gel materials that contain tethered polar groups which provide large dielectric constants. A key aspect of our

nanocomposites is the use of organophosphonic acid surface modifiers for metal-oxide nanoparticles that significantly improves the dispersion of the nanoparticles in polymer hosts and the dielectric properties of the nanocomposite films. Hybrid sol-gel materials also provide an interesting platform for designing materials with large dielectric constants and energy density, due to the strong silicate backbone and the flexibility in the attachment of a variety of polar groups. In this presentation, I will give an overview of our research in 1) surface modification of BaTiO₃ nanoparticles, 2) the development of high energy density fluoropolymer/BaTiO₃ nanocomposites and the impact of processing method, 3) trialkoxysilanes with high energy density, breakdown strength and extraction efficiencies of ~ 90%. Our studies have yielded important insight into factors governing the maximum energy density and the efficiency of nanocomposite and hybrid dielectrics.

10:30 AM

(EMA-S10-002-2014) Electrical Properties of Nanodielectrics Consisting of Polymers Containing Oxide Nanoparticles (Invited)

J. J. Fontanella*, J. F. Lomax, C. A. Edmondson, M. C. Wintersgill, U. S. Naval Academy, USA; M. A. Wolak, J. P. Calame, U. S. Naval Research Laboratory, USA; M. A. Westgate, U. S. Naval Academy, USA

The goal of the present work is to synthesize and characterize better materials for use in capacitive energy storage. The materials that have been studied are polymers containing oxide nanoparticles (NP). The polymers are polyetherimide (PEI), polycarbonate (PC) or polyphenylene oxide (PPO) while the NP are mostly 50 nm to 70 nm diameter barium titanate with (STNP) and without (UNP) surface treatment. In addition, measurements have been carried out on various size NP in a cavity. The primary results that have been obtained are relative permittivity, loss and breakdown strength though scanning electron microscopy, differential scanning calorimetry and thermogravimetric analysis studies have also been carried out. The electrical properties of the NP, themselves, exhibit interesting size effects. While the relative permittivity vs. NP concentration is well-behaved (follows a modified Hanai equation with reasonable characteristic parameters) for the PEI nanocomposites, the results for PC and PPO containing UNP are anomalous. However, the relative permittivity vs. NP concentration for STNP in PC and PPO is well-behaved. In the case of PC, neither type of NP significantly affects the gamma relaxation. However, the dielectric loss at room temperature and above is significantly lower with the use of STNP and the room temperature breakdown strength is significantly higher.

11:00 AM

(EMA-S10-003-2014) Interface-modified Multilayer Polymer Films for High Energy Density Capacitors (Invited)

M. A. Wolak*, J. S. Shirk, US Naval Research Laboratory, USA; M. Mackey, Z. Zhou, E. Baer, Case Western Reserve University, USA

Multilayer polymer composites containing alternating layers of polycarbonate (PC) and polyvinylidene fluoride (PVDF) show great promise as the active dielectric material in high energy density capacitors. The dielectric strength of these films is increased relative to monolithic PC or PVDF because the interfaces serve as barriers to the propagation of an electrical breakdown. The energy density of the film is proportional to the square of the applied field. First generation PC/PVDF multilayer films show breakdown strength (E_b) greater than 750 V/ μm and energy densities (U_d) as high as 13 J/ cm^3 . To further increase the dielectric strength and energy density, we have prepared two new types of interface-modified structures: graded permittivity multilayer composites and enhanced adhesion multilayer composites. Both types of composites contain thin interfacial layers positioned between the discreet layers of PC and PVDF, designed to take advantage of subsequent changes in the dielectric or mechanical properties of the film. These composites show increased dielectric strength ($E_b = 900 \text{ V}/\mu\text{m}$) and energy density ($U_d = 16 \text{ J}/\text{cm}^3$) relative to standard multilayer films without interface

modification. The talk will also focus on structure and failure analysis on interface-modified films using advanced imaging techniques such as AFM, TEM, and FIB/SEM.

11:30 AM

(EMA-S10-004-2014) Performance of Wide-Temperature, High-Power Ceramic Filter Capacitors (Invited)

K. Bridger*, A. V. Cooke, D. Kohlhafer, E. Passaro, Activesignaltech.com, USA; W. Schulze, R. Dempsey, S. Arrasmith, Alfred University, USA; J. Weigner, Lockheed Martin, USA; F. Duva, Novacap, USA

Today's military power conversion electronics are exposed to high temperatures, and future generations will see even higher temperatures. Capacitors can occupy almost 50% of the real estate in some power converters and often carry very high currents at high frequencies in both dc-dc converters and dc-ac inverters. Dissipation at high power levels can lead to internal capacitor temperatures at least 50°C above their ambient and so for military hybrid electric vehicles (HEVs) capacitors are expected to reach at least 150°C and possibly 200°C, while future aircraft component temperatures are expected to exceed 250°C. A new family of high-temperature dielectrics based on sodium bismuth titanate has been developed and capacitors are now available from Novacap under the trade name "Type H" or "Type HA". Type H has relatively flat dielectric constant and low loss from -40 to 200°C, while the HA offers a considerably higher dielectric constant at 250°C. This paper examines performance at high-frequency and high-current as well as the 60-Hz operation at 120-VAC and includes an estimate of internal heating. It also presents the challenges involved in developing a true wide temperature capacitor that has both high dielectric constant and low loss at low temperatures (<0°C), and the same at high temperatures (>200°C), while also having good insulation resistance and long lifetime at the high temperatures.

12:00 PM

(EMA-S10-005-2014) Continuous Fabrication of Piezoceramic Fibers and Ribbons by a Novel Alginate Gelation Method and Electrical Properties of 1-3 Piezocomposites

S. Alkoy*, Gebze Institute of Technology, Turkey; E. Mensur-Alkoy, Maltepe University, Turkey; R. Olukkent, S. Dursun, Gebze Institute of Technology, Turkey; A. Berksoy-Yavuz, ENS Piezodevices Ltd., Turkey; M. Kaya, Gebze Institute of Technology, Turkey

In this study, fabrication of piezoelectric ceramic fibers and ribbons, and the electrical properties of piezocomposites with 1-3 connectivity have been investigated. Continuous fabrication of the fibers and ribbons from lead zirconate titanate - PZT [$\text{Pb}(\text{Zr}_x\text{Ti}_{1-x})\text{O}_3$], potassium strontium niobate - KSN [$\text{KSr}_2\text{Nb}_5\text{O}_{15}$] and potassium sodium niobate - KNN [$\text{K}_{0.5}\text{Na}_{0.5}\text{NbO}_3$] powders were done through a novel alginate gelation method. The ion-exchange reaction that occurs between Na^+ and Ca^{2+} ions and the resultant gelation during the extrusion of a water based slurry process provides the three dimensional network structure that holds the ceramic powders in place and retains the fiber or ribbon form. Crystallographically textured KSN ceramic fibers and textured KNN ceramic ribbons have also been fabricated by the combination of alginate gelation and templated grain growth methods. 1-3 piezocomposites were prepared from fibers and their electrical characteristics were investigated. In the PZT fiber composites, dielectric constant was found to range 100 to 770 and piezoelectric charge coefficient (d_{33}) from 40 to 230 pC/N. The dielectric constant of the KNN fiber composites ranged from 67 to 190 and a fully recoverable electrostrain of 0.023% was obtained under an electric field of 4 kV/mm.

12:20 PM

(EMA-S10-006-2014) DNA based Bio-Polymer Hybrid Thin Films for Capacitor Applications

D. Joyce*, AFRL, USA

Deoxyribonucleic acid (DNA) based hybrid films incorporating sol-gel-derived ceramics have shown strong promise as insulating dielectrics for high voltage capacitor applications. Our studies of DNA-CMTA complex/sol-gel hybrid thin film devices have demonstrated reproducibility and stability in temperature- and frequency-dependent dielectric properties as well as reliability in DC voltage breakdown measurements, attaining values consistently in the 300 V to 350 V/ μm range. Functionally layered devices have also been designed, fabricated and characterized to determine any added benefit in dielectric applications. The electrical/dielectric characteristics of DNA-CTMA with sol-gel-derived ceramics as well as layered films were examined to determine their effect on vital dielectric parameters for voltage breakdown and energy storage.

S13: Highlights of Undergraduate Student Research in Basic Science and Electronic Ceramics

Student Finalist Presentations, Wednesday

Room: Coral A

Session Chair: Geoff Brennecke, Sandia National Laboratories

12:50 PM

(EMA-S13-001-2014) Conductivity in nanostructured ceria: space- and time- resolved mapping of ionic dynamics

J. Ding*, Georgia Institute of Technology, USA; E. Strelcov, S. Kalinin, Oak Ridge National Laboratory, USA; N. Bassiri-Gharb, Georgia Institute of Technology, USA

Nanostructured CeO_2 is widely used in catalytic devices and as mixed ionic-electronic conductor in solid oxide fuel cells. However, the origin of its conductive behavior is still subject to controversy. Anisotropic bulk conduction, as well as proton-based conduction facilitated by surface water adsorption, has been reported in nano-crystalline ceria. Here we investigate the regimes under which each of the above becomes the dominant mechanism. Nanostructured ceria is prepared by chemical solution deposition (CSD) and physical vapor deposition (PVD) on Si_3N_4 -coated Si, and quartz substrates. Cr/Pt electrodes, patterned by photolithography, are created on ceria stripes (on Si/ Si_3N_4) and beneath a continuous ceria film (on quartz). The local transport phenomena are studied as a function of atmospheric gas and humidity content from 25 to 125 °C, through use of time-resolved Kelvin Probe Force Microscopy (tr-KPFM). Two different mechanisms are found to contribute to the conductivity in nanostructured ceria at low temperatures: at high humidity and below 50 °C, proton-assisted conductivity mediated by adsorbed water plays a dominant role in surface charge distribution and conductivity; at higher temperatures, oxygen vacancy-based bulk and surface conductivity are dominant. Additionally, the effects of presence of triple points and conductivity of the substrates will be discussed.

1:05 PM

(EMA-S13-002-2014) Crystallization Kinetics of Phase Change Memory Films by Atomic Force Microscopy

J. L. Bosse*, B. D. Huey, University of Connecticut, USA; I. Grishin, O. V. Kolosov, Institute of Materials Science, United Kingdom

Chalcogenide phase change materials have been identified as promising candidates for data storage systems, combining the nonvolatility of flash memory with the speed of random access memory. Since the crystallization process is the time limiting step, the aim of the research community is to not only identify

stoichiometries with extremely fast switching, but also nanoscale characterization techniques to quantify the crystallization kinetics. In the current work, the amorphous to crystalline phase transition is observed for nucleation (GeTe) and growth (Ge₂Sb₂Te₅) dominated thin films with nanoscale temporal and spatial resolution by AFM. Current maps with conductive AFM are acquired throughout to quantify the crystalline nucleation and growth properties. For comparison with such electrically stimulated phase changes, nucleation and growth effects are also investigated for thermally induced phase transitions based on ultrasonic force microscopy.

1:20 PM

(EMA-S13-003-2014) Investigation of Defect Dipole Kinetics in the Ferroelectric and Paraelectric Phases of Acceptor Doped BaTiO₃ Single Crystals

R. Maier*, T. Pomorski, P. Lenahan, C. Randall, The Pennsylvania State University, USA

Room temperature conductivity in perovskites containing acceptor dopants or impurities is controlled by the concentration of oxygen vacancies and the interaction of those vacancies with oppositely charged dopant ions. Coulombic forces and relaxation of lattice strain provide driving forces for the formation of defect associates. Knowledge of the energy of association between acceptor sites and oxygen vacancies is necessary to properly interpret properties like ionic conductivity which have the important role of determining aging and resistance degradation behavior. A comprehensive study will be presented on the interaction of iron and manganese defects with oxygen vacancies in BaTiO₃ crystals. The effects of defect dipole orientation and dissociation kinetics on aging rates measured by the evolution of internal bias in ferroelectric hysteresis loops, ionic conductivity measured by low temperature impedance spectroscopy, and domain wall mobility measured by Rayleigh analysis will be presented. Careful high temperature equilibration of doped crystals in different oxygen atmospheres has been performed in order to present a detailed analysis with the aid of electron paramagnetic resonance on the effect of dopant valence state on low temperature defect associate formation and the resulting impact on the ferroelectric and dielectric properties.

1:35 PM

(EMA-S13-004-2014) Investigation of the nature and mechanism of resistive switching in TiO_{2-x}

A. Motallebgh*, E. C. Dickey, NC State University, USA

Resistive random access memories (RRAM) have attracted intense interest for potential use in next-generation non-volatile memory. In TiO₂ and other oxides, the redistribution of intrinsic point defects under applied electric field is largely responsible for the formation and functioning of these devices. In general, there are two stages to the redistribution process and thus device functionality. One involves the local modulation of stoichiometry near the electrode interfaces, which affects the effective Schottky barrier. The second stage, which arises under more aggressive biasing, is the electroformation of conductive filaments that shunt the electrodes. This research focuses on single crystalline rutile TiO₂, with a well-controlled initial defect chemistry state, as a model material to understand these two types of redistribution processes. The experimental approach is to combine electrical characterization measurements with electron microscopy analysis to understand the mesoscopic redistribution of point defects as a function of electric field and time. In particular, we utilize a combination of cathodoluminescence spectroscopy (CL) and electron energy loss spectroscopy (EELS), which provide spatially resolved information about local stoichiometry. We find CL to be particularly useful for distinguishing the type of point defect that dominates the redistribution process.

S1: Functional and Multifunctional Electroceramics for Commercialization

Dielectrics: Design and Synthesis

Room: Pacific

Session Chairs: Igor Levin, National Institute of Standards and Technology; Anthony West, University of Sheffield

2:00 PM

(EMA-S1-008-2014) Commercialising Research: Materials Discovery to Prototype Devices (Invited)

I. M. Reaney*, University of Sheffield, United Kingdom

Pure ceramic research may be commercialised but great care must be taken to ensure that the 'new material' has a unique combination of properties that are genuinely competitive or superior to those commercially available and is economically viable. This presentation will illustrate how combinatorial synthesis may be used to aid materials discovery of potentially commercial dielectrics. Prototype devices may also be fabricated to illustrate commercial potential but such research is difficult and time consuming. This presentation illustrates how a combined knowledge of MW materials and electrophoretic deposition has been used to generate novel dielectrically loaded antennas for satellite navigation.

2:30 PM

(EMA-S1-009-2014) Phase transition and strain glass in (1-x)(Bi_{1/2}Na_{1/2})TiO₃-xBaTiO₃ (x < 7%)

Y. Yao, Y. Yang*, Xi'an Jiaotong University, China; X. Tan, Iowa State University, USA; X. Ren, Xi'an Jiaotong University, China

(1-x)(Bi_{1/2}Na_{1/2})TiO₃-xBaTiO₃ has been the most studied Pb-free piezoelectric material in the last decade; however, puzzles still remain about its phase transitions, especially around the important morphotropic phase boundary (MPB). By introducing the strain glass transition concept from the ferroelastic field, it was found that the phase transition from tetragonal (T, P4bm) to rhombohedral (R, R3c) was affected by a strain glass transition at higher temperature for x > 4%. In these compositions, the T-R transition was delayed or even totally suppressed and displayed huge thermal hysteresis upon cooling and heating. Also, isothermal phase transitions were predicted and realized successfully in this crossover region, where the interaction between the T-R transition and the strain glass transition was strong. Our results revealed the strain glass nature in compositions around the MPB in this important material, and also provide new clues for understanding the transition complexity in other (Bi_{1/2}Na_{1/2})TiO₃-based Pb-free piezoelectric materials.

2:45 PM

(EMA-S1-010-2014) Crystal Chemical Strategies for Reducing the Dielectric Loss for Commercially Significant Polycrystalline Temperature-Compensated Microwave Dielectric Oxides using "Non-Critical" Materials (Invited)

M. D. Hill*, Trans-Tech Inc., USA

Shifts in the state of the art in filter design for modern wireless communication systems demand that new temperature-compensated ceramic material solutions be developed. One of the properties that is most critical for performance is the Q factor, which is the inverse of the dielectric loss tangent. Modern commercially significant materials include the tantalum-free temperature compensated double-perovskite barium zinc cobalt niobate with a dielectric constant of 34 and a Q > 50000 at 2 GHz for TE mode filters. The focus of the Q improvement efforts for this material is on stabilizing the high-loss anti-phase domain boundaries. The increased use of TM mode filters has brought forth a need for temperature compensated materials with a dielectric constant between 65 and 75. A number of different variants of the barium lanthanide titanate

orthorhombic tungsten bronze show Q values > 10000 at 1 GHz with some compositions not including the critical element neodymium. Data shows that specific ionic substituents on each cation site can improve the Q of this polycrystalline ceramic material.

3:15 PM

(EMA-S1-011-2014) Thin Films of High-k Dielectric Material LaGdO₃ for Logic and Memory Devices

S. P. Pavunny*, University of Puerto Rico, USA; J. F. Scott, University of Cambridge, United Kingdom; R. S. Katiyar, University of Puerto Rico, USA

As stated in the International Technology Roadmap for Semiconductors (ITRS), targeted equivalent oxide thicknesses (EOTs) of ~6.5 Å and ~3 Å are required for alternative high-k dielectric materials in the 20-nm logic and 28-nm DRAM technology generations, which may be unfeasible with the materials used at present, due to their relatively low dielectric constant ≤ 15 . This situation requires that new candidate materials be identified soon. To this end we have developed a promising inter-lanthanide oxide-based high-k material, LaGdO₃, and characterized it as a potential candidate for capacitors for future sub-nanometer logic (MOSFETs) and memory nodes (DRAM and MIM structures). Excellent features of this ternary oxide material, such as high and linear permittivity (~22), large band gap (~5.6 eV), sufficient electron (~2.57 eV) and hole (~1.91 eV) band offsets on silicon, good thermal stability with silicon, and lower leakage current densities within the ITRS specified limits at sub-nanometer electrical functional thickness in both HKMG MOS and MIM configurations are desirable for complementary metal-oxide-silicon (CMOS), bipolar (Bi), and BiCMOS chip applications. Structural, optical, interfacial, dielectric, and electrical transport properties of this new electronic device material will be presented.

4:00 PM

(EMA-S1-012-2014) Affecting Factors on the Microwave Dielectric Properties of CaMgSi₂O₆ Glass-Ceramics

Y. Eoh, B. Choi, E. Kim*, Kyonggi University, Republic of Korea

Effect of crystallization behaviors on microwave dielectric properties of CaMgSi₂O₆ (diopside) glass-ceramics was investigated. The crystalline behaviors of glass ceramics were controlled by nucleation agent, particle size, and two-step heat treatment process, which first step gives high density of nuclei, and the second step allows crystal growth of nuclei. Crystallization behaviors were evaluated by DTA, SEM and XRD analysis with Rietveld and reference intensity ratio (RIR) methods. Microwave dielectric properties (K and Qf) of the specimens were dependent on the crystallite size and degree of crystallization of glass ceramics. The quality factor (Qf) of the specimens heat-treated at 900°C for 1h with 6.88 μm showed 43,200 GHz and enhanced to 50,470 GHz by two-step heat treatment process and 0.5wt% Cr₂O₃ as nucleation agent. Dependence of the dielectric constant (K) and temperature coefficient of resonant frequency (TCF) on the crystallization behaviors was also discussed.

4:15 PM

(EMA-S1-013-2014) Synthesis of BaTiO₃ Nanopowders using TiO₂ Nanoparticles by Hydrothermal Method

J. Han*, M. Joung, J. Kim, Y. Lee, S. Nahm, Korea University, Republic of Korea; Y. Choi, Samsung Chemicals Nanotechnology, Material R&D Team, Republic of Korea

Anatase TiO₂ nanoparticles, obtained by hydrolyzing titanium isopropoxide in distilled water, were used to synthesize BaTiO₃ (BT) nanopowder by the hydrothermal method. When titanium isopropoxide was used, BT nanopowder with a low tetragonality of 1.0070 was formed because of the presence of OH⁻ ions in the oxygen sites and Ba vacancies. However, by changing the titanium source from titanium isopropoxide to TiO₂ nanoparticles, a homogeneous BT nanopowder with similar particle size and a high tetragonality of 1.0081 was synthesized. The size of the BT

nanopowder particles was decreased by reducing the synthesis time. In particular, BT nanopowder synthesized at 220°C for 16 h with a Ba:Ti molar ratio of 4.0 exhibited a high tetragonality of 1.0083 and a small particle size of 126.0 nm.

4:30 PM

(EMA-S1-014-2014) Effects of Bi(Mg_{1/2}Ti_{1/2})O₃ addition on the nanostructure and dielectric properties of modified SrTiO₃ by LPP(Liquid Phase Precursor) method

S. Song*, SungKyunKwan Univ., Republic of Korea

Single-Crystalline Strontium titanate(SrTiO₃) has been widely used a lot of fields such as catalytic materials, semiconducting and dielectric. SrTiO₃ is a typical perovskite-type oxide whose physical properties strongly depend on its chemical composition, structure, shape, size and crystallinity. In this work, the effects of Bi(Mg_{1/2}Ti_{1/2})O₃ addition on the nanostructure and dielectric properties of Si-Mn-modified SrTiO₃ were investigated to develop nano-sized particles and low temperature fired SrTiO₃-based ceramics with stable temperature characteristics. SrTiO₃-Bi(Mg_{1/2}Ti_{1/2})O₃ powder X-ray diffraction studies of the powders after calcining at 800°C similar to SrTiO₃. Transmission electron microscopic studies spherical particles of 60-90 nm size for SrTiO₃-Bi(Mg_{1/2}Ti_{1/2})O₃. The dielectric constant of SrTiO₃-Bi(Mg_{1/2}Ti_{1/2})O₃ is found from 900 to 1200(at 1kHz) for samples sintered at 1200°C. So this new composition SrTiO₃-Bi(Mg_{1/2}Ti_{1/2})O₃ can be applied nano-sized dielectric materials for various field.

4:45 PM

(EMA-S1-015-2014) Enhanced Dielectric and Ferroelectric Characteristics in Ba_{1-x}Ca_xTiO₃ Ceramics

X. Chen*, X. Zhu, W. Zhang, Zhejiang University, China

Synergic modification of BaTiO₃ ceramics was investigated by Ca-substitution, and the superior dielectric and ferroelectric properties were determined together with the structure evolution. X-ray diffraction (XRD) analysis demonstrated a large solubility limit above x=0.25 in Ba_{1-x}Ca_xTiO₃ solid solution where the fine grain structure was observed with increasing x. Room temperature dielectric constant as high as 1655 was achieved in the present ceramics together with the significantly reduced dielectric loss of 0.013 (x=0.20 at 100 kHz), where the Curie temperature kept almost a constant while other two transition temperatures decreased continuously with increasing x. More importantly, the remanent polarization Pr and dielectric strength Eb were significantly enhanced by Ca-substitution, and the best Pr (11.34 μC/cm²) and the highest dielectric strength Eb (75 kV/cm) were acquired at x=0.25. The present ceramics should be very desirable for the applications such as high density energy storage devices.

5:00 PM

(EMA-S1-016-2014) Nanocrystalline Diamond as a Dielectric Material

R. Singh, N. Govindaraju*, Oklahoma State University, USA

Diamond is a wide bandgap semiconductor with high dielectric breakdown strength, superior electron and hole mobilities, high thermal conductivity, and superior radiation hardness. The above material properties of diamond make it well suited for emerging areas of technology such as energy storage, power electronics, microelectromechanical, chemical and biological sensor applications. Room temperature and high temperature dielectric properties of nanocrystalline and microcrystalline diamond thin films are presented. In particular, it will be shown that by controlling the gas composition it will be possible to synthesize nanocrystalline and microcrystalline diamond films whose dielectric properties exceed that of standard dielectric materials at temperatures above 300 °C. Also, the recent development of multilayered diamond films with tailored morphology and structure will be presented. The implications of this research for developing devices for advanced

technology applications will be presented. Our findings demonstrate that it is possible to synthesize smooth, high electrical quality nano- and microcrystalline diamond films for high temperature and high power electronics and microelectromechanical system applications.

S2: Multiferroic Materials and Multilayer Ferroic Heterostructures: Properties and Applications

Theory and Modeling

Room: Indian

Session Chair: Pamir Alpay, IMS, University of Connecticut

2:00 PM

(EMA-S2-009-2014) Antiferroelectricity and Antiferroelectric Domain Walls (Invited)

A. K. Tagantsev*, Swiss Federal Institute of Technology, EPFL, Switzerland;
A. K. Tagantsev, Ioffe Physical Technical Institute, Russian Federation

Antiferroelectrics constitute a large group of dielectric materials that exhibit a structural phase transition between two non-polar phases with a strong dielectric anomaly at the high temperature side of the transition. A proper insight into the phenomenon can be gained by identifying the antiferroelectricity as a result of the interruption of an imminent ferroelectric phase transition having Curie temperature of T_0 by a structural phase transition at a slightly higher temperature T_A . This interruption occurs due to a repulsive interaction between polarization and a structural order parameter appearing at T_A . This approach also enables the identification of the antiphase boundaries in antiferroelectrics as promising candidates for the occurrence of ferroelectricity in domain boundaries of a non-polar material. This paper addresses the properties of the classical antiferroelectric, lead zirconate, in the context of the aforementioned approach. The data of a comprehensive experimental characterization (X-ray inelastic and diffuse scattering, Brillouin scattering and electron microscopy) of the material are presented and analyzed in view of the results of Landau theory and first principals calculations.

2:30 PM

(EMA-S2-010-2014) Switching Magnetic Ordering by an Electric field in Multiferroics (Invited)

L. Bellaiche*, University of Arkansas, USA

A systematic control of the magnitude and crystallographic direction of magnetic order parameters by an electric field is attractive for the design of original devices. The aim of this Talk is to report the results of ab-initio calculations that predict two different novel ways to achieve such control in multiferroic BiFeO_3 (BFO). - One way is via the existence of an energy term that (i) directly couples magnetic moments and electric polarization, P , and (ii) is linear in P . A particular example is the spin-current model. We demonstrate that this term allows an electric-field-driven and ultrafast switching of the magnetic chirality in the ground state of BFO. This switching is further found to involve original intermediate magnetic states. - Another way to control magnetic quantities by an electric field is "indirect": there is a trilinear "structural-only" coupling between polarization and two different structural quantities that leads to the reversal of one of these two structural quantities when switching the polarization. Then, this reversal can result in the change of direction of a magnetic order parameter, via a second physical energy. We show that such "indirect" coupling can indeed exist in BFO films, and provide the analytical expression and original physical quantities of these two energies.

3:00 PM

(EMA-S2-011-2014) Multiscale Atomistics for Defects in Electronic Materials (Invited)

K. Dayal*, J. Marshall, Carnegie Mellon University, USA

Ionic solids are important for electronic and energy storage/conversion devices. Examples include ferroelectrics and solid oxides. Defects in these materials play a central role in enabling their properties: for example, the electromechanics of ferroelectrics occurs by the nucleation and growth of domain wall defects, and solid oxide ionic conduction is through the motion of point defects. I will talk about our efforts to develop multiscale atomistic methods to understand the structure of defects in these materials. These materials have long-range electrostatic interactions between charges, as well as electric fields that exist over all space outside the specimen. I will describe a multiscale methodology aimed at accurately and efficiently modeling defects in such materials in complex geometries. Our approach is based on a combination of Dirichlet-to-Neumann maps to consistently transform the problem from all-space to a finite domain; the quasicontinuum method to deal with short-range atomic interactions, and rigorous thermodynamic limits of dipole lattices from the literature. We apply the method to understand the electromechanics of a ferroelectric under complex electrical loading.

4:00 PM

(EMA-S2-012-2014) Dynamics of the soft mode in ferroelectric PbTiO_3 from atomistic simulations (Invited)

I. Ponomareva*, University of South Florida, USA

Ferroelectric PbTiO_3 occupies a special place among ferroelectric materials owing to its unique status as a prototype displacive ferroelectric. However, despite its unique role there still exist some uncertainties and controversies regarding the soft mode dynamics in this classic ferroelectric. Here we present our recent methodological development that allows studying of soft mode dynamics in PbTiO_3 from the atomistic viewpoint. Application of such approach to trace the soft mode dynamics in a wide temperature range provides an atomistic insight into the nature of the phase transition in PbTiO_3 that remains controversial for many years. In particular, we find an order-disorder component in the phase transition near the Curie point. Next we focus on how the dynamics of soft mode in PbTiO_3 is modified by different mechanical boundary conditions that include hydrostatic pressure, biaxial and uniaxial stresses and strains. Our computational data reveal some unusual features of such dynamics and provide insight into some experimental findings in ferroelectric epitaxial films.

4:15 PM

(EMA-S2-013-2014) Theoretical Design Strategies for New Multiferroics (Invited)

J. Rondinelli*, Drexel University, USA

There are two main routes to accelerate materials discoveries: serendipitous realization through conventional synthesis or computationally guided growth of novel materials through artificial atomic scale structure. Within this setting, I describe the design methodology and theoretical discovery of a new class of "rotation-induced" ferroelectric materials using applied group theory and density functional calculations. Bottom-up engineering of the atomic framework structure, specifically rotations of transition metal octahedra at the unit cell level, is applied to realize ferroelectricity in artificial ABO_3 -structured composites formed by interleaving two bulk materials with no tendency to such behavior. This emergent form of octahedral rotation-induced ferroelectricity offers a reliable means to externally address and achieve deterministic electric-field control over magnetism. I discuss the required crystal-chemistry criteria to select the compositions and stoichiometries giving polarizations comparable to the best known ferroelectric oxides in magnetically ordered double perovskites. I then extend the approach to A_2BO_4 Ruddlesden-Popper (RP) oxides with disconnected layers

of corner-sharing octahedra to design improper multiferroism in a class of manganites using (pseudo)-rotations that describe Jahn-Teller distortions. I conclude by suggesting new materials families to search for unconventional forms of ferroic behavior.

4:30 PM

(EMA-S2-014-2014) Electromagnetic Modeling of Microwave-Assisted Low-Temperature Growth of Thin Films in Solution (Invited)

K. Yang*, B. Reja-Jayan, K. Harrison, C. Wang, University of Texas at Austin, USA; M. Cole, U.S. Army Research Laboratory, USA; A. Manthiram, A. E. Yilmaz, University of Texas at Austin, USA

An FFT-accelerated integral-equation based simulator is developed to predict the selective heating of thin films in microwave ovens. This simulator was used to analyze, understand, and improve microwave-assisted low-temperature growth of titanium dioxide (TiO_2) films. Initial experiments showed that TiO_2 thin films can be grown on indium tin oxide (ITO) coated glass substrates immersed in a growth solution at temperatures as low as 150°C within 60 minutes; however, the films were not uniform — they were thicker at the edges. By using the proposed simulator to model the coated glass substrate, the solution, the quartz vessel holding the solution, the rotor holding the vessel, the microwave oven, and the rotor's motion in the oven, it was found that (i) the ITO coating selectively absorbs microwave energy, (ii) the predicted energy absorption pattern in the coating is strongly correlated to the thickness of the resulting TiO_2 thin film, and (iii) the film uniformity can be improved by adjusting the ITO conductivity. The electromagnetic simulator developed in this study can supplement and guide microwave-assisted growth experiments by enabling the prediction of energy absorption by thin films. This simulator can also be used to predict the heating of ferroelectric thin films; initial results will be shown at the symposium.

S3: Structure of Emerging Perovskite Oxides: Bridging Length Scales and Unifying Experiment and Theory

Local Structure and Ferroelectric Domains

Room: Coral B

Session Chairs: Pamela Thomas, University of Warwick; David Cann, University of Oregon

2:00 PM

(EMA-S3-006-2014) The physics of relaxors in relation with other complex systems (Invited)

S. Prosandeev, Laboratoire SPMS, Ecole Centrale Paris - CNRS, France; S. Prosandeev, Physics Department and Institute for Nanoscience and Engineering, University of Arkansas, USA; B. Dkhil*, Laboratoire SPMS, Ecole Centrale Paris - CNRS, France

In this presentation, the main idea is to demonstrate that relaxors share common features with many other systems; these features being related to various and exotic phenomena like the weak crystallization in lipids, the Bose condensation in Helium II state or the pseudo-gap in superconductors. The tempting proximity of these phenomena will be discussed and used to propose a unified microscopic picture of relaxors. As a matter of fact, two new order parameters will be introduced to characterize the transitions occurring at Burns temperature and that at T^* which marks the crossover between a spherical glass and a quadrupole glass state.

2:30 PM

(EMA-S3-007-2014) Diffuse scattering in lead-containing perovskites (Invited)

A. Bosak*, European Synchrotron Radiation Facility, France; D. Chernyshov, Swiss-Norwegian Beam Lines at the ESRF, France; R. Burkovsky, M. Krisch, European Synchrotron Radiation Facility, France; S. Vakhrushev, Ioffe Physico-Technical Institute, Russian Federation

Diffuse scattering contains the information on the local deviations from the periodic average structure: it can refer to the static disorder, to the phonons, or to the slow dynamics. We extensively studied the diffuse x-ray scattering in a number of lead-containing materials with perovskite structure, including relaxor $\text{PbMg}_{1/3}\text{Nb}_{2/3}\text{O}_3$ (PMN) and prototypical antiferroelectric PbZrO_3 (PZO). The characteristic x-ray diffuse scattering, observed in PMN, was quantified in a wide range of temperatures (100-500 K) and pressures (0-10 GPa) with high-flux and high-resolution mapping of reciprocal space. It can be successfully parameterized in terms of pseudo-dynamical matrix, mimicking the scattering from low-energy phonons. Such a parameterization allows us to use plain waves to generate the disordered atomic configurations, related to the correlated Pb displacements. Static snapshots of the relaxor structure correspond to a specific dipole glassy state that can be characterized by local polarisation and its projection. The same kind of parameterization works extremely well for the high-temperature cubic phase of PZO, while the static disorder, considered being important for the relaxor state, is naturally absent. The similarity of the driving forces of phase transitions (well-defined for antiferroelectric, hidden for the relaxor) thus may be suspected, with strong implications of frozen-in disorder in relaxors.

3:00 PM

(EMA-S3-008-2014) Local structure analysis on complex $\text{PbZr}_{1-x}\text{Ti}_x\text{O}_3$ (Invited)

H. Yokota*, Chiba University, Japan; N. Zhang, Simon Fraser University, Canada; P. Thomas, University of Warwick, United Kingdom; M. Glazer, University of Oxford, United Kingdom

$\text{PbZr}_{1-x}\text{Ti}_x\text{O}_3$ (PZT) is one of the most commonly used materials for various applications due to its high piezoelectric and pyroelectric coefficients. Around the Ti concentration of 48%, so called a morphotropic phase boundary (MPB) which separates rhombohedral and tetragonal phase, piezoelectric coupling constant and electromechanical constant sharply increase to the maximum. A lot of researches have been carried out to understand the origin of the large properties around the MPB. The idea of polarization rotation has been accepted since the discovery of monoclinic Cm phase at the MPB region on PZT and this concept is adopted for the other solid solution systems. However, there is still ambiguity on its crystal structure. Recently, we carried out neutron diffraction experiments and found that monoclinic Cm phase exist in the whole area of the phase diagram, which means there is no single phase below the Curie temperature. Single crystal studies reported by Gorfman et al also suggested the mixture model around the MPB region. Although the phase mixture model seems to provide a better description on PZT phase diagram, we have to be careful about the result as it is very difficult to distinguish different phase models with similar R factors in Rietveld refinement. Therefore we performed a pair distribution function (PDF) analysis to understand the local structure of PZT. The details of PDF analysis will be discussed.

4:00 PM

(EMA-S3-009-2014) The role of domain wall displacement in achieving superior properties of lead-free ceramics: insights from in situ diffraction (Invited)

J. L. Jones*, North Carolina State University, USA

Microstructure plays a key role in determining emergent properties of ferroelectric polycrystalline materials. For example, polycrystalline barium titanate (BaTiO_3) exhibits maximum room temperature

relative permittivity (ϵ_r) at a grain size of approximately 1-2 μm and ϵ_r decreases below and above this grain size. Two widely accepted theories attribute this behavior to either internal residual stress or non-180° domain wall motion, though a direct measurement of the exact origin of such grain size effects has, to date, elucidated researchers. Here, using in situ, high-energy X-ray diffraction during application of electric fields, we show that 90° domain wall motion during both strong (above coercive) and weak (below coercive) electric fields is greatest at these inter-mediate grain sizes, correlating with the enhanced permittivity and piezoelectric properties observed in BaTiO_3 . This result validates the long-standing theory of Arlt et al. in attributing the size effects in polycrystalline BaTiO_3 to domain wall displacement. It is now empirically established that a doubling or more in the piezoelectric and dielectric properties of polycrystalline ferroelectric materials can be achieved through domain wall displacement effects; such mechanisms are suggested for use in the design of new ferroelectric materials with enhanced properties.

4:30 PM

(EMA-S3-010-2014) Ferroelectric phase transitions and large energy conversion in domain engineered ferroic crystals (Invited)

P. Finkel*, A. Amin, Naval Undersea Warfare Center, USA; S. Lofland, Rowan University, USA

It is well known that ferroelectric single crystals display both a linear piezoelectric effect and a non-linear electro-mechanically coupled phase transformations. Domain engineered ferroelectric single crystals deliver an order of magnitude improvement compared to conventional PZT. We demonstrate that under specially compressive stresses ferroelectric relaxors single crystals exhibit low field induced reversible and sustainable strain associated with ferroelectric-ferroelectric phase switching and unusual and unexpected lack of fatigue after several millions cycles is believed due to strain accommodation occurring in ferroics (Finkel et al. Phys. Status Solidi A, 10,1002 (2012)). These phase transformations result in extremely large changes in polarization in response to relatively small stress changes, a property that is well suited to enhancing mechanical energy conversion demonstrated in certain ternary ferroelectric relaxor single crystals. X-ray diffraction are in a very good agreement with macroscopic observation and phenomenological model confirming proposed transformational path. The phenomena presented here is universal in domain engineered ferroics enabling mechanical stress to be used for strain and polarization control of electromechanical energy conversion offering a significant opportunity to increase the efficiency of ferroelectric energy harvesters.

4:45 PM

(EMA-S3-011-2014) Correlation of Domain Processes and Properties in Future Piezoceramics

M. C. Ehmke*, J. Blendell, Purdue University, USA; K. J. Bowman, Illinois Institute of Technology, USA

The ambitious goal to replace versatile piezoceramics such as lead zirconium titanate (PZT) with non-toxic lead-free alternatives requires an understanding of the fundamental physical processes taking place in piezoelectric materials. It has been shown before that compositions at the morphotropic phase boundary (MPB) are essential for producing large piezoelectric strains. In addition, a phase convergence region, such as in the $\text{Ba}(\text{Zr}_{0.2}\text{Ti}_{0.8})\text{O}_3$ -x $(\text{Ba}_{0.7}\text{Ca}_{0.3})\text{TiO}_3$ (BZT-BCT) system, can promote even larger piezoelectric performance, up to 1600 pm/V. Here, we use in situ x-ray diffraction in combination with electromechanical measurements of BZT-BCT to identify and quantify intrinsic piezoelectric, extrinsic ferroelastic, and field-induced symmetry change processes and correlate them with macroscopic electromechanical properties. Moreover, the anisotropy of these properties is identified to be crucial for a complete understanding of the high macroscopic response. The investigation sheds new light onto how those processes interact and thus impact design criteria for new piezoelectric materials.

5:00 PM

(EMA-S3-012-2014) Depolarization Mechanisms in High Temperature Piezoceramics

T. Ansell*, D. Cann, Oregon State University, USA

Piezoelectric ceramics are used in a number of applications such as an accelerometer, spark igniter, or piezoelectric stack actuator found in piezoelectric fuel injectors. The ubiquitous lead zirconate titanate (PZT), exhibits excellent piezoelectric properties with a TC = 390 °C. However, for emerging high temperature applications, Curie temperatures (TC) must exceed 400 °C. The solid solution of lead titanate and bismuth scandate (PT-BS) has an increased TC = 450 °C and also a higher piezoelectric coefficient than undoped PZT. Ternary solid solutions of PbTiO_3 - BiScO_3 - $\text{Bi}(\text{X}_{1/2}\text{Ti}_{1/2})\text{O}_3$, where X = Mg, Zn, or Ni, were developed to increase TC while lowering the percent of expensive scandium oxide. A number of compositions in all three ternary systems exhibited transitions above 400 °C. However, a transition from normal ferroelectric to relaxor behavior is observed, especially in PT-BS-BNIT where relaxor behavior is most pronounced in compositions with high nickel content. This work will determine the phase transition temperature in the ternary and, most importantly, to determine the depolarization mechanisms in the relaxor compositions.

5:15 PM

(EMA-S3-013-2014) Bridging Length Scales in the Design of Advanced Perovskite Materials

S. C. Tidrow*, University of Texas - Pan American, USA

Through appropriate use of atomic substituents, Perovskites provide an enormous range of material properties and the potential for multi-functionality. Evidence indicates that Goldschmidt's formalism no longer adequately guides the research and development of new Perovskite materials. In this presentation, the evolving planar constrained Perovskite model, through mapping transformation, is shown to provide significant improvements, compared with Goldschmidt's formalism, in modeling fundamental material properties, crystal symmetry and lattice parameter over extended temperature ranges. As obtained using the model, new "effective" ionic radii and linear thermal expansion coefficients for numerous coordination dependent substituents within Perovskites are reported. Using the improved lattice parameters coupled with the Clausius-Mossotti relation, it is shown that significant improvement in quantitative values for the dielectric constant of materials can be obtained. Also, it is shown that the temperature for some polarization induced structural phase transitions can be emulated. This simplistic model that can be used to model a wide range of material properties is extensible to other materials and crystal symmetries. This material is based upon work supported by, or in part by, the U.S. Army Research Laboratory and the U.S. Army Research Office under contract/grant number W911NF-08-1-0353.

S7: Computational Design of Electronic Materials

Design of Materials with Novel Architectures

Room: Coral A

Session Chairs: Tim Mueller, Johns Hopkins University; Blas Uberuaga, Los Alamos National Laboratory

2:00 PM

(EMA-S7-007-2014) The Inverse Problem in Nano science and in materials theory: (Invited)

A. Zunger*, University of Colorado,Boulder, USA

The history of material research generally proceeded via accidental discoveries of materials configuration with interesting physical property (semiconductivity, ferromagnetism; superconductivity,

etc.). The question posed in this talk is: Given that structure /configuration often decides the material's property, and given that many (in fact, an astronomic number of) possible structures can be made, does it make sense to first declare the material property you really want, then find that structure and material that has this? Current examples of Inverse Design include (i) Design of nanostructure band gap (e.g. which superlattice sequence of GaAs/AlAs will have a given value of band gap? Can one find a sequence of Si/Ge/Si... that has a truly direct and optically strong gap?) (ii) Impurity by design (e.g. which arrangement of nitrogen impurities in GaP will have the deepest, or the shallowest impurity level?) (iii) Ferromagnetism by design (e.g. can one find a structure of Mn in GaAs with a given Curie temperature?) (iv) Excitonic spectra by design (e.g. can one find a structure of a quantum dot that has a given sequence—barcode—of excitonic lines?). (v) Search of transparent conductors (e.g., look for those structures that would have high hole conductivity).

2:30 PM

(EMA-S7-008-2014) Controlling the Conductivity of Two-Dimensional Conductors (Invited)

C. G. Van de Walle*, H. Peelaers, University of California, USA

The example of graphene has demonstrated that two-dimensional materials can have exciting applications as electronic materials. However, the lack of a band gap in graphene is an important obstacle, and other materials, such as transition-metal chalcogenides, are being actively explored. Bringing the electronic properties under control is still a major task, which we will illustrate with the example of MoS_2 . We are using cutting-edge first-principles calculations (based on density functional theory using hybrid functionals that also include van der Waals interactions) to calculate key materials parameters such as band gaps and effective masses, and to investigate how strain and alloying can be used for band-structure engineering. An in-depth study of electron-phonon interactions provides fundamental insights in mobility. We are also investigating how various dopants and defects are affecting the conductivity. The determination of these fundamental properties paves the way towards rigorous understanding and exploitation of these exciting materials.

3:00 PM

(EMA-S7-009-2014) First-Principles Assisted Design of Molecular Scale Graphane Analogues (Invited)

W. Windl*, O. D. Restrepo, J. Goldberger, The Ohio State University, USA

Graphene's success has shown that it is not only possible to create stable, single-atom thick sheets of a crystalline material, but that these materials can have electronic structures that are fundamentally different than the parent, and that are significantly influenced by the environment. Recent work at The Ohio State University has shown that unique single-layer 2D materials based on silicon and germanium can be synthesized, stabilized by appropriate ligands. In this talk, we will show theoretical calculations of the electronic properties of two-dimensional silicon and germanium sheets, which are strongly dependent on the stabilizing molecules. For our calculations, we will use density-functional theory with hybrid functionals that predict the band gaps in excellent agreement with experiment. We will examine the dependence between orbital structure and calculated bands and discuss the origin of the observed changes in the band structure with changing ligands. We will also discuss the relationship between the observed large band gaps for silicon and germanium and the Dirac-cone type band structure case of graphene, and the dependence of the observed properties on the geometric parameters of the atomic structure.

4:00 PM

(EMA-S7-010-2014) Density functional theory and microscopy: A combination tool for the design of new materials (Invited)

S. T. Pantelides*, Vanderbilt University, USA; S. J. Pennycook, Oak Ridge National Laboratory, USA

Density functional theory has evolved into a powerful and accurate method for the calculation of structural, electronic, and magnetic properties of materials and nanostructures. At the same time, aberration corrections now allow scanning transmission electron microscopy to achieve sub-Angstrom resolution in imaging complex material structures. This talk will highlight specific examples of combining the two approaches to elucidate the structure, dynamics, and electronic and magnetic properties of complex materials systems suitable for energy and medical applications, providing direct guidance of the design of novel functional structures. More specifically, we will describe the possibility of defect and strain engineering in the battery material LiFePO_4 , the discovery of a novel form of crystalline structure in CuInS_2 nanocrystals that is uniquely suitable for thermoelectric applications, passivation of magnetite nanoparticles for enhanced magnetism in bioapplications, and the design of passivated and stable nanovoids in graphene for DNA sequencing and molecular translocation.

4:30 PM

(EMA-S7-011-2014) First-principles design of organo-Sn polymeric dielectrics

H. D. Tran*, A. Kumar M.K., C. Wang, A. Baldwin, R. Ma, G. Sozting, R. Ramprasad, Institute of Materials Science, University of Connecticut, USA

Following on from recent computation-based suggestions that Sn-containing polymers may be promising dielectrics, one of them, poly (dimethyltin glutarate) (pDMTG), has been synthesized. The measured dielectric constant of pDMTG is $\epsilon \approx 7.4$, significantly higher than the current standard material used for high-energy-density applications, namely, polypropylene ($\epsilon \approx 2.2$). By performing first-principles calculations at the level of density functional theory and using the minima-hopping method to predict the stable structures (given that just the composition is provided), we propose four structural models of pDMTG. Based on these models, various physical properties of pDMTG, e.g., dielectric constant, infrared spectra and refractive index, are determined to closely agree with experimental data. The calculated band gap of pDMTG is high ($E_g \approx 6.1$ eV), implying that pDMTG is a promising candidate for high-energy-density materials. The strategy that has led to the synthesis and understanding of pDMTG shows that density functional theory is a powerful method to study and design new materials. Our work is supported by the Office of Naval Research through the Multidisciplinary University Research Initiative (MURI).

4:45 PM

(EMA-S7-012-2014) Theoretical Study on Strain Induced Variations in Electronic Properties of Ultrathin MoS_2 Sheets

L. Dong*, A. Dongare, University of Connecticut, USA; R. Namburu, T. O'Regan, M. Dubey, U.S. Army Research Laboratory, USA

Since the discovery of graphene, there has been a fast-growing interest in fabricating ultrathin 2-dimensional (2D) films and nano flakes out of materials with layered structures. Among all these materials, molybdenum disulfide (MoS_2) is a semiconductor that shows significant promise for use in electronics, optoelectronics, and catalytic applications. In this study, we will present a first principles study based on density functional theory to analyze the electronic properties of monolayer and bilayer MoS_2 under three 2D mechanical boundary conditions (MBCs): biaxial strain, uniaxial strain, and uniaxial stress. Our results show that for all these MBCs, the MoS_2 ultrathin sheets experience direct-indirect and/or indirect-indirect band gap transitions as the degree of in-plane strain varies from -6% to 6% in the basal plane. The strain and stress also modify the

effective masses of electrons and holes significantly. The relative stability of the electronic structure as well as the energetics of various bilayer MoS_2 stacking sequences are investigated under the presence of in-plane strain/stress conditions.

5:00 PM

(EMA-S7-013-2014) Defect kinetics in oxides from long time simulations (Invited)

B. P. Uberuaga*, Los Alamos National Laboratory, USA

Defect kinetics are key to the performance of oxides in a wide range of applications, from fast ion conductors to radiation tolerant materials. To understand and predict performance for such applications, one must first identify the underlying atomic scale mechanisms associated with the migration of defects that underpin that performance. However, especially as the complexity of the oxide increases, this can be a challenging task that defies intuition. Here, we describe the insights gained regarding defect kinetics in a number of oxides using accelerated molecular dynamics (AMD) methods. The AMD methods allow for the simulation of much longer times than conventional molecular dynamics while retaining full atomistic fidelity. We have used AMD methods to examine defect kinetics in a number of situations relevant for mass transport and radiation damage evolution. In particular, we examine interstitial clustering in simple oxides where large clusters exhibit interesting kinetic behavior. In more complex oxides, such as pyrochlore and perovskite, we find that the evolution of defects produced under irradiation is very circuitous, with certain varieties of defects being unstable. In every material considered, the AMD simulations reveal kinetic processes that were both surprising and with important consequences for understanding the behavior of defects within the material.

S8: Advances in Memory Devices

Ferroelectric and Resistive Data Storage

Room: Mediterranean B/C

Session Chair: Bryan Huey, University of Connecticut

2:00 PM

(EMA-S8-001-2014) Ferroelectric tunnel junctions (Invited)

V. Garcia*, Unité Mixte CNRS/Thales, France

After being conceptualized in the early 1970's, ferroelectric tunnel junctions (FTJs), where an ultrathin ferroelectric film is sandwiched between two electrodes, have remained elusive for more than 30 years. At room temperature, we use piezoresponse force microscopy (PFM) to show robust ferroelectricity in BaTiO_3 ultrathin films, and conductive atomic force microscopy to demonstrate the non-destructive resistive readout of the polarization state via its influence on the tunnel current [Nature 460 (2009) 81-84]. Solid-state FTJs based on BaTiO_3 show OFF/ON ratio >100 with fast and low energy resistive switching correlated to ferroelectric switching [Nat. Nanotech. (2012) 101-104]. By varying the voltage pulse amplitude, intermediate resistance states are reachable and PFM imaging reveals a direct correlation between resistance and ferroelectric domains configuration. The FTJs behave as memristors where quasi-continuous resistance variations with cumulated voltage pulses in the ns range can be interpreted by ferroelectric domains dynamics [Nat. Mater. 11, 860-864 (2012)]. More recently, we observed giant tunnel electroresistance (OFF/ON ratio $>10,000$) in solid-state FTJs based on ultrathin films of BiFeO_3 . These devices emerge as an alternative to other resistive binary or analog memories with the advantage of not being based on voltage-induced migration of matter at the nanoscale, but on a purely electronic mechanism.

2:30 PM

(EMA-S8-002-2014) Enhanced ferroelectric properties in epitaxial La-doped PZT films at low concentrations of La-doping

M. Hordagoda*, D. Mukherjee, University of South Florida, USA; D. Ghosh, J. Jones, University of Florida, USA; P. Mukherjee, S. Witanachchi, University of South Florida, USA

As a leading ferroelectric (FE) material in many applications from non-volatile memory to actuators and sensors, there is a high degree of interest in $\text{Pb}(\text{Zr}_{1-x}\text{Ti}_x)\text{O}_3$ (PZT), and in particular in improving upon its properties. Recent reports suggest that doping bulk PZT with La, has a desirable effect on its FE properties while reports on La doped thin films of PZT (PLZT) remain disparate. In this work epitaxial films of PLZT were grown with different atomic % of La (0.1%, 0.5%, 1%). Thin film capacitors were developed using pulsed laser ablation on SrTiO_3 (STO) substrates with $\text{La}_{0.7}\text{Sr}_{0.3}\text{MnO}_3$ as top and bottom electrode. The epitaxial nature of the films were confirmed using X-ray diffraction analysis. Smooth surface morphologies with roughness values of 10 nm were revealed from AFM scans and HRTEM images showed atomically sharp interfaces. The structures showed enhanced remnant polarization values compared to undoped PZT thin films. By performing an XRD strain analysis, in-plane compressive strains in the PLZT films were discovered which lead to increased tetragonality of the PZT unit cell. A model combining donor induced defect-dipoles and a strain-compression relaxation mechanism is proposed to explain the results.

2:45 PM

(EMA-S8-003-2014) Composition-Dependence of Piezoresponse in Ferroelectric Nanotubes

T. Field*, N. Bassiri-Gharb, Georgia Institute of Technology, USA

Ferroelectric nanostructures have high potential for a wide variety of dielectric and electromechanical applications; however, user-controlled fabrication processes for nanostructures without deleterious effects on the ferroelectric properties are still limited. Previous efforts in our group have proved the suitability of soft-template infiltration for creation of high aspect-ratio ferroelectric nanostructures. However, use of a passive Al_2O_3 film as a chemical barrier for template infiltration resulted in an order of magnitude increase in the driving voltages for the PZT nanostructure with respect to thin films. In this work, we report the effects of use of a thin layer of TiO_x , instead of alumina, deposited by ALD. The titania layer is incorporated in the ferroelectric nanotubes during the crystallization of the PZT layers, resulting in a reduction of the overall driving voltages, comparable to thin films of similar thickness. Furthermore, we investigated use of Zr-rich solutions to compensate for the TiO_x incorporation in the nanotubes. The effects of chemical composition as well as nanotube thickness on the piezoresponse of the ferroelectric nanostructures will also be discussed.

3:00 PM

(EMA-S8-004-2014) Ferroelectric Circuit Equations

J. T. Evans*, Radiant Technologies, Inc., USA

Ferroelectric capacitors cannot easily be modeled mathematically for use in classical circuit equations. This difficulty severely limits the usefulness of ferroelectric capacitors for electrical engineers in any circuit other than digital memory. The author has derived a set of theoretical equations describing the response of a ferroelectric capacitor in an electrical circuit. For these equation to be accurate, the capacitance of a ferroelectric capacitor must be fully defined. Borrowing from the model of a ferroelectric capacitor introduced in 1990 by Radiant Technologies for its then new RT66A Ferroelectric Tester, ferroelectric capacitance can be defined with seven components, three of which are sufficient to make circuit equations accurate enough to model circuit function. $C(\text{ferroelectric}) = C(\text{linear}) + C(\text{paraelectric}) + C(\text{remanent})$ The true shape of the paraelectric and remanent components of a ferroelectric hysteresis loop are still an open question but they can be reasonably fit using

Gaussian distributions. The distributions can be derived directly from the hysteresis loop of the targeted ferroelectric capacitor by taking the derivative of the hysteresis loop. The derivation of the circuit equations plus the ferroelectric model will be presented along with comparisons of circuit simulations with actual circuits.

3:15 PM

(EMA-S8-005-2014) Grain boundary initiated DC breakdown of Ferroelectric films and push-pull failures of series connected capacitors (Invited)

D. Varghese*, Texas Instruments, USA; M. Masuduzzaman, Purdue University, USA; J. Rodriguez, S. Krishnan, Texas Instruments, USA; M. Alam, Purdue University, USA

Ferroelectric films show promise as decoupling capacitors in integrated circuits due to their high permittivity, where they are subjected to DC bias over the product lifetime. Unlike the breakdown in classical materials like SiO₂, ferroelectric films under a DC bias show wider distribution in breakdown times for a given thickness. We use conductive AFM measurements on PZT to show that defect generation and breakdown under DC conditions occur along the grain boundaries of the polycrystalline film. Classical percolation theory adapted to the localized trap generation along grain boundaries in PZT explains the wide breakdown time distribution. Series connected capacitors may be used to ensure low failure rates at operating conditions despite the wide lifetime distribution of single capacitors. We show that such series connected capacitors exhibit oscillatory push-pull voltage sequence that makes the breakdown among individual capacitors correlated and has important implications for the lifetime of the overall capacitor.

4:15 PM

(EMA-S8-006-2014) On the electro-optical properties and applications of phase change materials (Invited)

P. Hosseini, C. Rios, G. Rodriguez-Hernandez, University of Oxford, United Kingdom; Y. Au, C. Wright, University of Exeter, United Kingdom; W. H. Pernice, Karlsruhe Institute of Technology, Germany; H. Bhaskaran*, University of Oxford, United Kingdom

We have experimentally demonstrated the operation of a phase change material in the Mixed-Mode electro-optical domain; herein, we present recent work with collaborators on the use of Ge₂Sb₂Te₅ in the mixed electro-optical mode. Some preliminary results of experiments probing the amorphous-to-crystalline transition in such materials, as well as their use in advanced photonics as well as electronic devices will be explored. These are preliminary results and require further characterization; however this indicates the first such measurements on nanoscale devices, and shows the potential for devices based on these materials in the combined optical and electrical domain, especially in nanophotonic devices.

4:45 PM

(EMA-S8-007-2014) Crystallization Kinetics of Phase Change Memory Films by Atomic Force Microscopy

J. L. Bosse*, B. D. Huey, University of Connecticut, USA; I. Grishin, O. V. Kolosov, Institute of Materials Science, United Kingdom

Chalcogenide phase change materials have been identified as promising candidates for data storage systems, combining the nonvolatility of flash memory with the speed of random access memory. Since the crystallization process is the time limiting step, the aim of the research community is to not only identify stoichiometries with extremely fast switching, but also nanoscale characterization techniques to quantify the crystallization kinetics. In the current work, the amorphous to crystalline phase transition is observed for nucleation (GeTe) and growth (Ge₂Sb₂Te₅) dominated thin films with nanoscale temporal and spatial resolution by AFM. Current maps with conductive AFM are acquired throughout to quantify the crystalline nucleation and growth properties. For comparison with such electrically stimulated phase changes,

nucleation and growth effects are also investigated for thermally induced phase transitions based on ultrasonic force microscopy.

5:00 PM

(EMA-S8-008-2014) Ceria Nanocrystals Based Memristors

A. Younis*, University of New South Wales, Australia

We report a novel approach to improve the resistive switching performance of metal oxide based memristors. In the first approach, the vertically aligned ZnO (NR) arrays were grown on transparent conductive glass by electrochemical deposition while CeO₂ quantum dots (QDs) were prepared by a solvothermal method. Subsequently, the as-prepared CeO₂ QDs were embedded into ZnO NRs array by dip-coating to obtain CeO₂-ZnO nano-composite. Interestingly, such a device exhibits excellent resistive switching properties with much higher ON/OFF ratios, better uniformity and stability over the pure ZnO and CeO₂ nanostructures. The origin of resistive switching was studied and the role of hetero-interface was discussed. Secondly, self-assembled CeO₂ nanocubes based resistive switching device was fabricated by hydrothermal process. The device was proven to exhibit excellent resistive switching performance. The origin of switching behaviour on the basis of filament model and inter cube junctions was presented. The present devices demonstrate to have the potential for next generation non-volatile memory applications.

5:15 PM

(EMA-S8-009-2014) An 8MHz 165uA/MHz Zero Leakage Non-Volatile Logic based Microcontroller Exhibiting 100% Digital State Retention at VDD=0V with <400ns Wakeup and Sleep Transitions

J. Rodriguez*, S. Bartling, S. Khanna, M. Clinton, H. McAdams, S. Summerfelt, Texas Instruments, USA

We demonstrate a non-volatile logic (NVL) System on Chip that backs up its working state (all flip-flops) upon receiving a power interrupt, has zero leakage in sleep mode, and needs less than 400ns to restore the system state upon power-up. For energy harvesting applications, NVL is a "must have" because there is no constant power source available to keep flip-flops operational, and even when the intermittent power source is available, boot-up code alone may consume all of the harvested energy. For handheld devices with limited cooling and battery capacity, zero-leakage IC's with "instant-on" capability are ideal.

Poster Session

Room: Atlantic/Arctic

(EMA-S1-P001-2014) Effect of viscosity and thickness in PZT-PZNN tape casting process for energy harvesting system

D. Song*, M. Woo, D. Cho, T. Sung, Hanyang University, Republic of Korea; S. Nahm, Korea University, Republic of Korea

Tape casting method of slurry is widely used for its convenience in commercialization. So, we have designed a tape casting process for piezoelectric energy harvesting system to study effect of density to output power of piezoelectric ceramic controlled by viscosity. First, the powder was prepared for energy harvesting system with 0.69Pb(Zr_{0.47}Ti_{0.53})O₃-0.31Pb{(Ni_{0.6}Zn_{0.4})^{1/3}Nb_{2/3}}O₃. Raw powders such as PbO, ZrO₂, TiO₂, NiO, ZnO, Nb₂O₅ were used to compose total weight of 1,000 g. After powder is ready, the slurry was prepared by mixing powder with solvent, binder, and dispersing agent. After ball milling, viscosity was controlled by degassing time of 0, 30 and 60 min. Each degassed slurry was tape casted by various heights of cutting blade from 200, 300 to 400 μm. As results, the viscosity of slurry was increased linearly from 1074, 1800 and 2681 cP as degassing time increases from 0, 30 and 60 min. Also, as the blade height was increased from 200, 300 and 400 μm, the thickness of the film was increased 48, 58, 80 μm for 0 min, 48, 68, 84 μm for 30 min and 53, 69, 93 μm for 60 min degassing. Then the piezoelectric properties

were analyzed by measuring d_{33} and g_{33} and the relationship between density and piezoelectric property was established. This study investigated the effect of viscosity and thickness in PZT-PZNN tape casting process for energy harvesting system.

(EMA-S1-P002-2014) Mechanism behind enhanced piezoresponse in high performance piezoceramics

A. K. Kalyani*, Indian Institute of Science, India; A. James, DMRL, India; R. Ranjan, Indian Institute of Science, India

A novel powder poling technique has been developed to study the mechanism of high piezoelectric response in morphotropic phase boundary (MPB) piezoceramics. A high performance La modified PZT ($d_{33} \sim 500$ pC/N) was investigated using this technique. A comparative structural and dielectric study of poled and unpoled specimen of the systems revealed that the high piezo response of associated with the field induced irreversible lattice distortion of the coexisting phases accompanied by a concomitant miniaturization of ferroelectric domains.

(EMA-S1-P004-2014) Thickness Optimization of 0.69PZT-0.31PZNN thick film for energy harvesting module

M. Woo*, D. Song, D. Cho, T. Sung, Hanyang University, Republic of Korea; S. Nahm, Korea University, Republic of Korea

In this study, we investigated the energy harvesting property according to the thickness of piezoelectric thick film fabricated by a tape casting process. The $0.69\text{Pb}(\text{Zr}_{0.47}\text{Ti}_{0.53})\text{O}_3$ - $0.31\text{Pb}\{(\text{Ni}_{0.6}\text{Zn}_{0.4})_{1/3}\text{Nb}_{2/3}\}\text{O}_3$ (0.69PZT-0.31PZNN) powder was prepared to make 70 μm thick sheets. The thickness of PZT-PZNN thick film was adjusted by laminating multiple sheets such as 2, 3 and 4 sheets. After sintering, electrode printing and polarization process, piezoelectric properties were measured by impedance analyzer and d_{33} meter. In order to find the optimized sintering temperature, the varying thickness of thick film was annealed for 2 h at various temperatures from 900 to 1050 °C. The thick film which laminated with 2 and 3 sheets was bent that sintered at 1000 °C and 4 sheets laminated thick film was bent at the sintering temperature of 1050 °C. This bending has resulted in a decrease of the piezoelectric properties. The thick film which laminated with 4 sheets and sintered at 1000 °C had a highest transduction coefficient ($d_{33} \times g_{33}$) of $10,127 \times 10^{-12}$ m²/N. This study investigated the thickness optimization of PZT-PZNN thick film for energy harvesting module.

(EMA-S1-P005-2014) Studies on magnetic and structural properties of Ba(Co_{1-x}Mn_x)O_{3-δ} using synchrotron X-ray spectroscopy

R. Shinoda*, Osaka Prefecture University, Japan; Y. Okamoto, Japan Atomic Energy Agency(JAEA-Tokai), Japan; A. Iwase, T. Matsui, Osaka Prefecture University, Japan

We have ever found that Ba(Co_{1-x}Mn_x)O_{3-δ} (BCMO) sintered samples show a variety of magnetic properties and of structural properties depending on the Mn substitution amount x . In particular, $x=0.15$ BCMO sintered samples indicated a ferromagnetic behavior under 32K and maximum saturation magnetization. The origin of their magnetic ordering was suggested to super-exchange coupling between the Co ions and Mn ions through O ions [1]. It is very important to know the valence state or the coordination state of transition metals, as well as the bonding angle between O ions for identifying the super-exchange coupling. In the present research, we used X-ray Photoelectron Spectroscopy (XPS) and X-ray Absorption Spectroscopy (XAS). These spectroscopies are unique techniques to analyze the fine structure and the chemical bonding state. The BCMO samples having the x value between 0 to 0.25, are mainly composed of the mixture of the phases with the 2H, 10H and/or 12H hexagonal crystal structure. The XPS measurement revealed that the valence state of the Mn ions was tetravalent (3d⁵). We have clearly observed the XANES and EXAFS spectra around the Mn-K absorption edge. In the conference, we will discuss the valence state of Mn ions and local lattice structure near Mn ions by using these XAS

spectra with Mn substitution amount x . [1] R. Shinoda et al., J. Appl. Phys. 113, 17E307 (2013).

(EMA-S1-P006-2014) Fabrication of Textured Lead-free (K,Na)NbO₃ Ceramics by Alginate Gelation and Templated Grain Growth

E. Mensur-Alkoy*, Maltepe University, Turkey; A. Berksoy-Yavuz, ENS Piezodevices Ltd., Turkey; S. Alkoy, Gebze Institute of Technology, Turkey

Lead zirconate titanate (PZT) is the piezoelectric material of choice applications, but lead-free alternatives have actively been pursued in recent years due to environmental and health concerns. The properties and performance of the lead-free piezoelectrics are tried to be improved through doping and producing them with a crystallographic texture through preferred grain orientation. However, studies in the literature on textured lead-free piezoelectrics have a common and fundamental drawback, namely; the techniques that are used to obtain texture are not adaptable for continuous fabrication of bulk textured ceramics or they require costly equipments. In this study, a new approach is utilized to overcome these problems: A new and novel technique called alginate gelation, was used together with the templated grain growth (TGG) method for the first time to fabricate textured (K,Na)NbO₃ based lead-free bulk piezoceramics in cm scale dimensions. KNN was fabricated continuously in ribbon form and then packed to obtain bulk ceramics. Development of crystallographic texture as a result of varying sintering time and temperature was evaluated through rocking curve analysis and a texture with Lotgering factor of 0.92 was achieved. The electrical properties of textured ceramics were evaluated through polarization and strain vs. electric field measurements.

(EMA-S1-P007-2014) Effect of buffer layer and microstructure on the thermochromic properties of VO₂ thin film

H. Koo, J. Cho, S. Bae, C. Park*, S. Ahn, Seoul National University, Republic of Korea

Through reversible metal-to-insulator transition(MIT) near room temp, VO₂ shows abrupt change in conductivity over 3 orders of magnitude, which made VO₂ a material with high potential for thermochromic(TC) smart window. However, it is difficult to deposit highly crystallized VO₂ film on soda lime glass(SLG) directly due to diffusion of alkali ions during deposition. Moreover, TC properties, such as amplitude of transition or hysteresis width, of VO₂ films on SLG should be improved for practical use. In this work, in order to improve TC properties of VO₂ films on SLG, two methods were applied: one is introducing buffer layers between SLG and film, the other is controlling microstructure of VO₂ film. First, silicon nitride buffer layer was applied to prevent alkali ion diffusion from SLG. Secondly, various oxide buffer layers such as zinc oxide, titanium oxide, tin oxide and ceria were applied to investigate effect of crystal structure and crystallinity of buffer layers on the properties of VO₂ film. Finally, microstructure change was induced by controlling the sputtering power during film deposition process. Electrical/optical properties were measured to evaluate TC properties, and microstructures were analyzed by combining XRD analysis and TEM measurements. The relation between alkali ion diffusion, buffer layer material, sputtering power and TC properties of VO₂ film will be discussed.

(EMA-S1-P008-2014) Dielectric properties of rare earth doped BaTiO₃ ceramics and Curie Weiss law

V. Mitic*, V. Paunovic, M. Miljkovic, B. Jordovic, University of Nis and Institute of Technical Sciences of SASA, Serbia

The doped BaTiO₃ ceramics, with different rare earth content, ranging from 0.01 to 1.0 wt% (Er, Yb or Ho), were investigated regarding their microstructural and dielectric characteristics in this paper. Doped BaTiO₃ were prepared using conventional method of solid state sintering at 1380 °C for four hours. SEM analysis of BaTiO₃ doped ceramics showed that in samples doped with a rare-earth ions low level, the grain size ranged from 20-40 μm , while

with the higher dopant concentration the abnormal grain growth is inhibited and the grain size ranged between 2-10 μ m. Dielectric measurements were carried out as a function of temperature up to 180 °C. The low doped samples sintered at 1380 °C, display the high value of dielectric permittivity at room temperature, from 2400 for 0.01Ho/BaTiO₃ to 3200 for 0.01Yb/BaTiO₃. A nearly flat permittivity-response was obtained in specimens with higher (1.0 wt%) additive content. The Curie temperature of doped samples were ranged from 128 to 130 °C. The Curie constant for all series of samples decrease with increase of dopant concentration and the lowest values were measured from samples doped with 0.01 at% of additive. Some parameters as Curie constant (C), Curie temperature (T_c) and a critical exponent of nonlinearity (γ) were calculated by using a Curie-Weiss law.

(EMA-S1-P009-2014) Influence of Li-B-Si and Ba-Zn-B additions on the sintering and microwave dielectric properties of Ba-Nd-Ti ceramics

E. Li*, S. Zhang, University of Electronic Science and Technology of China, China

The effect of Li₂O - B₂O₃ - SiO₂ (LBS) and BaO - ZnO - B₂O₃ (BZB) additions on the sintering behavior, microstructure and microwave dielectric properties of tungsten bronze type Ba₄Nd_{9.3}Ti₁₈O₅₄ (BNT) ceramics has been investigated. It was indicated that the LBS and BZB has an obvious effect on lowering the sintering temperature without damaging the microwave dielectric properties of the BNT ceramics. And BNT ceramics doped with 3 wt% LBS and 2wt% BZB can be well sintered at 875 °C for 3h and showed good properties of: $\epsilon_r=68.94$, $Q \times f=4704$ GHz (f=4.2 GHz).

(EMA-S1-P010-2014) The thermal and dielectric properties of Mn-doped (1-x) ZrTi₂O₆-xZnNb₂O₆ filled PTFE composites

Y. Yuan*, C. Zhong, Univ. of Electron. Sci. and Tech. of China, China

High dielectric constant and low loss (1-x) ZrTi₂O₆-xZnNb₂O₆ ceramic fillers have been prepared by the conventional solid-state reaction technique. The main phase is indexed to solid solution ZrTi₂O₆ and the second phase rutile TiO₂ is formed. Ceramic filled polytetrafluoroethylene (PTFE) microwave composite substrates were fabricated through the hot-pressing process. The relative dielectric constant (ϵ_r) and loss tangent ($\tan\delta$) of the composites increase with an increase of x in the (1-x) ZrTi₂O₆-xZnNb₂O₆ ceramic. At the optimum filler loading of 46 vol%, the coefficient of thermal expansion (CTE) and the absolute value of temperature coefficient of dielectric constant ($\tau\epsilon_r$) decrease as increasing x in the (1-x) ZrTi₂O₆-xZnNb₂O₆ ceramic, which is owe to the decrease of the second phase and the change of thermal properties of ZrTi₂O₆ by substitution in the filler. The 0.55ZrTi₂O₆-0.45ZnNb₂O₆ filled PTFE composite exhibits a dielectric constant of 7.32 with a loss tangent of 0.0015 (10 GHz), the $\tau\epsilon_r$ is -84 ppm/°C and the CTE is 17.5 ppm/°C at an optimum filler loading of 46 vol%. The present study shows that the CTE of the composite matches well with copper and the composite exhibits an acceptable temperature coefficient of dielectric constant, which make the (1-x) ZrTi₂O₆-xZnNb₂O₆/PTFE composites promising candidates for high dielectric constant microwave substrate applications.

(EMA-S1-P011-2014) Kinetics and equilibria of Schottky defect formation in the radiation detector TlBr

S. R. Bishop*, M. Kuhn, H. Tuller, Massachusetts Institute of Technology, USA

Thallium Bromide (TlBr) is an attractive material for high energy radiation detection due to its large molecular weight and wide energy band gap. However, TlBr exhibits levels of ionic conductivity that can lead to undesirable dark current leakage, believed to result in polarization of the material with consequent long term degradation in performance. The role of donor and acceptor dopants in controlling the ionic conductivity of single crystals of TlBr was investigated. Their bulk electrical properties were examined as a

function of temperature (20-300°C) with frequency dependent impedance spectroscopy, resulting in the formulation of a predictive ionic conductivity and defect equilibria model based on contributions from Br and Tl vacancies. Due to the ~5 orders of magnitude higher mobility of Br vacancies, as compared to Tl vacancies, an optimum level of approximately 4 ppm donor concentration is required to minimize the dark ionic conductivity. Additionally, a temperature induced conductivity relaxation method was developed to probe the extent of mechanical damage in samples. A dislocation density of $\sim 10^{10}$ cm⁻² was estimated.

(EMA-S1-P012-2014) Effect of K-doping on the antiferroelectric to ferroelectric phase transition in (Ag_{0.05}Na_{0.95})NbO₃ ceramics

Y. Xu*, X. Tan, Iowa state university, USA; Y. Feng, Xi'an Jiaotong University, China

Lead-free ceramics (1-x)(Ag_{0.05}Na_{0.95})NbO₃-xKNbO₃ (x=0.00-0.04) are synthesized via the solid state reaction method. Their structure analysis and electrical properties measurements indicate that the antiferroelectric order is weakened while the ferroelectric order is strengthened with increasing x (K content). For compositions x=0.00, 0.01 and 0.02, the critical electric field, E_F, exceeds the dielectric breakdown strength of the ceramic. However, the composition x=0.04 is ferroelectric at room temperature. The electric field-induced antiferroelectric to ferroelectric phase transition can only be realized in the compositions x=0.023 and 0.03; however, it is an irreversible transition with the induced ferroelectric phase preserved after the field removal. This allows detailed structural analysis in these two compositions before and after the phase transition. The original antiferroelectric phase is orthorhombic (Pbcm) while the induced ferroelectric phase is in monoclinic (Pm) symmetry. This phase transition corresponds to a volume expansion. It is interesting to notice that the metastable ferroelectric phase can be partially transformed to the antiferroelectric phase with an electric field of 51 kV/cm in the reversed direction. The volume expansion associated with the phase transition is also explored for a possible phase transition toughening effect.

(EMA-S1-P013-2014) Effects of Annealing in Pb(Yb_{1/2}Nb_{1/2})O₃-PbTiO₃ Ceramics Near the Morphotropic Phase Boundary

R. Sumang*, Naresuan University, Thailand; S. Prasertpalichat, Oregon State University, USA; T. Bongkarn, Naresuan University, Thailand; D. Cann, Oregon State University, USA

In this study, ceramics of the composition (1-x)Pb(Yb_{1/2}Nb_{1/2})O₃-xPbTiO₃ [(1-x)PYN-xPT with 0.48≤x≤0.505] near the morphotropic phase were prepared by the wolframite precursor method. The effect of annealing on the stoichiometry in PYN-PT ceramics were investigated by means of various electrical and structural characterization techniques including x-ray diffraction (XRD), scanning electron microscopy (SEM), dielectric spectroscopy and ferroelectric hysteresis measurements. A small amount of excess PbO (2 wt.%) was added to compensate for Pb loss during calcination and sintering. The results show that phase pure compounds over the composition 0.48 ≤ x ≤ 0.505 could be obtained. The crystal structure of PYN-PT changed from rhombohedral to tetragonal symmetry when the amount of PT increased. The non-stoichiometric PYN-PT ceramic exhibited excellent electrical properties as compared to pure PYN-PT.

(EMA-S2-P039-2014) Electrocaloric Materials and Dielectric Refrigeration: Novel Developments and Future Perspectives

Z. Kutnjak*, B. Rozic, B. Malic, H. Ursic, Jozef Stefan Institute, Slovenia; Q. M. Zhang, The Pennsylvania State University, USA

Although ECE has been studied for many decades, the relatively small ECE observed <2.5 °C, made it unsuitable for practical applications. Recently, however, materials with large ECE have been predicted to exist based on indirect observations thus opening the possibility of realizing dielectric refrigeration which is more

environmentally friendly compared to other techniques [1,2]. The later direct confirmation of large ECEs in ferroelectric polymers and ceramic thin films have attracted great interest for developing new cooling devices that have the potential to reach better efficiency than the existing cooling technologies [3]. A review of recent ECE findings obtained in polymeric and perovskite ceramic relaxor materials including thick ceramic multilayers, substrate-free thick films, thin films and liquid crystals will be given. Besides the materials progress, recent advances in development of practical cooling devices utilizing different approaches and materials will be presented. 1. Mischenko A. S. et al.: Giant Electrocaloric Effect in Thin-Film $\text{PbZr}_{0.95}\text{Ti}_{0.05}\text{O}_3$. *Science*. 2006; 311: 1270 -1271. 2. Neese B. et al.: Large Electrocaloric Effect in Ferroelectric Polymers Near Room Temperature. *Science*. 2008; 321: 821-823. 3. Lu S.-G et al.: Organic and inorganic relaxor ferroelectrics with giant electrocaloric effect. *Appl. Phys. Lett.* 2010; 97: 162904-1-162904-3.

(EMA-S2-P040-2014) Improved pyroelectric performances of PMNT single crystals used for infrared detectors

H. Luo*, The Shanghai Institute of Ceramics, Chinese Academy of Sciences, China

Relaxor-based PMNT single crystals exhibit excellent pyroelectric performances, $p \sim 1.28 \times 10^{-3} \text{ C.m}^{-2} \text{ K}^{-1}$, $F \sim 4.44 \times 10^{-10} \text{ m/V}$, $F \sim 0.07 \text{ m}^2/\text{C}$, $F \sim 1.32 \times 10^{-4} \text{ Pa}^{-1/2}$, and the sensitivity of infrared detectors could be further improved if the dielectric loss $\tan \delta \sim 0.3\%$ could be reduced. Several elements were used for doping PMNT single crystals in order to improve their performances, and only Mn-doping could significantly reduce the dielectric loss of PMNT single crystals. For example, the dielectric loss could be significantly reduced from 0.3% in undoped PMNT to 0.05% in Mn-doped PMNT at 1 kHz. Combined with the experiment of X-ray absorption fine structure (XAFS), the investigation of EPR and the activation energy from the temperature dependence of conductivity, is proposed to illuminate that Mn^{2+} is in B-site of perovskite structure, which will combine O vacancy in the closed layer to form a .. dipole defect. The dipole defect produce an inner electric field, and pin the movement of domain wall, thus they increase the coercive field E_c . Mn-doped PMNT single crystals reduce conductivity significantly, which result in the low dielectric loss. Mn-doped PMNT single crystals have been successfully used for fabricating high performances of infrared detectors, which reduce the intrinsic noise of dielectric loss and increase the specific detectivity as much as to $2.2 \times 10^9 \text{ cm.Hz}^{1/2}/\text{W}$.

(EMA-S2-P041-2014) Structure and ferroelectric/magnetic properties of Mn-doped bismuth iron titanate Aurivillius thin films

L. Keeney, T. Maity, M. Schmidt, N. Deepak, S. Roy, A. Amann, M. E. Pemble, R. W. Whatmore*, Tyndall National Institute, Ireland

Room temperature magnetoelectric multiferroic materials are interesting for applications in sensors and spin-based memory/logic devices. Recent work by the group has shown ferromagnetism and magnetic-field-induced switching of ferroelectric domains in thin films of $\text{Bi}_6\text{Ti}_2.8\text{Fe}_{1.52}\text{Mn}_{0.68}\text{O}_{18}$ which possesses 5 perovskite layers per half cell. This is the first report of such an effect occurring at room temperature. Here we report on the fabrication and detailed structural analysis of thin films with the composition $\text{Bi}_6\text{Ti}_x\text{Fe}_y\text{Mn}_z\text{O}_{18}$ with $2.3 \leq x \leq 3$, $1.4 \leq y \leq 1.95$ and $0.6 \leq z \leq 0.75$ in a study to explore the range of the 5-layer ($m=5$) structure and the ferroelectric and ferromagnetic properties of the resulting layers. Our earlier work indicated that as the ratio of Ti to Fe/Mn on the perovskite B-site changed, so should the percentage of Mn present as Mn^{4+} , which may be related to ferromagnetic behaviour in the films. XRD analysis indicated that the $m=5$ structure persists for $2.53 \leq x \leq 3$ with $1.4 \leq y \leq 1.77$. Preliminary analysis has indicated ferromagnetic behaviour in some of the films. More detailed structural, ferroelectric and ferromagnetic characterisation of these films will be reported and the implications of the results for multiferroic

behaviour in the structural family discussed. The support of SFI under the FORME SRC Award number 07/SRC/I1172 is gratefully acknowledged.

(EMA-S2-P047-2014) Strain Dependence of Polarization and Dielectric response in Epitaxial $(\text{Ba}_{1-x}\text{Sr}_x)\text{TiO}_3$ Thin Films

S. H. Bin-Omran*, King Saud University, Saudi Arabia

The potential of ferroelectric thin films for many applications, such as dynamic random access memories, nonvolatile ferroelectric random access memories and integrated devices, has recently attracted a lot of research attention on these low-dimensional systems. Intense effort has been made recently to determine if (and understand how) properties of these low-dimensional systems can differ from those of the corresponding three-dimensional bulk. As a result, recent studies revealed that electrical boundary conditions and mechanical boundary conditions play a dominant role in changing the properties of ferroelectric films. A first-principles-derived scheme is used to use a first-principles-derived technique to construct the temperature-versus-misfit strain phase diagrams for the whole BST composition range (i.e., $x=0.00, 0.20, 0.40, 0.60, 0.80, 1.0$). Moreover, we investigate the dependence of their dielectric and ferroelectric properties on the strain and the concentration.

(EMA-S3-P034-2014) Thin Film Growth by Pulsed Laser Deposition of Dielectric Materials

G. Kozlowski, J. Anders*, Wright State University, USA; C. Stutz, J. Jones, S. Smith, G. Landis, AFRL (Air Force Research Laboratory), USA

Thin films of $\text{Sr}_y\text{Ca}_{1-y}\text{Zr}_{1-x}\text{Ti}_x\text{O}_3$ (SCZT) with $x=0.8$, $y=0.01$, $\text{CaHf}_{1-x}\text{Ti}_x\text{O}_3$ (CHT) with $x=0.8$, and $\text{BiScO}_3 - (1-x)\text{BaTiO}_3$ with $x=0.36$ (BSBT(36/64)) showing a high permittivity are useful both in capacitor applications and in piezoelectrics. These dielectric thin films and SrRuO_3 (SRO) conductive bottom electrodes were prepared by using pulsed laser deposition on $\langle 100 \rangle \text{La}_{0.3}\text{Sr}_{0.7}\text{Al}_{0.65}\text{Ta}_{0.35}\text{O}_3$ (LSAT) single crystal substrates. In a search of optimal conditions to achieve epitaxially grown SCZT, CHT, BSBT(36/64), and SRO thin films, different substrate temperatures (600 C, 650 C, 750 C, and 800 C) and different partial pressures of oxygen (50 mTorr, 100 mTorr and 300 mTorr) in the chamber were used during deposition onto LSAT substrates. The optimized deposition conditions for conductive buffer layer of SRO film required 300 mTorr of oxygen partial pressure and substrate temperature of 750 C. The thorough structural and chemical studies of SCZT, CHT and BSBT(36/64) films were done by using SEM, AFM, and XRD measurements.

(EMA-S3-P035-2014) Electric-field induced microscopic strain response in functional ceramic/ceramic composite materials

N. H. Khansur*, J. Daniels, University of New South Wales, Australia

Electric-field induced strain response in newly developed ceramic/ceramic composite of relaxor and ferroelectric materials has been studied by means of in-situ high energy x-ray diffraction. This relaxor/ferroelectric composite at grain length scale has recently emerged as promising lead-free piezoelectric materials. Generally, a ferroelectrically (FE) active phase is incorporated in a large strain relaxor (RE) material to utilize the best of properties from each of the two materials. The RE phase material has large usable strain but the triggering field to generate the strain is high ($\geq 6 \text{ kV/mm}$) whereas FE materials generate strain at relatively low field but with low usable strain. In this work, new compositional system has been designed with a large strain lead-free system $[\text{Bi}_{0.5}\text{Na}_{0.39}\text{K}_{0.10}\text{La}_{0.01}]\text{TiO}_3$ (BNKLT) as RE phase and BaTiO_3 as FE phase materials to investigate the strain generation mechanism in ceramic/ceramic composites by in-situ high-energy x-ray diffraction. Macroscopically measured strain behaviour shows drastic change in properties as a function of volume fraction of FE phase present. The variation in strain mechanism has been elucidated by high energy x-ray diffraction study under applied electric fields. We present novel structure property relationships for these kinds of emerging ceramic/ceramic composite.

(EMA-S3-P038-2014) Enhanced Light emission from Erbium Oxide nanoparticles for Electronic and Optical Devices Applications

M. Maqbool*, Qatar University, Qatar

Light emitting nanoparticles are getting special attention due to their use in optical technology and biomedical applications. The present work reports light emission from Erbium Oxide nanoparticles. The nanoparticles, with 43 nm diameter, were obtained in the form of nanopowder with 99.9% purity. These nanoparticles were characterized for their light emission under a 532 nm Nd:YAG laser excitation. A Photoluminescence (PL) system, made by Princeton Instrumentation, was used to detect fluorescence emission from the nanoparticles. The PL system consisted of Pixis brand CCD camera with a range of 300 to 2000 nm. The Erbium Oxide nanoparticles were also mixed in distilled water to obtain spectrum. Two emission peaks were observed around 554 nm and 813 nm from the Erbium Oxide nanoparticles. The green emission at 554nm was obtained as a result of $4I_{15/2} \rightarrow 4S_{3/2}$ transition, and the near infrared emission from $4I_{15/2} \rightarrow 4I_{13/2}$ transition. The process was also repeated in vacuum and it was found that the green emission enhances tremendously when the nanoparticles are excited in vacuum. This enhanced luminescence from the Erbium Oxide nanoparticles shows their potential importance in the electronic and optical devices applications.

(EMA-S3-P042-2014) The non-volatile control of 2DEG conductance at oxide interfaces

S. Kim*, Korea Institute of Science and Technology, Republic of Korea; D. Kim, Seoul National University, Republic of Korea; Y. Kim, S. Moon, M. Kang, J. Choi, Korea Institute of Science and Technology, Republic of Korea; H. Jang, Seoul National University, Republic of Korea; S. Kim, J. Choi, S. Yoon, H. Chang, C. Kang, S. Lee, Korea Institute of Science and Technology, Republic of Korea; S. Hong, Seoul National University, Republic of Korea; J. Kim, S. Baek, Korea Institute of Science and Technology, Republic of Korea

Epitaxial complex oxide thin film heterostructures have attracted a great attention for their multifunctional properties, such as ferroelectricity, and ferromagnetism. Two dimensional electron gas (2DEG) confined at the interface between two insulating perovskite oxides such as LaAlO₃/SrTiO₃ interface, provides opportunities to expand various electronic and memory devices in nano-scale. Recently, it was reported that the conductivity of 2DEG could be controlled by external electric field. However, the switched conductivity of 2DEG was not stable with time, resulting in relaxation due to the reaction between charged surface on LaAlO₃ layer and atmospheric conditions. In this report, we demonstrated a way to control the conductivity of 2DEG in non-volatile way integrating ferroelectric materials into LAO/STO heterostructure. We fabricated epitaxial Pb(Zr_{0.2}Ti_{0.8})O₃ films on LAO/STO heterostructure by pulsed laser deposition. The conductivity of 2DEG was reproducibly controlled with 3-order magnitude by switching the spontaneous polarization of PZT layer. The controlled conductivity was stable with time without relaxation over 60 hours. This is also consistent with robust polarization state of PZT layer confirmed by piezoresponse force microscopy. This work demonstrates a model system to combine ferroelectric material and 2DEG, which guides a way to realize novel multifunctional electronic devices.

(EMA-S3-P043-2014) Non-volatile electroresistive diode of PZT/LAO/STO heterostructure

S. Kim, Korea Institute of Science and Technology, Republic of Korea; C. Park, Seoul National University, Republic of Korea; J. Kim*, S. Baek, Korea Institute of Science and Technology, Republic of Korea

Complex oxide heterostructures have been emerged as one of the most fascinating fields in condensed matter physics. Especially, two dimensional electron gas (2DEG) at the interface between two insulating oxides, LaAlO₃ and SrTiO₃ has drawn a great attention due to its multifunctionality such as superconductivity, ferromagnetism,

and nanoscale control. Due to a few nanometer-thick confinement of 2DEG, an external electric field allows a large modulation of the 2DEG carrier concentration through depletion and accumulation. Therefore, the electrical leakage current from Pt top electrode to 2DEG through LAO in Pt/LAO/STO structure shows diode-behavior: electron can flow from 2DEG to Pt top electrode, but not the other way around. Here, we integrate ferroelectric epitaxial PZT thin films on LAO/STO to realize non-volatile electroresistive diode, equivalent to the serial connection of diode and non-volatile switch. We are able to control the leakage current by around one order of magnitude upon polarization reversal while blocking the current in the opposite direction. Our system will provide a promising platform to explore the artificial synapse.

(EMA-S3-P045-2014) Preparation and Characterization of Self-Assembled, Percolative BaTiO₃-CoFe₂O₄ Nanocomposites via Magnetron Co-sputtering

Q. Yang, W. Zhang, M. Yuan, L. Kang, J. Feng, J. Ouyang*, Shandong University, China

BaTiO₃-CoFe₂O₄ composite films were prepared on (100) SrTiO₃ substrates by using a radio-frequency magnetron co-sputtering method at 750°C. These films contained highly (001)-oriented crystalline phases of perovskite BaTiO₃ and spinel CoFe₂O₄, which can form a self-assembled nanostructure with BaTiO₃ well dispersed into CoFe₂O₄ under optimized sputtering conditions. A prominent dielectric percolation behavior was observed in the self-assembled nanocomposite. Compared with pure BaTiO₃ films sputtered under similar conditions, the nanocomposite film showed higher dielectric constants and lower dielectric losses together with a dramatically suppressed frequency dispersion. This dielectric percolation phenomenon can be explained by the "micro-capacitor" model, which was supported by measurement results of the electric polarization and leakage current.

(EMA-S4-P014-2014) Encapsulation Process of OLED Using a LMPA-Epoxy Double Layered Structure

H. Choi*, E. Im, C. Moon, Hoseo University, Republic of Korea

Encapsulation technology to ensure the blocking characteristics from the moisture and oxygen is an essential problem to be solved for the mass production of the OLEDs. Frit encapsulation using laser anneal is best in performance as a barrier, but crack is unavoidable due to the high temperature thermal stress. Thin film encapsulation is another choice, but the blocking characteristics from the moisture and oxygen are not so good due to the structural imperfectness of the organic thin film layers. In this study, we are to develop an encapsulation process using a LMPA-epoxy mixture. Low melting point alloy (LMPA) will play a role of barrier from the moisture and oxygen, and epoxy will provide an adhesion strength and fill the voids at the interface between the substrate and metal layer. To realize this idea, LMPA and epoxy were separated each other to form a double layer structure. We have changed some experimental factors such as annealing temperature and design of the materials, and a thin metal layer was used as a sacrificial layer to get a good separation characteristic. We could get a well-separated double layered structure using Sn-58Bi and epoxy mixture with 180°C annealing, which showed the possibility as a barrier layer from the moisture and oxygen.

(EMA-S4-P015-2014) Change of the Heat Dissipation Characteristics According to the Emissivity at the Surface of LED Module

K. Park*, C. Moon, Hoseo Univ, Republic of Korea

Heat dissipation is a critical factor which directly determines the reliability and lifetime of the LED module in connection with the junction temperature of LED chip, especially for the high power LED module. In most LED modules, heat dissipation is conducted using various types of heat sinks to dissipate the heat which have been conducted from the LED chips to the outside efficiently. A lot of works have been done about the heat conduction and convection

at the surface, but few works have been reported about the heat radiation. In this study, therefore, we are to study the heat radiation at the surface of the heat sink. At first, we have done FVM simulation works using Ansys ICEPAK V13.0 program to study the effects of the changes of the emissivity at the surfaces of the heat sinks combined with the change of the thermal conductivity. From the works, we have found that the emissivity at the surface could affect the heat dissipation characteristic, ultimately resulting in the change of the junction temperature. For a next step, we prepared some LED modules and estimated the emissivity at the surface of the heat sinks comparing the thermal image using IR camera and surface temperature using thermo couple. Lastly, we conducted a surface coating to change the surface emissivity experimentally, and investigated the effect on the junction temperature of the LED chip.

(EMA-S4-P017-2014) Effective activated carbon based counter electrode for dye sensitized solar cells: electrochemical study

Z. Li*, M. Akhtar, W. Lee, O. Yang, Chonbuk National University, Republic of Korea

Carbon based nanomaterials such as carbon blacks, carbon nanotubes and carbon fibers etc. have recently received great attention owing to their excellent properties like the high mechanical strength, thermal stability and their excellent electronic properties. In this work, the steam treated activated carbon (AC) powder was used to prepared effective counter electrode (CE) for the fabrication of dye sensitized solar cells (DSSCs). Well ordered and uniform AC thin film electrode was achieved by the mixing of AC and binder solution of nafion:ethanol (1:10, v/v%). Cyclic voltammetry analysis revealed that AC CE displayed the high redox current density, representing the better reduction of triiodide ions to iodide ions in redox electrolyte. The high electrocatalytic activity of AC CE was explained by measuring the electrochemical impedance spectroscopy (EIS) which showed the low charge transfer resistance at the interface of CE and electrolyte layer. AC CE based DSSC accomplished reasonable overall conversion efficiency of 3.91% with high short circuit current density of 8.56 mA/cm² and open circuit voltage of 0.773 V. The improved photovoltaic performance and high photocurrent were attributed to its high electrocatalytic activity towards the reduction of I³⁻ ions and low charge transfer resistance at the interface of CE and electrolyte.

(EMA-S5-P018-2014) Effect of MMT Addition on Tensile Properties of Graphene Oxide/Chitosan Nanocomposites

D. Kim*, Y. Mithlesh, K. Rhee, Kyunghee University, Republic of Korea

MMT is one of the most important layered silicates used for the preparation of these organic or inorganic nanocomposites. It is known that MMT/polymer nanocomposites frequently exhibit remarkably improved mechanical and materials properties such as a higher modulus, increased strength, decreased gas permeability and increased biodegradability of biodegradable polymers. In this work, the novel chitosan nanocomposites film with MMT and graphene oxide was successfully prepared by a simple solution mixing-evaporation method. The structure, thermal stability, and mechanical properties of the composite films were investigated. FTIR result indicates an enhanced hydrogen-bonding interaction between chitosan and the fillers by using both MMT and graphene oxide. FESEM studies illustrated the excellent dispersion of MMT and graphene oxide in the CS matrix, without aggregation. The XRD analysis of MMT/GO/CS nanocomposite film showed that the GO sheets were well exfoliated in the CS matrix. TGA results suggested that the (5% MMT)/(1% GO)/CS nanocomposite film is more thermally stable than the chitosan, GO/CS, MMT/CS. With incorporation of 5 wt % MMT and 1wt% GO, the tensile strength of the (5%) MMT/(1%) GO/CS nanocomposite was 9% and 27% higher than that of the (1%) GO/CS and chitosan, respectively

(EMA-S5-P037-2014) Redox behavior of (Ba,Sr)(Ti,Zr)O₃ systems

Y. Han*, G. Song, Sungkyunkwan University, Republic of Korea

Redox behavior of (Ba_{1-x}Sr_x)(Ti_{1-y}Zr_y)O₃ has been studied at P(O₂)=1atm by measurements of equilibrium electrical conductivity at various temperatures, (x=0~0.3, y=0~0.3). The substitution of isovalent impurities such as Sr and Zr would not introduce any charged compensating defect species. However, the replacement of Sr and Zr will systematically change the cell size; the Sr substitution decreases the lattice parameters of perovskite cell and the Zr substitution increases the size. In (Ba,Sr)(Ti,Zr)O₃ system, the oxidation enthalpy (ΔH_p) increased with Zr contents as well as with Sr contents. The system codoped with Sr and Zr, (Ba_{0.9}Sr_{0.1})(Ti_{1-y}Zr_y)O₃ shows larger oxidation enthalpies than Ba(Ti_{1-y}Zr_y)O₃ regardless of Zr contents. This result is contradictory to the Ca substituted (Ba,Ca)TiO₃ system, where the oxidation enthalpy decreases with Ca contents. In this paper, the enthalpy cost for oxidation in (Ba,Sr)(Ti,Zr)O₃ systems will be discussed in terms of unit cell size and space availability of oxygen vacancy around the substituted elements.

(EMA-S6-P019-2014) Marine and Automotive Thermoelectric Generators Development in the Frame of the EC - PowerDriver Project

Y. Gelbstein*, Ben Gurion University, Israel; J. Tunbridge, R. Dixon, Intrinsic Materials Ltd, United Kingdom; M. Reece, H. Ning, Queen Mary University of London, United Kingdom; R. Gilchrist, Jaguar Land Rover, United Kingdom; R. Summers, Halyard Ltd, United Kingdom; I. Agote, TECNALIA Research and Innovation, Spain; I. Dimitriadou, K. Simpson, European Thermodynamics Ltd, United Kingdom; C. Rouaud, P. Feulner, Ricardo, United Kingdom; S. Rivera, Nanoker Research SL, Spain; M. Husband, Rolls Royce PLC, United Kingdom; J. Crossley, I. Robinson, Thermex Ltd, United Kingdom

The EC granted PowerDriver project aims to develop thermoelectric generators in the range of 300-600W output electrical power for automotive applications (gasoline engines) by utilizing the waste exhaust heat generated into useful electrical power. The project has also a target of more than 1.5kW for marine (Diesel engines) applications. The PowerDriver project applies for the first time to marine applications, showing several clear advantages. Since maximizing the thermoelectric efficiency requires maximizing the hot side temperature and minimizing the cold side temperature, it is clear that marine applications are capable of much more effectively cooling the cold side using the large reservoir of cold sea water, compared to automotive applications which are limited by the coolant flow rate through the cars radiator. There are difference in operation between automotive applications and marine application on the hot side as well. Since both the automotive and the marine applications seem very promising, both of the approaches are investigated in the PowerDriver project. Silicide and telluride based thermoelectric materials are considered for marine and automotive applications, respectively.

(EMA-S6-P020-2014) Enhanced thermoelectric performance in bismuth telluride based alloys by multi-scale microstructural effects

T. Zhu*, L. Hu, Zhejiang University, China

Multi-scale microstructural effects have been introduced by a simple hot deformation process to obtain high-performance n-type bismuth telluride based alloys. The donor-like effect (an interaction of antisite defects and vacancies), which can be adjusted by varying hot deformation temperature, is also considered responsible for the remarkable enhancement in power factor. Highly preferred orientation enables a significant improvement in in-plane electrical conductivity. Besides, the in-plane lattice thermal conductivity is greatly reduced by in-situ nanostructures and high-density lattice defects generated during the hot deformation process. The present study experimentally demonstrates a successful combination of

microscale texture enhancement, atomic scale lattice defects and donor-like effect and recrystallization induced nanostructures as a new approach to improve thermoelectric properties. These effects led to a maximum ZT of 0.95 for the $\text{Bi}_2\text{Te}_2\text{Se}_1$ sample hot deformed at 823K, about 80% improvement than that without hot deformation.

(EMA-S6-P021-2014) Surface Flatness of Fe_2VAl -based Epitaxial Thin-films Prepared by Ion Beam Sputtering Technique

K. Kato*, K. Iwasaki, TOYOTA BOSHOKU CORPORATION, Japan;
Y. Furuta, T. Miyawaki, H. Asano, T. Takeuchi, Nagoya University, Japan

Fe_2VAl -based Heusler alloys possess a large thermoelectric power factor ($S^2 \rho^{-1} = 5.5 \text{ mW m}^{-1} \text{ K}^{-2}$, where S and ρ are the Seebeck coefficient and the electrical resistivity, respectively) at ca. 300 K. However, the thermoelectric figure of merit ($Z = S^2 \rho^{-1} \kappa^{-1}$, κ is the thermal conductivity) is kept below 0.1 due to the large κ ($28 \text{ W m}^{-1} \text{ K}^{-1}$). To make use of nanosized multilayered periodic structure is one of the effective methods for reducing κ because it enhances Umklapp process of phonon scattering. This superlattice effect on κ requires flat surface of multiple phases stacking alternately. In this study, therefore, we investigated the surface flatness of single-phased Fe_2VAl films prepared by ion beam sputtering (IBS). Out of plane and in-plane XRD patterns of a film grown on MgAl_2O_4 substrate at 773 K showed only $h00$ peaks. In the in-plane rocking curve, the 220 peaks of Heusler phase showed 4-fold symmetry. These data suggest the epitaxial growth of the Heusler phase. The root mean square roughness of the prepared film was 0.3 nm, even when the thickness of the film exceeded 150 nm. The value of 0.3 nm is smaller than the lattice constant of Fe_2VAl (0.576 nm). These results indicate that the IBS is one of the appropriate techniques to prepare superlattice films. The thermoelectric properties of the prepared films will be discussed.

(EMA-S6-P022-2014) Uncertainty analysis of Seebeck coefficient and electrical resistivity characterization

J. Mackey*, University of Akron, USA; A. Sehirlioglu, Case Western Reserve University, USA; F. Dynys, NASA Glenn Research Center, USA

In order to provide a complete description of a material's thermoelectric power factor, in addition to the measured nominal value, an uncertainty interval is required. The uncertainty may contain sources of measurement error including systematic bias error and precision error of a statistical nature. The work focuses specifically on the popular ZEM-3 (Ulvac Technologies) measurement system, but the methods apply to any measurement system. The analysis accounts for sources of systematic error including sample preparation tolerance, measurement probe placement, thermocouple "cold-finger" effect, and measurement parameters; in addition to including uncertainty of a statistical nature. Complete uncertainty analysis of a measurement system allows for more reliable comparison of measurement data between laboratories.

(EMA-S6-P023-2014) Transient thermoelectric solution employing Green's functions

J. Mackey*, University of Akron, USA; A. Sehirlioglu, Case Western Reserve University, USA; F. Dynys, NASA Glenn Research Center, USA

The study works to formulate convenient solutions to the problem of a thermoelectric couple operating under a time varying condition. Transient operation of a thermoelectric will become increasingly common as thermoelectric technology permits applications in an increasing number of uses. A number of terrestrial applications, in contrast to steady-state space applications, can subject devices to time varying conditions. For instance thermoelectrics can be exposed to transient conditions in the automotive industry depending on engine system dynamics along with factors like driving style. In an effort to generalize the thermoelectric solution a Green's function method is used, so that arbitrary time varying boundary and initial conditions may be applied to the system without reformulation. The solution demonstrates that in thermoelectric applications of a

transient nature additional factors must be taken into account and optimized. For instance, the material's specific heat and density become critical parameters in addition to the thermal mass of a heat sink or the details of the thermal profile, such as oscillating frequency. The calculations can yield the optimum operating conditions to maximize power output and/or efficiency for a given type of device.

(EMA-S6-P024-2014) Thermoelectric properties of $\text{Ba}_2\text{NaNb}_5\text{O}_{15}$ orient ceramics, and its hopping enhancement

H. Kakemoto*, T. Kawano, H. Irie, University of Yamanashi, Japan

Recently, n-type thermoelectric properties of reduced tungsten bronze type oxide (TB), $\text{Sr}_x\text{Ba}_{1-x}\text{Nb}_5\text{O}_{15}$ (SBN) single crystal is firstly reported about typical Seebeck coefficient (S) and electrical conductivity (σ) along c -axis. TB ceramic can be modified crystalline quality by crystallographic orientation technique, and is expected to increase dimensionless figure of merit (ZT). Here, we report about TE properties of oriented $\text{Ba}_2\text{NaNb}_5\text{O}_{15}$ (BNN) utilizing Harman method for ZT and thermal conductivity (κ). Mixture of BNN and needle-like BNN was used tape casting for *in-plane* orientation, and was sintered at 1340°C for 12h. The orient BNN was reduced at 1050°C-1100°C for 2-5h in CO atmosphere. Temperature dependence of S and that of σ for reduced BNN were measured from 20°C to 300°C. ZT and κ of BNN were measured by using Harman method. S and σ were measured about -260 $\mu\text{V/K}$ and 17.5 S/cm with weak temperature dependence, respectively. $\text{PF} (=S^2\sigma)$ was estimated to be $1.2 \times 10^{-4} \text{ W/mK}^2$. The behaviour of S was associated with small polaron. Heikes formula is introduced in view of ion hopping between Nb^{4+} and Nb^{5+} , and is expanded for temperature dependence in order to take account for hopping dynamics. In the presentation, the approaches of crystallographic orientation, reduction, and non-reduction for BNN will be emphasized about S for hopping enhancement, PF and ZT .

(EMA-S6-P025-2014) High Pressure Processing of Bulk Nanoscale Thermoelectrics

E. Gorzkowski*, J. Wollmershauser, B. Feigelson, Naval Research Laboratory, USA

Recent history has shown that materials exhibit unexpected and often exceptional properties when scaled down to nanostructures due to quantum confinement effects. In this paper we will discuss the use of the NRL developed "bottom-up" technologies to fabricate 3D monolithic thermoelectric materials comprised of carefully designed and retained bulk nanostructures. The NRL High Pressure Lab has developed techniques that provide an opportunity to overcome the limitations of previous attempts to form bulk monolithic nanostructured thermoelectrics with high ZT values. The integrated approach employs total environmental control for both nanopowder surface preparation and high pressure sintering. By forcing complete control over the processing conditions, sintering occurs at temperatures as low as 0.2 T_{melt} at ~5GPa. At such low temperatures and high pressures, bulk diffusional and grain coarsening processes are sluggish and complete densification of the nanopowder occurs via surface driven processes without modification to the overall nanostructure, including crystallographic phase.

(EMA-S7-P026-2014) Energetics for lead migration across Pt/PbTiO₃ and Pt₃Pb/PbTiO₃ interfaces: A computation study

F. Lin*, A. Chernatynskiy, S. R. Phillpot, J. C. Nino, University of Florida, USA; J. L. Jones, North Carolina State university, USA; S. B. Sinnott, University of Florida, USA

A number of current electronic devices utilize lead-based perovskite compounds like lead titanate (PbTiO_3 or PTO) in thin film form. These thin films are often in contact with metal (e.g Pt, Au, Ir, etc.) layers that serve as connecting electrodes. Over time, the formation of intermetallics like Pt_3Pb for example has been observed at the PTO/Pt interface. Density functional theory (DFT) calculations are used here to analyze the migration barriers of Pb atoms across Pt/

PTO and Pt3Pb/PTO interfaces and help determine how this migration depends on the composition and orientation of the interface. In particular, the DFT calculations are used to determine the interfacial energies and work of adhesion and the results are compared to experimental measurements. This work is supported by the National Science Foundation through grant DMR-1207293.

(EMA-S9-P027-2014) Design and fabrication of ceramic-based inverters using ZnO and TiO₂ films assembled by wet processing technique

L. C. Liao*, Y. Lin, Yuan Ze University, Taiwan

Ceramic-based inverters, composed of two p-channel metal-oxide-semiconductor field-effect transistors (p-MOSFETs), were designed and fabricated using the assembly of TiO₂ and ZnO films. The stacked ZnO and TiO₂ (ZnO/TiO₂) films, prepared by spin coating methods, were characterized as semiconductor diodes after annealed according to the current-voltage data analysis. The device of the p-MOSFET was first designed by a SiO₂ layer coated on ITO as a gate and ZnO was coated on top of the SiO₂ layer to fabricate the MOS structure. Two pieces of TiO₂ films, coated on ITO substrates, were stacked with the ZnO film of the MOS device, served as a source and a drain, respectively. Results show that this device performed as a p-channel thin film transistor by current-voltage (I-V) measurements. The ceramic-based inverter was prepared by the circuit connection of the two p-MOSFETs. The voltage transfer characteristics of the inverters were evaluated by the tests of the input voltage (V_{in}) versus the output voltage (V_{out}) data.

(EMA-S9-P028-2014) Optical properties of nanostructured anatase thin films formed by the low temperature aqueous sol gel – flow coating approach

O. Muñoz-Serrato*, J. Serrato-Rodríguez, Universidad Michoacana de San Nicolás de Hidalgo, Mexico; T. Ishibashi, Nagaoka University of Technology, Japan

Spectroscopic ellipsometry was used to measure porosity and optical properties of thin films formed from sol-gel alkoxides precursors. The 100nm thick low roughness films containing 4nm anatase particles were formed by flow coating. The coating velocity and the angle of film deposition influenced the porosity of the film. Results showed that films obtained at higher substrate velocity and high blade angles rendered porosities of 40%. While low substrate velocity and low angles resulted in 25%. Porosity affected the refractive index (n) and the band gap (E_g), n varied within 1.85-1.89 at λ 550nm. 3.55-3.44eV for E_g varied according to porosity. Such high band gap values are due to the small particle size and high porosity levels. Transmittance as measured by UVvis was found as high as 80% for the visible region that is the result of the 4nm particle size. Thin films were successfully nanostructured via sol-gel precursor-flow coating; Ellipsometry allowed to characterize processing parameters i.e. thickness and porosity as well as optical properties. Optical properties were closely related to porosity induced during flow coating. The 4nm particle size of the films was an outstanding feature of the material and largely explained the resulting high values of band gap and transmittance.

(EMA-S12-P029-2014) Cryogenic Propulsion Technologies for 45 Megawatt Electric Aircraft

G. Y. Panasyuk*, UES Inc., USA; T. J. Haugan, Air Force Research Laboratory, USA

Advantages of cryogenic power propulsion are demonstrated for two aircrafts: the Boeing 787-9 (“Dreamliner”) and the world’s largest turbo-prop airplane the Antonov AN-22. A simple model that describes fuel/energy consumption as well as time and distance dependence of the power used in these aircrafts and their hypothetical electric analogues is introduced. The major components of 45 MW drive-trains were considered for both cryogenic and Cu-wire propulsion systems. As is shown, the cryogenic style drive-train is 20

times lighter and provides 50-70% longer flight range than a Cu-wire drive-train, reducing fuel cost by several times.

(EMA-S12-P030-2014) Development of high energy density SMES devices with YBCO wire

D. Latypov, BerrieHill Research Corp., USA; T. Bullard, UES Inc., USA; T. Haugan*, The Air Force Research Laboratory, USA

Superconducting magnetic energy storage (SMES) devices offer attractive and unique features including no theoretical limit to specific power, high cycling efficiencies and charge/discharge rates, and virtually no degradation with cycling. The mass specific energy density (MSED) of SMES systems; however, falls short of many needs. This paper examines SMES energy densities of solenoid-type magnets achievable using present day technology and future technology advancements. Scaling of maximum energy density with the stored energy, length of the conductor and radius of the bore were established with numerical simulations, and studied for a range of stored energies up to 250 MJ and operating temperatures of 4.2, 18, 40 and 65 K. With dependence of critical current on field taken into account, the optimum magnet design for YBCO also including H//c is a pancake coil with scaling of energy density $\epsilon \sim E^{1/3}$. Thus, current and magnetics limits achievable ϵ only at a fixed E. The overall limit on ϵ is also imposed by the virial theorem. Without additional structural support ϵ of a YBCO magnet is limited to $\sim 30\text{Wh/kg}$. However with introduction of light-weight and strong support materials the upper limit MSED of SMES is expected to exceed that of the best batteries $\epsilon \sim 150\text{Wh/kg}$.

(EMA-S12-P044-2014) Stability of structures in K-intercalated iron selenide superconductors

G. Wang*, Y. Liu, T. Ying, X. Lai, S. Jin, X. Chen, Chinese Academy of Sciences, China

The discovery of superconductivity at about 30 K in metal-intercalated iron selenides has stimulated significant interest as their structural and physical characteristics are remarkably different from other iron-based superconductors. However, the real structure of superconducting (SC) phases in this family is still ambiguous for the ubiquitous presence of phase separations. Recently, we clarified that there are at least two SC phases with nearly completed FeSe layers in the K-intercalated iron selenides by a liquid ammonia method, determined mainly by K concentration. Here we report the investigation of structures in K-intercalated iron selenides using first-principles calculations for understanding the fact that SC phases are stable only at particular K doping level. It is demonstrated that K_{0.25}Fe₂Se₂ and K_{0.5}Fe₂Se₂ similar to the experimental results, which are based on $2\sqrt{2} \times 2\sqrt{2} \times 1$ and $\sqrt{2} \times \sqrt{2} \times 1$ supercells of KFe₂Se₂ respectively, are more stable compared to various other structures. Coulomb force and lattice dynamics are the key factors to determine the stability of these structures.

(EMA-S12-P018-2014) Optimizing Flux Pinning of YBCO Superconductor with BaSnO₃+Y₂BaCuO₅ Mixed Phase Additions

M. P. Sebastian, AFRL, USA; G. Y. Panasyuk, UES, USA; H. Wang, Texas A & M University, USA; T. J. Haugan*, J. N. Reichart, AFRL, USA

Adding nanophase defects to YBa₂Cu₃O₇ (YBCO) superconductor thin films is well-known to enhance flux pinning, resulting in an increase in current densities (J_c). Previously, most studies have focused on single-phase additions; however the addition of several phases simultaneously has shown strong improvements by combining different flux pinning mechanisms. This paper further explores the effect of mixed phase nanoparticle pinning, with the addition of insulating, nonreactive phases of BaSnO₃ (BSO) and Y₂BaCuO₅ (Y211). Processing parameters vary the volume % of BSO and deposition temperature of films prepared by pulsed laser deposition on LaAlO₃ and SrTiO₃ substrates. The addition of Y211 = 3 volume % is constant. Results comparing the contribution of strong and weak flux pinning, current densities, critical temperatures, and microstructures will be presented.

(EMA-S13-P031-2014) Lithium Titanate as Anode Material in Lithium-Ion Batteries

D. Seshadri*, Case Western Reserve University, USA; M. Shirpour, M. Doeff, Lawrence Berkeley National Laboratory, USA

Previous research has shown that $\text{NaTi}_3\text{O}_6(\text{OH}) \cdot 2\text{H}_2\text{O}$ (Sodium Titanate, abbreviated as NNT herein) is a viable and stable anode for use in sodium-ion batteries. Ion exchange between synthesized (via hydrothermal synthesis) NNT and LiNO_3 was performed to yield $(\text{Li}_x\text{Na}_{1-x})\text{Ti}_3\text{O}_6(\text{OH}) \cdot 2\text{H}_2\text{O}$ (Lithium Titanate, herein written as LNT). Electrodes for NNT and LNT were prepared using 70% Active Material, 25% Acetylene Black, and 5% Binder. Coin cells were assembled to study the electrochemical capacity of these materials. X-ray diffraction (XRD), Scanning Electron Microscopy (SEM), and Energy-Dispersive X-ray Spectroscopy (EDS) were performed to study the resultant LNT structure. Results show that the ion-exchange process was successful and verified the synthesis of $(\text{Li}_x\text{Na}_{1-x})\text{Ti}_3\text{O}_6(\text{OH}) \cdot 2\text{H}_2\text{O}$. It is shown that the electrochemical capacities of unmilled LNT at various C-rates were higher than that of NNT counterparts. Thus, we conclude that LNT is a stable and better anode choice for use in lithium-ion batteries.

(EMA-S13-P032-2014) Effects of High Energy X Ray and Proton Irradiation on Lead Zirconate Titanate Thin Films' Dielectric and Piezoelectric Response

Y. Bastani, A. Y. Cortes-Pena*, A. D. Wilson, Georgia Institute of Technology, USA; S. Gerardin, M. Bagatin, A. Paccagnella, University of Padova, Italy; N. Bassiri-Gharb, Georgia Institute of Technology, USA

Ferroelectric thin films with large dielectric permittivity, piezoelectric coefficients, and electromechanical coupling are attractive for a range of applications such as random access memories, multilayer capacitors, energy harvesting devices, micro- and nano-electromechanical sensors and actuators. Especially of interest are autonomous microsystems for use in locations in which high radiation exposure (nuclear power plants, space applications, etc.) might be harmful to humans. The effects of irradiation by X rays and protons on the dielectric and piezoelectric response of highly (100)-textured polycrystalline lead zirconate titanate (PZT) thin films have been studied. Low field dielectric permittivity, remanent polarization, and piezoelectric d_{33} response all degraded with exposure to radiation, for doses higher than 300 krad. At first approximation, the degradation increased at higher radiation doses, and was stronger in samples exposed to X rays, compared to the proton-irradiated ones. Post-radiation heat treatment samples at above the Curie temperature showed an almost full recovery of the response. Nonlinear and high-field dielectric characterization suggest a radiation induced reduction of the extrinsic contributions to the response, attributed to increased pinning of the domain walls by the radiation-induced point defects.

(EMA-S13-P033-2014) Co-fired Multilayer Ceramic Batteries for Safe Electrochemical Energy Storage

L. Gao*, A. Baker, S. S. Berbano, C. Randall, The Pennsylvania State University, USA

Solid-state batteries are safer than batteries with liquid electrolytes. Co-fired multilayer ceramic batteries, similar to co-fired multilayer ceramic capacitors (MLCC), have been demonstrated in the patent literature by NAMICS Corp. and represent an exciting and almost unexplored area of research. Using new chemistries, our goal is to examine the compatibility and functionality of thin (200 μm) $\text{Li}_{1.5}\text{Al}_{0.5}\text{Ge}_{0.5}(\text{PO}_4)_3$ (LAGP) solid electrolyte tape printed with various redox active phases (LiCoO_2 , LiMn_2O_4 , and $\text{Li}_3\text{V}_2(\text{PO}_4)_3$) and metallic powders (Ag and Pd). The $\text{Li}_3\text{V}_2(\text{PO}_4)_3$ material is of interest since it can behave as both a positive and negative electrode. Understanding the thermochemical compatibility and shrinkage characteristics are the major challenges while exploring the co-firing of new chemistries. This paper focuses on the processing and

characterization using (1) X-ray diffraction (XRD), (2) Scanning electron microscopy (SEM), (3) Density measurements, and (4) Impedance spectroscopy. For temperatures less than 800°C, the XRD patterns of unfired and co-fired LAGP are unchanged. SEM micrographs of LiCoO_2 -based electrodes showed well-defined layers. Fired samples were 88% dense with printed LiMn_2O_4 and 75% dense with printed $\text{Li}_3\text{V}_2(\text{PO}_4)_3$ compared with the theoretical density of LAGP. Impedance spectroscopy was employed between 0°C and 130°C to characterize fired LAGP tapes.

Thursday, January 23, 2014

Plenary Session II

Room: Indian

Session Chair: George Rossetti, University of Connecticut

8:30 AM

(EMA-002-2014) Lead-free piezoceramics: History, achievements, future (Invited)

J. Roedel*, Technische Universität Darmstadt, Germany

Legislation originating from Europe has enhanced scientific interest in the research on lead-free piezoceramics about 10 years ago, although earlier work was done 50 years ago and some companies started research in the 1990s. Therefore I will summarize the current legislation, the progress which has been made overall in eliminating lead from industrial products and briefly review its toxicity. The evolution in research in lead-free piezoceramics over the last 20 years is then highlighted and the chances for success evaluated. In particular, progress in alkali niobates is contrasted to bismuth-based piezoceramics and barium titanate-based piezoceramics and is discussed with reference to the salient properties required. The focus will be on application-relevant properties like temperature-dependence, stress dependence, cycle and frequency dependence of the materials in question. In the end I will discuss recent advances in product development and will suggest applications where PZT may be replaced soon. As guidance for researchers, I will outline the immediate needs for the next five years and try to sketch the road for lead-free piezoceramics after that period.

S1: Functional and Multifunctional Electroceramics for Commercialization**Multifunctional Properties in Oxides**

Room: Pacific

Session Chairs: Dragan Damjanovic, Swiss Federal Institute of Technology - EPFL; Pamela Thomas, University of Warwick

10:00 AM

(EMA-S1-017-2014) Polarization Mechanism and New Trend of Dielectric Study (Invited)

T. Tsurumi*, K. Takeda, T. Hoshina, Tokyo Institute of Technology, Japan

Dielectric response of materials is governed by the polarization induced by electric field. Polarization mechanisms are categorized into 4 mechanisms: i.e., electronic, ionic, dipole and interfacial polarizations. In this lecture, we will introduce our recent achievements and/or new trend of dielectric study related to each polarization mechanism. Refractive index is determined by the electronic polarization, and the change of refractive index with external field is referred to as the electro-optic (EO) effect. We have studied the origin of EO-effect to find that the EO-effect was not caused by the change of electric polarization with electric field but by the photo-elastic effect combined with piezoelectric and/or electrostrictive effects.

10:30 AM

(EMA-S1-018-2014) Using high resolution neutron diffraction to study the impact of Jahn-Teller active Mn³⁺ on strain effects and phase transitions in Manganites Perovskites (Invited)

B. J. Kennedy*, The University of Sydney, Australia

Mixed-valence manganites of the type Sr_{1-x}Ln_{0.x}MnO₃ display fascinating and potentially technologically important magnetic and electronic properties. Here I will describe some of our recent variable temperature high resolution powder neutron diffraction studies of a number of examples. These measurements have been supplemented by XANES measurements to quantify the Mn³⁺ content of the samples. We have focused on examples where the MnO₆ octahedra show a large Jahn-Teller type distortion due to the presence of Mn³⁺ and displaying a tetragonal to cubic transition at high temperatures. The structural and lattice parameter data have been used to determine the octahedral tilting and spontaneous strains associated with the structural, electronic and magnetic phase transitions in a number of examples. Using very high resolution we have quantified the effects of both the Jahn-Teller type distortion and magnetic ordering on the structures.

11:00 AM

(EMA-S1-019-2014) New Soft Composite Multiferroics and Solid Spin Modulated Multiferroics Structures

Z. Kutnjak*, B. Rozic, Jozef Stefan Institute, Slovenia; M. Jagodic, Institute of Mathematics, Physics and Mechanics, Slovenia; S. Gyergyeck, M. Drofenik, D. Arcon, Jozef Stefan Institute, Slovenia

Magnetoelectric behavior in recently synthesized soft composite multiferroic mixtures of ferroelectric liquid crystals (LC) with various magnetic nanoparticles (NPs) is reviewed. The indirect coupling between the magnetization and electric polarization via the LC director field is observed and the electric field control of the magnetization is confirmed via SQUID susceptometer. Furthermore, the layered FeTe₂O₅Cl system was studied by specific-heat, muon spin relaxation, nuclear magnetic resonance, dielectric, as well as neutron and synchrotron x-ray diffraction measurements. From the comparison of the magnetic structures and orientations of the electric polarizations, a tentative phenomenological model, explaining the observed magnetoelectric behavior is derived. The magnetoelectric coupling is proposed to originate from the temperature dependent phase difference between neighboring amplitude modulation waves similar to FeTe₂O₅Br [1]. [1] M. Pregelj, O. Zaharko, A. Zorko, Z. Kutnjak, P. Jeglic, P. J. Brown, M. Jagodic, Z. Jaglicic, H. Berger, and D. Arcon, Phys. Rev. Lett. 103, 147202 (2009). [2] M. Pregelj, A. Zorko, O. Zaharko, Z. Kutnjak, M. Jagodić, Z. Jaglicic, H. Berger, M. de Souza, C. Balz, M. Lang, and D. Arcon, Phys. Rev. B 82, 144438 (2010).

11:15 AM

(EMA-S1-020-2014) Photocatalytic property of ferroelectric (Na,K)NbO₃

N. Kato*, K. Kakimoto, Nagoya Institute of Technology, Japan; M. Wegner, A. Roosen, University of Erlangen-Nuremberg, Germany

Ferroelectric material has a potential to assist a photocatalytic reaction because the spontaneous polarization of ferroelectrics can separate photo-generated charge carriers. Ferroelectric (Na,K)NbO₃ ceramic is one of the attractive photo-catalysts due to its good ferroelectric properties as well as relatively high conduction band levels. In this work, NKN ceramics was produced and its photocatalytic reactivity was evaluated before and after poling treatment. (Na_{0.5}K_{0.5})NbO₃ ceramics were synthesized via spark plasma sintering route at 980 °C for 10 min followed by annealing at 900 °C for 4 h. The specimens were then mirror polished, then polarized in oil bath at 30 kV/cm for 30 min at room temperature. The photocatalytic reactivity was evaluated by reduction of NO₃⁻ ions to NO₂⁻ ions. NKN specimens were put into a NaNO₃ solution and irradiated by 350 nm of a Xe lamp. After irradiation for 120 min,

the amount of NO₂⁻ generated due to photo-catalytic reaction was estimated by a colorimetric method. It was found that the photocatalytic reactivity of the surface of polarized NKN specimens increased significantly after polarization. This indicates a remnant polarization of NKN would assist photocatalytic reaction.

11:30 AM

(EMA-S1-021-2014) Glass-like Thermal Conductivity of (010)-Textured Lanthanum-doped Strontium Niobate Synthesized with Wet Chemical Deposition

B. M. Foley*, University of Virginia, USA; H. J. Brown-Shaklee, M. J. Campion, D. L. Medlin, P. G. Clem, J. Ihlefeld, Sandia National Laboratories, USA; P. E. Hopkins, University of Virginia, USA

We measure the cross-plane thermal conductivity (κ) of (010)-textured, undoped and lanthanum-doped strontium niobate thin films via time-domain thermoreflectance (TDTR). The thin films were deposited on (001)-oriented SrTiO₃ substrates via the highly-scalable technique of chemical solution deposition (CSD). We find that both film thickness and lanthanum doping have little effect on κ , suggesting that there is a more dominant phonon scattering mechanism present in the system; namely the weak inter-layer-bonding along the b-axis in the strontium niobate parent structure. Furthermore, we compare our experimental results with two variations of the minimum-limit model for κ and discuss the nature of transport in material systems with weakly-bonded layers. The low cross-plane κ of these scalably-fabricated films is comparable to that of similarly layered niobate structures grown epitaxially.

11:45 AM

(EMA-S1-022-2014) Surface plasmon resonance based magnetic field sensor using N:ZnO thin film

K. Jindal, University of Delhi, India; M. Tomar*, Miranda House, University of Delhi, India; V. Gupta, University of Delhi, India

In the present work, we demonstrate the development of magnetic field sensor using SPR technique in ferromagnetic nitrogen doped ZnO (ZnO:N) thin film. A laboratory assembled prism coupling based SPR setup was used, where a p-polarized light from a He-Ne laser ($\lambda=633$ nm) is incident on film surface via a prism. A thin film of gold (40 nm) was deposited on hypotenuse face of a quartz prism in order to obtain prism-Au-air system. ZnO:N films (200 nm) (N = 0, 4%, 8% and 10%) were deposited on gold coated face of prism (prism-Au-ZnO:N) by pulsed laser deposition in oxygen ambient at 10mT pressure at a substrate temperature of 650°C. SPR reflectance measurements were made as a function of angle of incidence of laser and the data was fitted with Fresnel's equations in order to obtain the value of refractive index for ZnO:N thin films. MOKE was studied in transverse configuration (TMOKE) by applying an external magnetic field of varying strength. Refractive index of ZnO:N films have been studied as function of magnetic field using a SPR setup and the variation is attributed to MOKE. The reproducible linear dependence of θ on magnetic field with a sensitivity of about 50 o/Tesla demonstrates the potential application of ZnO:N thin film for magnetic field sensor.

12:00 PM

(EMA-S1-023-2014) Development of MEMS based E-nose for the detection of harmful gases

A. Sharma*, R. Gupta, P. Tyagi, A. Singh, L. Rana, M. Tomar, V. Gupta, University of Delhi, India

In the present work, an effort has been made towards the development of e-nose based on MEMS technology for the detection of harmful and toxic gases. Prepared e-nose comprises an array of four sensor structures fabricated over platform consisting of four microheaters to be operated at different temperatures. Platinum microheaters have been fabricated using bulk micromachining technique on silicon dioxide membrane which provided improved thermal isolation of active area. Microheaters were then integrated

with tin oxide based sensor structure for the faster detection of NO₂, H₂, LPG and H₂S gases. The temperature of microheaters could be controlled by varying the applied dc voltage. The microheaters have been found to obtain a maximum temperature of ~800°C at a dc voltage of 3V. For selective detection of the four gases different catalyst were integrated with the SnO₂ sensing layer using RF sputtering technique. For the detection of NO₂ gas bare SnO₂ was considered whereas for the detection of H₂, LPG and H₂S gases, nanoclusters of Pd, Pt and Cu were deposited respectively over the surface SnO₂ thin film. All the four sensor structures were operated at different temperatures in order to get the maximum sensing response with low power consumption (~5mW).

12:15 PM

(EMA-S1-024-2014) From the Heywang model to the fractal electronics properties intergranular capacity relations

V. Mitic*, V. Paunovic, L. Kocic, University of Nis and Institute of Technical Sciences of SASA, Serbia

Ceramics grains contacts are essential for understanding complex dielectric properties of electronic ceramics materials. Since the real intergrain contact surface is an irregular object, the theory of fractal sets can be introduced. Also we are introducing the Heywang model of intergranular capacity as a basic idea for further relations with fractal structure. BaTiO₃-ceramics, studied in this paper, has fractal form in, at least, two levels: shapes and distributions of grains and intergrains contacts. Using method of fractal modeling a reconstruction of microstructure configurations, like shapes of grains or intergranular contacts can be successfully done. Furthermore, the area of grains surface is calculated by using fractal correction that expresses the irregularity of grains surface through fractal dimension. This leads to word a more exact calculuties of ceramics dielectric properties as well as more realistic understanding of electrical behaviour of barium-titanate ceramics. In order to obtain an equivalent circuit model, which provides a more realistic representation of the electronic materials electrical properties, in this article we have determined and implemented an intergranular contacts model for the BaTiO₃ electrical properties characterization.

S2: Multiferroic Materials and Multilayer Ferroic Heterostructures: Properties and Applications

Multiferroic Devices

Room: Indian

Session Chair: Greg Carman, UCLA

10:00 AM

(EMA-S2-015-2014) Magnetoelectric Multiferroic Heterostructures and Low-Power Devices (Invited)

N. Sun*, Northeastern University, USA

The coexistence of electric polarization and magnetization in multiferroic materials provides great opportunities for realizing magnetoelectric coupling, including electric field control of magnetism, or vice versa, through a strain mediated magnetoelectric interaction effect in layered magnetic/ferroelectric multiferroic heterostructures. Strong magnetoelectric coupling has been the enabling factor for different multiferroic devices, which however has been elusive, particularly at RF/microwave frequencies. In this presentation, I will cover the most recent progress on novel layered microwave multiferroic heterostructures and devices, which exhibit strong magnetoelectric coupling. We will demonstrate strong magnetoelectric coupling in novel microwave multiferroic heterostructures. At the same time, we will demonstrate E-field modulation of anisotropic magnetoresistance, giant magnetoresistance and exchange bias at room temperature in different multiferroic heterostructures. New multiferroic devices will also be

covered in the talk, including ultra-sensitive nanoelectromechanical systems magnetoelectric sensors with picoTesla sensitivity, multi-ferroic voltage tunable bandpass filters, voltage tunable inductors, tunable bandstop filters, tunable phase shifters and spintronics.

10:30 AM

(EMA-S2-016-2014) Loss Mechanism in Modern Microwave Dielectrics (Invited)

N. Newman*, S. Zhang, L. Liu, Arizona State University, USA

I review my group's work using modern experimental and theoretical condensed matter methods to understand intrinsic & extrinsic factors involved in optimizing high-performance microwave dielectrics. We focus on BaZn_{1/3}Ta_{2/3}O₃ (BZT) & BaZn_{1/3}Nb_{2/3}O₃ (BZN), but also show that the conclusions are general for other common materials. BZT and BZN exhibit the unusual combination of a large dielectric constant & a small loss tangent. Ab-initio electronic structure calculations show the desirable properties arise from charge transfer between cation d-orbitals; providing a degree of covalent directional bonding that resists angular distortions between atoms. This results in a more rigid lattice with higher melting points & enhanced phonon energies & thus inherently low microwave loss. Properties of commercial materials are optimized by adding alloying agents, such as Ni, to adjust the temperature coefficient of resonant frequency to zero. At low temperatures, the dominant loss mechanism in these commercial materials comes from spin excitations of unpaired transition-metal d electrons in isolated atoms (light doping) or exchange coupled clusters (moderate to high doping). At higher temperatures, loss is observed that arises and can be dominated by hopping transport. We describe our efforts to develop tunable materials at sufficiently high temperatures & small enough magnetic fields for practical applications.

11:00 AM

(EMA-S2-017-2014) Strain mediated magnetoelectric coupling using substrate constrained thin film ferroelectrics (Invited)

C. S. Lynch*, J. Cui, J. Hockel, UCLA, USA

Strain mediated magnetoelectric coupling at small length scales has been demonstrated using thin film Ni nano features on a single crystal [011] cut and poled PMN-PT substrate. In this experimental arrangement the entire piezoelectric substrate undergoes the same strain. These Ni/PMN-PT heterostructures have provided a demonstration of the effect, but are not well suited to the development of strain mediated magnetoelectric coupling based devices that require magnetization control of the individual magnetic features. Going to thin film ferroelectric materials grown on a Si substrate presents the challenge of the substrate constraining the in-plane strain of the film. This work presents an approach to overcoming the substrate constraint without complicated etching processes. Finite element simulations have been used to generate electrode pattern designs that enable local strain control when the electrode separation is on the same size scale as the film thickness. The electrode designs were fabricated and demonstrated to switch the easy axis of a Ni film at the mm scale. Fabrication work is ongoing to demonstrate this effect at the micron scale and smaller.

11:15 AM

(EMA-S2-018-2014) Strain Mediated Multiferroics: Reorientation of Single Domain Magnetic Moments (Invited)

G. Carman*, UCLA, USA

This presentation describes the ongoing work of reorienting single domain magnetic structures attached to piezoelectric material using electric fields. Magnetic single domain structures are small in size and have large surface to volume ratios. The orientation of the magnetic moment is strongly dependent upon various anisotropy energies including magneto-crystalline, demagnetization, and magnetoelastic. These magnetic anisotropies are well described with classical Landau-Lifshitz-Gilbert micromagnetic equations. What

is not as well understood or described is the transfer of mechanical energy into the small single magnetic domain structures using electric field induced strain. In these structures it is inappropriate to use a constant strain assumption due to the relatively large surface area that produce significant non-uniform strain distributions. In this presentation these issues are discussed in the context of a fully couple LLG with mechanics model and validated with experimental data on a Ni/PMN-PT single domain multiferroic structure. Analytical and experimental data indicate geometric design of the magnetic single domain is a critical issue in creating a structure that can be significantly manipulated with a piezoelectric material through the magnetoelastic effect.

11:30 AM

(EMA-S2-019-2014) Field-directed Assembly of Ferrite-Ferroelectric Core-Shell Nanofibers and Studies on Magneto-electric Interactions (Invited)

G. Sreenivasulu, M. Popov, K. Sharma, G. Srinivasan*, Oakland University, USA

Multiferroic composites with ferroelectric and ferromagnetic phases have attracted considerable attention in recent years for studies on the nature of magneto-electric (ME) interactions. In this work we have synthesized ferrite-ferroelectric core-shell nano-fibers by electrospinning and allowed them to assemble in a magnetic and/or electric field. Systems studied include nickel ferrite and barium titanate (BTO) or PZT. Fibers with 1-2 micron in diameter and 0.2-0.4 micron ferrite of ferroelectric core with lengths ranging from 10-100 micron were prepared. Electron microscopy studies show the anticipated core-shell structure for the nanowires. The fibers were assembled into rings, parallel wires and mats in a static magnetic field gradient and ac or dc electric fields. The effects of the field strength and frequency on the structure of the resulting assembly were investigated. Data on polarization vs electric field under a bias magnetic field H , permittivity vs f under H , and low-frequency ME effects indicate strong strain mediated ME coupling in the samples. Studies over 16-42 GHz show evidence for strong magneto-dielectric effects in the composites.

11:45 AM

(EMA-S2-020-2014) Ferroelectric and Multiferroic Hetero-structure Devices for Adaptive RF Circuit Applications (Invited)

T. Kalkur*, University of Colorado, USA

Adaptive RF electronics is becoming very important in multiband communication systems. Tunable devices fabricated with ferroelectric capacitors are expected to play an important role in this area of research because of their voltage polarity independent tunability, fast tuning capability, absence of moving parts, small size and capability to be integrated on any substrate. These tunable devices can be used to fabricate tunable single band and multiband band-pass, band stop filters, power splitters, multiband power amplifiers, tunable antennas and tunable thin film bulk acoustic resonators. In this presentation, application of these ferroelectrics in a wide variety of RF blocks that can be used in RF wireless communication systems will be reviewed. In addition, the design, fabrication and implementation of RF blocks with tunable BST capacitors will be presented. The opportunities to implement a variety of circuit blocks such as DC-DC converters using switched polarization charges in ferroelectric capacitors will also be presented.

12:00 PM

(EMA-S2-021-2014) Synthesis and Integration of Multifunctional Materials based on Complex Oxides and their Heterostructures (Invited)

J. P. Chang*, UCLA, USA

The demand of engineering metal oxide thin films at an atomic level has grown immensely due to their versatile applications in numerous technologically advanced fields including microelectronics,

optoelectronics, photonics, spintronics, energy storage devices and sensors. In this talk, I will discuss current research advances in atomic layer deposition for synthesizing multifunction and complex metal oxides with tailored electronic, chemical, interfacial, thermal properties and microstructures. Specifically, I will highlight our most recent research on the engineering of multiferroics thin films and their integration, for applications in memory devices, antenna and motors.

12:15 PM

(EMA-S2-022-2014) PZT/FeGa non-linear microcantilevers as robust multiferroic memory devices

I. Takeuchi*, University of Maryland, USA

We are investigating the characteristics of microfabricated PZT/FeGa multiferroic cantilevers. The cantilevers can be driven by AC or DC magnetic and electric fields, and the device response can be read off as a piezo-induced voltage. The mechanical resonant frequency of the cantilevers was found to follow a hysteresis behavior with DC bias magnetic field applied in the cantilever easy axis. The cantilever dimensions are such that various energy scales (magnetic energies (Zeeman, anisotropy), mechanical energy) are comparable in magnitude, and the mechanical degree of freedom emerges as a key tunable device parameter. Driving them in the non-linear regime, enhanced mechanical coupling at the tunable resonant frequency can be used to perform versatile read/write memory operations. In such devices, electric field and/or magnetic field can be used as input. Our Si-based multiferroic devices are scalable with high fabrication yields, and have stable write/read operations at room temperature which have been tested for > 10⁶ cycles. Results of parametric amplification to boost the magnetoelectric coefficient will be discussed. This work is carried out in collaboration with T. Onuta, Y. Wang, and S. E. Lofland, and it was funded by DARPA.

S3: Structure of Emerging Perovskite Oxides: Bridging Length Scales and Unifying Experiment and Theory

Inhomogeneities, Nonstoichiometry, and Point Defects

Room: Coral B

Session Chairs: Philip Lightfoot, University of St Andrews; Alexei Bosak, European Synchrotron Radiation Facility

10:00 AM

(EMA-S3-014-2014) Peculiar Inhomogeneous States in Ferroelectrics and Multiferroics (Invited)

L. Bellaiche*, University of Arkansas, USA

The purpose of this Talk is to report and discuss highly inhomogeneous states that differ from conventional ferroelectric and magnetic arrangements and that were all recently found via the use of ab-initio and first-principles-based techniques. Examples are: 1) The occurrence of the so-called polar nanoregions in solid solutions made of Ba(Zr,Ti)O₃ relaxor ferroelectrics. 2) The formation of arrays of ferroelectric vortices, antivortices and phase-locking phases, in films made of multiferroic BiFeO₃ films and in nanocomposites. 3) The microscopic understanding of the complex magnetic cycloid of BiFeO₃, including its associated and newly observed spin density waves. 4) The discovery of a novel crystallographic state in a variety of ferroelectrics and multiferroics (e.g., BiFeO₃, PbTiO₃ and EuTiO₃ thin films, as well as PbTiO₃/BiFeO₃ superlattices), in which cations adopt a nanoscale zig-zag configuration. 5) The existence of nanoscale twinned phases in BiFeO₃ and EuTiO₃ bulk. These phases possess complex oxygen tilting patterns that are coupled with unusual antiferroelectricity. They also provide a successful explanation for puzzling experimental data, such as X-ray

spectra varying over a long-time period or a dramatic difference between short-range and average crystallographic structures.

10:30 AM

(EMA-S3-015-2014) Investigation of Defect Dipole Kinetics in the Ferroelectric and Paraelectric Phases of Acceptor Doped BaTiO₃ Single Crystals (Invited)

R. Maier*, T. Pomorski, P. Lenahan, C. Randall, The Pennsylvania State University, USA

Room temperature conductivity in perovskites containing acceptor dopants or impurities is controlled by the concentration of oxygen vacancies and the interaction of those vacancies with oppositely charged dopant ions. Coulombic forces and relaxation of lattice strain provide driving forces for the formation of defect associates. Knowledge of the energy of association between acceptor sites and oxygen vacancies is necessary to properly interpret properties like ionic conductivity which have the important role of determining aging and resistance degradation behavior. A comprehensive study will be presented on the interaction of iron and manganese defects with oxygen vacancies in BaTiO₃ crystals. The effects of defect dipole orientation and dissociation kinetics on aging rates measured by the evolution of internal bias in ferroelectric hysteresis loops, ionic conductivity measured by low temperature impedance spectroscopy, and domain wall mobility measured by Rayleigh analysis will be presented. Careful high temperature equilibration of doped crystals in different oxygen atmospheres has been performed in order to present a detailed analysis with the aid of electron paramagnetic resonance on the effect of dopant valence state on low temperature defect associate formation and the resulting impact on the ferroelectric and dielectric properties.

11:00 AM

(EMA-S3-016-2014) Dynamics of Point Defects in Perovskite Dielectric Materials

C. Randall*, D. P. Shay, R. A. Maier, J. A. Bock, The Pennsylvania State University, USA; S. Lee, KICET, Republic of Korea

Point defect distributions and dynamics are discussed in perovskite dielectrics in both the ferroelectric and paraelectric phases. We consider acceptor doped materials and the association/dissociation of oxygen vacancies with the acceptor cations. We also consider the dynamics of defect dipoles in relation to the interaction with the ferroelectric polarization. In the cases of large electromigration of oxygen vacancy, we contrast degradation kinetics and point out a new model to consider the non-linear hopping of oxygen vacancies. Techniques that we utilize include TEM, EPR, TSDC, and Impedance Spectroscopy to aid bridging a self-consistent picture of local to macroscopic data.

11:15 AM

(EMA-S3-017-2014) Impact of Non-Stoichiometry and Aliovalent Doping on Materials Properties of Functional Oxides – from Ferroelectrics to Lithium-Ion Battery Cathode Materials (Invited)

R. A. Eichel*, RWTH Aachen University, Germany

Point defects, such as transition-metal dopants or oxygen vacancies as well as their defect complexes, markedly impact materials properties and thus determine device performance and life time. By using dedicated spectroscopic techniques, the defect structure of oxide ceramics used for energy conversion and storage is analyzed and the impact of corresponding defect chemistry to enhance materials hardening (for piezoelectric compounds), improve the power density (for lithium-ion batteries) is demonstrated. Particularly, atomic-scale mechanisms that limit life time are presented for both types of applications.

11:45 AM

(EMA-S3-018-2014) Synthesis and Crystal Structure of Perovskite Dielectric (Na,Li)(Nb,Ta)O₃

J. J. Carter*, University of Florida, USA; I. Levin, NIST, USA

Capacitors are used in a wide variety of electronic devices but must operate below 130°C due to the phase transition of the most commonly used dielectric material, barium titanate. Many applications require capacitors to operate at elevated temperatures. Sodium lithium niobate tantalate is a material that could potentially serve as a high temperature dielectric. Several compositions of this material with varying amounts of lithium and tantalum ($y = 0, 0.05, 0.1, 0.15$; $x = 0, 0.2, 0.4, 0.6$) were prepared in air as well as in reducing atmospheres and at different temperatures to determine the effect of these variables on the structure of the material. X-ray diffraction and Rietveld refinement showed the existence of orthorhombic and/or rhombohedral phases in the samples. Unit cell volume was found to decrease with increasing amounts of tantalum, while a reducing atmosphere lowered the amount of rhombohedral phase present.

12:00 PM

(EMA-S3-019-2014) Effects of A-site Stoichiometry in 1-x(Bi_{0.5}Na_{0.5}TiO₃)-xBaTiO₃ Ceramics Near the Morphotropic Phase Boundary (MPB)

S. Prasertpalichat*, D. Cann, Oregon State University, USA

Stoichiometric and non-stoichiometric compositions based on 1-x(Bi_{0.5}Na_{0.5}TiO₃)-xBaTiO₃ where $x=0.055, 0.06$ and 0.07 (i.e. near the morphotropic phase boundary) were prepared by a solid state mixed oxide method. X-ray diffraction analysis of all samples showed a single perovskite phase with pseudo-cubic symmetry. In stoichiometric compositions, high levels of dielectric loss were dramatically decreased after annealing for 7 days. This can likely be attributed to the presence of oxygen vacancies ($V_o^{\bullet\bullet}$) which compensate for Bi vaporization at high sintering temperatures. In non-stoichiometric compositions, the donor-doped compositions resulted in a significant improvement in dielectric loss whereas the acceptor-doped compositions showed an increase in loss. Impedance data were used to gain a better understanding of the conduction mechanisms and the overall electrical homogeneity of the ceramics. The hardening and softening of the ferroelectric hysteresis loops was also observed in acceptor-doped and donor-doped compositions, respectively. The hardening is most likely due to the pinning of domain wall by defect dipoles. In the electromechanical strain data, no significant change in maximum strain was observed due to changes in stoichiometry.

S5: Structure and Properties of Interfaces in Electronic Materials

Transport at Interfaces

Room: Caribbean B

Session Chair: Nick Strandwitz, Lehigh University

10:00 AM

(EMA-S5-001-2014) The Role of Grain Boundaries in the Internal Reduction of Ni²⁺ in YSZ (Invited)

I. Reimanis*, Colorado School of Mines, USA; J. T. White, Los Alamos National Laboratory, USA; J. Tong, Colorado School of Mines, USA; J. R. O'Brien, Quantum Design, Incorporated, USA; A. Morrissey, Colorado School of Mines, USA

The kinetics of internal reduction of Ni²⁺ ions dissolved in polycrystalline 10 mol % Y₂O₃-stabilized ZrO₂ (10YSZ) is examined, and it is shown that YSZ grain boundaries dictate the behavior. Specimens with 0.01, 0.1 and 0.5 m/o Ni²⁺ in solid solution within 10YSZ were prepared via chemical methods followed by calcination. They were then heat treated in Ar – 2% H₂ at 1273 K for times ranging from 1 to 20 h. SQUID magnetometry was used

to quantify the amount of Ni metal (Ni^0) formed during the heat treatment. The formation of Ni^0 followed parabolic kinetics, and was well-described by a Schmalzried-type internal reduction model. Transmission electron microscopy revealed that internal reduction occurs in two stages: (1) at short times, Ni^0 precipitates at grain boundaries. (2) For longer times, Ni^0 forms inside the grains.

10:15 AM

(EMA-S5-002-2014) Dopant Effects on Cation Diffusion in α - Al_2O_3

L. Feng*, S. Dillon, University of Illinois at Urbana Champaign, USA

The effects of Mg^{2+} and Si^{4+} dopants on cation lattice and grain boundary diffusivities in polycrystalline α - Al_2O_3 have been investigated between 1100 degree celsius to 1400 degree celsius. Energy dispersive spectroscopy and secondary ion mass spectrometry are employed to measure Cr^{3+} diffusivity in the lattice and grain boundaries, respectively. Our preliminary results indicate that Cr^{3+} diffusivity is comparable to Al^{3+} diffusivity measured previously in undoped alumina and is larger than O^{2-} diffusivity. The results also suggest that the aliovalent cation dopants have negligible effect on the Cr^{3+} diffusivity. The results will be rationalized on the basis of defect interactions.

10:30 AM

(EMA-S5-003-2014) Transport mechanism by gas/solid interactions in metal-oxide semiconductor interfaces

J. Jung*, S. Lee, Kyungnam University, Republic of Korea

The interaction of gas with the sensing element in the electrode-oxide semiconductor interface can cause changes in electrical properties. Hydrogen molecules are adsorbed and dissociated on the outer metal surface. The atomic hydrogen permeates through the bulk lattice toward the metal/oxide semiconductor, causing a perturbation at this interface that gives rise to a change in the output signal. An oxide semiconductor gas sensor generally consists of a thin or thick film of particulate oxide semiconductor materials, whose macroscopic conductance is measured using a pair of electrodes with dimensions much larger than the particle size. Gas phase species can become adsorbed on the particles. If physisorption occurs, there is little direct effect on the macroscopic conductivity although occupation of surface sites by the physisorbed species may block adsorption of other species. If chemisorptions occurs, with charge transfer between the adsorbate and the oxide semiconductor, the charged surface layer produces bending of the conduction and valence band edges. When particles are essentially separate, with no grain intergrowth, the band-bending leads to a potential barrier between neighboring particles, and a change in the macroscopic conductance relative to that of a pristine film with no adsorbate.

Consequences of Interfaces

Room: Caribbean B

Session Chair: Shen Dillon, University of Illinois at Urbana-Champaign

10:45 AM

(EMA-S5-004-2014) Novel Ceramic Metal Nanostructures by Reduction of Mixed Oxides (Invited)

H. M. Chan*, M. Kracum, K. Anderson, A. Kundu, Lehigh University, USA

A long standing challenge in the field of materials has been, for a given application, combining the optimum properties from different classes of materials. In the case of metal ceramic microstructures, the type of morphologies that can be achieved is limited by the available processing techniques. In this talk, results will be presented showing that unique microstructures, comprising interpenetrating

mixtures of metallic and ceramic phases can be achieved from the reduction of complex oxides of the type $\text{M}^1\text{M}^2\text{O}_{x+y}$. The less stable oxide is reduced leaving the metal (M^1), and the other oxide (M^2O_y). Examples of ceramics which have been shown to be amenable to this approach include CuAlO_2 (delafossite) and CoTiO_3 . CuAlO_2 is of interest to the electronics community because it is a p-type transparent semiconductor. Processing of the bulk precursor oxides will be discussed, together with the influence of reduction conditions on the resulting ceramic-metal structures. In addition to the generation of unique micro/nano-structures, the findings of this study also have implications for the potential to develop metallic complexions at ceramic grain boundaries.

11:15 AM

(EMA-S5-005-2014) Interface-dependent electrochemical behaviour of nanostructured manganese (IV) oxide (Mn_3O_4)

V. Liu*, Y. Ng, B. Okatan, K. Bogle, R. Amal, V. Nagarajan, University of New South Wales, Australia

We present results of our work on understanding the role of interfaces in the electrochemical behaviour of nanostructured manganese oxide. Manganese Oxide (Mn_3O_4) nanocrystals have been deposited on Nb:doped Strontium Titanate (Nb:SrTiO_3) substrate via pulsed laser deposition. (001), (101) and (112) orientated nanocrystals were successfully grown on (100), (110) and (111) Nb:SrTiO_3 substrates respectively. Crystallographic analysis suggests nanostructure growth may be dependent upon polarity, rather than lattice misfit alone, where morphology of each surface orientation is such that electrostatic repulsion can be minimised. Cyclic voltammetry (CV) was performed to understand how specific capacitance values vary with changing lattice orientations. The maximum specific capacitance calculated for the (100) orientation was 34F/g at the 3000th cycle, after which the CV loop plateaus rapidly. Structural analysis of this sample revealed a morphological transformation from the (001) orientation to the (101) platelet structures after CV cycling. The observed transformation could be the result of lattice misfit relaxation and electrostatics. The maximum specific capacitance obtained was for the (112) sample (120F/g) suggesting that such non-primary planes in spinel oxides may be most attractive for electrochemical applications. The research is supported by an ARC Discovery project.

11:30 AM

(EMA-S5-006-2014) In Situ Testing of High Strength Niobium-Sapphire Interfaces at the Nanoscale

R. Hao*, E. Saiz, F. Giuliani, Imperial College London, United Kingdom

Ceramic-metal interfaces are a critical feature in many material structures for example thermal barrier coatings and microelectronics. The purpose of this study is to investigate the mechanical properties of extremely thin metallic interlayers (< 500 nm) within ceramic bi-crystals and the adhesion at the ceramic-metal interface. The samples were prepared using the following steps: (a) thin Niobium layers were sputtered on the surface of <0001> oriented sapphire substrates; (b) the sapphire crystals with the Niobium faces in between were diffusion bonded at temperatures ranging between 1200 °C and 1500 °C; (c) micro-pillars were produced with the focused ion beam, containing a single uniform metallic interlayer. The pillars were compressed in situ in the SEM, which provide real-time load-displacement data. The pillars can hold withstand a load of ~8GPa in compression until they fracture or sliding at the sapphire-Niobium interfaces. TEM observation of the interface before and after testing has been used to understand the fracture mechanism. In summary, we have demonstrated the fabrication of nanosized metallic interlayers and we have used them to test the interfacial strength in situ at the nanoscale. This has shown that the interfacial strength can reach values of 4GPa in shear.

11:45 AM

(EMA-S5-007-2014) Dielectric & Piezoelectric Enhancement of Potassium Niobate/Barium Titanate Nano-complex Ceramics with Parallel Configuration of Structure-gradient Regions

S. Wada*, University of Yamanashi, Japan

Barium titanate (BaTiO₃, BT) and potassium niobate (KNbO₃, KN) (BT-KN) nano-structured ceramics with artificial morphotropic phase boundary (MPB) structure were successfully prepared by solvothermal method at temperatures below 230 deg. C. Especially, structure-gradient region (SGR) can be expected to enhance piezoelectric and dielectric properties, and then, to induce parallel configuration of SGR, new preparation method was proposed and developed in this study. As the results, KN epitaxial layer was successfully deposited on BT nanoparticle accumulation with necking structure between neighbored BT nanoparticles. Various characterizations confirmed that the BT-KN nano-structured ceramics exhibited BT/KN molar ratio of 1, a porosity of around 30 % and heteroepitaxial interface between BT and KN. Their apparent piezoelectric constant d_{33}^* was estimated at 300 pC/N, and was eight times larger value than that of the 0.5BT-0.5KN dense ceramics, while dielectric constant was estimated at 1600 at room temperature. The concept proposed in this study can be a new way to create piezoelectric ceramics with artificial MPB region.

12:00 PM

(EMA-S5-008-2014) Cylindrical and Ring Micro and Nano laser on optical fibers and titanium oxide nanotubes/nanowires

M. Maqbool*, Qatar University, Qatar; G. Ali, Pakistan Institute of Engineering & Applied Sciences, Pakistan

We have observed and report lasing action in titanium doped aluminum nitride deposited around an optical fiber. Optical fibers of 12 microns diameter were coated with a sputter deposited layer (4 micron thick) of titanium (1 at. %) doped amorphous aluminum nitride. When optically pumped by a Nd:YAG green laser at 532 nm, laser action was observed in whispering gallery modes around the fiber (in a ring shape) at 780.5 nm with a quality factor $Q > 1500$. Other modes were also observed between 775 nm and 800 nm. The primary and secondary modes give a mode separation of 4.6 nm. Along with its applications in optics and photonics the AlN:Ti micro laser we produced is very important from a biomedical applications point of view. Based on the successful achievement of microlaser action in optical fibers we are paying attention towards a nanolaser in titanium oxide nanowire or nanotube. We are in the process of growing titanium oxide nanowires and nanotubes. Thin film like AlN:Ti will be deposited on those nanowires/tube to achieve nanolaser.

S7: Computational Design of Electronic Materials**Design of Energy Materials**

Room: Coral A

Session Chair: Mina Yoon, Oak Ridge National Laboratory

10:00 AM

(EMA-S7-014-2014) Computationally Guided Design of Nanostructured Soft Matter and Multicomponent Materials for Energy Science (Invited)

B. Sumpter*, Oak Ridge National Laboratory, USA

The vital importance of energy to society requires the relentless pursuit of energy responsive materials that bridge fundamental chemical structures at the molecular level and achieve functionality, such as efficient energy conversion, over multiple length scales. This can potentially be realized by harnessing the power of self-assembly – a spontaneous process where molecules or much larger entities

form ordered aggregates as a consequence of predominately non-covalent (weak) interactions. However, predicting electronic transport and response of self-assembled molecular and hybrid architectures is complicated by the lack of understanding and control over nanoscale interactions, mesoscale architectures, and macroscale order. Unraveling the physicochemical processes that control structure and macroscopic properties requires tight integration of theory, modeling and simulation with precision synthesis, advanced experimental characterization and device measurements. This is the approach we use to understand how to design/manipulate the nanoscale organization of nanomaterials and their hybrid assemblies in order to achieve improved structure, properties, and functionality. Results discussed highlight progress for energy storage (supercapacitors), energy conversion (organic optoelectronics/photovoltaics) and lightweight structural materials.

10:30 AM

(EMA-S7-015-2014) Virtual high-throughput and Big Data techniques for the discovery and design of new organic semiconductors (Invited)

J. Hachmann*, University at Buffalo, SUNY, USA

The Harvard Clean Energy Project is concerned with the computational screening and development of new materials for organic electronics, in particular for photovoltaic applications. We have developed an automated, high-throughput framework for the virtual study of material candidates on an unprecedented scale. It utilizes quantum chemistry (augmented by techniques from materials informatics and machine learning) to characterize millions of molecular motifs and assess their potential for application as electronic materials. The Clean Energy Project represents the most extensive quantum chemical investigation ever conducted: we have so far screened 3 million compounds in 200 million DFT calculations, and generated a data volume of 500TB. The results are compiled and analyzed in an extensive database, which is openly available to the community. It is designed as an information hub and allows our partners to readily identify candidates with specific property combinations. In addition, it also facilitates our study of global trends using the results in its entirety. The extensive data collection provides a unique foundation for the study of the underlying structure-property relations, and the gained insights can open the door to a rational, systematic, and accelerated development of future high-performance materials.

11:00 AM

(EMA-S7-016-2014) Evolutionary search for the Crystal Structures of Novel Polymer Dielectrics

V. Sharma*, C. Wang, University of Connecticut, USA; Q. Zhu, Los Alamos National Laboratory, USA; G. Pilania, Stony Brook University, USA; A. R. Oganov, Los Alamos National Laboratory, USA; G. Sotzing, University of Connecticut, USA; S. Kumar, Columbia University, USA; R. Ramprasad, University of Connecticut, USA

We are involved in a search for new classes of polymers superior to polypropylene using first principles computations. Essential to this search are (i) strategies to efficiently navigate through the polymer chemical space (ii) schemes to identify promising building block motifs using our 'high-throughput' first principles computations¹, and (iii) identification of the stable crystal structures for these promising polymers. The present work involves aspect (iii). From our high-throughput first principles computations, it has been already determined that systems containing at least one aromatic group and at least one of the following moieties: -NH-, -CO-, or -O-, is desirable. In order to predict the stable structure of these polymeric materials, a new constrained evolutionary algorithm based computational approach, which has been implemented in the USPEX code, has been applied to a set of polymers for which reliable crystal structure information is already available experimentally. Next, we apply our methodology to predict the crystal structures for the identified new class of polymeric materials with high dielectric constant and

*Denotes Presenter

high band gap. The dielectric properties computed for these new polymers in the optimized crystal structures indicate that the identified polymers are of sufficient technological importance, which are hence currently going through a synthesis cycle.

11:15 AM

(EMA-S7-017-2014) Charge transport in lithium peroxide: relevance for rechargeable metal-air batteries (Invited)

M. Radin, D. Siegel*, University of Michigan, USA

The mechanisms and efficiency of charge transport in lithium peroxide (Li_2O_2) are key factors in understanding the performance of non-aqueous Li-air batteries. Towards revealing these mechanisms, we use first-principles calculations to predict the concentrations and mobilities of charge carriers in Li_2O_2 as a function of cell voltage. Our calculations reveal that changes in the charge state of O_2 dimers controls the defect chemistry and conductivity of Li_2O_2 . Negative lithium vacancies and small hole polarons are identified as the dominant charge carriers. The electronic conductivity associated with polaron hopping (10-20 S/cm) is comparable to the ionic conductivity arising from the migration of Li-ions (10-19 S/cm), suggesting that charge transport in Li_2O_2 occurs through a mixture of ionic and polaronic contributions. These data indicate that the bulk regions of crystalline Li_2O_2 are insulating, with appreciable charge transport occurring only at moderately high charging potentials that drive partial delithiation. The implications of limited charge transport on discharge and recharge mechanisms are discussed, and a two-stage charging process linking charge transport, discharge product morphology, and overpotentials is described. We conclude that achieving both high discharge capacities and efficient charging will depend upon access to mechanisms that bypass bulk charge transport.

11:45 AM

(EMA-S7-018-2014) Understanding the origin of high-rate intercalation pseudocapacitance in Nb_2O_5 crystals

P. Ganesh*, Oak Ridge National Laboratory, USA; A. Lubimtsev, Pennsylvania State University, USA; P. Kent, B. Sumpter, Oak Ridge National Laboratory, USA

Pseudocapacitors aim to maintain the high power density of supercapacitors while increasing the energy density towards those of energy dense storage systems such as lithium ion batteries. Recently discovered intercalation pseudocapacitors (e.g. Nb_2O_5) are particularly interesting because their performance is seemingly not limited by surface reactions or structures, but instead determined by the bulk crystalline structure of the material. We study ordered polymorphs of Nb_2O_5 and detail the mechanism for the intrinsic high rates and energy density observed for this class of materials. Using a combination of complementary theoretical method, such as: cluster-expansion, monte-carlo, global optimization and molecular dynamics, we rationalize this effect in $\text{Li}_x\text{Nb}_2\text{O}_5$ for a wide range of compositions and at finite temperatures. Multiple adsorption sites per unit-cell with similar adsorption energies and local charge transfer result in high capacity and energy density, while the interconnected open channels lead to low cost diffusion pathways between these sites, resulting in high power density. The nano-porous structure exhibiting local chemistry in a crystalline framework is the origin of high-rate pseudocapacitance in this new class of intercalation pseudocapacitor materials. This new insight provides guidance for improving the performance of this family of materials.

S12: Recent Developments in High-Temperature Superconductivity

New Superconductors and Their Progress

Room: Mediterranean B/C

Session Chair: Haiyan Wang, Texas A&M University

10:00 AM

(EMA-S12-001-2014) High T_c via the Mesoscopic Structure Route (Invited)

C. Chu*, L. Deng, Texas Center for Superconductivity at the University of Houston, USA

To determine the hidden cause for our recent detection of non-bulk superconductivity(SC) with an unexpectedly high onset- T_c s up to 49K in rare-earth-doped CaFe_2As_2 (Ca122) single crystals and the report by Xue's group of a T_c up to 50's K in unit-cell FeSe epi-films, we carried out detailed chemical, structural, and magnetic study of single crystalline Ca122 doped with La, Ce, Pr, and Nd. A special technique has also been developed and applied to the magnetic study of the 3-4 unit-cell FeSe-films. We have shown a doping-level independent T_c , the simultaneous appearance of superparamagnetism and SC, the existence of mesoscopic-2D structures in rare-earth doped Ca122 single crystals and thus provided evidence for the possible interface-enhanced T_c in Fe-based superconductors. Such mesoscopic-structures can be attributed to the rare-earth-doping-induced defects as evident from the presence of superparamagnetism detected in these SC samples. Similar observations were also obtained in the FeSe thin epi-films. We have observed in the 3-4 unit-cell FeSe-films Meissner effect below 1Oe with extensive weak-links up to ~20K; unconnected small SC patches up to ~40K; and an unusual dispersion of magnetic moment with frequency up to 70K. The weak-links and relaxation of the diamagnetic moment observed in the films suggest that the SC state of the FeSe films below 20K may be a glassy state.

10:30 AM

(EMA-S12-002-2014) Pushing the T_c - J_c - H_{c2} Boundaries of Iron-Chalcogenide Superconductors (Invited)

Q. Li*, Brookhaven National Lab, USA

Recently, we have demonstrated that the iron chalcogenide superconductors have a superior high-field performance over low temperature superconductors at 4.2 K.[Nature Communications (2013); Rep. Prog. Phys. (2011)] Although their superconducting transition temperatures (T_c) are typically lower than those of iron pnictides, iron chalcogenides exhibit low critical current anisotropies with very high upper critical field slopes near T_c . In this presentation, I will discuss recent progress in the superconducting films and coated conductors of iron chalcogenides. With a CeO_2 buffer, critical current densities (J_c) over 7 MA/cm² were observed in $\text{FeSe}_{0.5}\text{Te}_{0.5}$ films grown on single-crystalline and coated conductor substrates. Furthermore, these films have significantly higher T_c (>20K) as compared to bulk samples (bulk T_c ~15 K) for the entire doping regime of $\text{FeSe}_{1-x}\text{Tex}$. Structural analysis revealed that these films generally have significantly smaller c-axis and a-axis lattice constant than the bulk value, suggesting that the crystal structure changes have a dominating impact on the superconducting transition in iron-based superconductors. High J_c , low magnetic field anisotropies and relatively strong grain coupling make iron-chalcogenide coated conductors particularly attractive for high-field applications at liquid helium temperatures.

11:00 AM

(EMA-S12-003-2014) Role of Excess Fe in Iron Chalcogenide Superconductor (Invited)

H. Okazaki*, T. Yakaguchi, T. Watanabe, K. Deguchi, S. Demura, S. Denholme, T. Ozaki, National Institute for Materials Science, Japan; Y. Mizuguchi, Tokyo Metropolitan University, Japan; H. Takeya, National Institute for Materials Science, Japan; T. Oguchi, Osaka University, Japan; Y. Takano, National Institute for Materials Science, Japan

11-type iron chalcogenides are the simplest system with stacked only superconducting layers among the iron-based superconductors. Therefore, the iron chalcogenides are very suitable material to elucidate the mechanism of Fe-based superconductivity. However, excess Fe between superconducting layers in iron chalcogenides suppresses its superconductivity and results in the weak superconductivity. We extracted several thin crystals from the same $\text{FeTe}_{1-x}\text{Se}_x$ single crystal using the mechanical exfoliation and observed the inhomogeneous superconductivity by excess Fe [1]. Moreover, we successfully observed the Shubnikov-de Haas (SdH) oscillations in both superconducting and non-superconducting thin crystal. This is the first report of the SdH oscillation for the 11-type compound [2]. The SdH oscillations show that the inhomogeneity due to excess Fe is caused by the change of Fermi surface. We additionally found the annealing technique to induce bulk superconductivity [3,4]. Our results clearly show that the excess Fe plays an important role in the superconductivity of iron chalcogenides. References [1] H. Okazaki et al, J. Phys. Soc. Jpn. 81, 113707 (2012). [2] H. Okazaki et al, arXiv1207.6578. [3] Y. Mizuguchi et al., EPL 90, 57002 (2010). [4] K. Deguchi et al., Supercond. Sci. Technol. 24, 055008 (2011).

11:30 AM

(EMA-S12-004-2014) Fe-based Superconducting Thin Film Case Studies: From Fundamental Properties to Functional Devices (Invited)

S. Haindl*, University of Tuebingen, Germany

Fe-based superconductors bridge a gap between MgB_2 and the cuprate high temperature superconductors as they exhibit multi-band character and transition temperatures up to around 55 K. Investigating Fe-based superconductors thus promises answers to fundamental questions concerning the Cooper pairing mechanism, competition between magnetic and superconducting phases, and a wide variety of electronic correlation effects. The question addressed in this talk, however, is whether this new class of superconductors is also a promising candidate for technical applications? Superconducting film-based technologies are ranging from high-current and high field applications for energy production and storage to sensor development for communication and security issues and have to meet relevant needs of today's and future's society. In this talk we will highlight and discuss selected key issues for Fe-based superconducting thin film applications. We initially focus our discussion on the understanding of physical properties and actual problems in film fabrication based on a comparison of different observations made in the last years. Subsequently we address the potential for technological applications according to the present status.

12:00 PM

(EMA-S12-005-2014) Progresses on the study of iron selenide based superconductors (Invited)

X. Chen*, Institute of Physics, Chinese Academy of Sciences, China

The discovery of superconductivity (SC) at about 30 K in $\text{K}_0.8\text{Fe}_2\text{Se}_2$ and then in other alkali metals and thallium intercalated iron selenide has aroused a surge of research interests as these iron chalcogenides possess distinct characteristics of crystal structure and electronic structure from their iron pnictide counterpart superconductors. Considerable progresses have been made in the study of this class of superconductors. In this talk, I will report our recent studies and new insights on the structural and physical aspects, covering

the synthesis of smaller alkali metals, alkaline earths and some rare earths intercalated iron selenide superconductors through an ammonothermal route, crystal growth, identification of the superconducting phases, the structural stability, doping effects and other properties. Finally I will some review new progresses on related compounds and some controversial issues as well.

S13: Highlights of Undergraduate Student Research in Basic Science and Electronic Ceramics**Student Finalist Presentations, Thursday**

Room: Coral A

Session Chair: Geoff Brennecke, Sandia National Laboratories

12:40 PM

(EMA-S13-005-2014) Glass-like Thermal Conductivity of (010)-Textured Lanthanum-doped Strontium Niobate Synthesized with Wet Chemical Deposition

B. M. Foley*, University of Virginia, USA; H. J. Brown-Shaklee, M. J. Campion, D. L. Medlin, P. Clem, J. Ihlefeld, Sandia National Laboratories, USA; P. Hopkins, University of Virginia, USA

We measure the cross-plane thermal conductivity (κ) of (010)-textured, undoped and lanthanum-doped strontium niobate thin films via time-domain thermoreflectance (TDTR). The thin films were deposited on (001)-oriented SrTiO_3 substrates via the highly-scalable technique of chemical solution deposition (CSD). We find that both film thickness and lanthanum doping have little effect on κ , suggesting that there is a more dominant phonon scattering mechanism present in the system; namely the weak inter-layer-bonding along the b-axis in the strontium niobate parent structure. Furthermore, we compare our experimental results with two variations of the minimum-limit model for κ and discuss the nature of transport in material systems with weakly-bonded layers. The low cross-plane κ of these scalably-fabricated films is comparable to that of similarly layered niobate structures grown epitaxially.

12:55 PM

(EMA-S13-006-2014) In-situ investigation of dewetting kinetics in polycrystalline platinum thin films via confocal laser microscopy

S. Jahangir*, N. Valanoor, University of New South Wales, Australia; J. Ihlefeld, Sandia National Labs, USA

Metals and ceramic materials possess distinct diametric bonding characteristics, which is responsible for instability of the interface between these two materials. The aim of this work is to describe the kinetics of dewetting and subsequent morphological evolution in Platinum thin films grown on zinc oxide buffered (001) silicon substrates ($\text{Pt}/\text{ZnO}/\text{SiO}_2/(\text{001})\text{Si}$). We use a custom made confocal laser microscope coupled with a laser heating system to perform live imaging of the thin film dewetting under a range of heating and quenching ambients. Events including hillock formation, hole formation, hole growth leading to a network of Pt ligaments, break up of Pt ligaments to individual particles and subsequent Pt particle reorientation are observed in chronological fashion. These findings are corroborated by ex-situ atomic force microscopy and secondary electron microscopy quantitative analysis. The formation of meta-stable holes before film rupture is revealed to be critical stage that can not be captured with ex-situ methods. S.J and V.N acknowledge funding from the Australian Research Council. Sandia National Laboratories is a multi-program laboratory managed and operated by Sandia Corporation, a wholly owned subsidiary of Lockheed Martin Corporation, for the U.S. Department of Energy's National Nuclear Security Administration under contract DE-AC04-94AL85000.

1:10 PM

(EMA-S13-007-2014) New models for polarization reversal in poled ferroelectric ceramics

C. Cozzan*, University of Florida, USA; J. E. Daniels, University of New South Wales, Australia; J. L. Jones, North Carolina State University, USA

Polarization reversal involves reorienting spontaneous polarization by applying a field in an opposite direction. In the present work, the domain switching kinetics associated with polarization reversal are studied. Reversal in electrically poled, or biased, materials with large internal stresses was investigated using time-resolved high-energy X-ray diffraction. Additionally, a unique high-speed detection system was used in conjunction with ex situ macroscopic electro-mechanical strain measurements. Unexpectedly, a two-step reversal process is observed that can be modeled using two distinct time constants. Residual stress was studied by evaluating peak positions. The unique combination of these measurements provides evidence of the underlying physical mechanism of the two-step behavior, thereby improving the existing understanding of polarization reversal. This information is then used to develop a new mathematical model for domain reorientation during polarization reversal in ferroelectric/ferroelastic ceramics.

1:25 PM

(EMA-S13-008-2014) Microstructural origin for the piezoelectricity evolution in $(K_{0.5}Na_{0.5})NbO_3$ -based lead-free ceramics

H. Guo*, Iowa State University, USA; S. Zhang, Pennsylvania State University, USA; S. P. Beckman, X. Tan, Iowa State University, USA

The real-time evolution of the domain morphology and crystal structure under electrical poling fields of a model material, $0.948(K_{0.5}Na_{0.5})NbO_3-0.052LiSbO_3$, was directly visualized using *in situ* transmission electron microscopy. The original *Amm*2/*P4mm* polymorphic phase boundary is not stable against poling, and is finally replaced by the *Pm* phase. Complicated domain switching and phase transitions are observed to occur. At 8 kV/cm, the original herringbone domain patterns of mixed tetragonal and orthorhombic phases change to thin lamellar domains; this process involves domain switching as well as some extent of tetragonal to orthorhombic phase transition. At 14 kV/cm, a *Pm* phase with anti-parallel cation displacement (most likely combined with the $a^0b^+c^0$ oxygen octahedra tilting) is formed, as manifested by the appearance of blotchy domains and $1/2\{0eo\}$ superlattice diffraction spots. These microstructural changes are found irreversible, and hence they dictate the macroscopic properties of poled ceramics. The electromechanical response to the poling fields measured on the bulk ceramics correlate extremely well with the *in situ* observations. The microstructural mechanism for the enhanced piezoelectricity is the presence of the *Pm* phase at 14 kV/cm, where the large number of equivalent polar axis (24) makes the poling easier and more thorough.

1:40 PM

(EMA-S13-009-2014) Temperature dependent thermal conductivity of nano-grained Barium Titanate ($BaTiO_3$)

B. F. Donovan*, B. M. Foley, University of Virginia, USA; J. Ihlefeld, B. McKenzie, Sandia National Laboratories, USA; P. Hopkins, University of Virginia, USA

Barium Titanate ($BaTiO_3$) is a critical component of a wide array of devices including multi-layered ceramic capacitors, thermistors, and sensors. Performance and size scaling of devices, particularly multi-layered ceramic capacitors, has necessitated a scaling of $BaTiO_3$ grains to sub-100nm sizes. While the dielectric and structural properties of nano-grained $BaTiO_3$ has been widely studied, less is known about the thermal properties; in fact, discrepancies in the reputed values of the thermal conductivity of $BaTiO_3$ currently exist in literature. Accordingly, we study the effect of grain size on thermal conductivity of thin film barium titanate over

temperatures ranging from 77K to 500K. Nano-grained thin films were fabricated via chemical solution deposition, utilizing controlled annealing to modify average grain size. Time-domain thermoreflectance was used to determine the thermal conductivity of films with grain sizes ranging from 36nm-63nm. We show that at room temperature, the thermal conductivity of $BaTiO_3$ decreases with decreasing grain size, which is attributed to an increase in phonon scattering from grain boundaries. Additionally, the thermal conductivity of the samples was measured over a range of temperatures with special attention paid to regions of known structure transitions. We explore the results in the context of a model that incorporates phonon grain boundary scattering.

S1: Functional and Multifunctional Electroceramics for Commercialization

Defect Dynamics, Disorder, and Reliability

Room: Pacific

Session Chairs: Susan Trolier-McKinstry, Penn State; Clive Randall, Penn State University

2:00 PM

(EMA-S1-025-2014) Electrochemical Point Defect Dynamics in Ionic Ceramics (Invited)

E. C. Dickey*, A. Moballegh, North Carolina State University, USA

The electromigration of lattice point defects in ionic ceramics is a phenomenon that can lead to long-term degradation of electro-ceramic devices or that can be utilized to create unique device functionalities. This talk discusses the thermodynamics and kinetics of point-defect and interfacial reactions in rutile TiO_2 as a function of the initial point defect equilibrium, temperature and voltage biasing. The relationship between local microchemistry and electrical transport is studied through a combination of electrical transport measurements and electron microscopy techniques, and the local microchemistry at the electrode interfaces is found to be particularly important for the device leakage current. In particular, low oxygen activities at the cathode lead to high concentrations of point defects, eventual coalescence of point defects into higher dimensional lattice defects and even the condensation of new crystalline phases. All of these phenomena can modify the interfacial resistivity and thus global transport properties of the device.

2:30 PM

(EMA-S1-026-2014) Local-Structure Origins of Properties in Perovskite Ferroelectrics: A Combined-Technique Approach (Invited)

I. Levin*, NIST, USA

Differences between the local and average structures, even subtle ones, often control the exploitable properties of advanced materials. Therefore, determination of the local atomic arrangements is key to establishing structure-property relations for the design of new materials. Today, various measurement techniques exist for probing the local atomic order. Nonetheless, finding accurate comprehensive structural solutions still remains a challenge because any one of the existing methods yields only a partial view of the structure. We addressed this problem by developing a computational framework for local-structure determination in polycrystalline materials using simultaneous fitting of neutron total scattering, X-ray absorption fine structure, and single-crystal diffuse scattering data. The multiple-technique approach enables explicit determination of instantaneous atomic positions with accuracy and detail that are inaccessible by single-technique analyses. We will use representative perovskite-like electroceramic systems as examples of how detailed knowledge of the local structure can elucidate the origin of functional properties.

3:00 PM**(EMA-S1-027-2014) Voltage-dependent resistance phenomena in electroceramics (Invited)**

A. R. West*, University of Sheffield, United Kingdom

There are numerous ways in which the electrical resistance of ceramics may vary on application of a dc bias. These range from Schottky barrier phenomena to dielectric breakdown at high voltages. There is much recent interest in thin film memristive effects associated with redox reactions at sample-electrode interfaces; the associated charge injection into samples lead to resistance changes that are reversible only on application of a reverse bias. A related, but different, effect is the generation of filamentary conduction under the action of a dc bias which may, or may not, be reversible on removal of the bias. In bulk ceramics, resistances obey Ohm's law unless, in some way, there is a variation in carrier concentration under a dc bias. Apparent departures from Ohm's law of this kind have been found recently in acceptor-doped BaTiO₃ and CaTiO₃, in which the bulk resistance decreases reversibly on application of a small dc bias. (2) An overview of this effect will be presented, including the key role of oxygen redox equilibria at sample surfaces and the location of holes in p-type conductivity ceramics. 1. H. Belltran et al, J. Amer. Ceram. Soc, 93 500 (2010)., M. Prades et al, J Mater.Chem., 20 5 335 (2010); 2. M. Prades et al, Phys. Stat. Solidi A209 2267 (2012)

4:00 PM**(EMA-S1-028-2014) Electrical Partial Discharge as a Non-destructive Method for Reliability Evaluation of Piezoelectric Ceramics**

T. Hang*, J. Glaum, B. Phung, M. Hoffman, The University of New South Wales, Australia

In piezoelectric ceramics, defects such as pores and cracks are the main source of structural failure both without and under electric field. Such defects are difficult to eliminate and the failure of the ceramics can be unexpected and catastrophic. Currently, structural reliability is tested with destructive methods such as mechanical flexure tests rendering large amounts of material unusable. Therefore non-destructive methods for reliability evaluation are needed. In this work we have carried out electrical partial discharge tests on lead-zirconate-titanate bulk ceramics. In ceramics, partial discharges may occur under relatively low electric field due to the existence of structural defects where the permittivity and breakdown strength are lower. By comparing the results of partial discharge and four-point flexure tests, we find that the partial discharge inception field and the flexure strength are statistically related. We also examine the influence of partial discharge test on the piezoelectric ceramics by analysis of microstructure and electrical property characterization. Our results show that the partial discharge test can be an alternative non-destructive method to determine the structural reliability of piezoelectric ceramics.

4:15 PM**(EMA-S1-029-2014) Impedance spectroscopy and material design of lead-free alkali niobate piezoelectric ceramics**

M. Watanabe*, K. Kakimoto, I. Kogomiya, Nagoya Institute of Technology, Japan

In polycrystalline ceramic, both of grains and their boundaries can play key roles to the functionality of electric properties. However, such information is still a lack in lead-free alkali niobate piezoelectric ceramics, since they are likely to show a complex defect structure which may be caused by the evaporation of alkali oxides during sintering step. In this study, the roles of the bulk and grain boundaries against high-temperature electric conductivity for alkali niobate system were investigated by using an impedance

spectroscopic technique, which allows to determine the dominant factors of the conductive mechanism. The temperature dependence of the complex impedance was monitored by a frequency response analyzer for (Li,Na,K)NbO₃ (LNKN) ceramics having different microstructures and chemical stoichiometry. It was found for LNKN ceramics with Li content of 6 mol% that the conductivity of grain boundary (1.1×10^{-10} [W⁻¹cm⁻¹]) showed lower than that of the bulk (5.4×10^{-10} [W⁻¹cm⁻¹]). This finding indicated that grain boundaries would prefer to block the pass of charge carriers transporting across them, and became a new guideline of the material design for alkali niobate ceramics which could show better electrical properties. Various types of LNKN ceramics was subjected and compared in this study in order to understand the differences in their conductive behavior.

4:30 PM**(EMA-S1-030-2014) Fatigue mechanisms in Pb-free Piezoelectric Ceramics**

N. Kumar*, T. Ansell, D. Cann, Oregon State University, USA

Lead-free Bi(Mg_{1/2}Ti_{1/2})O₃-(Bi_{1/2}K_{1/2})TiO₃-(Bi_{1/2}Na_{1/2})TiO₃ (BMT-BKT-BNT) ceramics have been shown to exhibit fatigue-free behavior. To investigate the role of point defects on the fatigue characteristics, the composition 5BMT-40BKT-55BNT was doped to incorporate acceptor and donor defects on the A and B sites by adjusting the Bi/Na and Mg/Ti stoichiometries. Acceptor doping resulted in the stabilization of typical ferroelectric-like polarization and strain loops while donor-doped compositions exhibited characteristics of an ergodic relaxor phase. Fatigue measurements were carried out on all compositions under a bipolar driving field of 50 kV/cm. While the A-site acceptor-doped composition showed a small degradation in maximum strain after 10⁶ cycles, the other three were essentially fatigue free. Impedance measurements were used to identify the important conduction mechanisms in these compositions. As expected, the defects did not strongly influence the fatigue behavior in donor-doped compositions owing to the nature of their reversible field-induced phase transformation. Even for the acceptor-doped compositions which had stable domains in absence of electric field, there was minimal to no degradation in maximum strain due to fatigue. This suggests that either defects do not play a prominent role in fatigue in these systems or it is compensated by decrease in coercive field, an increase in ergodicity or other factors.

4:45 PM**(EMA-S1-031-2014) Electrochemically and optically derived oxygen stoichiometry and redox kinetics of (Pr,Ce)O_{2-δ} thin films (Invited)**

S. R. Bishop*, Kyushu University, Japan; J. Kim, D. Chen, Massachusetts Institute of Technology, USA; L. Zhao, Kyushu University, Japan; H. Tuller, Massachusetts Institute of Technology, USA

Many oxides exhibit advantageous properties in energy conversion and storage applications, such as solid oxide fuel cells (SOFCs), heterogeneous catalysis, photoelectrochemical cells, and batteries, due in part to their high temperature stability, corrosion resistance, and dopant cation solubility, respectively. Oxygen vacancies in these materials play key roles in electronic and ionic transport as well as mechanical properties. Additionally, as length scales are reduced, the energetics for vacancy formation have been shown to be modified. In this presentation, recent work using optical absorption as a probe to examine oxygen content and the corresponding redox kinetics on thin films will be presented. Enhanced oxygen nonstoichiometry of films, corroborated with electrochemical measurements, was observed. Additionally, differences in redox kinetics between the optical and electrochemical measurement techniques will be discussed.

5:15 PM

(EMA-S1-032-2014) "Phased and Confused": Exploring the Evolution of Phase Chemistry in NaSICON Ion Conducting Ceramics

E. Spörker*, N. Bell, J. S. Wheeler, C. Edney, D. Ingersoll, Sandia National Laboratories, USA

Growing interest in sodium-based battery systems has motivated renewed exploration of solid state sodium ion conductors, such as NaSICON (Sodium Super Ion Conductor). To be commercially viable, these ceramics must be capable of physically separating materials such as molten sodium from incompatible catholytes, while providing high sodium ion conductivity for effective battery performance. Naturally, these properties are strongly dependent on the phase chemistry of the ceramic. Here, we examine NaSICON with the composition $\text{Na}_3\text{Zr}_2\text{PSi}_2\text{O}_{12}$, an electrolyte with excellent sodium ion conductivity, but one traditionally been plagued by deleterious secondary phases (e.g., ZrO_2 , silicates, and phosphates) formed during high temperature syntheses ($>1200^\circ\text{C}$). We explore a lower temperature ($<1200^\circ\text{C}$) sol-gel synthesis, evaluating the influences of temperature and sodium content on ceramic composition. We characterize the evolution of phase chemistry during NaSICON synthesis and investigate the potential influences of secondary phase formation on electrolyte stability and performance. Insights from these studies may inform improved NaSICON syntheses and enhanced ceramics for developing sodium battery systems.

5:30 PM

(EMA-S1-033-2014) Bulk Ionic Conductivity of Glass and Glass-Ceramic Lithium Thiophosphate Solid Electrolytes for Solid-state Batteries & Electrochemical Capacitors

S. S. Berbano*, M. Mirsaneh, M. T. Lanagan, C. A. Randall, The Pennsylvania State University, USA

Lithium solid electrolytes are important for safe energy storage and have the possibility to operate at higher voltages than liquid electrolytes. Solid electrolytes with high ionic conductivity are important to minimize the equivalent series resistance of solid-state batteries and electrochemical capacitors. To maximize the ionic conductivity, it is important to consider the relative impact of an optimized microstructure, phase assemblage, composition, and density. Mechanically milled powders of the compositions $x\text{Li}_2\text{S} + (1-x)\text{P}_2\text{S}_5$ (mol fraction), $x = 0.70, 0.75$, and 0.80 , were cold-pressed ($\sim 75\%$ dense) and pressed near their glass transition temperatures ($\sim 95\%$ dense) at constant pressure. Density and impedance spectroscopy measurements suggest that ionic conductivity is improved by increasing the bulk conduction volume rather than by increasing the surface area. Higher density compacts had higher ionic conductivity with little change in the activation energy for conduction in a given composition. Impedance spectroscopy characterization on dense, crystallized $x = 0.80$ samples below room temperature revealed lower ionic conductivity when heated $> 350^\circ\text{C}$. It is possible that bulk lithium loss (oversintering) at high temperatures limited the improvement in ionic conductivity from crystallization in glass-ceramics heated $> 350^\circ\text{C}$.

5:45 PM

(EMA-S1-034-2014) Conductivity in nanostructured ceria: space- and time- resolved mapping of ionic dynamics

J. Ding*, Georgia Institute of Technology, USA; E. Strelcov, S. Kalinin, Oak Ridge National Laboratory, USA; N. Bassiri-Gharb, Georgia Institute of Technology, USA

Nanostructured CeO_2 is widely used in catalytic devices and as mixed ionic-electronic conductor in solid oxide fuel cells. However, the origin of its conductive behavior is still subject to controversy. Anisotropic bulk conduction, as well as proton-based conduction facilitated by surface water adsorption, has been reported in nano-crystalline ceria. Here we investigate the regimes under which each of the above becomes the dominant mechanism. Nanostructured

ceria is prepared by chemical solution deposition (CSD) and physical vapor deposition (PVD) on Si_3N_4 -coated Si, and quartz substrates. Cr/Pt electrodes, patterned by photolithography, are created on ceria stripes (on Si/ Si_3N_4) and beneath a continuous ceria film (on quartz). The local transport phenomena are studied as a function of atmospheric gas and humidity content from 25 to 125°C , through use of time-resolved Kelvin Probe Force Microscopy (tr-KPFM). Two different mechanisms are found to contribute to the conductivity in nanostructured ceria at low temperatures: at high humidity and below 50°C , proton-assisted conductivity mediated by adsorbed water plays a dominant role in surface charge distribution and conductivity; at higher temperatures, oxygen vacancy-based bulk and surface conductivity are dominant. Additionally, the effects of presence of triple points and conductivity of the substrates will be discussed.

S2: Multiferroic Materials and Multilayer Ferroic Heterostructures: Properties and Applications

Materials Synthesis and Epitaxial Systems

Room: Indian

Session Chair: Valanoor Nagarajan, University of New South Wales

2:00 PM

(EMA-S2-023-2014) Domain structure of (100)/(010)-oriented epitaxial PbTiO_3 -based thin films with in-plane polarization (Invited)

H. Funakubo*, Y. Ehara, T. Nakashima, Tokyo Institute of Technology, Japan; T. Yamada, Nagoya University, Japan

Control of crystal orientation and ferroelectric domain structures is an essential issues to obtain the desired properties for PbTiO_3 -based films. In the present study, (100)-oriented epitaxial PbTiO_3 films with thickness of from ~ 2 to 30 nm were grown at 600°C on (100) KTaO_3 substrates. Crystal structure of the films was characterized by high-resolution x-ray diffraction (XRD) and piezoelectric force microscopy (PFM). For PbTiO_3 film with film thickness below 30 nm , only PbTiO_3 $h00$ diffraction peaks were observed on out-of-plane θ - 2θ patterns. On the other hands, PbTiO_3 $h00/00l$ peaks were observed on in-plane θ - 2θ patterns using grazing incidence XRD measurements (GIXRD). PbTiO_3 $h00/00l$ peaks separated into sub peaks representing in-plane tilting of the domains with a tilt angle from ~ 1.05 to $\sim 1.15^\circ$ with increasing film thickness from 2 to 30 nm . This is due to a coherent junction between two adjacent variants of a domains, a_1 and a_2 domains. This tilting angle (ω) was a good agreement with the equation based on the tetragonal distortion, $\{\omega = [(2\tan^{-1}(c/a) - 90^\circ)/2]\}$. Relatively small value in the measured tilt angle compared to the theoretical value of 3.6° implies that the in-plane tilting of these a domains is highly clamped by the substrate. These PbTiO_3 thin films have a unique domain structure along in-plane direction.

2:30 PM

(EMA-S2-024-2014) Ferroic order and switching controlled by reversible elastic strain (Invited)

K. Dorr*, E. Guo, MLU Halle-Wittenberg, Germany; M. D. Biegalski, H. M. Christen, ORNL, USA; S. Das, IFW Dresden, Germany; R. Roth, MLU Halle-Wittenberg, Germany; L. Schultz, A. Herklotz, IFW Dresden, Germany

Magnetic and ferroelectric ordering in complex oxide films can be very sensitive to elastic strain. This has been exploited in many strain-coupled thin-film structures of magnets with ferroelectrics for obtaining a substantial magnetoelectric response. The origins of strain sensitivity, however, are multiple. They are fundamentally understood and modeled in rather few cases. The impact of lattice defects leads to a strong obstacle for identifying the effects of

elastic strain by comparing films grown on differently mismatched substrates. We have introduced the application of piezoelectric substrates for reversible strain control in epitaxial ferroic films, allowing one to study the same thin film in different strain states. In my presentation, I will discuss the influence of reversible strain on the ferroelectric switching of BiFeO_3 capacitors. Domain dynamics in BiFeO_3 films under reversibly controlled elastic strain has been complementarily studied by piezoresponse force microscopy. In the second part of my talk, I will give an overview on phenomena of reversible-strain-induced magnetic order in epitaxial films of several magnetic oxides ($\text{La}_{1-x}\text{Sr}_x\text{MO}_3$, $M = \text{Mn}$ or Co ; SrRuO_3 ; CoFe_2O_4).

3:00 PM

(EMA-S2-025-2014) The effect of interfacial octahedral behavior in ferromagnetic manganite heterostructures (Invited)

E. Moon, S. May*, Drexel University, USA

Magnetism at oxide interfaces has attracted considerable interest as advances in thin film deposition have enabled studies of high quality ABO_3 perovskite heterostructures. This talk will focus on how rotations and distortions of the BO_6 octahedra can play a key role in the magnetic properties of ultrathin oxide films and superlattices, using the canonical ferromagnet $\text{La}_{0.7}\text{Sr}_{0.3}\text{MnO}_3$ (LSMO) and reduced bandwidth $\text{Eu}_{0.7}\text{Sr}_{0.3}\text{MnO}_3$ (ESMO) compounds as model systems. We find that LSMO films grown under the same strain state but on substrates with different octahedral rotations exhibit increasingly different magnetic behavior as the thickness is reduced below 15 unit cells. Additionally, the magnetic and electronic properties of isovalent (LSMO)/(ESMO) superlattices, in which the MnO_6 rotations are modulated throughout the superlattice, will be presented.

4:00 PM

(EMA-S2-026-2014) Biphasic Magnetoelectric Multiferroic Nanocomposite Films (Invited)

M. Jain*, University of Connecticut, USA

Indirect magnetoelectric (ME) coupling is observed via strain in biphasic ME composites in which the magnetic (in magnetostrictive materials, such as CoFe_2O_4) and electric (in piezoelectric materials, such as $\text{PbZr}_x\text{Ti}_{1-x}\text{O}_3$) order parameters arise in separate but intimately connected phases. In nanocomposite ME films, the connectivity and distribution of the two phases strongly affects its ME performance. Magnetostrictive phase, being more conductive, causes leakage problems in such films. In this work two solution synthesis methods were employed for the fabrication of $\text{PbZr}_x\text{Ti}_{1-x}\text{O}_3$: CoFe_2O_4 nanocomposite thin films in order to mitigate the leakage effect by limiting the amount of magnetic phase while maintaining high interfacial area between the two phases. The films were evaluated by various characterization techniques, such as x-ray diffraction, ferroelectric measurements, atomic force microscopy, transmission electron microscopy, and ME measurements. It was found that by limiting the amount of CoFe_2O_4 and achieving desirable distribution, large ME coupling values could be achieved.

4:15 PM

(EMA-S2-027-2014) Exotic functional domain walls in multiferroics (Invited)

D. Meier*, ETH Zürich, Switzerland

In ferroic oxide materials natural interfaces spontaneously arise in the form of domain walls. Just like artificially constructed interfaces such domain walls are a rich source for fascinating physics resulting from their low symmetry, geometric confinement, electrostatics, and strain. In addition, they can be created, moved, and erased at will offering great potential for novel device paradigms and new opportunities for interface engineering. Particularly interesting are domain walls in multiferroics, where the interplay of electric and magnetic

(or structural) long-range order gives rise to rather exotic interface states. Here, I will present two examples of multiferroic domain walls with specific functionalities: (i) Hybrid walls with inseparably entangled magnetic and electric order parameters and (ii) charged walls that owe their stability to the presence of topologically protected structural singularities. Results gained by cathode-lens microscopy, scanning-probe microscopy, and nonlinear optics will be discussed providing insight to the domain wall physics on nano- to mesoscopic length scales.

4:30 PM

(EMA-S2-028-2014) Multiferroics Within a Fiber: Janus-type Nanomaterials Synthesized via Electrospinning and Electrospray Techniques

J. D. Starr*, J. S. Andrew, University of Florida, USA

Recent research on nanocomposite multiferroics has focused on techniques for synthesizing thin films due to the ease of achieving an epitaxial relationship between phases. However, these films suffer from numerous limitations: layer-by-layer deposition processes are often slow, and magnetoelectric properties can be dampened due to substrate clamping. In this work, we present a new method of fabrication that overcomes many of these limitations, and show how Janus-type nanofibers and nanoparticles can be synthesized via electrohydrodynamic spinning and atomization. These methods create composite multiferroics within a single particle or fiber by simultaneously establishing magnetostrictive (CoFe_2O_4) and piezoelectric (BaTiO_3) phases that are localized in opposite hemispheres. The segregation of these phases is confirmed through electron microscopy and energy dispersive spectroscopy. These nanocomposites maintain a large contact area between phases and form anisotropic building blocks that could eventually be used to form more complicated devices. While this platform was initially created for bilayer configurations, we show how it can easily be extended to multilayer designs, and demonstrate how altering the order and arrangement of the layers can impact magnetoelectric coupling through magnetization measurements made near the ferroelectric Curie temperature of BaTiO_3 .

4:45 PM

(EMA-S2-029-2014) Magnetic and ferroelectric property enhancement of PZT/LSMO multiferroic thin films using dual laser ablation

M. Hordagoda, D. Mukherjee*, H. Robert, P. Mukherjee, S. Witanachchi, University of South Florida, USA

$\text{PbZr}_{0.52}\text{Ti}_{0.48}\text{O}_3/\text{La}_{0.7}\text{Sr}_{0.3}\text{MnO}_3$ (PZT/LSMO) heterostructures are of great interest due to their ferroelectric and multiferroic behavior. Growing both, LSMO and PZT using pulsed laser ablation (PLD) is particularly challenging owing to the precipitation of a Mn_2O_4 impurity phase in the LSMO layer and the non-congruent ablation of PZT. This report presents evidence for the epitaxial growth of PZT/LSMO thin films on SrTiO_3 and MgO substrates using a novel dual laser ablation (DLA) technique which combines a CO_2 laser with the KrF excimer laser PLD. Higher excitation of the ablated species, as evidenced by the emission spectroscopy data of the DLA plume, leads to better film morphology and crystallinity. This technique also yields particulate free uniform films over large areas due to the broader angular distribution of the plume as seen by inspecting the ICCD images of the plume. The single crystalline nature of the films were confirmed using XRD while AFM scans showed surfaces with roughness as low as 1 nm. Defect free interfaces were seen in the cross sectional HRTEM images. The remnant polarization of the DLA deposited films $70\text{--}90\text{ }\mu\text{C}/\text{cm}^2$, when compared with the $30\text{--}45\text{ }\mu\text{C}/\text{cm}^2$ value of the films deposited using PLD shows a considerable enhancement. A higher saturation magnetization of $250\text{--}280\text{ emu}/\text{cm}^3$ and in-plane magnetic anisotropy were also observed.

5:00 PM

(EMA-S2-030-2014) The effect of La doping on the ferroelectric and magnetic properties of PZT/LSMO multiferroic heterostructures

M. Hordagoda*, D. Mukherjee, University of South Florida, USA; D. Ghosh, J. Jones, University of Florida, USA; P. Mukherjee, S. Witanachchi, University of South Florida, USA

The recent revival of interest in $\text{Pb}(\text{Zr}_{1-x}\text{Ti}_x)\text{O}_3/\text{La}_x\text{Sr}_{1-x}\text{MnO}_3$ (PZT/LSMO) heterostructures, with respect to applications in novel spintronic devices, is due to the reports of a large charge-driven magnetoelectric (ME) coupling. The results of reducing the space charge effect of bulk PZT by replacing Pb^{2+} by an off-valent donor such as La^{3+} is also reported. In the present work La doped PZT (PLZT)/LSMO bilayers were grown with La concentrations of 0.1%, 0.5% and 1% on MgO and SrTiO_3 substrates using pulsed laser deposition. XRD data showed single crystal epitaxial film growth and allowed the calculation of the residual strains in the individual layers. The PZT layers exhibited roughness values as low as 1.6 nm, measured using atomic force microscopy (AFM). Ferroelectric (FE) measurements were made by growing a thin film capacitor with PLZT as the dielectric and LSMO top and bottom layers. Square polarization hysteresis loops were measured at a nominal voltage of 5V. Enhancement due to the La doping were observed as evidenced by the remnant polarization value of $60\mu\text{C}/\text{cm}^2$ for 0.1% La doping as compared to $40\mu\text{C}/\text{cm}^2$ for undoped films. At 300K the PLZT/LSMO films showed saturated magnetization values of $420\text{ emu}/\text{cm}^3$ when grown on MgO and $360\text{ emu}/\text{cm}^3$ on STO. An explanation involving a strain compression-relaxation mechanism is being developed to explain the behavior.

S5: Structure and Properties of Interfaces in Electronic Materials

Thermodynamics of Interfaces

Room: Caribbean B

Session Chair: Edwin Garcia, Purdue University

2:00 PM

(EMA-S5-009-2014) Orientation relationships of copper crystals on sapphire surfaces: how much does the interface matter? (Invited)

D. Chatain*, Aix-Marseille University, CNRS, France

We aim to understand how and why two materials like a fcc metal and an oxide, very different in chemistry, structure and cohesive bonding chose to form particular hetero-interfaces. Wetting and interface structure characterizations at the macroscopic and the atomistic scales were performed by electron and near-field microscopies on submicron copper crystals equilibrated on sapphire substrates of different orientations ($c(0001)$, $a(11-20)$, $r(1-102)$ and $m(10-10)$). The energetics of the interface and its anisotropy, the orientation relationships, and the interface and triple line shapes were investigated. We find that there are particular and recurrent crystallographic alignments of copper and sapphire crystal directions whatever the orientation of the sapphire substrate. We also show that the triple line may foster drastic shape changes of the interface and of the oxide surface. These results may be helpful in explaining the properties of metallic crystals prepared on oxide substrates, which are used in technologically important applications, such as catalysis and optics.

2:30 PM

(EMA-S5-010-2014) Extending CALPHAD Methods to Model Grain Boundaries and Nanocrystalline Materials (Invited)

N. Zhou, J. Luo*, UCSD, USA

Bulk phase diagrams, along with CALPHAD methods, are among the most useful tools for materials science. Materials researchers have long recognized that interfaces and nanomaterials that have a large amount of interfaces can exhibit thermodynamic stability that drastically differs from bulk materials. A series of recent studies, which were documented in a review article [J. Am. Ceram. Soc. 95: 2358 (2012)], have successfully extended the bulk CALPHAD methods to model the thermodynamic stability of nanometer-thick, quasi-liquid, intergranular films (as a type of grain boundary "phase" or complexion). Our recent efforts have been focused on using a regular-solution lattice model to develop a systematic set of more rigorous grain boundary complexion (phase) diagrams with well-defined transition lines and critical points. In another recent study, we further extended bulk CALPHAD methods to model binary poly/nanocrystalline alloys and developed a new kind of thermodynamic stability diagram for equilibrium-grain-size alloys. These stability diagrams for grain boundaries and nano-grained materials (as extensions to bulk phase diagrams) can be used as general tools to accelerate materials design in the spirit of the "Materials Genome" initiative.

3:00 PM

(EMA-S5-011-2014) Equilibrium State of the Solid-Solid Ni-YSZ(111) Interface (Invited)

H. (Bratt) Nahor, H. Meltzman, W. D. Kaplan*, Technion - Israel Institute of Technology, Israel

The stability of metal films on oxide surfaces is important for the performance of devices such as solid oxide fuel cells (SOFCs). Ni - yttrium stabilized zirconia (YSZ) serves as an anode material in SOFCs, where it is subjected to high temperatures and a reducing atmosphere, which can lead to Ni coarsening and a decrease in Ni/YSZ/fuel-gas triple line length. A better understanding of the equilibrated Ni-YSZ interfacial structure and energy can lead to improved adhesion and long-term stability of SOFCs. In this work, solid-state dewetting of thin Ni films on YSZ substrates was used to form equilibrated Ni-YSZ interfaces at $T=1350^\circ\text{C}$ in Ar-H_2 at an oxygen partial pressure $P(\text{O}_2)=10^{-20}$ atm. The equilibrium crystal shape (ECS) of the Ni crystals was determined, and the orientation relationship (OR) for equilibrated particles and the interfacial structure was investigated using high resolution electron microscopy. The solid-solid interfacial energy was measured using Winterbottom analysis. The low-energy OR₁ was found to be $\text{Ni}[1-10](111)||\text{YSZ}[1-10](111)$ with an interface energy of $1.8\pm0.1\text{ J}/\text{m}^2$. A second OR₂ was found with a 180° rotation to the first, $\text{Ni}[-110](111)||\text{YSZ}[1-10](111)$ and an interface energy of $2.1\pm0.1\text{ J}/\text{m}^2$. A model which explains the two different ORs, based on twinning during grain growth which accompanies the solid-state dewetting process, will be presented.

Structure and Composition of Interfaces

Room: Caribbean B

Session Chair: John Blendell, Purdue University

4:00 PM

(EMA-S5-012-2014) Phase and Orientation Relationships for Interfaces in Electronic Ceramic Heterostructures Determined by Combinatorial Substrate Epitaxy (Invited)

G. Rohrer*, P. Salvador, Carnegie Mellon University, USA

The majority of heteroepitaxial growth studies use single crystal substrates with low index surfaces. From an interface crystallography point of view, this work is restricted to a very narrow region of epitaxial orientation space and focuses on what should be considered extremely special interfaces. A simple question arises: does

epitaxial growth on special surfaces reflect the preferred epitaxial orientation between two crystals in general? To address this question, we have developed combinatorial substrate epitaxy (CSE) to explore growth throughout epitaxial orientation space. In CSE, films are deposited on polished polycrystalline substrates, and local orientations of the film and substrate are mapped using electron backscatter diffraction, and the film-substrate orientation relationships (ORs) are computed for hundreds of different pairs. Using CSE, we investigated the growth of TiO₂ on BaTiO₃ and BiFeO₃, and the epitaxial growth of hematite (Fe₂O₃) on SrTiO₃ over the entire range of epitaxial orientation space. Collectively, those studies show that well-prepared polycrystalline surfaces can be treated locally as single-crystal growth surfaces and that the closest-packed networks in the film and substrate are essentially continuous. This proves to be a more general description of TiO₂ growth perovskite surfaces than previous descriptions.

4:30 PM

(EMA-S5-013-2014) Crystallization of Atomic Layer Deposited Aluminum Oxide Films (Invited)

N. C. Strandwitz*, D. Weisberg, Lehigh University, USA

We report studies of the crystallization of atomic layer deposited amorphous aluminum oxide films on sapphire, silicon and silicon dioxide substrates. Using controlled thermal treatments coupled with ex-situ SEM-EBSD we examined the effects of temperature and annealing time on the crystallization growth behavior. We found that amorphous alumina films of approximately 90 nm thickness crystallize fully in the alpha phase when grown and annealed (800 °C) on alpha alumina substrates. Further studies of attempts to modify the crystallization behavior will also be discussed.

4:45 PM

(EMA-S5-014-2014) Molecular Dynamics Simulations of the Lu in Silicate Intergranular Films in Silicon Nitride: Growth and the Role of Oxygen on Adsorption (Invited)

S. H. Garofalini*, Y. Jiang, Rutgers University, USA

Molecular dynamics (MD) computer simulations have been used to evaluate the behavior of rare earth-doped silicon oxynitride intergranular films (IGFs) in silicon nitride ceramics. The simulations reproduce the specific adsorption of Lu and La at the sites observed in HAADF-STEM studies, but show the important role that oxygen plays on Lu adsorption. The simulations show that the presence of oxygen at specific N surface lattice sites plays a significant role on Lu adsorption, but has almost no effect on La adsorption. EELS studies have shown that oxygen is present at sites on the prism surface of silicon nitride in contact with the oxide IGF. The energetics of Lu at specific surface adsorption sites on the prism-oriented silicon nitride surface is consistent with the observed positions. Growth of the prism surface outward along its surface normal is affected by the different rare earths and the simulations reproduce this difference.

5:15 PM

(EMA-S5-015-2014) Comparative method behavior interaction potential surface to a structure (Al₂O₃(ZnO/SnO₂)+TiO₂,1O₂) in low isotropic model with multiple harmonic oscillators single bond

O. Rodriguez Pinilla*, Universidad Autónoma de Colombia, Colombia

In this paper, we present the results of the simulated behavior and experimental measurement of the chemical potential or potential interaction for a raw ceramic phase structure (Al₂O₃(ZnO/SnO₂)+TiO₂,1O₂) used the theoretical model of multiples single harmonic oscillators. The above results were obtained considering the application of such materials by contact field sensors. In turn, was taken as the approximate basis for the interaction potential as a nonlinear function of: temperature, relative electric permittivity, relative humidity, type of charge carriers (n) and (p) of the material and surface voltage. On the other hand, was calculated and simulated

the thermal behavior responsible for the chemical potential energy propagation in the structure of the compound under study.

5:30 PM

(EMA-S5-016-2014) The Study of Magnetic Properties of A_{1-x}Mn_xA' (A=Zn,Cd and A'=S,Te,Se) at Critical Region Using High Temperature Series Expansion Extrapolated with Pade Approximants

H. D. Berry*, Dilla University, Ethiopia

In the present work we explore magnetic properties especially spin glass, antiferromagnetic and paramagnetic states of diluted magnetic semiconductors(A_{1-x}Mn_xA' (A=Zn,Cd and A'=S,Te,Se)) at critical region using classical Heisenberg model with high temperature series expansion extrapolated with pade approximants. We use this technique to determine the critical temperature (T_c), critical exponents in magnetic susceptibility (γ=1.38±0.1) and correlation function (ν=0.8±0.1).

S7: Computational Design of Electronic Materials

Computational Methods for Novel Oxides

Room: Coral A

Session Chair: Ghanshyam Pilania

2:00 PM

(EMA-S7-019-2014) A Phenomenological Theory for Ferroelectric Solid Solutions (Invited)

G. A. Rossetti*, University of Connecticut, USA; A. A. Heitmann, Naval Undersea Warfare Center, USA

A thermodynamic theory for the diffusionless phase diagrams of ferroelectric solid solutions will be presented. A particular form of the Ginzburg-Landau theory is adopted that places special emphasis on the role played by the crystallographic anisotropy of polarization at inter-ferroelectric transitions. Relations are developed that specify the stability of the proper symmetry ferroelectric phases in terms of the coefficients of the Landau series. Analytical expressions are derived that describe key topological features of binary and ternary phase diagrams, dielectric and piezoelectric property maps are computed, and relationships between the crystallographic anisotropy of polarization and the extrema in properties are illustrated. The computations demonstrate how the mixing of anisotropy energies for differing end member compounds controls the topologies of their phase diagrams and provides insight into experimental observations of nanodomain structure, low-symmetry ferroelectric phases, and extrinsic contributions to electromechanical properties. The inherent simplicity of the theory, together with the unified analytical parameterization scheme employed, is expected to be useful for guiding experimental investigations of ferroelectric solid solutions, in generating free energy functions for phase field simulations, and for developing first-principles-derived thermodynamic descriptions for ferroelectric materials.

2:30 PM

(EMA-S7-020-2014) Modeling Electrothermal Properties of Polarizable Dielectric Materials (Invited)

S. Alpay*, G. A. Rossetti, University of Connecticut, USA

Electrothermal (electrocaloric and pyroelectric) properties of ferroelectric thin films have many applications in active solid-state cooling and infrared sensing devices. We use here a nonlinear thermodynamic model based on Landau-Ginzburg-Devonshire formalism to analyze the electrothermal properties of perovskite ferroelectric materials such as BaTiO₃, PbTiO₃, and the incipient ferroelectric SrTiO₃ under different electrical and mechanical boundary conditions. The results show how these boundary conditions alter the electrothermal properties for a given material

composition. It is further demonstrated that thermal stresses that develop during processing can have a significant influence on the electrothermal properties of polycrystalline ferroelectric films on IC-friendly substrates. Therefore, appropriate choices of the ferroelectric material, substrate, growth or annealing temperature, and electrode configuration can be used to optimize the electrothermal properties.

3:00 PM

(EMA-S7-021-2014) Generalized Atomistic Models for Metal-Metal Oxide Composites (Invited)

S. Valone*, Los Alamos National Laboratory, USA; M. I. Baskes, University of California San Diego, USA; X. Liu, R. L. Martin, Los Alamos National Laboratory, USA; K. Kolluri, University of Pennsylvania, USA; S. R. Atlas, University of New Mexico, USA; G. Pilania, Los Alamos National Laboratory, USA

The Fragment Hamiltonian (FH) model was conceived for the express purpose of subsuming separate models for metals and ceramics into a single atomistic model. These models rely on fundamentally different variables to describe the states of atoms in a material. One variable is the usual net charge on an atom or fragment. The other variable, ionicity, accounts for charge fluctuations that do not change the number of electrons on a fragment. FH model establishes a relationship between these disparate variables. The resulting energy for each fragment incorporates both variables. Generalized Mulliken electronegativities and absolute hardnesses (or Hubbard U) appear explicitly, as expected. Both are determined from changes in the number of electrons on a fragment by an integer value. Charge-transfer, electron hopping also appears and serves to regulate both charge flow and gap energies. One can take derivatives of the fragment energies with respect to either net charge or ionicity to produce differential definitions of electronegativity and hardness. The differential definitions join charge-transfer hopping effects with the finite-difference definitions, to modify the chemical potentials and open and close gaps. These theoretical developments for the FH model and its applications to Be/BeO and Ni/NiO interfaces will be presented to illustrate the efficacy of the model.

4:00 PM

(EMA-S7-022-2014) Computational design of multifunctional layered oxides across length scales (Invited)

S. Nakhmanson*, University of Connecticut, USA

Compared to their “mundane” parent compounds (like, e.g., ABO₃ perovskite structures), layered oxides possess a variety of additional “dials” that could be adjusted to manipulate their properties and create new, and advanced functionalities. Utilizing first-principles-based computational techniques, we study and predict intriguing behavior in a variety of epitaxial layered-perovskite compounds, including Goldstone-like excitations, incommensurate structural distortions and unusual affinity for molecular absorption. The results of first-principles computations can also be distilled into simple energy expressions that can be used to study mesoscale behavior of nano- and microstructures made out of these materials. For conducting such simulations we are developing a highly scalable real-space finite-element code (Ferret) that can treat systems with coupled polar and elastic degrees of freedom. The computational approach is built on MOOSE, Multiphysics Object Oriented Simulation Environment that is being developed at Idaho National Laboratory. In this presentation we will provide an overview of our approach and some examples of applications we are working on in collaboration with experimental groups.

4:30 PM

(EMA-S7-023-2014) Accurate descriptions of Hellmann-Feynman forces in understanding ferromagnetic ZnOCoH

A. Pham*, M. H. Al Assadi, University of New South Wales, Australia; C. J. Gil, University of Florida, USA; A. Yu, S. Li, University of New South Wales, Australia

We demonstrate through the use of hybrid functional that Co-H-Co complex is not stable in ZnOCoH due to the underestimation of the Coulombic and electronic contributions of Hellman-Feynman forces in previous study [Phys. Rev. Lett. 94, 127204 (2005)]. The improved geometry optimization increases the overlapping between O's 2p and H's 1s making the Co-H-Co complex unstable and results in a new stable Co-H-O-Co complex. Within this new geometry, ferromagnetism is stabilized by a combination of large Jahn-Teller distortion and double exchange interaction due to the unequal valence states of Co ions.

S9: Thin Film Integration and Processing Science

Epitaxial and Functional Oxide Thin Films

Room: Coral B

Session Chairs: Brady Gibbons, Oregon State University; Rudeger Wilke, The Pennsylvania State University

2:00 PM

(EMA-S9-001-2014) Strain engineering via octahedral distortions in epitaxial perovskite oxide films (Invited)

A. Vailionis*, Stanford University, USA; H. Boschker, M. Huijben, G. Koster, G. Rijnders, University of Twente, Netherlands

Complex perovskite oxides have emerged as multifunctional materials of remarkable tunability and exhibit a wide spectrum of electronic properties including high mobility, magnetism and superconductivity. The perovskite unit cell is composed of A -site cation and BO_6 octahedron where central transition metal cation B is octahedrally coordinated with its oxygen nearest neighbors. Many of the properties are strongly coupled to distortions of the BO_6 building block such as rotations (variation of $B-O-B$ bond angle) and/or deformations (change in the $B-O$ bond length). In this talk we will show that the BO_6 octahedral distortions act as an effective way for substrate-induced stress accommodation and are an important tuning mechanism of the physical properties in epitaxial ABO₃ thin films. Moreover, due to interatomic coupling across the film-substrate interface the coherently strained layer inherits octahedral rotation pattern of the underlying substrate. This coupling effect is more pronounced at the vicinity of the interface, i.e. in ultrathin layers, and diminishes with film thickness. As a result, functional properties of oxide thin films are expected to vary with thickness. We demonstrate how strain-induced octahedral distortions affect physical properties of epitaxial ABO₃ films by using two examples: La_{1-x}Sr_xMnO₃ and SrRuO₃.

2:30 PM

(EMA-S9-002-2014) Epitaxial integration of commensurate cubic oxides on GaN

C. T. Shelton*, E. Paisley, E. Sachet, I. Bryan, NCSU, USA; M. Bügler, TU Berlin, Germany; M. Biegalski, Oak Ridge National Laboratory, USA; J. LeBeau, B. Gaddy, S. Mita, R. Collazo, Z. Sitar, D. Irving, NCSU, USA; A. Hoffmann, TU Berlin, Germany; J. Maria, NCSU, USA

The interface properties of heteroepitaxially grown polar materials have received much attention due to the existence of quantum confined 2D carrier gasses. Integration of lattice-matched rocksalt oxides with wide-bandgap semiconductors offers a path toward 2D interface conductivity at an oxide-nitride interface. Unfortunately, a smooth, commensurate, single domain oxide-nitride interface with

an intrinsic carrier source to populate the 2DEG remains elusive. Recently, however, a new surfactant-assisted MBE growth technique has been used to prepare smooth (111) MgO and CaO rocksalt oxides on GaN. We extend these methods to a new rocksalt system, CdO and solid solutions of CdO-MgO. Cd_{1-x}Mg_xO (CMO) is a wide-bandgap n-type oxide semiconductor with the rocksalt structure. In this work we demonstrate growth of lattice matched CMO on GaN using Plasma-assisted MBE. Optical characterization of the rocksalt thin films as well as transport properties will be presented. In addition, we will introduce evidence for an epitaxial origin of the two in-plane rotation domains commonly observed in rocksalts on GaN. Finally, we will share early efforts to control the surface morphology of MOCVD grown GaN substrates by removing the characteristic *c*/2 bilayer fluctuation. Collectively these techniques open new avenues for integration of oxides on GaN and observation of unique interface phenomena.

2:45 PM

(EMA-S9-003-2014) In-situ X-ray Studies of the Synthesis and Properties of Polar and Ferroelectric Thin Film Heterostructures (Invited)

M. Highland*, E. Perret, C. Folkman, Argonne National Laboratory, USA; C. Thompson, Northern Illinois University, USA; D. Fong, S. Streiffer, G. Stephenson, J. Eastman, P. Fuoss, Argonne National Laboratory, USA

In recent years there has been interest in understanding the properties of polar oxide surfaces, with particular emphasis on the behavior of buried heterointerfaces and as well as bare ferroelectric surfaces compensated by chemical environments. By precisely controlling these interfaces and the environments in which they are synthesized we may be able to create and enhance desired emergent interfacial states and properties. To realize this level of control we utilize in-situ synchrotron x-ray scattering to probe the growth environment during Metal Organic Chemical Vapor Deposition (MOCVD) and rf-magnetron sputtering of oxide thin films. I will describe recent studies of the deposition of various oxide overlayers (such as LaGaO₃ and ZrO₂) onto thin films of the prototypical ferroelectric PbTiO₃, in an effort to exploit the surface polarization of the ferroelectric to augment the properties of the oxide over layer. These results will suggest new pathways for enhancing and manipulating emergent states at oxide interfaces.

3:15 PM

(EMA-S9-004-2014) Carbon Nanotubes Integrated with Superconducting NbC

G. Zou*, Soochow University, China; H. Luo, NMSU, USA; T. McCleskey, Q. Jia, LANL, USA

The formation of carbon nanotube and superconductor composites makes it possible to produce new and/or improved functionalities that the individual material does not possess. In this talk, we will give a brief summary about carbon nanotubes integrated with superconducting niobium carbide (NbC) by a chemical solution process. Here, coating well-aligned carbon nanotubes with superconducting NbC does not destroy the microstructure of the nanotubes in two different ways. NbC also shows much improved superconducting properties such as a higher irreversibility and upper critical field. An upper critical field value of ~5 T at 4.2 K is much greater than the 1.7 T reported in the literature for pure bulk NbC. Furthermore, the aligned carbon nanotubes induce anisotropy in the upper critical field, with a higher upper critical field occurring when the magnetic field is parallel to the carbon nanotube growth direction. These results suggest that highly oriented carbon nanotubes embedded in superconducting NbC matrix can function as defects and effectively enhance the superconducting properties of the NbC.

4:00 PM

(EMA-S9-005-2014) High mobility CdO: Towards monolithically integrated plasmonic devices (Invited)

E. Sachet*, C. T. Shelton, M. Kang, S. Franzen, J. Maria, North Carolina State University, USA

CdO is a prototypical transparent conducting oxide with excellent n-type ability and high charge carrier mobility. This presentation will describe advances in heteroepitaxial thin film growth of CdO on various substrates and explore the possibilities for monolithic integration of high mobility CdO thin films for optoelectronic and plasmonic devices operating in the mid-IR. We will present a plasma assisted molecular beam epitaxy (MBE) growth technique that employs Dysprosium as an n-type dopant. This approach allows for tuning of the carrier concentrations from 1E19 up to 5E20 cm⁻³, which corresponds to plasma frequencies covering the entire mid-IR range (2-10 μm). Thin heteroepitaxial films grown by this method routinely exceed mobilities of 400 cm²/(Vs) (CdO single crystal mobility=600 cm²/(Vs)), making them ideal candidates for the next generation of plasmonic sensors where low loss and high optical confinement are needed. We will discuss optical properties of CdO:Dy and describe the doping mechanisms and donor states in the CdO:Dy system. Results will be compared to density functional theory (DFT) calculations to further describe the origin of conductivity and the high charge carrier mobility in CdO. Finally, experimental results demonstrating the applicability of a CdO based monolithic plasmonic biosensor will be presented, as well as finite element modeling (FDTD) of prototype sensor device designs.

4:30 PM

(EMA-S9-006-2014) High kt²×Q, Multi-frequency Lithium Niobate Resonators (Invited)

S. A. Bhavé*, Cornell University, USA

To satisfy the ever-increasing demand for spectrum, commercial markets desire integrated multi-frequency “band”-select duplexer and diplexer filters, with fractional bandwidth (BW) ranging from 3% to 10% and steep roll-off for high stop band rejection. The achievable bandwidth of such filters is ultimately limited by the electro-mechanical coupling factor (kt²) of the resonators, while the roll-off is determined by resonator quality factor (Q). Therefore, resonators with both high kt² and high Q are desired for large BW, steep roll off band-pass filters. This paper presents the fabrication technology and design of thin-film lithium niobate (LN) contour-mode resonators. By carefully positioning the inter-digital transducer (IDT), we achieved CMRs with kt²×Q of 148 (IDT @ node) or resonators with very high kt² of 12.3% and spur-attenuated response (IDT @ anti-node). In addition, we demonstrated resonators with frequencies ranging from 400MHz to 1.9GHz on a single chip.

5:00 PM

(EMA-S9-007-2014) Ba_{0.5}Sr_{0.5}TiO₃ Thin Film Capacitors for Microwave Antenna

B. Malic*, Jozef Stefan Institute, Slovenia; S. Glinsek, Brown University, USA; B. Kmet, T. Pecnik, Jozef Stefan Institute, Slovenia; V. Furlan, Centre of Excellence SPACE.SI, Slovenia; M. Vidmar, University of Ljubljana, Slovenia

The Ba_xSr_{1-x}TiO₃ (x=0–1) solid solution is suitable for tunable microwave applications. In the case of solution-derived thin films, knowledge and control of the microstructure-dielectric properties relations is crucial for integration into devices. In this contribution we present the processing of Ba_{0.5}Sr_{0.5}TiO₃ (BST) thin-film capacitors and the study of the relationships between the microstructure, thickness and the RF- and MW-range dielectric properties. The acetate-alkoxide derived solutions were spin-coated on polished alumina substrates. The as-deposited films were rapidly thermally annealed at 900 °C. By repeating the deposition and annealing steps films with thicknesses in the 100 nm to 500 nm range were prepared. Patterning of copper electrodes for the antenna was

performed by lift-off photolithography and magnetron sputtering. The kHz- and MHz- range properties of the planar capacitors with different film thicknesses were measured. The about 170 nm thick films reached the values of the dielectric permittivity of ~1300 and ~1200, measured at 100 kHz and 10 GHz, respectively. The tenability, expressed as the ratio of the permittivities at 0 V and 40 V at 100 kHz, was 3.98. To observe the capacitor behavior at lower end of the X frequency band, planar capacitors were simulated at frequencies between 7 and 9 GHz using the dielectric properties of the films measured at 10 GHz.

5:15 PM

(EMA-S9-008-2014) VO₂ Thin Film Electrochromic Window Behavior Dependence on Doping and Strain State

P. Clem*, C. Edney, J. Custer, C. Nordquist, T. Jordan, J. Hunker, Sandia National Laboratories, USA

VO₂ thin film electrochromic behavior, and the ability to shift metal insulator transition temperature by chemical doping, enables tunable solar transmission windows. Chemical solution deposition and sputtered films were used to increase the solubility of dopants in VO₂ thin films over that possible in prior single crystal and vapor-deposited film studies, to elucidate effects of doping on transition behavior. A range of dopants have been evaluated to raise (Al, Cr, Ge, Fe) or lower (W, Mo, Nb) VO₂ transition temperature from 60°C to tune transitions from below 0°C to 85°C. A comparison of chemically doped vs. 0-0.4% tensile strained films suggests large cation doping with W and Mo causes lattice strain effects similar to tensile stress, increasing metallic state resistivity and decreasing transition temperature. Implications on these dopant choices for tailored device applications, including demonstrations of environmentally-activated thermochromic windows, are discussed. This work was supported by the Laboratory Directed Research and Development (LDRD) program office at Sandia National Laboratories. Sandia National Laboratories is a multi-program laboratory managed and operated by Sandia Corporation, a wholly owned subsidiary of Lockheed Martin Corporation, for the U.S. Department of Energy's National Nuclear Security Administration under contract DE-AC04-94AL85000.

5:30 PM

(EMA-S9-009-2014) Nanoscale Mapping of Microscale Piezoactuators (Invited)

M. Rivas, J. L. Bosse, L. Ye, University of Connecticut, USA; R. Keech, S. Trolier-McKinstry, Penn State University, USA; R. Polcawich, U.S. Army Research Laboratory, USA; B. D. Huey*, University of Connecticut, USA

Piezoactuating MEMS devices are investigated during in-situ actuation using Atomic Force Microscopy. For periodic vibrations, the amplitude and phase of the MEMS components are mapped as a function of driving amplitude as well as frequency. In this manner, resonance frequencies, resonant modes, and resonance nodes can be directly visualized with nanoscale resolution. The influence of pulsed actuation is also studied for signals down to 100 nsec. In each case, the electro-mechanical forces imparted by the MEMS device can also be recorded, allowing direct detection of mechanical latching devices. Finally, piezoactuation is considered for bulk PZT ceramics, thin films, and microfabricated piezoelectric structures at the nanoscale. Piezoactuation is thereby characterized as a function of feature dimensions, particularly with respect to edge effects as well as the influence of grains and grain boundaries.

S12: Recent Developments in High-Temperature Superconductivity

Superconductors and Their Applications

Room: Mediterranean B/C

Session Chair: Timothy Haugan, Air Force Research Laboratory

2:00 PM

(EMA-S12-006-2014) Development of MgB₂ and (Ba(Sr),K)Fe₂As₂ wires (Invited)

H. Kumakura*, S. Ye, Z. Gao, A. Matsumoto, K. Togano, National Institute for Materials Science, Japan

Internal Mg diffusion (IMD) method is effective in enhancing J_c and J_e of MgB₂ wires. Recently we succeeded in fabricating high performance MgB₂ wires using the 4mol% C-coated high quality B powder (from SMI Co.). The C₈H₁₀ addition decreased Cl in SMI B powder and increased the B packing density, which are responsible for the increase of J_c and J_e values. High J_c of 76 kA/cm² and J_e of 5.3 kA/cm² were obtained at 20 K & 5 T. At 10 K, the J_c of the wire was actually higher than that for Nb-Ti wires at 4.2 K in magnetic fields below 8 T. The high density MgB₂ layer, uniform and small MgB₂ grain size, C substitution for B in MgB₂ lattice are considered to be the main reasons of high critical current properties we obtained. The K-doped BaFe₂As₂ and SrFe₂As₂ superconductors are potentially useful for magnet applications due to their high H_{c2}. In this study, we investigated the effects of intermediate mechanical deformation and annealing process on J_c of the Ba(Sr)-122/Ag tapes fabricated by ex-situ powder-in-tube method. The results show that the J_c can be significantly enhanced by improving the various processing parameters. Especially, the addition of uni-axial pressing in the final stage is very effective to heal cracks formed by the previous rolling, resulting in further significant increase of J_c. High transport J_c above 30 kA/cm² in 10 T at 4.2 K has been obtained for the 7-filamentary Ba-122 tape.

2:30 PM

(EMA-S12-022-2014) Slow Abrikosov to fast moving Josephson vortex transition in REFeAs(O,F) (Invited)

P. J. Moll, ETH Zurich, Switzerland; L. Balicas, National High Magnetic Field Laboratory, USA; D. Geshkenbein, G. Blatter, J. Karpinski, N. D. Zhigadlo, B. Batlogg*, ETH Zurich, Switzerland

We have observed a transition from well-pinned Abrikosov-like to highly mobile Josephson-like vortices in the iron pnictide high-T_c superconductor SmFeAs(O,F) (T_c ~ 50 K). This A-to-J transition between the two regimes upon cooling through the temperature T* is hallmarked by an extraordinary jump of vortex mobility and a pronounced peak in the critical current density. The dissipation below T* reaches significant fractions of the normal state resistance at all temperatures and fields, far below H_{c2}/√2, estimated well above 100 T at low temperatures. We show the temperature T* to coincide with the temperature at which the interlayer coherence length ξ_c equals the SmO layer thickness, hence leading to Josephson-like vortices below and Abrikosov-like vortices above T*. This transition is unusual, as the material is an only moderately anisotropic superconductor (γξ ~ 5-7, γλ ~ 10), unlike strongly anisotropic, clearly two-dimensional cuprates. The observation of this A-to-J transition highlights the significance of structural layeredness and gives microscopic information about the order parameter in SmFeAs(O,F). This profound change in the nature of the vortex matter in these compounds has eluded discovery until now, as its detection poses two main experimental challenges:

3:00 PM**(EMA-S12-008-2014) Grain structure in macroscopically untextured Bi2212 round wires – Where does the current flow? (Invited)**

F. Kametani*, J. D. Jiang, N. Craig, M. Matras, E. E. Hellstrom, D. C. Larbalestier, National High Magnetic Field Laboratory, USA

In order to fully understand whether HAGBs in macroscopically untextured Bi2212 round wires are superior to those in Bi2223 or REBCO, or whether other mechanisms compensate obstructing effects of HAGBs, we extensively study the grain and GB structure of Bi2212 round wires by using the electron backscatter diffraction (EBSD) method. EBSD revealed that Bi2212 grains can plastically bend and/or twist by themselves during the grain growth in such a way that quite large (>10 deg.) long range GB misorientation can be accommodated. The inverse pole figure derived from long – range EBSD scanning on the 700 μm longitudinal cross section of Bi2212 single filament also show the out-of-plane misorientation is quite large, ± 80 deg. in the radial direction which is consistent to the macroscopically untextured filament, but ± 15 deg. in the longitudinal direction, which is smaller than expected. In addition, we found that in-plane misorientation of Bi2212 grains in the round wire filaments is surprisingly small, ± 15 deg. Our microstructural analysis starts to reveal the unique grain structure in Bi2212 round wires that enables high J_c in the macroscopically untextured wire architecture.

4:00 PM**(EMA-S12-009-2014) AC loss in coated conductor coils in DC bias current (Invited)**

E. Pardo*, J. Souc, J. Kovac, Institute of Electrical Engineering, Slovak Academy of Sciences, Slovakia

Changing magnetic fields in windings made of coated conductor create AC loss, which reduces the efficiency and complicates cooling. Therefore, it is needed to predict the AC loss and reduce it by optimization. This contribution studies the AC loss in windings with a bias transport current by means of numerical modelling and measurements. The model assumes either the critical state or a smooth current-voltage relation for the superconductor. This model takes into account the details of the magnetization currents and their interaction between turns. With this model, we analyze stacks of pancake coils from few turns up to thousands in ripple current and a racetrack coil under ripple magnetic field. The measurements, done by electrical means, are performed for the same situations, although the stack of pancake coils contains only around 100 turns. We found that the model agrees with the measurements. In addition, considering the interaction of the magnetization currents between all the turns in one pancake is important, although the interaction between pancakes up to neighbours of second order is enough. For a DC bias current in ripple current, the power loss for the increasing half of the current cycle is much larger than for the decreasing one. In conclusion, the model presented follows the necessary requirements for virtually any number of turns. In addition, ripple AC loss can be measured by electrical means.

4:30 PM**(EMA-S12-010-2014) Recent Progress of R&D Project of Fundamental Technologies for Accelerator Magnets Using Coated Conductors (Invited)**

N. Amemiya*, Kyoto University, Japan; T. Kurusu, Toshiba Corporation, Japan; T. Ogitsu, High Energy Accelerator Research Organization, Japan; Y. Mori, Kyoto University, Japan; K. Noda, National Institute of Radiological Sciences, Japan; M. Yoshimoto, Japan Atomic Energy Agency, Japan

An R&D project of fundamental technologies for accelerator magnets using coated conductors is in progress: “Challenge to functional, efficient, and compact accelerator systems using high T_c superconductors” under Strategic Promotion of Innovative Research and Development Program funded by the Japan Science and

Technology Agency. Our targets are cryo-cooler-cooled magnets for the accelerators for carbon cancer therapy or accelerator-driven subcritical reactor. Although there are various potential advantages such as the reduction of electricity consumption and better thermal stability, many intrinsic fundamental technologies have to be developed before the realization of cryo-cooler-cooled accelerator magnets wound with coated conductors. In our project, we have been designing magnets which are compatible with the designs of accelerators for carbon cancer therapy and ADSR, considering the mechanical properties of coated conductors. We are developing the winding technologies which enable the designed magnets. Some more fundamental issues have been studied: the influence of the tape magnetization on the field quality, the radiation tolerance of magnet materials, etc. The latest status of the project will be presented. This work was supported by Japan Science and Technology Agency under Strategic Promotion of Innovative Research and Development Program.

5:00 PM**(EMA-S12-011-2014) Cryogenic and superconducting drivetrains and components for all-electric or hybrid-electric aircraft propulsion (Invited)**

T. Haugan*, The Air Force Research Laboratory, USA; G. Y. Panasyuk, T. Bullard, UES Inc., USA; D. Latypov, BerrieHill Research Corp., USA

Hybrid-electric-vehicle (HEV) or electric-vehicle (EV) propulsion is well understood from the automotive industry, and achieves very significant increases of energy efficiencies of 2-3x from the use of non-combustion technologies and ‘smart’ energy management including brake regeneration. The possibility of hybrid-electric propulsion for aircraft has increasingly been considered in the last 5 years, and has been successfully implemented in 2 and 4 passenger aircraft. This paper will summarize recent progress in this field for aircraft, and present case studies of how cryogenic electric power systems can positively impact hybrid-electric or all-electric power systems and capabilities, for different size and power level aircraft. Cryogenic drivetrain and components will be studied include generators and motors, power transmission cables, power storage devices including Li-batteries and superconducting magnetic energy storage (SMES), power electronics including inverters, and cryogenic technologies. Properties of cryogenic systems and components will be compared to Cu-wire based systems. Acknowledgments: Air Force Office of Scientific Research (AFOSR), and Aerospace Propulsion Directorate of The Air Force Research Laboratory (AFRL/RQ).

5:30 PM**(EMA-S12-012-2014) Electric Aircraft Concept: Impact of Superconductor/Cryogenic Power Systems for Aircraft Propulsion**

G. Y. Panasyuk*, UES Inc., USA; T. J. Haugan, Air Force Research Laboratory, USA

We consider a concept of an electric aircraft that takes advantages of using ultra-light cryogenic power propulsion. A model that describes fuel/energy and power consumption for conventional and conceptual electric aircrafts is developed. The model provides, in particular, a simple description of how the aircraft’s altitude, horizontal velocity, and the total power change during its ascending to the cruise regime for several conventional aircrafts and compares these quantities to the ones of the corresponding electric counterparts. It also estimates the maximum travelling distance for an electric aircraft. The model shows clear advantages of using cryogenic electric power systems (which include superconducting motor and cables) over conventional power systems based on combustion as well as electric systems that use traditional copper wiring. The advantages come from significant decrease of weight and increase of drive-train efficiencies. Using state-of-the-art Li-batteries with energy densities = 400 Wh/kg, flight distances ~ 10% of those achieved with jet fuel combustion (of the order of 1000 miles for 45

MW class aircrafts such as the Boeing 787 Dreamliner aircraft) are expected, which are very significant.

5:45 PM

(EMA-S12-013-2014) An Investigation into the Nickel Doped Paratacamite Group of Minerals as Potential Superconducting Materials

T. Bullard*, UES Inc., USA; T. Haugan, The Air Force Research Laboratory, AFRL/RQQM, USA; L. Brunke, University of Dayton Research Institute, USA

A quantum spin liquid (QSL) state known as the resonating valence bond (RVB) state has been proposed as an explanation for high temperature superconductivity in cuprate compounds. Recent research suggests that a QSL has been realized in the $x=1$ member of the zinc-paratacamite group of minerals (also known as Herbertsmithite) due to its unique crystalline structure. However Herbertsmithite does not possess superconducting properties; therefore we investigate the magnetic properties of nickel doped zinc paratacamite for superconducting behavior. Specifically we vary the ratio of zinc to nickel ($\text{Zn}_x\text{Ni}_{1-x}\text{Cu}_3(\text{OH})_6\text{Cl}_2$) in the crystal structure and examine the resulting magnetization as a function of applied field $M(H)$ and the susceptibility as a function of temperature $\chi(T)$. Phase analysis and powder purity are obtained via X-ray diffraction and induction coupled plasma (ICP) analysis.

Friday, January 24, 2014

Plenary Session III

Room: Indian

Session Chair: Haiyan Wang, Texas A&M University

8:30 AM

(EMA-003-2014) Functional Electronic Materials in Integrated Commercial Building and Aerospace Systems (Invited)

J. Mantese*, United Technologies Research Center, USA

Commercial building and aerospace platforms are undergoing a consolidation of subsystems towards creating holistic approaches to intelligent buildings and aircraft design. Using analogies from a similar rationalization of automotive systems, this talk will look at the role of functional electronic materials development and component processing as enabling technologies for future distributed sensing needs and energy generation/consumption. With an eye toward lessons learned from the automotive industry; opportunities for functional and electronic materials will be identified, particularly in the areas of: closed-loop-sensing, local power generation/storage, and material/device processing for cost-effective manufacturing.

S1: Functional and Multifunctional Electroceramics for Commercialization

Lead-Free Piezoelectrics

Room: Pacific

Session Chairs: Takaaki Tsurumi, Tokyo Institute of Technology; Sean Bishop, Kyushu University

10:00 AM

(EMA-S1-035-2014) Processing and Microstructure Control of (Na,K)NbO₃-based Lead-free Piezoceramics (Invited)

K. Kakimoto*, Nagoya Institute of Technology, Japan

(Na,K)NbO₃ (NKN)-based alkali niobate ceramic system has been considered to be one of the most attractive compositions in the research field of lead-free piezoelectrics. However, there are still problems in the processing and the reliance in the electric properties.

Our current interests are focused to well-designed processing and microstructure control. One of these key technologies is the development of fine powders derived from a new aqueous-based citrate precursor technique, which is classified to a chemical solution process. This route is now extended to engineer NKN-based film and fiber structure, too. In this talk, not only such elaborated processing routes but critical grain size for inducing high piezoelectric properties in bulk ceramics are also addressed for better understanding of alkali niobate materials. The results of the model experiments clearly showed the distinguishing of different ferroelectric and piezoelectric properties on the basis of the microstructure of NKN-based ceramics.

10:30 AM

(EMA-S1-036-2014) Recent Developments on Lead Free Ferroelectric Materials (Invited)

S. Zhang*, T. Shrout, Pennsylvania State University, USA

The scientific and technical impacts of lead free materials are contrasted with "soft" and "hard" PZTs. On the scientific front, the intrinsic nature of the dielectric and piezoelectric properties are presented in relation to the existence of MPB or PPT. Analogous to PZT, enhanced properties are noted for MPB compositions in NBT-BT. Though comparable with respect to TC, the high piezoelectricity reported in KNN based materials are result of enhanced polarizability, associated with the PPT being at RT. Technologically, lead free materials are discussed in relation to general applications. Finally, manufacturability plays an important role in the implementation of materials into actual devices. For successful implementation of the lead free, the following progresses have been achieved: 1. For KNN family, the PPT was shift downward to below RT to improve temperature stability while maintaining high piezoelectric. 2. Acceptor dopant was used to reduce the power dissipation for the potential high power application. The material properties were evaluated at hard drive condition, revealing NBT-based lead free possessing stable mechanical Q, superior to "hard" PZTs, closely associated with their high coercive field, ~35kV/cm. 3. Fundamentally, in-situ TEM was employed to study the domain structure as a function of applied electric field, the relationship between microstructure and macroscopic properties has been established.

11:00 AM

(EMA-S1-037-2014) Large electric field-induced strain in La-modified [(Bi_{1/2}Na_{1/2})_{0.95}Ba_{0.05}]_{1-x}La_xTiO₃ lead-free ceramics

X. Liu*, X. Tan, Iowa State University, USA

Lead-free perovskite [(Bi_{1/2}Na_{1/2})_{0.95}Ba_{0.05}]_{1-x}La_xTiO₃ ceramics ($x = 0.00, 0.01, 0.02, 0.025, 0.03, 0.04, 0.05, 0.06$) were fabricated via the solid state reaction method and their crystal structures and electrical properties were systematically investigated. It was found that the ceramics with lanthanum contents lower than 3 at. % exhibited a ferroelectric rhombohedra phase, while further increase in La turned the crystal structure into pseudo-cubic. This indicated the existence of a morphotropic phase boundary (MPB) between 2.5% and 3.0% La³⁺ concentration. With the addition of La³⁺, the thermal depolarization temperature (T_d) was shifted to below room temperature and the dielectric constant (ϵ_r) became stable against temperature. The piezoelectric coefficient (d_{33}) rose with La³⁺ content initially, giving the highest value of 145 pC/N when $x = 0.02$, and then abruptly dropped down. Polarization and strain hysteresis loops demonstrated that the long range ferroelectric order was disrupted by the addition of La³⁺. The largest remanent polarization (P_r) of 39 $\mu\text{C}/\text{cm}^2$ was observed in the composition $x = 0.01$ while the highest strain of 0.36 % was achieved in $x = 0.04$. Although the strain in the compositions $x = 0.05$ and 0.06 fell down, the almost temperature-independent ϵ_r above 120 °C suggests great potential of these compositions for high-temperature dielectric applications.

11:15 AM

(EMA-S1-038-2014) Preparation of (K,Na)(Nb,Ta)O₃ based Lead Free Piezoelectrics Using Novel Sintering Aid

K. Kikuta*, EcoTopia Science Institute, Nagoya University, Japan

Alkali niobate tantalate based materials have been studied as a candidate for novel lead free piezoelectrics. Dense (K,Na)(Nb,Ta)O₃ based ceramics were successfully prepared using a sintering aid including transition metals such as copper or cobalt. We already reported that hard KNNT material can be made by the addition of K-Cu-Ta-O compounds. In this work, the effect of sintering aids was examined using the composition of 99.5KNNT – (0.5/y)(KxCyTazO_δ) from the view point of sinterability and electric properties. The prepared samples showed that the relatively “soft” properties compared with those samples doped with K-Cu-Ta-O sintering aids. The prepared KNNT based piezoelectrics has the d₃₃ over 290 pC/N and Q_m around 100 by controlling the phase transition behavior.

11:30 AM

(EMA-S1-039-2014) Piezoelectric properties of lead-free niobate ceramics with controlled grain size

K. Kato*, K. Kakimoto, Nagoya Institute of Technology, Japan; K. Hatano, K. Kobayashi, Y. Doshida, Taiyo Yuden Co., Ltd., Japan

Recently the grain size effect of ferroelectric ceramics has attracted attention because of the control of the electrical behavior. It is well recognized that piezoelectric properties depend on grain sizes. In case of BaTiO₃ ceramics, the grain size and its corresponding property correlation is well established. On the other hand, such investigations on alkali niobates, a potential candidate for lead-free piezoelectric ceramics, are remained scarce because of the difficulty in grain-size control during sintering. The aim of this study was to control the grain size of Li-substituted (Na,K)NbO₃ (LNKN) ceramics and to evaluate the electrical properties. LNKN ceramics were synthesized at various sintering parameters such as heating schedules with one-step or two-step plateau under various Po₂ atmospheres for controlling grain size. In these experiments, grain sizes with specific range indeed showed the maximum piezoelectric properties for LNKN.

11:45 AM

(EMA-S1-040-2014) Electric field-induced structure in NBT-based relaxors (Invited)

P. A. Thomas*, D. I. Woodward, D. S. Keeble, D. Walker, S. Anand, University of Warwick, United Kingdom

In recent years, Na_{0.5}Bi_{0.5}TiO₃ (NBT) based solid solutions have emerged as potential replacements for conventional lead-based piezoelectric materials. NBT is a relaxor ferroelectric that forms the basis of a number of lead-free piezoelectric systems. Perovskites that are relaxors are characterised by the presence of nano-sized polar regions and an apparently pseudo-cubic structure on the macroscopic scale. NBT is perhaps unusual in that it has, in addition to relaxor behaviour, a series of macroscopic phase transitions [Jones & Thomas, 2002] and planar defects of some type [eg Kreisel et al., 2003] that make a full description of the structure and identification of its individual changes particularly challenging. Functional electroceramics are poled by applying an external electric field. In relaxor materials this can cause a significant change in the macroscopic structure. In classical ferroelectrics such as Pb(Zr, Ti)O₃ (PZT), this polarisation is lost when the material is heated through a phase transition, but NBT ceramics spontaneously depole when heated above T_D ~ 150 °C [Davies et al., 2011] via a mechanism that is not well-understood but does not coincide with a change in symmetry [Gorfman et al., 2012] and cannot be thought of as a conventional phase transition. This depolarisation temperature is observed in many NBT-based systems and has been frequently mistaken for a conventional phase transition.

12:15 PM

(EMA-S1-041-2014) Correlation between Piezoelectric Properties and Phase Co-existence in (Ba,Ca)(Ti,Zr)O₃ Ceramics

Y. ZHANG*, J. Glaum, University of New South Wales, Australia; C. Groh, Technische Universität Darmstadt, Germany; M. C. Ehmke, J. Blendell, Purdue University, USA; M. Hoffman, University of New South Wales, Australia

Lead-free piezoceramic materials must show comparable or better piezoelectric performance compared to materials currently used in order to be considered as an alternative to lead-based piezoceramics. (Ba_{100-x}Ca_x)(Ti_{100-y}Zr_y)O₃ (BCTZ) piezoceramics are a promising lead-free alternative due to the high piezoelectric coefficients observed. In this study, six BCTZ compositions were selected which, based on a review of previous studies, are expected to have high piezoelectric coefficients at room temperature. Samples were produced using a conventional solid oxide route and electric-field-dependent polarization, strain, and piezoelectric coefficient were measured. All compositions exhibit well-developed hysteresis loops and large piezoelectric coefficient around 310 ~ 475 pm/V at room temperature. X-ray diffraction and temperature-dependent permittivity measurements revealed that the good piezoelectric performance is due to the co-existence of several phases. The XRD results also suggest that the phase co-existence appears within a broad temperature range. A relationship between the tetragonal-orthorhombic phase transition temperature and the Ca₂₊ to Zr₄₊ ratio is proposed. This enables tailoring of BCTZ compositions with high piezoelectric coefficient to a desired operation temperature.

S2: Multiferroic Materials and Multilayer Ferroic Heterostructures: Properties and Applications**Novel Multiferroic Materials and Other Functional Oxides I**

Room: Indian

Session Chair: Jonathan Spanier, Drexel University

10:00 AM

(EMA-S2-031-2014) Characteristics of PZTFT: A New Room-Temperature Multiferroic (Invited)

D. M. Evans, Queens University Belfast, United Kingdom; M. Alexe, University of Warwick, United Kingdom; J. F. Scott, University of Cambridge, United Kingdom; M. Gregg*, Queens University Belfast, United Kingdom

Research into multiferroic systems has undergone a renaissance in the last decade. This has partly been driven by renewed scientific curiosity, but also partly by a strong desire to demonstrate new proof-of-principle electronic devices. The majority of proposed device structures are based on a strongly coupled magnetoelectric response, which has only been seen at room temperature to date in composite systems, rather than single-phase materials. Recently, however, a new room-temperature multiferroic based on a solid-solution of lead zirconate titanate and lead iron tantalate (PZTFT) was reported. In this talk, the coupling behaviour in PZTFT will be explored more fully than in literature published to date. Thin single crystal lamellae have been incorporated into coplanar capacitor devices, allowing the switching of ferroelectric domains using both electric and magnetic fields to be monitored using piezoresponse force microscopy (PFM). In addition, the effect of applied magnetic fields on device capacitance was measured directly. It has been found that the effects of applied magnetic fields on ferroelectric domain states is very strong after the capacitor has been poled electrically. Indeed, levels of magnetic-field induced switching are comparable to those seen after electrical switching.

Analysis of magnetocapacitance using a Landau formalism confirms the distinctly coupled behaviour in the material.

10:30 AM

(EMA-S2-032-2014) Polymer-assisted deposition for a wide range of epitaxial ferroic metal-oxide films (Invited)

Q. X. Jia*, Los Alamos National Laboratory, USA; M. Jain, University of Connecticut, USA; H. Luo, Texas A&M University, USA; E. Bauer, Los Alamos National Laboratory, USA; H. Wang, Texas A&M University, USA; T. M. McCleskey, A. K. Burrell, Los Alamos National Laboratory, USA

Chemical solution approaches offer the advantages large area coatings, easy setup, and potentially low cost to grow thin films. However, many functional compound materials cannot be deposited and the growth of high quality epitaxial films is not always controllable by the existing chemical solution approaches owing to differences in chemical reactivity among the metals. I will discuss our approach, polymer-assisted deposition (PAD), to the growth of a wide range of ferroic metal-oxide thin films. The use of polymer as the binding agent for metal ions has several advantages. First, the formation of covalent complexes between the polymer and the metal cations make it possible to prepare almost any metal precursor solutions that are impossible to achieve by the commonly available chemical solution deposition techniques. Secondly, the viscosity of the solution can be effectively controlled by the polymer. Thirdly, the precursor solutions are environmentally friendly as metal salts and commercially available polymers are used as the source materials. The unique chemistry and processing design of PAD deliver stable and homogeneous solutions at a molecular level that enables the epitaxial growth of high quality epitaxial ferroic thin films. The processes, microstructures, and physical properties of different ferroic films grown by PAD will be discussed in this talk.

11:00 AM

(EMA-S2-033-2014) Controlling Metal-to-Insulator Transitions in Complex Oxide Heterostructures (Invited)

S. Stemmer*, University of California, Santa Barbara, USA

Complex oxides and correlated electron materials offer new opportunities for electronic switching devices, such as unique band structures, high electron densities, and potentially electronically tunable phase transitions and magnetism. We will start with an overview of the basic properties of these materials, their physics, and recent advances in controlling growth and interface properties. We will report on our recent work on electrostatic carrier doping of perovskite based complex oxide heterostructures, controlling and understanding of metal-insulator transitions, and the development of tunnel devices with these materials. The work was done in collaboration with Evgeny Mikheev, Adam Hauser, Jinwoo Hwang, Santosh Raghavan and Jim Allen.

11:15 AM

(EMA-S2-034-2014) Vertical interface effects in multiferroic nanocomposite thin films (Invited)

H. Yang*, Soochow University, China; H. Wang, Texas A&M University, USA; J. L. MacManus-Driscoll, University of Cambridge, United Kingdom; Q. Jia, Los Alamos National Laboratory, USA

For epitaxial metal oxide films, interfaces always play a critical role in controlling structural and electrical properties. In a film-on-substrate geometry, interfaces can be created in two forms: horizontal and vertical. Both experimental and theoretical works have demonstrated the impact of horizontal interface on physical properties of either single-phase thin films or superlattices. Compared with the horizontal interface, the effects of vertical interface on the physical properties is profound. Recently, we fabricated vertically aligned nanocomposite thin films based on BiFeO₃, BaTiO₃, and EuTiO₃ materials. The vertical interface effectively manipulates strain state and the physical properties. More details will be presented in the talk.

11:30 AM

(EMA-S2-035-2014) Electronic and Vibrational Properties of Complex Metal Oxides (Invited)

S. Zollner*, New Mexico State University, USA

The electronic and vibrational properties of complex metal oxides can be investigated using spectroscopic ellipsometry (from the vacuum-UV to the mid-IR). My talk presents examples of undergraduate ellipsometry research on metal oxides. (1) For spinel (MgAl₂O₄) and LaAlO₃, we determined the dispersion of the refractive index and its temperature dependence over the visible and near-UV range. In the vacuum-UV, we find absorption peaks (near 8 eV for spinel) due to optical interband transitions. In the IR, the optical constants are influenced by lattice absorption of infrared-active phonons. (2) In NiO, the absorption is moderate (but non-zero) in the visible and rises in the UV, where we find a strong absorption peak at 4 eV. The optical constants of NiO and their temperature dependence are very similar to Si up to 700 K. At higher temperatures, NiO deteriorates under UHV annealing. In the IR, we find not only the single TO phonon expected for the rocksalt structure, but also a zone-folded mode due to antiferromagnetic ordering. (3) In CeO₂ films grown on a-plane sapphire by liquid solution deposition with (100) texture, we find an absorption peak at 4 eV. Samarium doping (to create oxygen vacancies) significantly reduces the grain size and lowers the refractive index, but does not change the band gap. A similar variation of the refractive index with grain size has been found in pure CeO₂ films produced by PVD.

11:45 AM

(EMA-S2-036-2014) Ferroelectric behaviour in strained thin films of anatase TiO₂ (Invited)

N. Deepak, M. E. Pemble, L. Keeney, R. W. Whatmore*, Tyndall National Institute, Ireland

This paper reports the first-ever observation of room-temperature ferroelectric behaviour in anatase-phase titanium dioxide (a-TiO₂). It is shown that ferroelectric behaviour is induced in ultra-thin (20nm to 80nm) biaxially-strained epitaxial films of a-TiO₂ deposited by liquid injection chemical vapour deposition onto (110) single crystal neodymium gallium oxide (NGO) substrates. The structural properties of the films were analysed by XRD & high-res TEM and ferroelectricity by PFM. The films showed: switchable dielectric spontaneous polarization, retention of polarization information for several hours and at temperatures up to 100°C without loss, and the disappearance of polarisation between 180 and 200°C, indicative of a Curie temperature. This is believed to constitute strong experimental evidence for ferroelectricity, which has not hitherto been reported in a-TiO₂ and opens up the possibility for a range of new devices and materials applications. An explanatory model for the observations is presented based on the structural effects of large in-plane strains. The support of ICGEE (International Centre for Graduate Education in Micro & Nano Engineering), Science Foundation Ireland (SFI) under the FORME Strategic Research Cluster Award number 07/SRC/I1172 is and the Higher Education Authority Program for Research in Third Level Institutions (2007-2011) via the INSPIRE program are gratefully acknowledged.

12:00 PM

(EMA-S2-037-2014) Energy Landscape in Frustrated Systems: Cation Hopping in Pyrochlores (Invited)

J. C. Nino*, U of Florida, USA

Dielectric relaxation in pyrochlore insulator compounds is a well known phenomenon that can lead to high dielectric losses at high frequencies. While this is an undesired characteristic from the technological point of view, this relaxation phenomenon has also been associated with the very useful dielectric tunability observed in these compounds. Here, the dynamics of the local environment and electronic structure in inherently dipolar frustrated pyrochlore compounds are presented to help identify the fundamental nature of

dipolar disorder in pyrochlore systems and determine the necessary and sufficient conditions for dielectric relaxation. The energy landscape associated with cation hopping events in three compounds is mapped and used to correlate the hopping pathway with experimental dielectric response. In addition, a detailed comparison of the vibrational modes and relaxation behavior in Bi₂Ti₂O₇ (BTO), Ca_{1.5}Ti_{1.5}NbO₇ (CTN), and Bi_{1.5}ZnNb_{1.5}O₇ (BZN) will be discussed. Through comprehensive analysis of this combined experimental and computational work, rules to predict the occurrence of relaxation and cation hopping pathways will be postulated.

12:15 PM

(EMA-S2-038-2014) Formation mechanisms and functionalities in a new supercell structure by the co-growth of BiFeO₃ and BiMnO₃

A. Chen*, Los Alamos National Laboratory, USA; Y. ZhU, Texas A&M University, USA; Z. Bi, Los Alamos National Laboratory, USA; H. Zhou, North Carolina State University, USA; J. L. MacManus-Driscoll, University of Cambridge, United Kingdom; J. Narayan, North Carolina State University, USA; Q. Jia, Los Alamos National Laboratory, USA; H. Wang, Texas A&M University, USA

Multiferroic materials, which exhibit the coexistence of ferromagnetism and ferroelectricity, have attracted extensive interest owing to their potential applications as multifunctional devices and fascinating physical phenomena. A new epitaxial BFM0322 thin films with SC structure have been grown on LAO substrates with a thin pseudo-perovskite BFM0 interlayer. The new structure demonstrates both room-temperature ferrimagnetic and ferroelectric responses. The STEM results show the unique bismuth SC structures interlayered with double-row Fe-O-Mn layers with a zigzag arrangement. Strain mapping analysis at heterointerfaces found that not only a sufficient lattice misfit is required through substrate selection and to be preserved in initial coherent epilayer growth, but also an appropriate interfacial reconstruction is crucial for triggering the growth of the new supercell structure.

S6: Thermoelectrics: Defect Chemistry, Doping and Nanoscale Effects

Theory and Novel Materials

Room: Coral A

Session Chair: Doreen Edwards, Alfred University

9:45 AM

(EMA-S6-001-2014) Recent Progress in the Development of Thermoelectric Generators (Invited)

J. D. Koenig*, Fraunhofer IPM, Germany

Most important challenges in the near future are an increase of the energy efficiency and a reduction of CO₂ emission in industrial processes and transportation. The quest for methods of converting high amounts of lost heat partly into electrical energy leads to a well-known technology: Thermoelectricity. Currently, thermoelectric energy harvesting is enjoying high popularity. It demand has triggered a worldwide research race for materials, modules and systems with better conversion capabilities in particular for high temperatures. As a first order assessment of the recent and current material development it is reasonable to expect "high-temperature material" in technical ripeness within a short-term time scale. Therefore additional aspects like availability, processability, long-term stability, commodity prices, environmental and recycling will play a decisive role for the choice of the finally "best" high temperature material. Here, a survey of most recent achievements in material development will be presented including an assessment on their technical ripeness. Parallel to this progress increasing efforts have been started to fabricate new modules. In addition the state of art of high temperature module development based on Half-Heusler compounds,

silicides and Skutterudites at Fraunhofer IPM will be summarized and some aspects of high temperature system integration for thermoelectric will be discussed.

10:15 AM

(EMA-S6-002-2014) Methods of Thermoelectric Efficiency Enhancement for Power Generation Applications (Invited)

Y. Gelbstein*, Ben-Gurion University, Israel

Thermoelectrics as a direct energy conversion method between heat and electricity is mainly used for electrical power generation and cooling applications. A large variety of materials, such as intermetallic compounds, silicides and chalcogenides have been investigated as thermoelectric materials due to high ZT values at different temperature ranges. Global trends for improving the thermoelectric efficiency via maximizing the ZT values include, electronic doping optimizations; generation of Functionally Graded Materials (FGMs) with an optimal maximal ZT envelope over a wide temperature range; and nanostructuring formation for reduction of the lattice thermal conductivity. Nanostructures generation can be achieved by nano-powdering using energetic ball-milling followed by a rapid consolidation method such as Spark Plasma Sintering (SPS). Yet, due to the demand for high stability characteristics, required for long operation periods at high temperatures, one approach for avoiding nano-features coarsening and thermoelectric properties degradation, is based on utilizing thermodynamically driven nanostructures, due to physical metallurgy based effects such as spinodal decomposition and nucleation and growth reactions. All of the mentioned above general trends will be discussed during the talk.

10:45 AM

(EMA-S6-003-2014) Nano-scale Enhancement via Bottom-up Processing of Thermoelectric Materials

K. Wei*, G. S. Nolas, University of South Florida, USA

The efficiency of thermoelectric (TE) devices is directly related to the TE materials properties, therefore new, exotic, rare and costly materials are typically investigated. By offering the potential for controlling both thermal and electrical properties, nanostructured TE materials are currently of interest. We have developed a bottom-up strategy in order to prepare nanocomposites that involve the compositional and size controlled synthesis of TE materials by hydrothermal, colloidal and facile solution-based processes. Spark Plasma Sintering is then applied to densify the nanocrystals into dense polycrystalline solids. By optimizing the TE properties antimonide and chalcogenide nanocomposites achieved enhanced TE properties as compared to that of bulk materials. For example, after densification, Sb-doped PbS nanocrystals results in higher carrier concentrations, thereby possessing higher ZT values, compared to the undoped specimen. The approach whereby direct doping of the nanocrystals results in an increase of the polycrystalline carrier concentration is a promising approach to nanoscale TE materials enhancement and one that we've employed for some time. In addition, FeSb₂ nanocomposites achieved higher ZT values than that of the bulk due to significant phonon scattering. The effect of defects on the electrical and thermal transport properties will also be discussed.

11:00 AM

(EMA-S6-004-2014) Alkaline earth hexaborides: the effect of dopant additions on thermoelectric properties

M. Alberga*, D. D. Edwards, Alfred University, USA

Thermoelectric generators (TEGs) can be used to convert waste heat into usable electrical energy. Metal hexaborides (MB₆ with M = Ca, Sr, Ba) have received interest as thermoelectric materials due to their high electrical conductivity and Seebeck coefficient values. However, the thermal conductivities of these materials exceed 10 W/(m K); considered high relative to other candidate materials. In this work, the effects of alloying between these alkaline earth cations

were studied with the goal of reducing thermal conductivity, thereby increasing the figure of merit, ZT. Additionally, the effects of both donor and acceptor type dopants on the electrical properties were explored. High relative density was achieved for all samples through spark plasma sintering (SPS).

11:15 AM

(EMA-S6-014-2014) Synthesis of nanostructured Oxides and Oxynitrides for thermoelectric converters

A. Weidenkaff*, W. Xie, X. Xiao, L. Sagarna, G. Saucke, P. Thiel, L. Karvonen, A. Shkabko, EMPA, Switzerland

Ceramic oxides are promising candidates for high temperature conversion of solar - or exhaust gas heat. The broad application of thermoelectric converters in future energy technologies requires the development of low cost scalable synthesis methods for highly efficient thermoelectric materials. Various soft chemistry synthesis methods are applied, tested and compared for the synthesis of nanostructured titanates, cobaltates, manganates and zinc oxides. Aerosol processes such as Ultrasonic Spray combustion and Flame Spray Synthesis enable a continuous feed and decomposition of tailored liquid precursors as well as the deposition of coatings and dense films on substrates. Ammonolysis of the oxides leads to conductive oxynitrides with enhanced conductivity. The nanostructuring, composition, oxidation state and defect structure can be controlled by the precursor chemistry and defined synthesis conditions which is shown in X-ray diffraction and electron microscopic studies. Suitable candidates are being selected from the synthesized products according to their temperature dependent ZT values, and compatibility factors to produce performing thermoelectric converters delivering a high energy density. These converters are tested under ambient air at temperatures of $T > 900$ °C and applied in an exhaust gas stream of a custom made hybrid vehicle, solar thermal converters, metal casting furnaces and solid oxide fuel cells.

11:30 AM

(EMA-S6-006-2014) High Performance, High Efficiency Rare-Earth-Based Thermoelectric Materials for Space Power Generation Applications (Invited)

S. Bux*, T. Vo, Jet Propulsion Laboratory/California Institute of Technology, USA; J. Grenkemper, Y. Hu, University of California Davis, USA; J. Ma, S. Clarke, University of California Los Angeles, USA; J. Pfluger, California Institute of Technology, USA; C. Huang, D. Uhl, T. Caillat, P. Von Allmen, Jet Propulsion Laboratory/California Institute of Technology, USA; S. Kauzlarich, University of California Davis, USA; J. Fleurial, Jet Propulsion Laboratory/California Institute of Technology, USA

Since the 1960s, the state-of-the-art power systems for space applications has typically been based up on either SiGe or PbTe. Although reliable and robust, the thermoelectric performance of these systems remains fairly low. In recent years, complex materials such as n-type $\text{La}_{3-x}\text{Te}_4$ and p-type $\text{Yb}_{14}\text{MnSb}_{11}$ have emerged as new high efficiency, high temperature thermoelectric materials with ZTmax on the order of 1.2 at 1275 K. The high performance of these Zintl phases is attributed to their favorable characteristics such as: semi-metallic behavior due to small band gaps, very low glass-like lattice thermal conductivity values due to structural complexity and reasonably large thermopower values near their peak operating temperatures. We will present an overview of recent research efforts at JPL and collaborating institutions on these systems and will discuss approaches and preliminary results on the properties of these rare earth compounds through suitable experimental chemical substitutions coupled with guidance from first principle electronic structure simulations.

12:00 PM

(EMA-S6-007-2014) Discovering New and Old Thermoelectrics Using Transport Theory (Invited)

D. J. Singh*, Oak Ridge National Laboratory, USA

There is no known thermodynamic or other fundamental physical principle that limits the possible values of the thermoelectric figure of merit, ZT. However, thermoelectric performance requires combinations of materials properties that do not normally occur together, for example, high thermopower combined with high conductivity and high carrier mobility with low lattice thermal conductivity. As a result, high thermoelectric performance is typically found not in materials that follow standard text-book behavior, but in materials with unusual features such as highly non-parabolic or other complex band structures, proximity to lattice instabilities, unusual bonding, etc. In this presentation we discuss different ways of obtaining high ZT along with materials examples and also suggest new directions and possible realizations of them.

S9: Thin Film Integration and Processing Science

Processing and Integration of Ferroelectric Thin Films

Room: Coral B

Session Chair: Jon Ihlefeld, Sandia National Laboratories

10:00 AM

(EMA-S9-019-2014) Understanding dewetting in metallic thin films through in-situ scanning confocal laser microscopy (Invited)

N. Valanoor*, University of New South Wales, Australia

Buoyed by the installation of a custom designed in-situ hot stage scanning confocal microscope in my lab, a number of unsuccessful attempts were made to investigate various kinetic phenomena in ferroic materials systems. It was only in late 2012 that we found the ideal problem, rather the ideal undergraduate who came to us with the ideal problem- to understand dewetting phenomena in metallic thin films. In my talk I will show our results of understanding how dewetting proceeds in metallic thin films. Most of the talk will focus on polycrystalline gold films sputtered on various buffer layers and how the buffer layers affect dewetting. The second part will cover recent work on understanding the thermal stability of Ni islands. For the first time real-time images render the various stages such as rim formation, faceting and pinch off. This work is partly supported by the Australian Research Council and is a collaborative effort between UNSW, Sandia, North Carolina State and MIT.

10:30 AM

(EMA-S9-011-2014) Flux-assisted growth of BaTiO_3 thin films

D. T. Harris*, M. J. Burch, J. Ihlefeld, P. G. Lam, J. Li, E. C. Dickey, J. Maria, North Carolina State University, USA

In this presentation we demonstrate that by incorporating a low melting temperature flux into BaTiO_3 , we can enhance grain growth, crystallization, and the nonlinear dielectric properties important for devices like ferroelectric varactors. BaTiO_3 films with $\text{BaO-B}_2\text{O}_3$ flux were grown on c-sapphire using PLD from ceramic target compositions containing between 1% and 5% of the borate-based flux. Films were prepared at room temperature, then annealed at temperatures above the flux melting temperature of 869 °C. Average grain sizes of 0.3 μm were observed in samples grown with 3% flux, compared to < 0.1 μm for conventional material. Enhancement of the relative tuning from 20% to 70% is associated with improved crystallinity and larger grain size. Capacitance temperature measurements reveal a shift in the Currie temperature of 50 °C, in agreement with phenomenological theory, expected residual strain, and x-ray strain

measurements. X-ray diffraction and TEM were employed to search for evidence of secondary phases, and an interface reaction between our films and sapphire was discovered. $\text{BaO-V}_2\text{O}_5$ (BVO) and $\text{Bi}_2\text{O}_3\text{-BaB}_2\text{O}_4$ offer the opportunities for lower processing temperatures. Films grown with liquid BVO exhibit enhanced density, as well as texture that is not present when grown with no liquid layer.

10:45 AM

(EMA-S9-012-2014) Microstructural Characterization of Flux-Grown BaTiO_3 Thin Films

M. J. Burch*, D. T. Harris, J. Li, J. Maria, E. C. Dickey, North Carolina State University, USA

BaTiO_3 is an important material because of its potential for applications in tunable microwave devices. Methods of increasing the tunable properties of BaTiO_3 thin films have been extensively studied recently. One method to improve the tunability of the films is to add a liquid forming flux to the thin film during deposition. The flux leads to an enhanced microstructure by increasing the size and crystalline perfection of the BaTiO_3 grains, which leads to enhanced tunability. BaTiO_3 thin films were deposited approximately 500 nm thick by pulsed laser deposition with concentrations up to 5% barium-borate flux on several different orientations of sapphire (A, R and C) and subsequently annealed in air at 900°C. Transmission electron microscopy, electron energy loss spectroscopy and energy dispersive x-ray spectroscopy were used to characterize the thin films. Secondary phases of barium aluminate were found to be present in all of the films characterized. However, the secondary phases and overall microstructure of the BaTiO_3 varied dramatically between the different sapphire substrate orientations. Nonetheless, all of the fluxed films exhibited superior electrical properties when compared to unfluxed films.

11:00 AM

(EMA-S9-013-2014) Chemical Solution Processing of High Performance Piezoelectric Thin and Ultra-Thin Films (Invited)

N. Bassiri-Gharb*, Y. Bastani, S. Brewer, Georgia Institute of Technology, USA

Silicon-integrated ferroelectric thin films have been leveraged over the last two decades for fabrication of high performance piezoelectric microelectromechanical systems (MEMS) sensors, actuators and transducers. Ceramic PZT thin films have been often the material of choice, due to their large electromechanical response, especially at morphotropic phase boundary compositions (MPB). However, ferroelectric thin films suffer from extrinsic size effects that lead to deterioration of the piezoelectric properties in thin and ultra-thin films. Here we report two different strategies for processing of thin films with enhanced piezoelectric response with respect to traditionally processed PZT thin films. Specifically, we will discuss preparation of superlattice-like (SL), polycrystalline PZT thin films and polycrystalline relaxor-ferroelectric (PMN-PT) by chemical solution deposition on platinized Si substrates. Compositions were targeted at the MPB for both materials and PZT seed layers were used for texturing of the films. ~200 nm-thick SL PZT films showed effective piezoelectric coefficients ($d_{33,f}$) of ~100pm/V, which is comparable to the piezoelectric response of films of ~2 μm in thickness. PMN-PT thin films with $d_{33,f}$ up to ~220 pm/V were obtained for ~800nm-thick films.

11:30 AM

(EMA-S9-014-2014) In situ x-ray diffraction during crystallization of solution-derived ferroelectric films (Invited)

J. L. Jones*, North Carolina State University, USA; S. Mhin, University of Florida, USA; G. L. Brennecke, J. Ihlefeld, Sandia National Laboratories, USA; R. G. Polcawich, L. M. Sanchez, US Army Research Laboratory, USA

Solution deposition is an attractive method for synthesis of ferroelectric thin films due to its low cost and easy scalability. Synthesis of such films involves heating of an initially amorphous layer to

high temperatures during which diffusion and chemical reactions may occur at the interfaces and surfaces. These effects can have either deleterious or beneficial effects on the resulting film chemistry, microstructure, texture, and properties. In order to study these effects in situ and guide materials synthesis, we have developed and applied an in situ X-ray diffraction approach to probe films at sub-second time scales during heating at rates of 0.5°C/s to over 100°C/s. In this talk, we will present in situ measurements of a variety of film chemistries (lead zirconate titanate (PZT) and lead titanate (PT)) derived from different chemical routes (IMO and 2-MOE). We will also show the influence of the substrate by contrasting film evolution on commercial platinized silicon substrates to substrates prepared at the Army Research Laboratory, the latter of which have a very strong degree of texture and high density. Sandia National Laboratories is a multi-program laboratory managed and operated by Sandia Corporation, a wholly owned subsidiary of Lockheed Martin Corporation, for the U.S. Department of Energy's National Nuclear Security Administration under contract DE-AC04-94AL85000.

12:00 PM

(EMA-S9-015-2014) Compositional Study of Solution Deposited $(\text{Bi}_{0.5}\text{Na}_{0.5})\text{TiO}_3$ - $(\text{Bi}_{0.5}\text{K}_{0.5})\text{TiO}_3$ - $\text{Bi}(\text{Mg}_{0.5}\text{Ti}_{0.5})\text{O}_3$ Thin Films

J. E. Mendez*, J. Walenza-Slabe, N. Kumar, D. P. Cann, B. J. Gibbons, Oregon State University, USA

In this study, the pseudo-ternary system of $(\text{Bi}_{0.5}\text{Na}_{0.5})\text{TiO}_3$ - $(\text{Bi}_{0.5}\text{K}_{0.5})\text{TiO}_3$ - $\text{Bi}(\text{Mg}_{0.5}\text{Ti}_{0.5})\text{O}_3$ (BNT-BKT-BMgT) is studied in order to understand the effect that BMgT, an unstable perovskite, has on the binary BNT-BKT system. In bulk and thin film embodiments these materials have exhibited very promising piezoelectric properties, although there are differences in where the maximum properties are exhibited in terms of BMgT content. Here, the compositional space is explored in the following fashion: $(72.5 - .5x)(\text{Bi}_{0.5}\text{Na}_{0.5})\text{TiO}_3$ - $(22.5 - .5x)(\text{Bi}_{0.5}\text{K}_{0.5})\text{TiO}_3$ - $x\text{Bi}(\text{Mg}_{0.5}\text{Ti}_{0.5})\text{O}_3$, where x varies from 0-50 in increments of 5. Thin films are produced using chemical solution deposition (CSD). Solutions made from acetate precursors, with appropriately overdoped solutions to account for cation volatility, are spin-cast onto platinized silicon substrates, then pyrolyzed and crystallized at 300°C and 700°C, respectively. The resulting films range from 250 nm-300 nm in thickness, as measured by ellipsometry, and are phase pure perovskite, as determined from x-ray diffraction. The resulting films gave a monotonically increasing trend in d_{33} , E_3 , and P_r values as the percent of BMgT phase increased, which is in disagreement with bulk ceramic results. Further efforts to explain these discrepancies between the BNT-BKT-BMgT thin film and bulk embodiments will be presented.

12:15 PM

(EMA-S9-016-2014) Solution-Derived $\text{Bi}(\text{Zn,Ti})\text{O}_3$ - BaTiO_3 Thin Films with Bulk-like Permittivity

R. P. Wilkerson, University of California - Berkeley, USA; K. E. Meyer, New Mexico Institute of Mining and Technology, USA; P. G. Kotula, G. L. Brennecke*, Sandia National Laboratories, USA

Weakly-coupled relaxor dielectric systems based on solid solutions of BaTiO_3 and Bi-based perovskites have received interest in recent years because of their large permittivity values which are stable under large electric fields and across broad temperature ranges. While chemical homogeneity has been shown to be critical to achieving bulk-like permittivity in pure BaTiO_3 thin films, parallel work suggests that the attractive permittivity stability of bulk $\text{Bi}(\text{Zn}_{0.5}\text{Ti}_{0.5})\text{O}_3$ - BaTiO_3 is due in part to chemical heterogeneity at the sub-grain scale. Here we report the fabrication of thin films in the $\text{Bi}(\text{Zn}_{0.5}\text{Ti}_{0.5})\text{O}_3$ - BaTiO_3 system which exhibit the frequency dispersion that is characteristic of relaxor dielectrics and similar magnitudes of permittivity values when compared to bulk ceramic samples of the same compositions, representing an opportunity to explore the role of multi-scale cation distribution on permittivity scaling and relaxor response. This work was supported in part by

the Energy Storage program managed by Dr. Imre Gyuk for the Department of Energy's Office of Electricity Delivery and Energy Reliability. Sandia National Laboratories is a multi-program laboratory managed and operated by Sandia Corporation, a wholly owned subsidiary of Lockheed Martin Corporation, for the U.S. Department of Energy's National Nuclear Security Administration under contract DE-AC04-94AL85000.

S12: Recent Developments in High-Temperature Superconductivity

YBCO based Coated Conductors, Pinning Properties and Applications

Room: Mediterranean B/C

Session Chair: Judy Wu, University of Kansas

10:00 AM

(EMA-S12-014-2014) Improvement of Spatial Homogeneity and In-field Critical Current in RE-123 Coated Conductors (Invited)

T. Kiss*, K. Higashikawa, S. Gangi, K. Imamura, M. Inoue, Kyushu University, Japan; T. Taneda, A. Ibi, T. Yoshida, M. Yoshizumi, T. Izumi, Y. Shiohara, International Superconductivity Technology Center, Japan; K. Kimura, T. Koizumi, N. Aoki, T. Hasegawa, SWCC Showa cable systems Co., Ltd, Japan

Practical performance of RE-123 coated conductors depends strongly on spatial homogeneity and in-field critical current (I_c) of the tape. It has been pointed out that local obstacle can be an origin of thermal instability and/or degradation of coil windings and also magnetization current induced in the tape strand prevent field homogeneity or stability of a magnet. To challenge these issues, 1) we have developed a novel method to visualize in-plane I_c distribution in long length superconducting tapes in the range of 100s of meters with high spatial resolution based on reel-to-reel scanning Hall probe microscopy, 2) we also carried out in-field transport measurement and magnetic moment measurement by use of both four-probe methods and SQUID magnetometer, respectively. Based on these studies, we will summarize recent progress of spatial homogeneity in several types of long length coated conductors obtained from different processes including MOD, standard PLD process and artificial pinning center (APC) addition using BaHfO₃. Influence of in-plane texturing and APC on the in-field current transport properties over 9 decades of electric field ranges from flux creep to flux flow regime will also be discussed.

10:30 AM

(EMA-S12-015-2014) Status of coated conductor development for coil applications in high magnetic fields at low temperatures (Invited)

V. Selvamanickam*, A. Xu, Y. Liu, N. Khatri, L. Delgado, E. Galtsyan, X. Li, G. Majkic, University of Houston, USA

At the University of Houston, we are developing coated conductors with improved critical currents in magnetic fields of 2.5 T to 30 T in temperatures of 4.2 K to 40 K. In particular, (Gd,Y)Ba₂Cu₃O_x (GdYBCO) coated conductors made by metal organic chemical vapor deposition (MOCVD) with high levels of Zr addition (> 15 mol.%) are being explored. Pinning force levels over 300 GN/m³, 450 GN/m³ and 1700 GN/m³ have been achieved at 40 K, 30 K and 4.2 K respectively in 15 mol.% added GdYBCO superconductors in the orientation of field perpendicular to the conductor. Fascinating correlations have been found between critical currents at 77 K in low magnetic fields (up to 3 T) and those at low temperatures.

11:00 AM

(EMA-S12-016-2014) Laser Chemical Vapor Deposition for High- J_c YBa₂Cu₃O_{7-δ} films (Invited)

A. Ito*, P. Zhao, T. Goto, Institute for Materials Research, Tohoku University, Japan

YBa₂Cu₃O_{7-δ} (YBCO) films with a high critical current density (J_c) were prepared on a multilayer-coated Hastelloy C276 substrate by laser chemical vapor deposition (laser CVD) using a single liquid source precursor. CVD is promising for the preparation of coated conductors because it not only provides a rapid deposition and uniform coverage but can also be adapted to a reel-to-reel continuous production system for long-length wires. Although Y, Ba, and Cu solid compounds were used as precursors in previous study, the use of a liquid precursor to continuously and stably supply a precursor for a prolonged period is feasible. Y(dpm)₃, Ba(dpm)₂(tmod)₂, and Cu(dpm)₂ precursors were dissolved in tetrahydrofuran and the source solution was delivered into the evaporation chamber using a plunger pump. A Nd:YAG laser beam was introduced into the CVD chamber through a quartz window. A multilayer-coated Hastelloy C276 tape was used as a substrate. Deposition was lasted for 180 s. The as-deposited films were heat treated in an O₂ atmosphere. A *c*-axis-oriented YBCO film was grown epitaxially on a (100) CeO₂ layer. Deposition rate was 11 μm h⁻¹. A screw dislocation and stacking faults were observed in the cross-section of the YBCO film. The J_c of the YBCO film reached 2.7 MA cm⁻². The screw dislocations perpendicular to the film plays the role of pinning centers and be responsible for the enhancement of J_c .

11:30 AM

(EMA-S12-017-2014) Kinetics and dynamics of double doping nanostructure self-assembly in YBCO films (Invited)

J. Wu*, J. Baca, J. Shi, University of Kansas, USA; T. Haugan, M. Sabastian, U.S. Air Force Research Laboratory, USA; B. Maiorov, T. Holesinger, Los Alamos National Laboratory, USA

In this work, we investigate the role of Y₂O₃ nanoparticles on the growth of BZO nanorods in order to understand the mechanisms governing their self-assembly in YBCO films strained differently via selection of different substrates. By examining the microstructure and current-carrying capacity of BZO-doped YBCO films, we show that the nanorod growth dynamics are significantly enhanced when compared to films doubly-doped with BZO and Y₂O₃ nanoparticles. We find that the average nanorod length and associated critical current densities increase at a significantly higher rate in the absence of Y₂O₃ nanoparticles when the growth temperature is increased. When additional strain is added to the YBCO matrix through substrate/film interface, the dynamics is considerably affected. We show the interactive effects of multiple dopants and YBCO matrix strain that must be considered to fully control the defect landscape in oxide films. A theoretical model based on the elastic strain theory was developed to quantify the interfacial strain at the coherent or semi-coherent interface between dopants and YBCO matrix, and that between the YBCO matrix film and substrate and interplay of these two interfacial strains could results in a variety of nanostructure morphology and an excellent agreement with experiment has been obtained.

12:00 PM

(EMA-S12-019-2014) Designed Flux Pinning Landscapes in YBa₂Cu₃O_{7-δ} Thin Films by incorporating CoFe₂O₄:CeO₂ Vertically Aligned Nanocomposites

J. Huang*, C. Tsai, L. Chen, H. Wang, Texas A&M University, USA

Multifunctional vertically aligned nanocomposites (VAN) combined ferromagnetic CoFe₂O₄ with non-ferromagnetic CeO₂ have been introduced into YBa₂Cu₃O_{7-δ} (YBCO) thin films as both cap and buffer layers to enhance flux pinning properties of the YBCO films. A pulsed laser deposition (PLD) technique was applied to prepare all the samples. The composition of CoFe₂O₄ in the VAN nanolayer

was varied from 10%, 30% to 50%, which results in ordered CoFe₂O₄ and CeO₂ nanopillars to obtain tunable flux pinning properties. XRD, high resolution XTEM and STEM along PPMS are used for microstructure and superconducting performance measurements. The results show that all the samples have a T_c Value of about 90K, and there is an obvious self-field and in-field J_c enhancement for all the doped samples compared to the reference YBCO sample. The results suggest that VAN provides effective pinning centers by both defect and magnetic nanoinclusions. The 50% CoFe₂O₄ VAN cap doped sample shows the best J_{csf} of 17.1 MA/cm², 48.3 MA/cm² and 132 MA/cm² at the temperature of 65K, 40K and 5K, respectively. Furthermore, tunable pinning properties can be achieved by tuning the density of magnetic pinning centers in the VAN nanolayer.

S1: Functional and Multifunctional Electroceramics for Commercialization

Piezoelectric Energy Harvesting

Room: Pacific

Session Chair: Shujun Zhang, Penn State University

1:30 PM

(EMA-S1-042-2014) Synthesis of KNbO₃ Nanowires and Their Application to Flexible Piezoelectric Energy Harvesters (Invited)

S. Nahm*, M. Joung, H. Xu, J. Kim, I. Seo, Korea University, Republic of Korea; S. Yoon, C. Kang, Korea Institute of Science and Technology, Republic of Korea

Tetragonal KNbO₃ (KN) nanowires were formed when the synthesis was carried out at 1200°C for 48 h. However, when the fabrication was conducted at high temperatures ($\geq 1500^\circ\text{C}$) or at 1200°C for a long period of time (≥ 72 h), orthorhombic KN nanowires were obtained. Moreover, the KN nanowires synthesized at 1200°C for 60 h showed a morphotropic phase boundary (MPB) structure in which both tetragonal and orthorhombic structures coexisted. A tetragonal KN nanowire exhibited a d₃₃ value of 137.1 pm/V, which is larger than that of the orthorhombic KN nanowire (104.5 pm/V), probably because of the softening effect of the metal vacancies. The MPB KN nanowires exhibited a larger d₃₃ value of 146.0 pm/V. Three types of the KN nanowires were mixed with PDMS and these mixtures were deposited on the Au-coated PI substrate. Finally, the Au-coated PI was covered on the PI/Au/PDMS-KN device to fabricate the piezoelectric energy harvester. In these work, three types of KN piezoelectric energy harvesters were fabricated and the output power of these harvesters were investigated. Moreover, the magnitude of their output power was explained based on the structural and piezoelectric properties of the KN nanowires.

2:00 PM

(EMA-S1-043-2014) Confinement Printing of Thin Film Lead Zirconate Titanate (Invited)

S. Trolier-McKinstry*, A. Welsh, Penn State, USA; D. Dezest, L. Nicu, CNRS, France

This work explores the confinement printing of lead zirconate titanate (PZT) liquid precursors from stamp wells (rather than stamp protrusions as is used in microcontact printing). The confinement printing of solutions uses an initial sacrificial printing step in order to remove solution from the protrusions of the stamp. The second stamping cycle deposits the solution from the wells of stamp. Printing from wells doubled the thickness (e.g. from 25 to 50 nm) of deposited solution per stamping cycle over microcontact printing. This work studies the printing characteristics of this patterning technique, including line edge resolution, feature thickness, sidewall angles, and achievable lateral feature size. Arrays of PZT features were printed, characterized and compared to continuous PZT thin films of similar thickness. One micron thick PZT features exhibit

a permittivity of 1030 and a loss tangent of 0.024. The hysteresis loops are well formed, without pinching of the loops. The patterned features showed remanent polarizations of 29 $\mu\text{C}/\text{cm}^2$, and coercive fields of 52 kV/cm. The piezoelectric response of the features produced an e_{31f} of -7 C/m².

2:30 PM

(EMA-S1-044-2014) Microstructural origin for the piezoelectricity evolution in (K_{0.5}Na_{0.5})NbO₃-based lead-free ceramics

H. Guo*, Iowa State University, USA; S. Zhang, Pennsylvania State University, USA; S. P. Beckman, X. Tan, Iowa State University, USA

The real-time evolution of the domain morphology and crystal structure under electrical poling fields of a model material, 0.948(K_{0.5}Na_{0.5})NbO₃-0.052LiSbO₃, was directly visualized using *in situ* transmission electron microscopy. The original *Amm*2/*P4mm* polymorphic phase boundary is not stable against poling, and is finally replaced by the *Pm* phase. Complicated domain switching and phase transitions are observed to occur. At 8 kV/cm, the original herringbone domain patterns of mixed tetragonal and orthorhombic phases change to thin lamellar domains; this process involves domain switching as well as some extent of tetragonal to orthorhombic phase transition. At 14 kV/cm, a *Pm* phase with anti-parallel cation displacement (most likely combined with the a^bc⁰ oxygen octahedra tilting) is formed, as manifested by the appearance of blotchy domains and 1/2{*o*o*o*} superlattice diffraction spots. These microstructural changes are found irreversible, and hence they dictate the macroscopic properties of poled ceramics. The electromechanical response to the poling fields measured on the bulk ceramics correlate extremely well with the *in situ* observations. The microstructural mechanism for the enhanced piezoelectricity is the presence of the *Pm* phase at 14 kV/cm, where the large number of equivalent polar axis (24) makes the poling easier and more thorough.

S2: Multiferroic Materials and Multilayer Ferroic Heterostructures: Properties and Applications

Novel Multiferroic Materials and Other Functional Oxides II

Room: Indian

Session Chair: Nick Sbrokey, Structured Materials Industries, Inc.

2:00 PM

(EMA-S2-039-2014) Metal-insulator transition-based oxide electronics (Invited)

S. Ramanathan*, Harvard Univ, USA

Oxide semiconductors are gaining interest as active device components for future electronic, photonic and energy device technologies. Within this class, correlated oxides that display sharp phase transitions are particularly interesting due to their reversibly collapsible band gap. In this presentation, we will emphasize two sets of oxide systems: VO₂ and SmNiO₃ in the rutile and perovskite family respectively. Vanadium dioxide undergoes a sharp metal-insulator transition around 67 degC while SmNiO₃ undergoes a transition at 130 degC in bulk form. The proximity of the phase transition to room temperature creates interest in both fundamental ceramic science studies and device-level research. Scientific issues concerning such oxides are plenty. A deep understanding of the structural and electrical nature of the interfaces between such oxides and gate insulators (both solid state and ionic liquids) are crucial. In this presentation, we will discuss few inter-related topics: (a) growth of phase pure oxide thin films by physical vapor deposition and new synthesis techniques for thermodynamic phase control including on

non-lattice matched substrates, (b) methods to electrically actuate the phase transition and non-volatile memory and (c) emerging opportunities in programmable fluidic circuits that utilize complex oxides.

2:30 PM

(EMA-S2-040-2014) Reversible redox reactions in epitaxial SrCoOx oxygen sponges (Invited)

H. Lee*, Oak Ridge National Laboratory, USA

Ionic defects, such as oxygen vacancies, in perovskite oxides with multivalent transition metal elements play a central role in the performance of many advanced energy technologies, including solid-oxide fuel cells, rechargeable batteries, oxygen-separation membranes, memristers, and resistive random access memories. Strontium cobaltites are good candidates due to the potential for mixed ionic and electronic conductivity and good catalytic activities owing to the multivalent nature of Co ions. However, the successful growth of phase pure, fully oxidized SrCoO₃ has not been reported so far due to the metastable Co⁴⁺ state. Here, we will present epitaxial growth of two SrCoO_{3-x} phases, i.e. the 'brownmillerite' SrCoO_{2.5} and the 'perovskite' SrCoO₃, by pulsed laser epitaxy. Results from a systematic study with XRD, XAS, XMCD, SQUID, and PPMS will be presented, comparing the structural and physical properties between two phases. In particular, based on real-time XRD and spectroscopic ellipsometry, we will show that those two phases can be topotactically reversible at drastically reduced temperatures as low as 200 °C, which may lead to the discovery of new oxygen membranes and cathode materials for high performance energy storage. *The work was supported by the U.S. Department of Energy, Basic Energy Sciences, Materials Sciences and Engineering Division.

3:00 PM

(EMA-S2-041-2014) Voltage Tunable Microwave Resonators Fabricated with MOCVD deposited Ba_xSr_{1-x}TiO₃ Films (Invited)

N. M. Sbrockey*, Structured Materials Industries, Inc., USA; T. Kalkur, E. Nowe, University of Colorado at Colorado Springs, USA; S. Alpay, H. Khassaf, University of Connecticut, USA; G. S. Tompa, Structured Materials Industries, Inc., USA

Resonators are critical components in radio frequency (RF) communication, radar and wireless data applications. The development of voltage tunable resonators will greatly reduce cost and manufacturing complexity for RF systems, as well as enable frequency agile operation. Voltage induced piezoelectric effects have been well documented for Ba_xSr_{1-x}TiO₃ (BST) and SrTiO₃ thin films. Voltage tunable film bulk acoustic resonators (FBAR) devices have been demonstrated with films deposited by sputtering and pulsed laser deposition. This work is developing FBAR devices using BST films deposited by metal organic chemical vapor deposition (MOCVD). The resonator parameters such as Q and k² are dependent on the properties of the BST films, which are correlated to the MOCVD deposition parameters. Computer simulation is used to predict performance for tunable RF filters fabricated using the voltage controlled FBAR devices.

3:15 PM

(EMA-S2-042-2014) Deposition of YIG and BST Films on Metals and Growth of Low-Damping Nanometer-Thick YIG Films (Invited)

M. Wu*, Y. Sun, T. Liu, H. Chang, M. Kabatek, Y. Song, W. Schneider, Colorado State University, USA; V. Vlaminck, H. Schultheiss, A. Hoffmann, Argonne National Laboratory, USA

This presentation will touch on two issues on thin film depositions: (1) the deposition of oxide thin films on metals and (2) the growth of low-damping nm-thick yttrium iron garnet (YIG) films. Issue (1) is important because some device applications require the growth of

oxide films on metallic electrodes. Such growth is challenging due to problems with the oxidation, diffusion, and breakup of electrodes during the deposition of oxide films. The first half of this presentation will report the development of a new sandwich-type bottom electrode and the growth of YIG and barium strontium titanate (BST) thin films on the electrodes. The electrodes consist of a Cu layer sandwiched between two cladding layers made of high entropy alloy nitride (HEAN). The HEAN layers have high oxidation resistance and good thermal stability and thereby facilitate the growth of YIG and BST films on the electrodes. Issue (2) arises in line with the emergence of a new research field - "spintronics using YIG," which creates a demand for YIG films that have a thickness in the nm range and also exhibit low damping as in YIG crystals. The second half of this presentation will report the growth of low-damping nm-thick YIG films by pulsed laser deposition (PLD) and sputtering. The 10-nm PLD films showed a damping of 3.2×10⁻⁴. The 10-nm sputtering films showed a damping of 12×10⁻⁴.

4:00 PM

(EMA-S2-043-2014) Monolithic Multiferroic Thin Film Heterostructure Fabrication via an Automated Chemical Solution Deposition Process (Invited)

X. Guo*, H. Song, Y. Wang, K. K. Li, Y. K. Zou, H. Jiang, Boston Applied Technologies, Inc., USA; S. S. Puranam, A. Gopinath, University of Minnesota, USA; M. Wu, Colorado State University, USA

This research is aimed to develop electrically tunable microwave devices based on a multiferroic heterostructure for reduced bias field, faster tuning, and minimized device size at low cost. In this work, M-type barium hexagonal ferrite (BaM) and barium strontium titanate (BST) are chosen as the ferromagnetic and ferroelectric layer materials, respectively. Monolithic heterostructures of highly textured BaM and BST thin films with preferred crystalline orientations were fabricated with an automated chemical solution deposition process. Effects of buffer layers, processing parameters and precursor solutions on microstructures and ferromagnetic and ferroelectric properties of the heterostructures were studied. X-ray diffractometry, scanning electron microscopy, magnetic hysteresis, and ferromagnetic resonance measurements were carried out. The results indicated the good quality of the thin film heterostructures and the promise of the low-cost solution-processed monolithic multiferroic heterostructures for frequency-agile RF electronics.

4:15 PM

(EMA-S2-044-2014) MOCVD of Complex Oxides for Multiferroic and Multiferroic Composite Thin Film Production (Invited)

G. S. Tompa, N. M. Sbrockey*, Structured Materials Industries, Inc., USA

Multiferroic thin films have received a great deal of attention recently because of their unique properties and potential in multiple applications. Multiferroics are unique because of their coupling of effects such as charge, elasticity, and magnetism; and more importantly the capability to influence these couplings by external stimuli such as electrical field or mechanical strain. Such combinations of manipulative interactive properties have been proposed for making hybrid memory cells, tunable RF components and many other unique devices. Multiferroics encompass a wide class of materials; including single phase materials such as BiFeO₃ and composite materials such as BaTiO₃/CoFe₂O₄. The properties of multiferroic and multiferroic composite thin films are highly dependent on their structure, which is in turn controlled by the film deposition process. Approaches to make multiferroics include: MOSD, Sputtering, PLD, MBE and MOCVD. Each of these techniques have advantages and disadvantages. This talk will briefly review and compare these techniques and then focus on the MOCVD process. We believe the MOCVD process offers the best overall solution to large area, reproducible production of multiferroic and multiferroic composite thin films.

4:30 PM

(EMA-S2-045-2014) A facile route for single-crystal heteroepitaxial ferroic perovskite oxide thin films (Invited)

J. Spanier*, Drexel University, USA

Growth of high-quality single-crystal epitaxial thin films of complex oxides typically requires high deposition temperature and high vacuum. Atomic layer deposition (ALD), an attractive, versatile, and inexpensive low-temperature and low vacuum thin film deposition technique, is not generally regarded as a candidate for producing chemically complex films of exceptional crystalline quality. I will present on our recent work involving the use of ALD to obtain epitaxial thin films of ferroic perovskite oxides. I will discuss how a low-temperature and low-vacuum surface reaction rate-limiting process, with brief thermal annealing, can be used to obtain stoichiometric and high-quality epitaxial perovskite thin films with atomic structural quality and physical properties comparable to high-vacuum and high-temperature routes. Our results unambiguously challenge the widely held notion that atomic layer deposition is not appropriate for high-quality epitaxial thin film growth and demonstrate its applicability as an inexpensive, facile and highly scalable route for producing epitaxial complex oxide thin films. In my talk will also highlight some of my group's other work involving ferroelectrics, particularly for renewable energy applications. Work supported by ARO and the NSF/SRC.

4:45 PM

(EMA-S2-046-2014) Hardware Modifications of ARL's MOCVD System and Fabrication of SrTiO₃ Thin Films

E. Enriquez*, UTSA, USA; D. Shreiber, M. Will-Cole, Army Research Lab, USA

Hardware modifications were made to an existing Metalorganic Chemical Vapor Deposition (MOCVD) system in attempts to improve film purity and quality. A loading chamber was installed with a "wobblestick" load arm to protect samples from impurities in the main MOCVD chamber prior to deposition. Camera and light sources to provide a live video feed of the main MOCVD chamber was also installed, to assist with the transportation of samples from the load chamber to the sample heater. Strontium Titanate (STO) thin films were grown on Platinized Silicon substrates (Pt/TiO₂/SiO₂/Si), hereafter abbreviated as PTSi, and were characterized by X-Ray Diffraction (XRD), Scanning Electron Microscopy (SEM), Atomic Force Microscopy (AFM) and Energy Dispersive Spectroscopy (EDS). A study of mass flow rates and total gas flow rates were performed to investigate their respective roles in the resulting homogeneity and film thickness of resulting STO films. Investigations have shown a notable increase in the quality of the fabricated STO thin films as compared to samples grown prior to the hardware and growth parameter modifications.

5:00 PM

(EMA-S2-047-2014) CoWO₄ nanoparticles synthesized by microwave-hydrothermal technology: catalytic oxidation of terpenes

A. Dias, P. Robles-Dutenhefner*, UFOP, Brazil

Metal-transition orthotungstates are currently studied as promising candidates for applications as multiferroic materials. Among the methods employed to produce nanostructured ceramics, the microwave-assisted synthesis has become a most promising route. The main advantage in comparison with conventional methods is the low-energy consumption associated with faster precipitation kinetics. In this work, CoWO₄ powders were synthesized under microwave-hydrothermal conditions in temperatures as low as 110°C and times ranging from 1 to 60 minutes. Structural and morphological properties were carefully investigated through X-ray diffraction, Raman spectroscopy, nitrogen adsorption, and transmission electron microscopy. The results are discussed in terms of the relationship between the crystal structure, morphological features

and the final properties. CoWO₄ was used as a heterogeneous catalyst for the liquid-phase aerobic oxidation of the monoterpenes citronellol, (+)-limonene and (-)-beta-pinene. Catalytic activity of CoWO₄ was assessed in the oxidation reaction of beta-citronellol, (+)-limonene and (-)-beta-pinene in a free solvent system. Results obtained demonstrated that this material was promising catalysts for the oxidation of monoterpenes. Reactant conversion ranged from 49 to 78% and a combined selectivity up to 59% for the oxidation products was achieved.

S6: Thermoelectrics: Defect Chemistry, Doping and Nanoscale Effects**Oxides, Films and Defects**

Room: Coral A

Session Chair: Sabah Bux, Jet Propulsion Laboratory/California Institute of Technology

2:00 PM

(EMA-S6-008-2014) Understanding the defect chemistry to control electrical conduction in polar titanates (Invited)

D. Sinclair*, University of Sheffield, United Kingdom

This talk will focus on the influence of chemical doping and non-stoichiometry on the electrical properties in polar titanates, including BaTiO₃, Na_{1/2}Bi_{1/2}TiO₃, Sr₃Ti₂O₇, and TiO₂. We will focus on: (i) the origin and influence of so-called Rare-earth (electronic) donor doping, eg $\text{La} + e \rightarrow (\text{Ba}, \text{Sr})$ and oxygen-loss (reduction) mechanisms in BaTiO₃ and Sr₃Ti₂O₇ by a combination of atomistic simulations, Impedance Spectroscopy and Seebeck coefficient measurements; (ii) the remarkable influence of the Na:Bi A-site starting ratio on the conduction properties of Na_{1/2}Bi_{1/2}TiO₃. In this case we use a combination of Impedance Spectroscopy, electro-motive force (emf) measurements and O₁₈ Tracer Diffusion measurements to prove the existence of (unexpected) high levels of oxide ion conduction; (iii) co-donor and acceptor doping (Nb, In) of TiO₂ to highlight the important role of oxygen-loss that induces significant electrical heterogeneity in this material. If time permits, we will present thermal conductivity measurements on a range of undoped and doped cubic and hexagonal-type perovskites to assess their potential as novel thermoelectrics.

2:30 PM

(EMA-S6-009-2014) High temperature thermoelectric properties of SrTiO₃ under controlled pO₂

H. J. Brown-Shaklee*, P. A. Sharma, J. Ihlefeld, Sandia National Laboratories, USA

Many reports in the thermoelectric literature point to the link between oxygen activity achieved during processing and thermoelectric performance near room temperature. However, in situ measurement of thermoelectric oxides at elevated temperatures remains relatively understudied. Here, we discuss the role of oxygen vacancies and charge compensating defects on the thermoelectric transport properties of Nb-doped SrTiO₃ (Nb-STO) between 300 and 1200K. We developed an automated system to sequentially measure Seebeck coefficient and electrical conductivity as a function of temperature and pO₂. Our results show that thermoelectric power factor ($S\sigma^2$) of Nb-STO ceramics decreases by >3 orders of magnitude when allowed to equilibrate at high temperature under increasing oxygen activities ($10^{-23} < p\text{O}_2 < 10^0$ atm). By extension, the thermoelectric figure of merit, ZT, will also vary by orders of magnitude for identically donor doped ceramics due to charge compensation by strontium vacancies. This work was supported by the LDRD program at Sandia National Laboratories. Sandia National Laboratories is a multi-program laboratory managed and operated by Sandia Corporation, a wholly owned subsidiary of Lockheed Martin Corporation, for the U.S. Department of

Energy's National Nuclear Security Administration under contract DE-AC04-94AL85000.

2:45 PM

(EMA-S6-010-2014) The effects of niobium doping and oxygen partial pressure on the thermoelectric properties of beta-gallia rutile intergrowths

K. J. Scott*, M. Alberga, D. D. Edwards, Alfred University, USA

The development of oxide materials with improved n-type thermoelectric properties will enable the development of thermoelectric generators (TEGs) that can operate above 1000K. Beta-gallia rutile intergrowths, a homologous series expressed as $\text{Ga}_4\text{Tin-4O}_{2n-2}$, contain rutile-type blocks separated by thin beta-gallia layers. Oxides with layered crystal structures offer the opportunity to decouple the electrical and thermal properties and thereby increase the thermoelectric figure of merit (ZT). Optimization of these materials would involve limiting the thermal conductivity through phonon scattering at the intergrowth interfaces and increasing the electrical conductivity with different levels of Nb dopant and oxygen partial pressures ($p\text{O}_2$). In this work, we have investigated the thermoelectric properties of $\text{Ga}_4\text{Tin-4O}_{2n-2}$ ($n=13$ to $n=25$) both equilibrated at different $p\text{O}_2$ and with varying niobium dopant concentrations. Powders were consolidated using spark plasma sintering. The thermoelectric properties and the underlying defect chemistry will be discussed.

3:00 PM

(EMA-S6-011-2014) Temperature dependent thermal conductivity of nano-grained Barium Titanate (BaTiO_3)

B. F. Donovan*, B. M. Foley, University of Virginia, USA; J. Ihlefeld, B. B. McKenzie, Sandia National Laboratories, USA; P. E. Hopkins, University of Virginia, USA

Barium Titanate (BaTiO_3) is a critical component of a wide array of devices including multi-layered ceramic capacitors, thermistors, and sensors. Performance and size scaling of devices, particularly multi-layered ceramic capacitors, has necessitated a scaling of BaTiO_3 grains to sub-100nm sizes. While the dielectric and structural properties of nano-grained BaTiO_3 has been widely studied, less is known about the thermal properties; in fact, discrepancies in the reputed values of the thermal conductivity of BaTiO_3 currently exist in literature. Accordingly, we study the effect of grain size on thermal conductivity of thin film barium titanate over temperatures ranging from 77K to 500K. Nano-grained thin films were fabricated via chemical solution deposition, utilizing controlled annealing to modify average grain size. Time-domain thermoreflectance was used to determine the thermal conductivity of films with grain sizes ranging from 36nm-63nm. We show that at room temperature, the thermal conductivity of BaTiO_3 decreases with decreasing grain size, which is attributed to an increase in phonon scattering from grain boundaries. Additionally, the thermal conductivity of the samples was measured over a range of temperatures with special attention paid to regions of known structure transitions. We explore the results in the context of a model that incorporates phonon grain boundary scattering.

3:15 PM

(EMA-S6-012-2014) Spin-state control in cobalt oxides (Invited)

I. Terasaki*, Nagoya University, Japan

The spin state is a fundamental concept in transition-metal complexes and compounds. The spin states of Co^{3+} ions are particularly important in the sense that the low spin state is almost degenerate with the high spin state. The spin-state related transport has received a considerable interest since the discovery of the good thermoelectric properties in the layered cobalt oxide NaCoO_2 [1]. This particular oxide shows thermoelectric conversion efficiency as good as the state-of-the-art thermoelectric materials. Koshibae et al. [2] proposed that additional entropy coming from the spin state plays an important role in the thermopower of the cobalt oxides. We

show in this talk why and how the spin states affect the transport and magnetic properties in various cobalt oxides. The first one is the A-site ordered perovskite $\text{Sr}_3\text{YCo}_4\text{O}_{10.5}$ [3]. This material is a room temperature (weak)ferromagnet with a transition temperature of 370 K. We have found that the thermopower of this oxide is enhanced by external pressure, which is explained in terms of the pressure-induced spin state crossover. The second example is $\text{LaRh}_{1-x}\text{Co}_x\text{O}_3$, a solid solution of LaCoO_3 and LaRhO_3 [4]. [1] I. Terasaki et al., Phys. Rev. B56 (1997) R12685. [2] W. Koshibae, et al., Phys. Rev. B62 (2000) 6869. [3] I. Terasaki et al., Materials 3 (2010) 786. [4] S. Asai et al., J. Phys. Soc. Jpn. 80 (2011) 104705.

3:45 PM

(EMA-S6-013-2014) Thermoelectric transition metal oxides and sulfides: a comparison between itinerant ferromagnets

A. Maignan*, LABORATOIRE CRISMAT CNRS ENSICAEN UCBN, France

One unexpected feature of the TE power of transition metal oxides lies in the quasi T-independent $S(T)$ curve over a large T range. Consistently with the theory of the strongly correlated electron system [1], well above the temperature of the quasi particles formation, the S constant behaviour of perovskite ruthenates can be approximated by the generalized Heikes formula by taking into account the spin entropy term [2]. The case of CoS_2 , an itinerant ferromagnet crystallizing in the pyrite structure, will be considered [3] to evaluate the impact of spins on the transport properties in 3D sulfides as compared to 3D (simple or quadruple) perovskite ruthenates [2, 4]. References: [1] X. Deng et al, Phys. Rev. Lett. 110, 086401 (2013), [2] see for instance: Y.Klein et al, Phys. Rev. B 73, 052412 (2006), [3] S. Hébert et al, J. Appl. Phys. 114, 103703 (2013), [4] N. Hollman et al, Phys. Rev. B 87, 155122 (2013).

4:00 PM

(EMA-S6-005-2014) Si/Ge Nano-structured with Tungsten Silicide Inclusions

J. Mackey*, University of Akron, USA; A. Schirlioglu, Case Western Reserve University, USA; F. Dynys, Nasa Glenn Research Center, USA

Traditional silicon germanium high temperature thermoelectrics have potential for improvements in figure of merit via nano-structuring with a silicide phase. A second phase of nano-sized silicides can theoretically reduce the lattice component of thermal conductivity without significantly reducing the electrical conductivity. However, experimentally achieving such improvements in line with the theory is complicated by factors such as control of silicide size during sintering, dopant segregation, matrix homogeneity, and sintering kinetics. Samples are prepared using powder metallurgy techniques; including mechanochemical alloying via ball milling and spark plasma sintering for densification. In addition to microstructural development, thermal stability of thermoelectric transport properties are reported, as well as couple and device level characterization.

4:15 PM

(EMA-S6-015-2014) Cutting-Edge Room Temperature Thermoelectric Properties of AZO Thin Films

J. Loureiro*, R. Santos, J. Figueira, M. Ferreira, I3N-CENIMAT/UNINOVA, Portugal; S. Reparaz, C. Sotomayor, Catalan Institute of Nanoscience and Nanotechnology ICN2, Spain; R. Martins, I. Ferreira, I3N-CENIMAT/UNINOVA, Portugal

Improved thermoelectric properties of Aluminum Zinc Oxide (AZO) thin films deposited by rf and pulsed dc magnetron sputtering at room temperature are reported. It is confirmed that both Al doping from 0.5 to 2% and films thickness clearly control the thermoelectric, optical and structural properties of these films. Seebeck coefficients up to $-134 \mu\text{V/K}$, electrical conductivities up to $4 \times 10^4 (\Omega \cdot \text{m})^{-1}$ lead to attain power factors up to $4 \times 10^{-4} \text{ W/mK}^2$, which is above the state of art for similar materials almost by a factor of three. The thermoelectric I-V response of an optimized AZO

element with a planar geometry (4 mm x 1 mm) was measured and a maximum power output of 2.3 nW for a temperature gradient of 20 K near room temperature was obtained. Moreover, the low thermal conductivity (<1.19 W/mK) yields a ZT value above 0.1. This is an important result as it is at least three times higher than the ZT found in literature for AZO at room temperature opening new doors for applications of this inexpensive, abundant and environmental friendly material in a new era of thermoelectric devices.

4:30 PM

(EMA-S6-016-2014) All-solution processed InGaO₃(ZnO)m superlattice films with coarsened grains of c-axis preferred orientation

S. Cho*, Y. Kwon, H. Cho, Sungkyunkwan University, Republic of Korea

Recently, artificial oxide superlattice structures with semiconducting and insulating properties were reported, which was expressed by RAO₃(MO)_m (R=In or rare earth elements; A=Ga, In, Al, or Fe; M=Mg, Co, Cu, or Zn; m=integer). These materials have the periodic layered structure (superlattice), which consists of alternating stacks of RO₂- (conduction path) with low energy band gap and AO+(MO)_m (barrier layer) with large energy band gap. Low-dimensional nanostructures including superlattice structure change the density of state, effective mass of carriers, and phonon-dispersion relationship. In addition, the interfaces generated by periodic layered structure decrease dramatically thermal conductivity due to increased phonon-scattering. In this study, an all-solution process for fabricating InGaO₃(ZnO)_m superlattice structure was developed based on the chemical reaction of InGaZnO solution and reactive solid phase epitaxy growth proposed by the Hosono group. ZnO buffer and amorphous InGaZnO layer was spin-coated by solution process. Additionally, Thermal treatment for the crystallization was performed by furnace. The crystallinity was analyzed through X-ray diffraction and transmission electron microscopy. Additionally, Thermoelectric properties such as Seebeck coefficient, electrical conductivity and power factor were evaluated.

4:45 PM

(EMA-S6-017-2014) Thermoelectric Oxide Ga_{3-x}In_{5+x}Sn₂O₁₆ Properties Using Spark Plasma Sintering

C. E. Dvorak*, D. Edwards, Alfred University, USA

The development of oxide materials with improved n-type thermoelectric properties can facilitate the development of thermoelectric generators (TEGs) that can operate above 1000K. The transparent conducting oxide (TCO) Ga_{3-x}In_{5+x}Sn₂O₁₆ (0.6<x<1.6), which has an anion-deficient fluorite structure, has shown promise as an n-type thermoelectric oxide. In this work, Ga_{3-x}In_{5+x}Sn₂O₁₆ was prepared by solid state synthesis and then consolidated using conventional and spark plasma sintering. The comparison of thermoelectric properties of both conventionally sintered and SPS Ga_{3-x}In_{5+x}Sn₂O₁₆ will be presented.

5:00 PM

(EMA-S6-018-2014) Experimental determination of phonon mean free paths in complex crystals

P. Hopkins*, B. M. Foley, B. F. Donovan, R. Cheaito, J. T. Gaskins, University of Virginia, USA; H. J. Brown-Shaklee, J. Ihlefeld, Sandia National Laboratories, USA

The transport of phonons in crystals is driven by a bandwidth of phonons of various wavelengths. These various phonon wavelengths give rise to a spectrum of mean free paths, where each differential window of these mean free paths contributes some portion to the overall thermal conduction in the material. A greater understanding of this spectrum of mean free paths gives insight into phonon scattering, which is the primary contribution to thermal resistance in solids at non-cryogenic temperatures. In this work, we develop new experimental approaches to determine the mean free path

in complex crystals. First, we show that during time domain thermoreflectance measurements, the metal film transducer can act as a phonon emitter across the interface of solids, thereby controlling the mean free paths that are excited in the substrate. We show that for metal/silicon systems, the measured thermal conductivity is directly proportional to the Debye temperature of the metal film. From this, we determine the thermal conductivity accumulation and mean free path spectra in silicon. We then turn to frequency domain measurements, and develop means to extend the standard frequency domain thermal spectroscopy to upwards of 1 GHz. This results in experimental sensitivity during mean free path measurements on the order of 1-10 nm in complex oxides such as TiO₂ and SrTiO₃.

5:15 PM

(EMA-S6-019-2014) Thermoelectric modules using p-type CuZnO and n-type NiZnO thin film oxides

J. Loureiro*, R. Santos, J. Figueira, M. Ferreira, A. Rodrigues, R. Martins, I. Ferreira, I3N-CENIMAT/UNINOVA, Portugal

In this study it is shown the performance of thermoelectric (TE) devices made with p-type CuZnO and n-type NiZnO thin films deposited by e-gun evaporation and sputtering techniques. The p-type CuZnO thin films deposited on glass substrates have electric conductivity of $6.24 \times 10^5 \Omega\text{m}^{-1}$ and power factor of $2.5 \times 10^{-5} \text{ W/mK}^2$ with a Seebeck coefficient of $8.3 \mu\text{V/K}$, while for n-type NiZnO films these values are $6.30 \times 10^5 (\Omega\text{m})^{-1}$, $2.0 \times 10^{-4} \text{ W/mK}^2$ and $-18 \mu\text{V/K}$, respectively. The thermoelectric I-V response of the n-p pairs at room temperature is linear with the increase of thermal gradient and the maximum output power is proportional to the number of n-p pairs. A single n-p pair with 4 mm x 2 mm has a maximum output of 2.3 nW for a temperature gradient of 20 K around room temperature. The influence of the n-p TE pairs design on the output of the modules and their interconnection in series and parallel were evaluated leading to a TE device with 8 pairs in 11.4 cm^2 area responding with a maximum output of 18nW to the same temperature gradient of 20 K. Even though the achieved records of these oxides materials can not be competitive with commercial thermoelectric materials they can however be applied in low power consumption applications at room temperature. Besides that, due to their low thickness ($<100 \text{ nm}$) these ZnO-based alloys can be easily integrated in flexible devices broadening their range of applications.

S9: Thin Film Integration and Processing Science

Substrates, Metallization, and Integration

Room: Coral B

Session Chair: Edward Sachet, North Carolina State University

2:00 PM

(EMA-S9-017-2014) Seed Layer TiO₂ Structure Impact on {111}-Textured Pt Electrodes for PZT Devices (Invited)

G. R. Fox*, Fox Materials Consulting, LLC, USA; D. M. Potrepka, R. G. Polcawich, US Army Research Laboratory, USA; D. A. Cullen, Oak Ridge National Laboratory, USA

Thin film platinum electrodes have been used in the production of FRAM for nearly two decades and are also incorporated in most PZT MEMS devices. A Ti underlayer and the use of Pt films deposited near room temperature results in a thermally unstable electrode for subsequent PZT processing. Enhancement of thermal stability of the Pt electrode was achieved with a TiO₂ seed layer and Pt deposition at substrate temperatures above 450°C. These Pt/TiO₂/SiO₂/Si structures exhibit well defined interfaces, a Pt layer with improved density and {111}-texture, and enhanced device properties. X-ray diffraction, TEM, ellipsometry, and electrical property measurements were collected for a detailed analysis of the TiO₂ structure and to determine its impact on the Pt structure and properties. The TiO₂

films were formed by thermal oxidation of DC magnetron sputter deposited Ti films and the Pt films were deposited by DC magnetron sputter deposition at a substrate temperature of 500°C. TEM observations confirm that there is a discontinuity in the TiO₂ and Ti microstructures associated with the thickness induced changes in the TiO₂ metrics and specifically the minimization of the TiO₂ {200} misorientation distribution. The Pt {111} misorientation distribution (rocking curve FWHM) mimics the TiO₂ {200} distribution and exhibits a minimum width with a TiO₂ seed layer optimum thickness of 30 nm.

2:30 PM

(EMA-S9-018-2014) The Influence of Microscopic Degrees of Freedom on Equilibrated Orientation Relationships between Pt and SrTiO₃

G. Atiya, A. Altberg, V. Mikhelashvili, G. Eisenstein, W. D. Kaplan*, Technion - Israel Institute of Technology, Israel

This study focuses on Pt-SrTiO₃ interfaces, formed by solid-state dewetting, for processing nanometer length-scale particles for memory devices. Thin films of Pt were dewetted on (001) SrTiO₃ substrates with a TiO₂ termination to form equilibrated single crystal particles. Annealing (dewetting) was conducted at 1150°C using different partial pressures of oxygen (P(O₂)). Given the similar lattice parameters between Pt and SrTiO₃, a simple cube-on-cube orientation relationship was expected to form at equilibrium. However, at a low P(O₂) of 10⁻²⁰ atm, in addition to equilibrated Pt particles, a strontium oxide interfacial phase formed at the interface, and rod-shaped SrTiO₃ particles, slightly depleted in Ti, formed on the surface of the SrTiO₃ substrates. At a higher P(O₂) of 1.5x10⁻³ atm, only a preferred orientation of Pt {111} parallel to the SrTiO₃ {100} surface formed, without a low-index orientation relationship. Monochromated and aberration corrected high resolution transmission electron microscopy showed that different forms of SrTiO₃ surface and interface reconstruction evolved at the different oxygen partial pressures. This indicates the important role of surface/interface microscopic degrees of freedom on the macroscopic degrees of freedom (orientation relationship) at equilibrium.

2:45 PM

(EMA-S9-010-2014) Adaptive Optics Systems Based on PZT Thin Films with Integrated ZnO Electronics (Invited)

R. H. Wilke*, R. L. Johnson-Wilke, M. L. Wallace, The Pennsylvania State University, USA; J. I. Ramirez, T. L. Jackson, The Pennsylvania State University, USA; V. Cotroneo, S. McMuldroch, P. B. Reid, D. A. Schwartz, Harvard-Smithsonian Center for Astrophysics, USA; S. Trolrier-McKinstry, The Pennsylvania State University, USA

Adjustable X-ray optics, using PZT films deposited on slumped, thin glass substrates, are a candidate for next generation telescopes. The vision is to create a pixelated array of 1 cm² electrodes that are addressed using a row-column scheme, with ZnO transistors integrated onto the PZT to provide the control electronics. The PZT films are deposited on Corning Eagle glass substrates using RF magnetron sputtering. Crystallization is complete at 550 °C with piezoelectric properties that exceed the mission requirements. Influence function measurements of 2 μm thick films on flat glass substrates show a 1.5 μm out of plane deflection for 1 cm² actuators driven at 1.5 E_c. Preliminary depositions on curved substrates mimicking the shape of the proposed mirror demonstrate that the process can be transferred to non-planar geometries. For integration with the control electronics, ZnO thin film transistors are being fabricated using plasma enhanced atomic layer deposition. Incorporation of the ZnO processing shows no significant degradation to the PZT properties. The transistors exhibit rapid turn on times (~14 ms) and discharge times consistent with negligible source-drain leakage. Complete integration of the ZnO transistors with the PZT arrays will be discussed.

3:15 PM

(EMA-S9-020-2014) Electrochromism vs. the Bugs: Developing WO₃ Thin Film Windows to Control Photoactive Biological Systems

L. J. Small*, S. Wolf, E. Courchain, V. S. Vandelinder, D. R. Wheeler, G. Bachand, E. D. Spoeke, Sandia National Laboratories, USA

The ability to control the intensity of light incident on photoactive biological proteins allows for effective control of biological function. Electrochromic materials such as WO₃ provide a convenient means by which an external stimulus, such as voltage, may control the amount of light delivered to the biological system. In WO₃, the optical absorbance at specific wavelengths can be modulated by electrochemically reducing W⁶⁺ and simultaneously intercalating H⁺, Li⁺, or Na⁺ into the film. This talk will describe the sol-gel deposition of WO₃ thin films onto transparent conducting substrates and the effect of annealing temperature, film crystallinity, and film thickness on the electrochromic response in various aqueous environments. Subsequent integration of the WO₃ thin films with the photoactive protein bacteriorhodopsin from *Halobacterium salinarum* reveals the real-time response between the voltage-regulated optical transmission of WO₃ and the pH response of bacteriorhodopsin. Sandia National Laboratories is a multi-program laboratory managed and operated by Sandia Corporation, a wholly owned subsidiary of Lockheed Martin Corporation, for the U.S. Department of Energy's National Nuclear Security Administration under contract DE-AC04-94AL85000.

4:00 PM

(EMA-S9-021-2014) Molecular "Popoids": Assembling Functional Supramolecular Nanocrystal Films on Chemically-Modified Surfaces

E. Spoeke*, D. V. Gough, J. S. Wheeler, T. N. Lambert, V. Stavila, K. Leong, M. D. Allendorf, Sandia National Laboratories, USA

Self-assembled supramolecular materials offer tremendous technological potential, exhibiting a wide range of chemical functionalities and materials properties. With viable applications of these materials ranging from gas storage and catalysis to sensing and drug delivery, learning to control the nucleation, growth, and assembly of such structures on technologically relevant surfaces is extremely important. Here, we describe the controlled nucleation and growth of metal organic frameworks (MOFs), one especially promising class of crystalline supramolecular materials, as films on functional surfaces. Through careful control over solution-phase growth processes and manipulation of substrate surface chemistry, we show that it is possible to control the nucleation and growth of select MOF thin films and MOF thin film composites. In particular, we focus on the growth of opto-electronically active MOF constructs with potential applications in photovoltaics, solid-state lighting, or organic electronics.

4:15 PM

(EMA-S9-022-2014) Nucleation and Passivation of Al₂O₃ and TiO₂ Thin Films Formed by Atomic Layer Deposition on Polymeric Substrates

H. I. Akyildiz*, Y. Sun, J. S. Jur, North Carolina State University, USA

Passivation of polymer-based flexible electronics is a primary challenge due to the inherent incompatibility between inorganic material properties and processes with the organic substrates. In this work nucleation behavior and passivation properties of low-temperature Al₂O₃ and TiO₂ thin films by atomic layer deposition (ALD) is investigated on polyamide and polyimide films. A hybrid (organic-inorganic) nucleation layer beneath the oxide film is observed due to the infiltration and reaction of the ALD precursors into the polymer during processing. The hybrid layer formation is more prevalent at lower processing temperatures. As the processing temperature is increased, less infiltration is observed, eventually resulting in a uniform dense inorganic film. Mechanical properties

of the films are investigated by nanoindentation and crack formation analysis while bending the films. Specifically, the role of the hybrid layer on the modification of the mechanical behavior of the film and substrate is presented, as is the potential of these oxide/hybrid structured layers for passivation applications.

4:30 PM

(EMA-S9-023-2014) Fabrication of superhydrophobic silica-stainless steel composite through electrophoretic deposition

R. Corpuz*, MSU-IIT, Philippines; L. De Juan, University of the Philippines Diliman, Philippines

This study investigates fabrication of superhydrophobic coating on stainless steel using dimethylsiloxane modified silica particles using electrophoretic deposition. Results show that a uniform surface coating with thickness of around 2~3 microns as well as the presence of low surface energy methyl group resulted to a superhydrophobic surface with a contact angle of 163 to 165 degrees.

4:45 PM

(EMA-S9-024-2014) Sodium ion conductivity and scaling effects in NASICON thin films prepared via chemical solution deposition

J. Ihlefeld*, W. Meier, M. Rodriguez, B. B. McKenzie, A. Allen, M. Blea, A. McDaniel, Sandia National Laboratories, USA

We will present a methodology for preparing sodium zirconium phosphate and sodium zirconium silicon phosphate (NASICON) thin films via a chemical solution deposition approach. It will be shown that temperatures in excess of 700°C are required to crystallize the films and that the required temperature increases with increasing silicon content. Increasing silicon content was not accompanied by a significant increase in sodium-ion conductivity, as would be expected from bulk ceramic-based literature. Conversely, it was observed that grain size had a strong effect on the measured ionic conductivities. We will show how increasing grain size in the phosphate end-member via increased thermal budget results in properties consistent with those measured on bulk ceramics. Sandia is a multiprogram laboratory operated by Sandia Corporation, a wholly owned subsidiary of Lockheed Martin Company, for the United States Department of Energy's National Nuclear Security Administration under contract DE-AC04-94AL85000.

S12: Recent Developments in High-Temperature Superconductivity

New Superconductors, New Structures and Pinning Properties

Room: Mediterranean B/C

Session Chair: Claudia Cantoni, Oak Ridge National Laboratory

1:30 PM

(EMA-S12-020-2014) High critical current densities in Ba-122 thin films by self-assembled and artificial pin arrays (Invited)

C. Tarantini*, F. Kametani, J. D. Weiss, J. Jiang, E. E. Hellstrom, J. Jaroszynski, National High Magnetic Field Laboratory, USA; S. Lee, C. Eom, University of Wisconsin, USA; D. C. Larbalestier, National High Magnetic Field Laboratory, USA

In order to determine the potential of the recently discovered iron-based superconductors we study the pinning properties of Co-doped BaFe₂As₂ (Ba-122) thin films in high fields up to 45T. We deposited single and multilayer films on different substrates and with different density of defects in order to increase the in-field J_c performance and decrease the effective J_c anisotropy. We discovered that Ba-122 is quite unique since it accepts up to 15-20%vol. of pinning

centers effective over a wide temperature and field range without compromising the matrix properties. Ba-122 thin films deposited on SrTiO₃-templated (La,Sr)(Al,Ta)O₃ have a high density of self-assembled c-axis aligned nanorods and additional precipitates can be introduced by multilayer deposition. We obtained a strong increase of J_c that exceeds 10⁵A/cm² 20T and 4.2K with a weak angular dependence. Moreover the pinning force density F_p(4.2K) reaches 45-50 GN/m³ at 15-20T, close to H_{irr}/2. We also characterized Ba-122 films deposited on CaF₂ that induces an enhancement of T_c by strain. This strain effect plus the introduction of effective pinning center further improves the J_c performance with F_p(4.2K) reaching 74 GN/m³ at 22.5 T. We conclude that this Fe-based superconductor has enormous pinning tunability which exceeds even that of YBCO. In fact its pinning force is almost as tunable as Nb-Ti.

2:00 PM

(EMA-S12-021-2014) Exploring the variables controlling superconductivity in 122 arsenides by local-probe microscopy and spectroscopy techniques (Invited)

C. Cantoni*, M. Pan, K. Gofryk, A. Sefat, B. I. Saparov, A. F. May, W. Lin, M. A. Mc Guire, B. C. Sales, Oak Ridge National Laboratory, USA

A longstanding goal in the field of Iron-based superconductors (FBS) has been to decipher the interplay between chemical substitutions (doping), crystal structure, and electronic structure, as this might be the key to understand trends in T_c and expand FBS functionality. By using local probes such as aberration-corrected scanning transmission electron microscopy (STEM), electron energy loss spectroscopy (EELS), and scanning tunneling microscopy (STM), which can map crystal and electronic structures on the atomic scale, we discover that FBS are more complex than expected on the basis of bulk-sensitive measurements, which are not sensitive to nanoscale inhomogeneities. In this talk, I will discuss some types of nanoscale inhomogeneities present in FBS and their effect on local physical properties, including the superconducting gap and its spatial distribution. In particular, nanoscale dopant inhomogeneity gives rise to an inhomogeneous superconducting gap in Ba(Fe_{1-x}Cox)2As₂, and filamentary superconductivity in (Ca_{1-x}Pr_x)Fe2As₂. In both systems, nanoclusters with a superconducting gap larger than the measured macroscopic value exist; indicating higher T_c might be realized in FBS by controlling the dopant distribution. Research was supported by the Materials Sciences and Engineering Division Office of Basic Energy Sciences, U.S. Department of Energy.

2:30 PM

(EMA-S12-007-2014) MgB₂ thin films for electronics and RF applications (Invited)

X. Xi*, Temple University, USA

Superconductivity at 39 K in MgB₂ allows superconducting devices such as SQUID detectors and superconducting digital circuits to operate at above 20 K, a temperature attainable by smaller, more efficient and cheaper cryocoolers than required by the Nb-based devices and circuits. The larger energy gaps in MgB₂ could potentially lead to higher operating frequency than in Nb-based digital circuits. Our recent work on MgB₂ RSFQ TFF circuits demonstrated operation up to 180 GHz at low temperatures and 65 GHz at 20 K. Clean MgB₂ thin films have a low residual resistivity (<0.1 μΩcm) and a high T_c of 40 K, promising a low BCS surface resistance. Its thermodynamic critical field H_c is higher than Nb, potentially leading to a higher maximum accelerating field. The lower critical field H_{c1}, which marks the vortex penetration into the superconductor and the vortex motion related dissipation, is lower for MgB₂ than Nb, but it can be enhanced by decreasing the film thickness below the penetration depth. I will present results of research in two directions: enhancement of H_{c1} in thin MgB₂ films and multilayers, and the coating of RF cavities by MgB₂.

3:00 PM

(EMA-S12-023-2014) Artificially engineered superlattices of pnictide superconductor (Invited)

C. Eom, A. Ruosi*, University of Wisconsin-Madison, USA

Artificial layered pnictide superlattices offer unique opportunity towards tailoring superconducting properties and understanding the mechanisms of superconductivity by creating model structures which do not exist in nature. We have demonstrated that artificially engineered undoped Ba-122 / Co-doped Ba-122 compositionally modulated superlattices produce ab-aligned nanoparticle arrays by layering and self-assembled c-axis aligned defects that combine to produce very large J_c and H_{irr} enhancements over a wide angular range. We also demonstrate a structurally modulated SrTiO₃ (STO) / Co-doped Ba-122 superlattice with atomically sharp interfaces. Success in superlattice fabrication involving pnictides will serve to spur progress in heterostructured systems exhibiting novel interfacial phenomena and device applications. This work has been done in collaboration with S. Lee, C. Tarantini, P. Gao, J. Jiang, J. D. Weiss, F. Kametani, C. M. Folkman, Y. Zhang, X. Q. Pan, E. E. Hellstrom, and D. C. Larbalestier. The work at the University of Wisconsin was supported by funding from the DOE Office of Basic Energy Sciences under award number DE-FG02-06ER46327.

4:00 PM

(EMA-S12-024-2014) Vortex pinning and dynamics in Fe-based superconductors with naturally-grown and engineered pinning landscapes (Invited)

L. Civale*, Los Alamos National Laboratory, USA

Vortex pinning and dynamics in Fe-based superconductors is at least as complex as in oxide superconductors. Clean single crystals may have very simple pinning landscapes dominated by a single type of defects, resulting in a low critical current density (J_c) with rather featureless dependences on temperature (T), magnetic field strength (H) and orientation (Θ). In contrast, thin films frequently show much higher J_c arising from mixed pinning landscapes containing both uncorrelated and correlated disorder, as evidenced by angular dependences $J_c(\Theta)$ exhibiting peaks for $\Theta=0$ ($H||c$ axis) whose intensity varies with T and H . On top of these features in as-grown samples, several studies have shown that the pinning landscape can be effectively engineered by irradiation or by addition of non-superconducting second phases. A somewhat surprising characteristic of the vortex matter in Fe-based superconductors is that it tends to show large fluctuations effects similar, or even larger, than in oxide HTS, such as fast flux creep and extended liquid phases. This is the case even in compounds where simple estimates based on the value of the Ginzburg number (Gi) would suggest that fluctuation effects should be much smaller, similar for instance to MgB₂. I will present studies of the vortex pinning and dynamics in Fe-based superconductors with different landscapes and Gi numbers.

4:30 PM

(EMA-S12-025-2014) Improvement and limitations of critical current densities in K-doped ferropnictide BaFe₂As₂ bulks and wires (Invited)

J. D. Weiss*, J. Jiang, C. Tarantini, F. Kametani, A. Polyanskii, B. Hainsey, D. Larbalestier, E. Hellstrom, Florida State University, USA

Over the last two years, researchers have greatly improved the properties of superconducting (AE)Fe₂As₂ (AE = Sr, Ba) wires and bulks, increasing the critical current densities towards values needed for applications, generally thought to be of order 10^5 A/cm². It now seems that the best bulk, tape or round wire forms can get to this J_c value at self-field but that in-field J_c values are almost an order of magnitude smaller unless texturing techniques are used to align grains. Here we present results from several experiments designed to understand what limits the J_c of Ba_{0.6}K_{0.4}Fe₂As₂ bulks and round wires. We find that even high J_c wires (4.2 K, self-field >0.12 MAcm⁻²) show evidence for significant obstacles to current flow, as shown by $J_c(H)$ curves that are hysteretic between increasing and decreasing field, and by $J_c(H)$ plots that see little difference whether H and I are parallel or perpendicular to the length of the wire. We conclude that although long range connectivity does exist in our high J_c samples, there is also clear evidence for percolative current flow. Recent effort to raise J_c through texturing, impurity doping, and grain boundary engineering will be discussed for bulk materials as well as for single and multi-filament wires.

5:00 PM

(EMA-S12-026-2014) Enhanced Superconducting Properties of FeSe_{0.1}Te_{0.9} Thin Films on STO and Glass Substrates

L. Chen, J. Huang, C. Tsai, Y. Zhu, J. Jian, A. Chen, Z. Bi, F. Khatkhatay, Texas A&M University, USA; N. Cornell, A. Zakhidov, University of Texas at Dallas, USA; H. Wang*, Texas A&M University, USA

In this study Te-rich iron chalcogenide (FeSe_{0.1}Te_{0.9}) thin films with composition close to antiferromagnetic ordering have been deposited on SrTiO₃ (STO) substrates and glass substrates. The superconducting critical transition temperature (T_c) of the FeSe_{0.1}Te_{0.9} thin film ranges from ~12.5 K to ~13.3 K on STO substrates and ranges from 10 K to 12 K on glass substrates. The upper critical field is as high as 114 T and 43 T for thin film on STO and glass substrates, respectively, which is much higher than that of the FeSe_{0.5}Te_{0.5} thin films on STO substrates and glass substrates. The self-field critical current density (J_{csf}) is also much higher than that of FeSe_{0.5}Te_{0.5} thin film, and the FeSe_{0.1}Te_{0.9} thin film demonstrates superior pinning properties under applied magnetic field. Compared to the FeSe_{0.5}Te_{0.5}, which was considered as the optimum composition, FeSe_{0.1}Te_{0.9} presents even more promises for high field applications because of its high upper critical field and high critical current density as well as its compatibility on various substrates.

Author Index

* Denotes Presenter

A

Agote, I.	46
Aguirre, B. A.	30
Ahn, S.	42
Akhtar, M.	46
Akyildiz, H. I.*	80
Al Assadi, M. H.	64
Alam, M.	41
Alberga, M.	78
Alberga, M.*	71
Alexe, M.	69
Ali, G.	55
Alkoy, S.	42
Alkoy, S.*	33
Allen, A.	81
Allendorf, M.	31
Allendorf, M. D.	80
Alpay, S.	76
Alpay, S.*	63
Altberg, A.	80
Amal, R.	54
Amann, A.	44
Amemiya, N.*	67
Amin, A.	38
Anand, S.	69
Anders, J.*	44
Anderson, K.	54
Andrew, J. S.	61
Ansell, T.	59
Ansell, T.*	38
Anwar, F.	30
Aoki, N.	74
Arcon, D.	50
Arrasmith, S.	33
Asano, H.	47
Atiya, G.	80
Atlas, S. R.	64
Au, Y.	41

B

Baca, J.	74
Bachand, G.	80
Bae, S.	42
Baek, S.	27, 45
Baer, E.	32
Bagatin, M.	49
Baker, A.	49
Baldwin, A.	39
Balicas, L.	66
Barthelemy, A.	28
Bartling, S.	41
Baskes, M. I.	64
Bassiri-Gharb, N.	33, 40, 49, 60
Bassiri-Gharb, N.*	73
Bastani, Y.	49, 73
Batlogg, B.*	66
Bauer, E.	70
Beanland, R.*	29
Beckman, S. P.	58, 75
Bell, N.	60
Bellaiche, L.*	36, 52
Berbano, S. S.	49
Berbano, S. S.*	60
Berksoy-Yavuz, A.	33, 42
Berry, H. D.*	63
Bhaskaran, H.*	41
Bhave, S. A.*	65
Bi, Z.	71, 82
Biancoli, A.	26

Bibes, M.	28
Biegalski, M.	64
Biegalski, M. D.	60
Bin-Omrar, S. H.*	44
Bishop, S. R.*	43, 59
Blatter, G.	66
Blea, M.	81
Blendell, J.	38, 69
Bock, J. A.	53
Bogle, K.	54
Bongkarn, T.	43
Bosak, A.*	37
Boschker, H.	64
Bosse, J.	30
Bosse, J. L.	66
Bosse, J. L.*	33, 41
Bowman, K. J.	38
Boyn, S.	28
(Bratt) Nahor, H.	62
Bray, J. W.*	26
Brennecka, G. L.	73
Brennecka, G. L.*	73
Brewer, S.	73
Bridger, K.*	33
Brown-Shaklee, H. J.	50, 57, 79
Brown-Shaklee, H. J.*	77
Brunke, L.	68
Bryan, I.	64
Bügler, M.	64
Bullard, T.	48, 67
Bullard, T.*	68
Buongiorno Nardelli, M.	31
Burch, M. J.	72
Burch, M. J.*	73
Burkovsky, R.	37
Burrell, A. K.	70
Bux, S.*	72

C

Caillat, T.	72
Calame, J. P.	32
Campion, M. J.	50, 57
Cann, D.	38, 43, 53, 59
Cann, D. P.	73
Cantoni, C.*	81
Carman, G.*	51
Carrete, J.	31
Carter, J. J.*	53
Chan, C. K.*	30
Chan, H. M.*	54
Chang, H.	45, 76
Chang, J. P.*	52
Chatain, D.*	62
Cheaito, R.	79
Chen, A.	82
Chen, A.*	71
Chen, D.	59
Chen, J.	27
Chen, L.	28, 74, 82
Chen, P.	28
Chen, X.	48
Chen, X.*	35, 57
Chen, Z.	28
Chernatynskiy, A.	47
Chernyshov, D.	37
Cho, D.	41, 42
Cho, H.	30, 79
Cho, J.	42
Cho, S.	30
Cho, S.*	79

Choi, B.	35
Choi, H.*	45
Choi, J.	45
Choi, Y.	35
Christen, H. M.	60
Chu, C.*	56
Chun, S.	30
Chung, C.	26
Civale, L.*	53
Clarke, S.	72
Clem, P.	57
Clem, P. G.	50
Clem, P.*	66
Clinton, M.	41
Cole, M.	37
Collazo, R.	64
Cooke, A. V.	33
Cornell, N.	82
Corpuz, R.*	81
Cortes-Pena, A. Y.*	49
Cosgriff, M.	28
Cotroneo, V.	80
Courchaine, E.	80
Cozzan, C.*	58
Craig, N.	67
Crossley, J.	46
Cruz-Campa, J.	30
Cruz-Campa, J. L.	30
Cui, J.	51
Cullen, D. A.	79
Curtarolo, S.*	31
Custer, J.	66

D

Damjanovic, D.*	26
Daniels, J.	44
Daniels, J. E.	58
Das, S.	60
Davidson, B. A.*	27
Dayal, K.*	36
De Juan, L.	81
Deepak, N.	44, 70
Deguchi, K.	57
Delgado, L.	74
Dempsey, R.	33
Demura, S.	57
Deng, L.	56
Denholme, S.	57
Dezest, D.	75
Dias, A.	77
Dickey, E. C.	34, 72, 73
Dickey, E. C.*	58
Dillon, S.	54
Dimitriadou, I.	46
Ding, J.*	33, 60
Dixon, R.	46
Dkhil, B.*	37
Doeff, M.	49
Dong, L.*	39
Dongare, A.	39
Donovan, B. F.	79
Donovan, B. F.*	58, 78
Dorr, K.*	60
Doshida, Y.	69
Drofenik, M.	50
Dubey, M.	39
Dursun, S.	33
Duva, F.	33
Dvorak, C. E.*	79
Dynys, F.	47, 78

E

Eastman, J.	65
Edmondson, C. A.	32
Edney, C.	60, 66
Edwards, D.	79
Edwards, D. D.	71, 78
Ehara, Y.	28, 60
Ehmke, M. C.	69
Ehmke, M. C.*	38
Eichel, R. A.*	53
Eisenstein, G.	80
Enriquez, E.*	77
Eoh, Y.	35
Eom, C.	27, 81, 82
Evans, D. M.	69
Evans, J. T.*	40
Evans, P.*	28

F

Feigelson, B.	47
Feng, J.	45
Feng, L.*	54
Feng, Y.	43
Ferreira, I.	78, 79
Ferreira, M.	78, 79
Feulner, P.	46
Field, T.*	40
Figueira, J.	78, 79
Finkel, P.*	38
Fleurial, J.	72
Foley, B. M.	58, 78, 79
Foley, B. M.*	50, 57
Folkman, C.	65
Fong, D.	65
Fontanella, J. J.*	32
Foster, M.	31
Fox, G. R.*	79
Franzen, S.	65
Frederick, J.	27
Freeland, J. W.	27
Fueglein, E.	26
Funakubo, H.	28
Funakubo, H.*	60
Fuoss, P.	65
Furlan, V.	65
Furuta, Y.	47
Fusil, S.*	28

G

Gaddy, B.	64
Galtsyan, E.	74
Ganesh, P.*	56
Gangi, S.	74
Gao, L.*	49
Gao, Z.	66
Garcia, V.	28
Garcia, V.*	40
Garofalini, S. H.*	63
Garrity, K. F.*	32
Gaskins, J. T.	79
Gelbstein, Y.*	46, 71
Gerardin, S.	49
Geshkenbein, D.	66
Ghosh, D.	40, 62
Gibbons, B. J.	73
Gil, C. J.	64
Gilchrist, R.	46
Giuliani, F.	54
Glaum, J.	59, 69
Glazer, M.	37

Glinsek, S.	65
Gloter, A.	28
Gofryk, K.	81
Goldberger, J.	39
Gopinath, A.	76
Gorfman, S.	29
Gorzowski, E.*	47
Goto, T.	74
Gough, D.	31
Gough, D. V.	80
Govindaraju, N.*	35
Gregg, M.*	69
Grenkemper, J.	72
Grishin, I.	33, 41
Groh, C.	69
Grossman, J. C.	31
Guo, E.	60
Guo, H.	29
Guo, H.*	58, 75
Guo, X.*	76
Guorong, L.*	27
Gupta, R.	50
Gupta, V.	50
Gyergyek, S.	50

H

Hachmann, J.*	55
Haindl, S.*	57
Hainsey, B.	82
Han, J.*	35
Han, Y.*	46
Hang, T.*	59
Hao, R.*	54
Harris, D. T.	73
Harris, D. T.*	72
Harrison, K.	37
Hasegawa, T.	74
Hashemi Zadeh, S.	26
Hatano, K.	69
Haugan, T.	68, 74
Haugan, T. J.	48, 67
Haugan, T. J.*	48
Haugan, T.*	48, 67
Heitmann, A. A.	63
Hellstrom, E.	82
Hellstrom, E. E.	67, 81
Herklotz, A.	60
Higashikawa, K.	74
Highland, M.*	65
Hill, M. D.*	34
Hockel, J.	51
Hoffman, M.	59, 69
Hoffmann, A.	64, 76
Holesinger, T.	74
Hong, S.	45
Hopkins, P.	57, 58
Hopkins, P. E.	50, 78
Hopkins, P.*	79
Hordagoda, M.	61
Hordagoda, M.*	40, 62
Hoshina, T.	49
Hosseini, P.	41
Hu, L.	46
Hu, Y.	72
Huang, C.	72
Huang, J.	82
Huang, J.*	74
Huang, L.	27
Huey, B. D.	33, 41
Huey, B. D.*	30, 66
Huey, B.*	28
Huijben, M.	64

Hunker, J.	66
Husband, M.	46

I

Ibi, A.	74
Ihlefeld, J.	28, 50, 57, 58, 72, 73, 77, 78, 79
Ihlefeld, J.*	81
Im, E.	45
Imai, Y.	28
Imamura, K.	75
Ingersoll, D.	60
Inoue, M.	74
Irie, H.	47
Irving, D.	64
Ishibashi, T.	48
Ito, A.*	74
Itoh, M.	28
Iwasaki, K.	47
Iwase, A.	42
Izumi, T.	74

J

Jackson, T. L.	80
Jagodic, M.	50
Jahangir, S.*	57
Jain, M.	28, 70
Jain, M.*	61
James, A.	42
Jang, H.	45
Jaroszynski, J.	81
Jia, Q.	65, 70, 71
Jia, Q. X.*	70
Jian, J.	83
Jiang, H.	76
Jiang, J.	81, 82
Jiang, J. D.	67
Jiang, Y.	63
Jiao, J.*	27
Jin, S.	48
Jindal, K.	50
Jo, J.	28
Johlin, E.	31
Johnson-Wilke, R. L.	80
Jones, J.	40, 44, 62
Jones, J. L.	47, 58
Jones, J. L.*	37, 73
Jordan, T.	66
Jordovic, B.	42
Joung, M.	35, 75
Joyce, D.*	33
Jung, J.*	54
Jur, J. S.	80

K

Kabatek, M.	76
Kagomiya, I.	59
Kakemoto, H.*	47
Kakimoto, K.	50, 59, 69
Kakimoto, K.*	68
Kalinin, S.	33, 60
Kalkur, T.	76
Kalkur, T.*	52
Kalyani, A. K.*	42
Kametani, F.	81, 82
Kametani, F.*	67
Kang, C.	45, 75
Kang, L.	45
Kang, M.	45, 65
Kaplan, W. D.*	62, 80
Karpinski, J.	66

Karvonen, L.	72
Kassiba, A.	27
Katiyar, R. S.	35
Kato, K.*	47, 69
Kato, N.*	50
Kauzlarich, S.	72
Kawano, T.	47
Kaya, M.	33
Keeble, D.	29
Keeble, D. S.	69
Keech, R.	66
Keeney, L.	44, 70
Kellogg, G. L.	30
Kelso, J.	30
Kennedy, B. J.*	50
Kent, P.	56
Khanna, S.	41
Khansur, N. H.*	44
Khassaf, H.	76
Khatkhatay, F.	82
Khatri, N.	74
Kikuta, K.*	69
Kim, D.	45
Kim, D.*	46
Kim, E.*	35
Kim, J.	35, 45, 59, 75
Kim, J.*	45
Kim, S.	45
Kim, S.*	45
Kim, T.	27
Kim, Y.	45
Kimura, K.	74
Kiss, T.*	74
Kmet, B.	65
Kobayashi, K.	69
Kocic, L.	51
Koenig, J. D.*	71
Kohlhafer, D.	33
Koizumi, T.	74
Kolluri, K.	64
Kolosov, O. V.	33, 41
Koo, H.	42
Koster, G.	64
Kotula, P. G.	73
Kovac, J.	67
Kowalski, B.*	26
Kozlowski, G.	44
Kracum, M.	54
Krisch, M.	37
Krishnan, S.	41
Kuhn, M.	43
Kumakura, H.*	66
Kumar M, A.	39
Kumar, N.	73
Kumar, N.*	59
Kumar, S.	55
Kundu, A.	54
Kurusu, T.	67
Kutes, Y.	30
Kutnjak, Z.*	43, 50
Kwon, Y.	79
Kwon, Y.*	30

L

Lai, X.	48
Lam, P. G.	72
Lambert, T.	31
Lambert, T. N.	80
Lanagan, M. T.	60
Landis, G.	44
Larbalestier, D.	82
Larbalestier, D. C.	67, 81

Latypov, D.	48, 67
LeBeau, J.	64
Lee, D.	27
Lee, H.*	76
Lee, S.	45, 53, 54, 81
Lee, W.	46
Lee, Y.	35
Lenahan, P.	34, 53
Lenef, A.*	30
Leong, K.	31, 80
Leveille, J.	28
Levin, I.	53
Levin, I.*	58
Li, E.*	43
Li, J.	72, 73
Li, K. K.	76
Li, Q.*	56
Li, S.	64
Li, X.	27, 74
Li, Z.*	46
Liau, L. C.*	48
Lightfoot, P.*	29
Lim, E.	26
Lin, F.*	47
Lin, W.	81
Lin, Y.	48
Liu, L.	51
Liu, T.	76
Liu, V.*	54
Liu, X.	64
Liu, X.*	68
Liu, Y.	48, 74
Lluberes, A.	30
Lofland, S.	38
Lomax, J. F.	32
Lookman, T.*	32
Loureiro, J.*	78, 79
Lubimtsev, A.	56
Luo, H.	27, 65, 70
Luo, H.*	44
Luo, J.*	62
Lynch, C. S.*	51

M

Ma, C.	29
Ma, J.	72
Ma, R.	39
Mackey, J.*	47, 78
Mackey, M.	32
MacManus-Driscoll, J. L.	70, 71
Maier, R. A.	53
Maier, R.*	34, 53
Maignan, A.*	78
Maierov, B.	74
Maity, T.	44
Majkic, G.	74
Malic, B.	43
Malic, B.*	65
Mansfield, L.	30
Mantese, J.*	68
Manthiram, A.	37
Maqbool, M.*	45, 55
Maria, J.	64, 65, 72, 73
Marinova, M.	28
Marshall, J.	36
Martin, R. L.	64
Martins, R.	78, 79
Masduzzaman, M.	41
Matras, M.	67
Matsui, T.	42
Matsumoto, A.	66
May, A. F.	81

May, S.*	61
McGuire, M. A.	81
McAdams, H.	41
McCleskey, T.	65
McCleskey, T. M.	70
McClure, J. C.	30
McDaniel, A.	81
McDannald, A.	28
McKenzie, B.	58
McKenzie, B. B.	78, 81
McMuldorch, S.	80
Medlin, D. L.	50, 57
Meier, D.*	61
Meier, W.	81
Meltzman, H.	62
Mendez, J. E.*	76
Mensur-Alkoy, E.	33
Mensur-Alkoy, E.*	42
Meyer, K. E.	73
Mhin, S.	73
Michael, J. R.	30
Mikheleshvili, V.	80
Miljkovic, M.	42
Mingo, N.	31
Mirsaneh, M.	60
Mita, S.	64
Mithlesh, Y.	46
Mitic, V.*	42, 51
Miyawaki, T.	47
Mizuguchi, Y.	57
Moballeggh, A.	58
Moballeggh, A.*	34
Moffitt, B.	28
Moll, P. J.	66
Moon, C.	45
Moon, E.	61
Moon, S.	45
Mori, Y.	67
Morrissey, A.	53
Mueller, T.*	31
Mukherjee, D.	40, 62
Mukherjee, D.*	61
Mukherjee, P.	40, 61, 62
Muñiz-Serrato, O.*	48

N

Nagarajan, V.	54
Nahm, S.	35, 41, 42
Nahm, S.*	75
Nakashima, T.	60
Nakhmanson, S.*	64
Namburu, R.	39
Narayan, J.	71
Newman, N.*	51
Ng, Y.	54
Nicu, L.	75
Nielson, G. N.	30
Ning, H.	46
Nino, J. C.	47
Nino, J. C.*	70
Noda, K.	67
Nolas, G. S.	71
Nordquist, C.	66
Noufi, R.	30
Nowe, E.	76

O

O'Brien, J. R.	53
O'Regan, T.	39
Oganov, A. R.	55
Ogitsu, T.	67

Author Index

Oguchi, T.	57
Okamoto, Y.	42
Okatan, B.	54
Okazaki, H.*	57
Olukkent, R.	33
Ordenez, R.	30
Ouyang, J.*	45
Ozaki, T.	57

P

Paccagnella, A.	49
Paisley, E.	64
Pan, M.	81
Panasyuk, G. Y.	48, 67
Panasyuk, G. Y.*	48, 67
Pantelides, S. T.*	39
Pardo, E.*	67
Park, C.	45
Park, C.*	42
Park, K.*	45
Passaro, E.	33
Paunovic, V.	42, 51
Pavunny, S. P.*	35
Pecnik, T.	65
Peelaers, H.	39
Pemble, M. E.	44, 70
Pennycook, S. J.	39
Pernice, W. H.	41
Perret, E.	65
Perry, J. W.*	32
Pflugger, J.	72
Pham, A.*	64
Phillpot, S. R.	47
Phung, B.	59
Pilania, G.	31, 55, 64
Pimentel, A. A.	30
Piquette, A.	30
Podkaminer, J. P.	27
Polcawich, R.	66
Polcawich, R. G.	73, 79
Polomoff, N.	28
Polyanskii, A.	82
Pomorski, T.*	34, 53
Ponomareva, I.*	36
Popov, M.	52
Post, E.*	26
Potrepka, D. M.	79
Prasertpalichat, S.	43
Prasertpalichat, S.*	53
Prieto, H.	30
Prosandeev, S.	37
Puranam, S. S.	76

R

Rabe, K. M.	32
Radin, M.	56
Ramanathan, S.*	75
Ramirez, J. I.	80
Ramprasad, R.	31, 39, 55
Rana, L.	50
Randall, C.	34, 49, 53
Randall, C. A.	60
Randall, C.*	53
Ranjan, R.	42
Ranjan, R.*	29
Rao, B.	29
Reaney, I. M.*	28, 29, 34
Reece, M.	46
Reeja-Jayan, B.	37
Reichart, J. N.	48
Reid, P. B.	80

Reimanis, I.*	53
Ren, X.	34
Reparaz, S.	78
Restrepo, O. D.	39
Rhee, K.	46
Rijnders, G.	64
Rios, C.	41
Rivas, M.	66
Rivera, S.	46
Robert, H.	61
Robinson, I.	46
Robles-Dutenhefner, P.*	77
Rodrigues, A.	79
Rodriguez Pinilla, O.*	63
Rodriguez-Hernandez, G.	41
Rodriguez, J.	41
Rodriguez, J.*	41
Rodriguez, M.	81
Roedel, J.*	49
Rohrer, G.*	62
Rojac, T.	26
Rondinelli, J.*	36
Roosen, A.	50
Rossetti, G. A.	63
Rossetti, G. A.*	26, 63
Roth, R.	60
Rouaud, C.	46
Roy, S.	44
Rozic, B.	43, 50
Ruosi, A.*	82
Ryu, S.	27
Rzchowski, M. S.	27

S

Sabestian, M.	74
Sachet, E.	64
Sachet, E.*	65
Saenrang, W.	27
Sagarna, L.	72
Saiz, E.	54
Sakata, O.	28
Salazar, M. T.	30
Sales, B. C.	81
Salvador, P.	62
Sanchez, C.	30
Sanchez, L. M.	73
Santos, R.	78, 79
Saparov, B. I.	81
Saucke, G.	72
Sbrockey, N. M.*	76
Scheffler, M.*	31
Schmidt, M.	44
Schneider, W.	76
Schultheiss, H.	76
Schultz, L.	60
Schulze, W.	33
Schwartz, D. A.	80
Scott, J. F.	35, 69
Scott, K. J.*	78
Sebastian, M. P.	48
Sefat, A.	81
Sehirlioglu, A.	26, 47, 78
Sehirlioglu, A.*	26
Seidel, J.*	28
Selvamanickam, V.*	74
Seo, I.	75
Serrato-Rodriguez, J.	48
Seshadri, D.*	49
Sharma, A.*	50
Sharma, K.	52
Sharma, P. A.	77
Sharma, V.*	55

Shay, D. P.	53
Shelton, C. T.	65
Shelton, C. T.*	64
Shi, J.	74
Shimizu, T.	28
Shinoda, R.*	42
Shiohara, Y.	74
Shiraishi, T.	28
Shirk, J. S.	32
Shirpour, M.	49
Shkabko, A.	72
Shreiber, D.	77
Shrout, T.	68
Siegel, D.*	56
Simpson, K.	46
Sinclair, D.*	77
Singh, A.	50
Singh, D. J.*	72
Singh, R.	35
Sinnott, S. B.	47
Sitar, Z.	64
Small, L. J.*	80
Smith, S.	44
Song, D.	42
Song, D.*	41
Song, G.	46
Song, H.	76
Song, S.*	35
Song, Y.	76
Sotomayor, C.	78
Sotzing, G.	39, 55
Souc, J.	67
Spanier, J.*	77
Spoerke, E. D.	30, 80
Spoerke, E.*	31, 60, 80
Sreenivasulu, G.	52
Srinivasan, G.*	52
Starr, J. D.*	61
Stavila, V.	31, 80
Stemmer, S.*	70
Stephenson, G.	65
Strandwitz, N. C.*	63
Streffler, S.	65
Strelcov, E.	33, 60
Stutz, C.	44
Sumang, R.*	43
Summerfelt, S.	41
Summers, R.	46
Sumpter, B.	56
Sumpter, B.*	55
Sun, N.*	51
Sun, Y.	76, 80
Sung, T.	41, 42

T

Tagantsev, A. K.	36
Tagantsev, A. K.*	36
Tajiri, H.	28
Takano, Y.	57
Takeda, K.	49
Takeuchi, I.	28
Takeuchi, I.*	52
Takeuchi, T.	47
Takeya, H.	57
Tan, X.	34, 43, 58, 68, 75
Tan, X.*	29
Taneda, T.	74
Tarantini, C.	82
Tarantini, C.*	81
Terasaki, I.*	78
Thiel, P.	72
Thomas, P.	29, 37

Thomas, P. A.*	69
Thompson, C.	65
Tidrow, S. C.*	38
Togano, K.	66
Tomar, M.	50
Tomar, M.*	50
Tompa, G. S.	76
Tong, J.	53
Tran, H. D.*	39
Trolter McKinstry, S.	66
Trolter-McKinstry, S.	80
Trolter-McKinstry, S.*	75
Tsai, C.	74, 82
Tsurumi, T.*	49
Tuller, H.	43, 59
Tunbridge, J.	46
Tyagi, P.	50

U

Uberuaga, B. P.*	40
Uhl, D.	72
Ursic, H.	26, 43

V

Vailionis, A.*	64
Vakhrushev, S.	37
Valanoor, N.	57
Valanoor, N.*	27, 72
Valone, S.*	64
Van de Walle, C. G.*	39
Vandelinder, V. S.	80
Vanderbilt, D.	32
Varghese, D.*	41
Vidmar, M.	65
Villegas, J.	28
Vlaminck, V.	76
Vo, T.	72
Von Allmen, P.	72

W

Wada, S.*	55
Walenza-Slabe, J.	73
Walker, D.	69
Wallace, M. L.	80
Wang, C.	37, 39, 55
Wang, C.*	31
Wang, G.*	48
Wang, H.	48, 70, 71, 74
Wang, H.*	82
Wang, S.	27

Wang, X.	27
Wang, Y.	76
Watanabe, M.*	59
Watanabe, T.	57
Wegner, M.	50
Wei, K.*	71
Weidenkaff, A.*	72
Weigner, J.	33
Weisberg, D.	63
Weiss, J. D.	81
Weiss, J. D.*	82
Welsh, A.	75
West, A. R.*	59
Westgate, M. A.	32
Whatmore, R. W.*	44, 70
Wheeler, D. R.	80
Wheeler, J.	31
Wheeler, J. S.	60, 80
White, J. T.	53
Wilke, R. H.*	80
Wilkerson, R. P.	73
Will-Cole, M.	77
Wilson, A. D.	49
Windl, W.*	39
Wintersgill, M. C.	32
Witanachchi, S.	40, 61, 62
Wolak, M. A.	32
Wolak, M. A.*	32
Wolf, S.	80
Wollmershauser, J.	47
Woo, M.	41
Woo, M.*	42
Woodward, D. I.	69
Wright, C.	41
Wu, J.*	74
Wu, M.	76
Wu, M.*	76

X

Xao, X.	72
Xi, X.*	81
Xie, W.	72
Xiong, X.	27
Xu, A.	74
Xu, H.	75
Xu, Y.*	43

Y

Yakaguchi, T.	57
Yamada, H.	28
Yamada, T.	60

Yang, H.*	70
Yang, K.	31
Yang, K.*	37
Yang, O.	46
Yang, Q.	45
Yang, Y.*	34
Yao, Y.	34
Yasui, S.*	28
Ye, L.	28, 66
Ye, S.	66
Yilmaz, A. E.	37
Ying, T.	48
Yokota, H.*	37
Yoon, S.	45, 75
Yoshida, T.	74
Yoshimoto, M.	67
Yoshizumi, M.	74
Younis, A.*	41
Yu, A.	64
Yuan, M.	45
Yuan, Y.*	43

Z

Zakhidov, A.	82
Zeng, J.	27
Zhang, N.	37
Zhang, Q. M.	43
Zhang, S.	43, 51, 58, 75
Zhang, S.*	68
Zhang, W.	35, 45
ZHANG, Y.*	69
Zhao, L.	59
Zhao, P.	74
Zhao, W.	27
Zhao, X.	27
Zheng, L.	27
Zhigadlo, N. D.	66
Zhong, C.	43
Zhou, H.	71
Zhou, N.	62
Zhou, X.	30
Zhou, Z.	32
Zhu, Q.	55
Zhu, T.*	46
Zhu, X.	35
Zhu, Y.	71, 82
Zollner, S.*	70
Zou, G.*	65
Zou, Y. K.	76
Zubia, D.*	30
Zunger, A.*	38

Organizers:



100th ANNIVERSARY
1913-2013



Cosponsor:



MS&T'14[®]

Materials Science & Technology 2014

October 12-16, 2014

David L. Lawrence Convention Center
Pittsburgh, Pennsylvania USA

The leading forum addressing structure, properties, processing and performance across the materials community.
call for papers March 15, 2014

The technical program covers:

- Biomaterials
- Ceramic and Glass Materials
- Characterization
- Electronic, Optical, and Magnetic materials
- Fundamentals
- Green Manufacturing and Sustainability
- Iron and Steel (Ferrous Alloys)
- Materials Behavior and Performance
- Materials-Environment Interactions
- Nanomaterials
- Processing and Product Manufacturing
- Surface Modification
- Special Topics

www.matscitech.org

2014

The
American
Ceramic
Society
www.ceramics.org



Meetings & Expositions of THE AMERICAN CERAMIC SOCIETY

FEBRUARY 17 – 20, 2014

Materials Challenges in Alternative and Renewable Energy – MCARE 2014
Hilton Clearwater Hotel
Clearwater, Florida USA

MARCH 3 – 5, 2014

ACerS Structural Clay Products Division Meeting, in conjunction with NBRC Spring Executive Committee & Membership Meeting
Hilton Knoxville Hotel
Knoxville, Tennessee USA

MARCH 25 – 27, 2014

St. Louis Section/RCD 50th Annual Symposium
Hilton St. Louis Airport Hotel
St. Louis, Missouri USA

APRIL 7 – 9, 2014

4th Ceramic Leadership Summit – CLS 2014
Sheraton Inner Harbor Hotel
Baltimore, Maryland USA

APRIL 14 – 16, 2014

IMAPS/ACerS 10th International Conference and Exhibition on Ceramic Interconnect and Ceramic Microsystems Technologies (CICMT 2014)
Hotel Hankyu Expo Park
Osaka, Japan

MAY 25 – 29, 2014

Deutsche Glastechnische Gesellschaft and the Glass & Optical Materials Division Annual Meeting – DGG-ACerS GOMD Joint Annual Meeting, including the 10th International Conference on Advances in Fusion and Processing of Glass (AFPG)
Aachen, Germany

JUNE 17 – 18, 2014

ACerS/NSF Principal Investigator Workshop
Arlington, Virginia

JULY 9 – 11, 2014

5th Advances in Cement-based Materials: Characterization, Processing, Modeling and Sensing
Tennessee Technological University
Cookeville, Tennessee

JULY 30 – AUGUST 1, 2014

Innovations in Biomedical Materials: Focus on Ceramics
Hilton Columbus Downtown
Columbus, Ohio USA

AUGUST 4 – 7, 2014

3rd International Conference on Electrospinning – Electrospin 2014
Westin San Francisco Market Street
San Francisco, California USA

AUGUST 17 – 21, 2014

5th International Congress on Ceramics
Beijing International Conference Center
Beijing, China

OCTOBER 12 – 16, 2014

MS&T14 – Materials Science & Technology Conference and Exhibition, combined with ACerS 116th Annual Meeting
David L. Lawrence Convention Center
Pittsburgh, Pennsylvania USA

NOVEMBER 3 – 6, 2014

75th Conference on Glass Problems – 75thGPC
Greater Columbus Convention Center
Columbus, Ohio USA

strontium doped lanthanum II-IV nitride materials crystal growth cobalt metamaterials
organic metallics tantalum alloys cerium polishing powder thin film bioceramics
es **Li** **Be** dysprosium pellets atomic layer deposition rod
solid **Na** **Mg** aerospace ultra-light alloys iridium crucibles erbium
ite **K** **Ca** scandium-aluminum green technology ultra
misch **Rb** **Sr** **Y** **Zr** **Nb** **Mo** **Tc** **Ru** **Rh** **Pd** **Ag** **Cd** **In** **Sn** **Sb** **Te** **I** **Xe**
catho **Cs** **Ba** **La** **Hf** **Ta** **W** **Re** **Os** **Ir** **Pt** **Au** **Hg** **Tl** **Pb** **Bi** **Po** **At** **Rn**
solar e ClIGS superc

Ce	Pr	Nd	Pm	Sm	Eu	Gd	Tb	Dy	Ho	Er	Tm	Yb	Lu
Th	Pa	U	Np	Pu	Am	Cm	Bk	Cf	Es	Fm	Md	No	Lr

Now Invent.TM



platinum ink quantum dots nickel foam ultra high purity m
anti-ballistic ceramics osmium alternative energy ion

World's Leading Manufacturer of
Engineered & Advanced Materials
shape memory alloys Nd:YAG catalog: americanelements.com
rhodium sponge photovoltaics

© 2001-2011, American Elements is a U.S. Registered Trademark.